Drug Delivery Devices for Cancer and Posterior Eye

By

Hamad Alrbyawi

A dissertation submitted to the Graduate Faculty of
Auburn University
in partial fulfillment of the
requirements for the Degree of
Doctor of Philosophy

Auburn, Alabama
December 14, 2019

Keywords: Liposomal Drug Delivery, Melanoma Cancer, Breast Cancer, Daunorubicin, Ceramide, Cardiolipin

Approved by

Jayachandra Babu Ramapuram, Chair, Professor of Drug Discovery and Development
Robert D. Arnold, Co-chair, Professor of Drug Discovery and Development
Daniel L. Parsons, Professor of Drug Discovery and Development
William R. Ravis, Professor of Drug Discovery and Development
Feng Li, Assistant Professor of Drug Discovery and Development
Satyanarayana Pondugula, Associate Professor of Anatomy, Physiology and Pharmacology

Abstract

Skin cancer is by far the most common of all cancers. Among all types of skin cancer, malignant melanoma causes most of the deaths. Likewise, breast cancer is the most common cancer in women after skin cancer and the second leading cause of cancer death in women after lung cancer. Currently, conventional cancer treatments include chemotherapy, immunotherapy and targeted therapy. However, inefficient drug delivery and tumor penetration can reduce the response rate for these treatments. Stimuli-responsive lipid-based nanoparticles are a promising strategy for intratumor drug delivery. Enzymes, acidic tumor pH, mild hyperthermia and light can be utilized to trigger drug accumulation at the tumor site for deep penetration and effective tumor targeting. Different stimuli-responsive liposomes and their application in cancer treatment have been reviewed.

The ability of C6-ceramide to alter cancer cells membrane permeability was utilized to enhance the cellular uptake of daunorubicin toward B16-BL6 melanoma cells. Daunorubicin was encapsulated within liposomes where C6-ceramide acted as a component of the lipid bilayer. Liposomal formulation with ceramide exhibited a higher cytotoxic effect on B16-BL6 cell line than free daunorubicin, liposomes without ceramide and liposomes similar to DaunoXome®.

Cardiolipin increases membrane fluidity as its presence introduces a higher unsaturation degree to the membrane bilayer. pH-sensitive daunorubicin liposomal formulation enriched with cardiolipin was designed to target the tumor site and enhance the cellular uptake of daunorubicin toward B16-BL6 melanoma cells. Cardiolipin enriched liposomes exhibited a higher cytotoxic and cellular uptake effect on B16-BL6 cell line than liposomes similar to DaunoXome® and free daunorubicin.

Thermosensitive daunorubicin liposomal formulation enriched with cardiolipin was formulated to enhance the cellular uptake of daunorubicin, as cardiolipin triggers structural changes in the cell membrane making it more permeable, and to target the tumor site by release of their contents upon exposure to mild hyperthermia. Thermosensitive daunorubicin liposomal formulation with cardiolipin exhibited greater cellular uptake and higher cytotoxic effect on MDA-MB-231 breast cancer cells than the same formulation without cardiolipin, DaunoXome® , and free daunorubicin.

Ocular drug delivery to the posterior segment of the eye has been a major challenge due to a large number of ocular barriers. It is highly desirable to achieve effective drug concentration in the posterior eye in a noninvasive manner. The basics and recent developments of formulation in ocular drug delivery to the posterior segment have been reviewed.

Cyclosporine A loaded in polyvinyl pyrrolidone (PVP) based microneedles for delivery to the posterior segment of the eye were formulated. They promptly dissolved upon instillation in the eye and released their Cyclosporine A content.

Microneedles containing different amounts of PVP were evaluated for dissolution, failure force and drug content. Perfusion studies were performed using whole porcine eyes to determine Cyclosporine A distribution in the individual ocular tissues. Cyclosporine A concentration in different posterior segment tissues was significantly greater compared to the Cyclosporine A ophthalmic emulsion Restasis®.

Acknowledgments

There are numerous people that I must thank for their scientific assistance and career counseling. I would like to express my deepest gratitude to Dr. Jayachandra Babu Ramapuram for his support, guidance, and for giving me the opportunity to explore my scientific interests. I am indebted to Dr. Robert D. Arnold for the invaluable help and letting me use certain specialized equipment in his laboratory. I want to offer my special thanks to my dissertation committee members, Dr. Daniel Parsons and Dr. William R. Ravis, Dr. Feng Li, Dr. Satyanarayana Pondugula for participation in my dissertation committee and providing me with the guidance, advice and skills needed to pursue this degree. Also, I would like to thank Dr. Amol Suryawanshi for serving as an outside reader. I also would like to thank all the faculty members, staff and fellow students in the Department of Drug Discovery and Development for their support and help, especially Jennifer Johnston for her generous help whenever needed. I am thankful for everyone whom I have worked in the laboratory: Ahmed Alsaqr, Mohammed Fahad, Haley Shelley, Ishwor Poudel, Manjusha Annaji and Matthew Eggert. This journey would not have been possible without the support of my family and friends. To my family, thank you for encouraging me and inspiring me to follow my dreams. I am especially grateful to my mother who always gives me unconditional support and love that motivate me to complete my Ph.D. program smoothly and successfully. Finally, I would like to thank Saudi government and Taibah University for their financial support through my scholarship assistance.

Table of Content

List of Tables

List of Figures

List of Abbreviations

Akt	Protein kinase B (serine/threonine kinase)
CDs	Cyclodextrins
CHEMS	cholesteryl hemisuccinate
CL	Cardiolipin
C6-Ceramide	N-hexanoyl-D-erythro-sphingosine
DL	Drug loading
DNR	Daunorubicin
DOPE	1,2-dioleoyl-sn-glycero-3-phosphoethanolamine
DOPG	1,2-dioleoyl-sn-glycero-3-[phospho-rac-(1-glycerol)]
DPPC	1,2-dipalmitoyl-*sn*-glycero-3-phosphocholine
DSPC	1,2-distearoyl-*sn*-glycero-3-phosphocholine
EE	Encapsulation efficiency
EVA	Ethylene vinyl acetate
IC_{50}	The half maximal inhibitory concentration
MNs	Microneedles
MMPs	Matrix metalloproteinases
MSPC	1-myristoyl-2-stearoyl-*sn*-glycero-3-phosphocholine
NIPAAm	N-isopropylacrylamide
OA	Oleic acid
PAA	Poly (acrylic acid)
PBS	Phosphate-Buffered Saline

PCF	Polysulfone capillary fiber
PCL	Poly (ε-caprolactone)
PCNs	Polymer-caged nanobins
PEG	Polyethylene glycol
PGA	Polyglycolic acid
PI3K	Phosphoinositide 3-kinase
PLGA	Poly (d,l-lactic-co-glycolic acid)
POE	Polyoxyethylene
POPC	phosphoryl-oleoyl phosphatidylcholine
PVA	Polyvinyl alcohol
PVP	Polyvinylpyrrolidone
RES	Reticuloendothelial system
TSLs	Thermosensitive liposomes

Chapter 1. Introduction to Liposomes for Cancer Drug Delivery

1.1 Abstract

Liposomes have gained increasing attention as nanocarriers for several chemotherapeutic drugs. These vesicles of spherical shape that consist of one or more phospholipid bilayers are promising systems for drug delivery owing to their unique properties such as biocompatibility, bio-degradability, low toxicity, nonimmunogenicity and capability to incorporate both hydrophilic and hydrophobic compounds. The current field of liposomes focuses on the development of multifunctional liposomes that target cancer cells. Active targeting promotes tumor specificity, enhances therapeutic efficacy and reduces side effects of chemotherapeutic drugs. Stimuli-responsive liposomes are a promising approach to deliver and release chemotherapeutic drugs in the tumor site. The unique characteristics in the tumor microenvironment can act as an endogenous stimulus (pH, redox potential, or enzymatic activity) or external stimulus (heat or light) can be applied to trigger drug release from liposomes. This literature review focuses on new developments in stimuli-sensitive liposomal drug delivery systems.

1.2 Introduction

Advanced delivery systems with low costs, high efficiency, good targetability, and low toxicity for the delivery of chemotherapeutic drugs are highly required (Kumar et al., 2013). Nanocarriers generally possess a particle size below 200 nm, which can be associated with therapeutic and diagnostic agents for easy cellular penetration, site-specific delivery, detection and characterization of cancer in the tumor site (Wicki, Witzigmann, Balasubramanian, & Huwyler, 2015). The nanocarriers have many advantages such as (1) prolong circulation half-life, (2) targetability to cancer cells (3) reduce systemic side effects, (4) co-delivery of multiple drugs and (5) overcome drug resistance caused by drug efflux transporters (e.g. P-glycoprotein) (Kumari, Ghosh, & Biswas, 2016; Raj, Mongia, Kumar Sahu, & Ram, 2016). Currently, a wide variety of nanocarrier platforms are being developed for cancer treatment, including liposomes, nanotubes, micelles, gold nanoparticles, carbon nanotubes and solid lipid nanoparticles. Several chemotherapeutic agents with poor pharmacokinetics, solubility and biodistribution can be better delivered as nanocarrier systems (D. B. Chen, Yang, Lu, & Zhang, 2001).

Modification of certain nanocarrier properties, including their surface charge, shape and size, can allow better targeting of tumor tissue and superior release of drugs. Positively charged nanoparticles effectively target tumor vessels while neutral ones diffuse faster to the tumor tissue (Stylianopoulos et al., 2010). The shape of the nanocarriers may influence fluid dynamics and thus impact cellular uptake. Small nanoparticles can accumulate more easily in the

leaky blood vessels of tumors compared to large nanoparticles (Bregoli et al., 2016).

Effective delivery of chemotherapeutic drugs encapsulated within a nanocarrier presents a significant challenge due to the complexity of solid tumors (Takechi-Haraya, Goda, & Sakai-Kato, 2017). The nanocarriers can be made multifunctional 1) by adding a ligand such as polyethylene glycol prolonging the circulation time 2) by including a protein such as transferrin for promoting specific types of endocytosis 3) by including a biological lipid such as ceramide for enhancing cellular uptake into the tumor tissue (L. Chen, Alrbyawi, Poudel, Arnold, & Babu, 2019; Zhai et al., 2010). Several stimuli strategies, such as temperature, pH and redox, can be used in nanocarriers for enhanced delivery of chemotherapeutic agents to a specific location. The stimuli triggers instability in the liposomes at the target site, leading to the release of entrapped drug molecules (Movahedi, Hu, Becker, & Xu, 2015).

1.3 Cancer

Cancer is a life-threatening disease that leads to irregular and uncontrollable growth of malignant cells. Malignant cells can invade healthy tissues and organs. Cancer cells are able to spread to different organs through blood vessels and the lymphatic system. Cancer is responsible for over 8 million deaths worldwide and it is the second leading cause of death following heart disease (Zaorsky et al., 2017). Some of the well-known causes of cancer are smoking, radiation, and obesity (Hooper et al., 2018). The tumor microenvironment is characterized by hypoxia, acidosis, high interstitial fluid

pressure, and increased extracellular matrix rigidity (Riemann et al., 2016; Yang, 2017).

Although there are several chemotherapeutic drugs that can be used to treat cancer, they lack specificity and may damage both tumor and normal tissues. In addition, there are several biological barriers to effective drug delivery in cancer such as poor blood flow, poor vascularization, paracellular and transcellular transport across the endothelium and high interstitial fluid pressures (S. M. Kim, Faix, & Schnitzer, 2017). Since poor drug delivery and selectively can limit and even prevent therapeutic efficacy of chemotherapeutic drugs in the treatment of solid tumors, development of nanocarriers are urgently needed to overcome these significant barriers. Anticancer treatments typically depend on the ability of the drugs to reach their designated cellular and subcellular intended site of action (tumor), while minimizing collateral toxicity to healthy cells. Fabrication of nanotechnology-based drug delivery systems that can alter the biodistribution, tissue uptake, and pharmacokinetics of chemotherapeutic drugs and deliver them to tumors is increasingly common in cancer treatment. Over the past two decades, several nanocarriers, such as liposomes, nanoparticles, dendrimers, and carbon nanotubes, have been developed for cancer therapy. Furthermore, various strategies have been adopted for targeting nanocarriers to the tumor sites and enhancing their cellular uptake, including surface functionalization to identify various extracellularly overexpressed biomarkers and local stimuli-triggered release of encapsulated molecules (Huwyler, Drewe, & Krahenbuhl, 2008).

1.4 Liposomes as Nanocarriers

Liposomes are the most commonly investigated nanocarriers for drug delivery applications. The nanometer size, site-specific drug delivery, hydrophobic and hydrophilic characters make liposomes an excellent vehicle for chemotherapeutic drug delivery. Owing to their amphiphilic nature, liposomes can entrap and stabilize hydrophilic molecules in the aqueous core and lipophilic molecules in their lipid bilayers (Figure.1.1). In addition, they exhibit a high level of biocompatibility because they consist of phospholipid bilayers that resemble human membrane (Monteiro, Martins, Reis, & Neves, 2014). Liposomes are small artificial vesicles of spherical structure that can be made from cholesterol and natural non-toxic phospholipids. They self-assemble when an amphiphilic lipid is hydrated with an aqueous liquid. They can be categorized according to their size (small, intermediate, or large), layers (unilamellar or multilamellar, and preparation technique (reverse-phase evaporation vesicles or vesicle extruded method).

Both the size and the number of layers (lamellae) in the liposomal formulation are considered critical in determining the half-life and quantity of drugs encapsulated (Ong, Ming, Lee, & Yuen, 2016). Furthermore, the selection of bilayer components determines the rigidity, fluidity and charge of the liposomal bilayer. Unsaturated phosphatidylcholine lipids from natural sources (e.g. soybean phosphatidylcholine) form a more permeable liposomal bilayer, whereas saturated phospholipids with long acyl chains (e.g. dipalmitoylphos phatidylcholine) form a rigid bilayer (Allen, 1997).

Prolonged systemic circulation permits more extensive interaction of liposomes with their target tissue leading to enhanced permeability and retention effect (EPR). Sterically stabilized liposomes were introduced to increase stability and extend circulation periods. Polyethylene glycol (PEG), a hydrophilic polymer, is optimal for obtaining sterically stabilized liposomes. PEG molecules on the surface of liposomes form a protective layer that prevents their fusion, self-aggregation and interaction with blood components and hides them from uptake by the reticuloendothelial system (RES) (Allen, Hansen, Martin, Redemann, & Yau-Young, 1991). The RES is a part of the immune system, composed of circulating macrophages and monocytes, Kupffer cells and spleen and other lymphatic vessels, and its function is to remove foreign materials. Opsonin proteins play an essential role as they reduce the charge repulsion between phagocytic cells and foreign material, such as bacteria viruses and nanoparticles.

PEG is widely used to increase the blood circulation time of liposomes because of their lack of toxicity, low immunogenicity, biocompatibility, solubility in organic solvents, versatile molecular weights and simplicity to conjugate with lipids (Nag & Awasthi, 2013). Several mechanisms have been proposed by which PEG prevents opsonization including increasing surface hydrophilicity (as hydrophobic particles are more vulnerable to the RES), enhancing the repulsive interaction between liposomes and blood components and shielding of liposomes surface charge (van Vlerken, Vyas, & Amiji, 2007). Liposomal drug formulations with PEG can impact the pharmacokinetics and tissue distribution of the incorporated anticancer compound. Doxil® (PEGylated liposomal vehicle for

doxorubicin) enhances doxorubicin bioavailability approximately 90-fold compared to free drug and increases circulation half-life to 36 h (Gabizon, Shmeeda, & Barenholz, 2003; Laginha, Verwoert, Charrois, & Allen, 2005). In addition to increasing the half-life of the drug, liposomes enhance the solubility of drugs, provide targeted drug delivery, decrease the toxic effect of drugs, protect drugs against their environment and overcome multidrug resistance (Deshpande, Biswas, & Torchilin, 2013; Matsuo et al., 2001).

The adequacy of liposomes as a carrier system for drugs depends on several factors such as the bilayer structure, the nature of their lipid components, surface charge and the size of the particles. As a result, liposomes are distinguished as an ideal drug-carrier because their structure can be easily modulated to accommodate a broad spectrum of therapeutic agents. Since phospholipids are the main building blocks of liposomes, they have a great influence on liposome composition and function as a drug carrier. Typically, they are amphiphilic molecules that consist of a polar head (hydrophilic) and non-polar fatty acid backbone (hydrophobic). Because of their amphiphilic characteristic they can form lipid bilayers. Currently, there are two types of lipids are used typically in the preparation of liposomes 1) naturally occurring from natural sources like soybean, (e.g. phosphatidylcholine) 2) synthetic amphiphilic lipids, consisting of a phosphorus polar head and glycerol backbone incorporated with sterols, (e.g. dipalmitoyl phosphatidylcholine). Depending on the polar head charge, liposomes can be zwitterionic, positively or negatively charged. Lipids used in liposomal formulations are phosphatidylcholine (PC), 1,2-distearoyl-sn-

glycero-3-phosphoethanolamine-N-[methoxy(polyethylene glycol)-2000] (MPEG-DSPE), phosphatidylserine (PS), phosphatidylethanolamine (PE), dioleoyl phosphatidylethanolamine (DOPE), and 1,2-dioleoyl-3-trimethylammoniopropane (DOTAP). Lack of surface charge will increase liposome aggregation, hence decreasing their physical stability. In addition, neutral liposomes release a significant amount of drugs in the extracellular space since they do not interact significantly with cells (Zhao, Zhuang, & Qi, 2011). Compared with neutral liposomes, charged liposomes have several advantages. The existence of a surface charge on the liposomes induces electrostatic repulsion and prevents their aggregation and flocculation. Also, the presence of a charge on the surface of liposomes might promote their interaction with cells. The incorporation of cholesterol to the liposomal bilayer is crucial for structural stability. Cholesterol reduces liposomes permeability and increases their *in vivo* and *in vitro* stability as it increases the packing between the phospholipid molecules and prevents their transfer to high-density and low-density lipoprotein. Moreover, cholesterol influences the size of liposomes (increasing cholesterol concentration will proportionally increase liposomes size) and fluidity, and consequently modulates the release profile of encapsulated compounds. In the blood circulation, negatively charged liposomes are less stable and more toxic compared to neutral and positive liposomes. Anionic liposomes promptly interact with the biological system, including opsonin and other circulating proteins, which leads to rapid uptake by the RES and toxic effects such as pseudoallergy (Cullis, Chonn, & Semple, 1998).

The encapsulation efficiency of a compound and its localization in the liposomal membrane depends on its polarity and partition coefficient. Since hydrophobic molecules tend to localize in the acyl hydrocarbon chain of the liposome membrane, their encapsulation efficiency is greatly influenced by the properties of the chains, such as packing density, chain length and the drug-to-lipid ratio. Hydrophilic molecules reside in the aqueous core of liposomes; as a result, their encapsulation efficiency does not exhibit a strong dependence on the drug-to-lipid ratio (Mohan, Narayanan, Sethuraman, & Krishnan, 2014). The high encapsulation efficiency of drugs in liposomes does not always equate to improved therapeutic efficacy because drugs only exert their therapeutic effect when they are released at an appropriate rate from liposomes. Numerous anticancer drugs have intermediate solubility and when they are encapsulated in liposomes they exhibit a rapid release rate since they readily partition between the liposome bilayer and the interior aqueous phase. Therefore, the liposomes compositions must be optimized to enhance the release rate of encapsulated drugs. The experimental approaches usually include either altering the lipid bilayer or entrapping drugs that have physicochemical properties suitable for the purpose. For example, adjustment of the interior pH of the liposomes or the formation of complexes within the liposomes core can enhance the retention of weak bases, such as doxorubicin and daunorubicin, to a great extent and exhibit a desirable release profile (Mayer, Bally, & Cullis, 1986). Drugs that are not weak bases, such as docetaxel, can be converted to weak-base prodrugs, which will allow more encapsulation within liposomes (Zhigaltsev et al., 2010).

In conclusion, liposomes can alter the biopharmaceutical profile of the encapsulated molecules leading to reduced toxicity, modified pharmacokinetic behavior, and an enhanced therapeutic index. Liposomes have the ability to entrap, protect, and transfer greater amounts of drugs while being well tolerated in patients in comparison to the free form of the drug.

1.5 Targeting

Liposomes structure may be modified to increase the accumulation of drugs at the target tissue, enhance cellular internalization and organelle-specific delivery (Figure. 1.2). Active targeting methods utilize conjugation of targeting ligands to the surface of liposomes. These ligands have a high affinity to receptors and other cancer-specific biomarkers that are overexpressed on the surface of tumor cells. The primary purpose of conjugation of these ligands is to minimize non-specific uptake of liposomes by other tissue. Examples of ligands may include transferrin, enzymes, folic acid and macromolecules like proteins and carbohydrates (Deshpande et al., 2013). It is essential when selecting targeting ligands to consider negative impacts. The targeting ligands themselves could lead to immune response or might make liposomes too dense and recognized by the RES. Ligands for active targeting can be conjugated directly to the lipids or linked to the distal end of PEG chains. The targeting moiety must be attached in sufficient quantities to have an optimum affinity for receptors located on the cell surface. Multifunctional liposomes have been formulated to increase targetability, enhance therapeutic efficacy and overcome difficulties of liposomal formulations with a single function such as biological barriers. Liposomes having

two ligands on their surface or carrying two ligands and two anticancer agents (Y. Zhang et al., 2017) have been reported.

Targeting the tumor vasculature and microenvironment has several advantages compared with receptors targeting. First, targeting the tumor vasculature minimizes tumor metastasis. Second, the tumor vasculature is not specific for any cancer (Byrne, Betancourt, & Brannon-Peppas, 2008). Solid tumors grow new blood vessels that supply them with nutrients and oxygen. However, these newly formed blood vessels possess unique characteristics not generally observed in normal tissues. Specific unique characteristics of tumors include impaired lymphatic drainage, over-expressing of some receptors, excessive leakiness and permeability and extensive angiogenesis (Linton, Sherwood, Drews, & Kester, 2016). The examples of such targets include Vascular Cell-Adhesion Molecules (VCAMs), Matrix-Metalloproteases (MMPs), Integrins and Cluster-of-Differentiation 44 (CD44).

A new targeting method has been developed that uses an external trigger for improved efficiency of liposomal drug release. The idea of stimuli sensitivity is based on specific characteristics of the tumor microenvironment, such as a lower pH, higher temperature and excessive expression of some proteolytic enzymes (V. P. Torchilin, 2007). The stimuli-sensitive liposomes maintain their structure during circulation. However, they are formulated to undergo rapid changes when exposed to external stimuli or a particular tumor microenvironment, hence releasing the entrapped agent rapidly. In this chapter, the stimuli-responsive and triggered release liposomes will be discussed in detail.

1.6 Stimuli-Responsive and Triggered Release Liposomes

Recently, research has been significantly advanced in terms of liposomal drug delivery systems with an improved drug targeting potential in cancer treatment. An area has focused mainly on developing approaches for actively targeting and releasing drugs to the tumor site. Stimuli-responsive and triggered release liposomes release their therapeutic payloads utilizing pathological differences in the tumor's microenvironment or in response to an external stimulus. Stimuli can be either internal, such as low pH, high temperature and enzymes at the tumor site, or can be externally applied to trigger the drug release, such as ultrasound and light (Danhier, Feron, & Preat, 2010). The stability of PEGylated liposomes may not always be favorable for drug delivery because they might not release the entrapped compounds in tumor areas or cell compartments. Conjugation of PEG to the liposome surface decreases targeted liposomal accumulation and drug release at the tumor site (V. P. Torchilin et al., 1992). Furthermore, PEG decreases the interaction of the ligand-targeted liposomes with their ligand by steric hindrance (Sawant & Torchilin, 2012). Lipids in stimuli-sensitive liposomes typically include a triggerable component that plays an important role in the stability and permeability of the liposomal lipid bilayer.

1.6.1 pH-Responsive Liposomes

pH-sensitive liposomes have been developed to increase the ability of liposomes to mediate intracellular delivery of different biologically active compounds. These liposomes are formulated to be stable at physiological pH (pH 7.4) but undergo destabilization and fusogenic properties under acidic

conditions, thus leading to the release of their entrapped compounds. Tumor tissue exhibits an acidic environment as compared with healthy tissues. Extracellular pH values at tumor sites range from 6.8 to 7.0, but might reach as low as 5.7 (Felber, Dufresne, & Leroux, 2012). Extracellular acidification is primarily due to lactate secretion from anaerobic glycolysis (known as the Warburg effect). Due to the high rate of glycolysis, excess protons and carbon dioxide production, insufficient tumor oxygen supply and lack of functional lymphatic drainage systems, cancer cells produce large amounts of lactate, which would contribute to enhanced acidification of extracellular environment (J. W. Kim & Dang, 2006). pH-sensitive liposomes have been designed to undergo destabilization when submitted to acidic environments within the endosomes (pH 5.5), as occurs in the tumor extracellular matrix (Ferreira Ddos, Lopes, Franco, & Oliveira, 2013). Several lipids, organic functional groups and inorganic compounds, which exhibit considerably different physicochemical properties in response to pH change, have been used for the fabrication of pH-responsive liposomes for cancer treatment. Reduced pH is a general feature for most types of solid tumors (Khawar, Kim, & Kuh, 2015).

Tumor specific receptor targeting liposomes has shown limited success in their clinical trails due to significant patient-to-patient variations in receptor expressions and increased complexity and cost in developing such liposomes formulations (Du, Lane, & Nie, 2015). To achieve the pH-sensitive release of liposome content, liposomes are formulated with pH-sensitive components such

as pH-sensitive lipids, pH-responsive insertion peptides, pH-sensitive linkages (chemical bonds) and pH-sensitive moieties as listed in Table 1.1.

1.6.1.1 pH-Sensitive Liposomes Components and Their Application for The Delivery of Anti-Cancer Drugs

Different classes of pH-sensitive liposomes have been proposed. One of the most common established classes involves PE lipid or its derivatives, like DOPE, with compounds containing an acidic group (e.g. CHEMS) that acts as a stabilizer at neutral pH. PE has a minimally hydrated and small head group as compared to the hydrocarbon chains and exhibits a cone shape despite a lamellar phase. The cone shape tends to form an inverted hexagonal (H_{II}) phase in acidic conditions above the phase transition temperature as a result of the interaction of amine and phosphate groups of the polar head group (Seddon, Cevc, & Marsh, 1983). The inverted hexagonal (H_{II}) phase obstructs the formation of a lamellar phase (liposomal bilayers). However, non-bilayer lipids, such as PE, can be stabilized to form a bilayer structure by incorporation of amphiphilic molecules (e.g. CHEMS) containing a protonatable acidic group between PE molecules. Amphiphilic molecules between PE molecules favor electrostatic repulsion and facilitate the formation of liposomal bilayer structures, which leads to liposome formation at physiological pH and temperature (Duzgunes, Straubinger, Baldwin, Friend, & Papahadjopoulos, 1985).

Although stable liposomes are created at physiological pH, acidic conditions prompt protonation of the carboxylic groups of the amphiphilic molecules decreasing their stabilizing effect because PE molecules will revert into their original inverted hexagonal phase, leading to destabilization of

liposomes. DOPE also has a strong tendency to form an inverted hexagonal phase in acidic environment. Similar to PE, DOPE converted to a hexagonal inverted phase, leading to the formation of non-lamellar structures at acidic pH (Figure 1.3).

Liposomes composed of DOPE, CHEMS and DSPE-PEG in a 5.7:3.8:0.5 molar ratio were formulated to enhance the ability to release doxorubicin in an acidic environment for the treatment of bone metastases (Ferreira Ddos et al., 2016). pH-sensitive liposomes possessed remarkably stronger cytotoxicity against female nude BALB/c mice bearing MDA-MB-231 tumors due to the higher uptake of doxorubicin in the tumor area. Furthermore, lower uptake of doxorubicin in the heart was noticed suggesting a minimal cardiotoxicity. The more rapid release of doxorubicin from liposomes at pH 5 compared to pH 7.4 was observed and this could be explained by the destabilization of the lipid bilayer under an acidic environment.

The pH sensitivity was due to the presence of DOPE and CHEMS and increased circulation time was due to PEG. pH-sensitivity composed of DOPE/HSPC/CHEMS/CHOL/mPEG(2000)-DSPE at a molar ratio of 4:2:2:2:0.3 was designed to increase intracellular doxorubicin release rates within an acidic environment. (Ishida, Okada, Kobayashi, & Kiwada, 2006). A rapid doxorubicin release was observed as a result of membrane disruption when liposomes were incubated in acidic buffer. However, no doxorubicin leakage was noticed in HEPES buffered saline (pH 7.4). Folate receptor-targeted pH-sensitive liposomes composed of HSPC/CHOL/mPEG2000-DSPE/folate-PEG3350-CHEMS, at a

molar ratio of 55:40:4:1, exhibited efficient and stable encapsulation of imatinib with increased drug release at lower pH value (5.5). Folate-PEG3350-CHEMS decreases the rigidity and stability of liposomes bilayer at an acidic pH (Ye et al., 2014). Folate receptor-targeted pH-sensitive liposomes demonstrated higher internalization efficiency and cytotoxicity as folate PEG3350-CHEMS could effectively target the HeLa cells through the folate receptor. In addition to active targeting, pH sensitivity liposomes release the drug in endosomes after uptake by tumor cells or in the extracellular acidic environment.

Liposomal formulations conjugated with hydrazone and oxime have been used to enhance drug delivery into tumor sites. Such conjugates are labile to hydrolysis in acidic conditions due to the hydrolysis of carbon-nitrogen double bonds (Kalia & Raines, 2008) (Figure 1.4). However, hydrazone and oxime based bonds are stable at neutral pH (in the blood). pH-sensitive liposomes containing mPEG2000-Hz-CHEMS-modified paclitaxel have been investigated (D. Chen et al., 2011). The modified liposomes via cleavable pH-responsive hydrazone linkages efficiently removed by the lower pH (5.5) and esterase in the serum (half-life 6.7 hours). Due to the pH-sensitive hydrazone bond, the rate of PEG cleavage from PEG-Hz-CHEMS was higher than that from the same formulation without hydrazine (PEG-CHEMS). Regarding biodistribution of the modified liposomes, repeated injection of mPEG Hz-CHEMS liposomes caused no increase in liver and spleen accumulation compared with mPEG-PE liposomes.

Doxorubicin pH-sensitive liposomes targeted to the CD19 epitope on B-lymphoma cells and conjugated with thiol cleavable PEG-derivative, mPEG-S-SDSPE, exhibited enhanced doxorubicin delivery into the nuclei of the target cells with higher cytotoxicity *in vitro* and *in vivo* (Ishida, Kirchmeier, Moase, Zalipsky, & Allen, 2001). These pH-sensitive liposomes were composed of DOPE/CHEMS/ mPEG-S-S-DSPE/Mal-PEG-DSPE (6:4:0.24:0.06) and loaded with doxorubicin. Liposomes were stable in the culture media; however, doxorubicin was rapidly released in human plasma as a result of rapid cleavage of the disulfide linkage by blood components, such as cysteine. The liposomes conjugated with mPEG-S-SDSPE had a release half-life of about 8 h at pH 5.5. pH-sensitive formulation containing mPEGS-S-DSPE displayed more rapid nuclear accumulations of doxorubicin and increased cytotoxicity compared to free drug, on pH-sensitive liposomes and non-targeted liposomes. When SCID mice treated with 3 mg/kg free doxorubicin or liposome-encapsulated doxorubicin, doxorubicin/DOPE/CHEMS/mPEG SS-DSPE/Mal-PEG-DSPE [anti-CD19] formulation had significantly higher “increased life spans” (%ILS) than did the groups treated with non-targeted formulations.

A liposomal formulation for finely tuned pH-induced PEG release was designed using phenyl substituted-vinyl-ether-(PIVE)-PEG-DOG conjugates and DOPE (H. K. Kim, Van den Bossche, Hyun, & Thompson, 2012) . They showed pH-induced dePEGylation and content release at acidic pH (pH 3.5 or 4.5); however, they were stable at physiological pH. *In vitro* transfection studies on HEK 293 and COS-7 cells showed that mPEG-PIVE-DOG:DOPE had a higher

transfection efficiency compared to that of polyethylenimine (PEI) and non-acid-cleavable lipid (mPEG-DOPE) because pDNA was released rapidly at acidic condition inside the cells. Electron donating or withdrawing properties of the α-phenyl vinyl ether substituent influenced the hydrolysis rate of PIVE-PEG lipopolymers under acidic conditions.

In recent years, pH-responsive membrane-destabilizing polymers have been reported. Examples of polymers for generation of pH-responsive liposomes include poly(methacrylic acid), N-isopropylacrylamide, poly(diethylaminoethyl methacrylate), poly(acrylamide) and poly(acrylic acid) (Figure 1.5). At acidic pH, the destabilizing polymers display a transition from a hydrophilic state to a lipophilic state leading to enhance interactions with cell membranes. At low pH values, the pH-sensitive copolymers with carboxylic groups could be protonated to become hydrophobic (Chiang, Lyu, Wen, & Lo, 2018).

Highly stable polymer-caged nanobins (PCNs) around liposomes were designed to trigger the release of doxorubicin under acidic conditions. PCNs were prepared by insertion of cholesterol-modified poly (acrylic acid) (Chol-PAA) into the liposome (S. M. Lee, Chen, O'Halloran, & Nguyen, 2009). Insertion of Chol-PAA created PCNs around liposome templates whose doxorubicin payloads can be triggered to release under acidic conditions due to conformational collapse upon protonation of the free acrylate groups. Besides, folic acid was conjugated to PCNs in order to enhance tumor targeting. pH-sensitive polymer cages efficiently delivered doxorubicin into the cytoplasm through destabilizing of the liposomal membrane under acidic condition.

Furthermore, when cytotoxicities of the PCNs- doxorubicin formulations with and without folic acid were evaluated in KB human epithelial nasopharyngeal carcinoma cells, both formulations still showed better efficacy than doxorubicin-loaded bare liposomes, possibly as a result of acid triggered drug-releasing character of PCNs (S. M. Lee et al., 2009).

Hyaluronic acid (HA) based pH-sensitive polymer-modified liposomes with different contents of 3-methyl glutarylated (MGlu) units and 2-carboxycyclohexane-1-carboxylated (CHex) units were designed as a new class of pH-responsive polymers with a transition pH of about 5.4–6.7 (Miyazaki, Yuba, Hayashi, Harada, & Kono, 2018). Doxorubicin was encapsulated using active-loading method. HeLa cells were incubated with doxorubicin-loaded liposomes and intracellular doxorubicin distribution was investigated. HA-based pH-sensitive polymer-modified liposomes delivered doxorubicin into the nucleus due to pH-responsive membrane disruptive ability and high cellular association of HA.

The formation of pH-sensitive liposomes using materials such as oleic acid (OA) is a common technique for conferring pH sensitivity to a liposome formulation. OA is a negatively charged moiety that destabilizes the liposome structure through phase conversion at acidic condition (Fleige, Quadir, & Haag, 2012). pH-sensitive docetaxel (DTX)-loaded liposomes, consisting of PE/CHOL/OA/DTX (3:2:3:1, w/w), achieved 1.3-fold higher cumulative DTX release rate at pH 5.0 than at pH 7.4 after 72 h (H. Zhang, Li, Lu, Mou, & Lin, 2012). Pharmacokinetic analysis of DTX-liposomes gave a higher DTX concentration in plasma at each time point than free DTX indicating the stability

of liposomes in circulation. Negatively charged lipids such as OA decrease PE intermolecular interactions as they provide electrostatic repulsions, which prevent interbilayer interactions under physiological conditions. In acidic condition, the protonation of OA neutralizes their negative charges, and the liposomes become destabilized as the PE reverts to hexagonal II phase.

pH-responsive liposomes were designed by encapsulating bicarbonate ion (NH4HCO3) to produce CO2 effervescence upon acidification that will trigger drug release by creating pores in liposomes membrane (Liu, Ma, Wei, & Liang, 2012). pH-sensitive liposomes modified with sulfadimethoxine-based copolymer that initiates phase transitions upon ionization (Bersani, Vila-Caballer, Brazzale, Barattin, & Salmaso, 2014), and pH-sensitive ion channels liposomes that makes pores upon protonation (Pacheco-Torres et al., 2015) were also prepared.

1.6.2 Thermosensitive Liposomes

Inclusion of lipids with transition temperatures closer to physiological body temperature (40–45^{o}C) allows induction of drug release after external localized heating (Drummond, Noble, Hayes, Park, & Kirpotin, 2008). The first class developed are traditional thermosensitive liposomes. Liposomes lipid membranes have a specific phase transition temperature at which they undergo phase transition from a gel to a liquid (Li et al., 2014). During the liquid phase “melting transition”, liposomes undergo significant morphology changes, including formation of open liposomes and pore-like defects because the mobility of the lipid head groups rises. When the heat approaches the transition temperature of the lipid, the C-C single bonds in the hydrocarbon chains switch

from a *trans* to a *gauche* configuration (Casado, Sagrista, & Mora, 2014). As a result, encapsulated drugs are able to leak out as the membrane becomes fluidized and permeable.

Synergistic interaction has been validated in preclinical research since mild hyperthermia has been used as an adjunctive treatment with chemotherapy (Wust et al., 2002). Compared to chemotherapy alone, mild hyperthermia improved patient response (Nishimura et al., 1990). Use of thermosensitive liposomes might help targeted drug delivery to areas where mild hyperthermia, such as microwaves, radio frequencies and high-intensity ultrasound, are applied. Combination of thermosensitive liposomes with mild hyperthermia can improve therapeutic effectiveness by (i) increasing accumulation of liposomes in the tumors due to increase in the tumor vascular permeability (Huang et al., 1994), and (ii) promoting drug release from the thermosensitive liposomes into the tumor vasculature and interstitium. Additionally, mild hyperthermia might increase therapeutic effectiveness by enhancing blood flow at the exposed area (Kong, Braun, & Dewhirst, 2000). Tumor cells are more susceptible than healthy cells to thermal effect because tumor microenvironment stressed by low oxygen levels and pH may be less able to tolerate the added stress of heat.

The temperature of tumors increases more than surrounding normal tissues when applying mild hyperthermia because they have a disorganized and compact vascular structure making heat dissipation more difficult. Table 1.2 shows some lipids and polymers used to prepare thermosensitive liposomes (Zhu & Torchilin, 2013).

1.6.2.1 Thermosensitive Liposomes Components and Their Application for The Delivery of Anti-Cancer Drugs

DPPC based liposomes have been extensively investigated as a stimulus responsive drug delivery system. Such system has the advantage of thermosensitivity of DPPC (Tm = 41.4°C) alone or with DSPC (42.5 - 44.5°C). Liposomes formulation composed of DPPC with other lipids, predominantly DSPC, showed enhanced drug release when with mild hyperthermia. Lu and his coworkers examined the rapid release of thermosensitive liposomes at different DPPC/DSPC ratios during the phase transition (Lu & Ten Hagen, 2017). They proposed that inhomogeneous crystal grains consisting of membranes formed in DPPC-DSPC bi-component. Disordered arrangement of lipid molecules occurred because of different lattice orientation and it could enable rapid release of encapsulated compounds from liposomes (Figure 1.6). Thermosensitive liposomes composed of DPPC:DSPC (7:3 molar ratio) and encapsulated with methotrexate was one of the earliest thermosensitive liposomes developed to treat cancer (Weinstein, Magin, Yatvin, & Zaharko, 1979). When mice with a lung tumor were treated with the formulation, more than 4-fold higher methotrexate levels were reached with mild hyperthermia ($42^{o}C$) applied to the tumor site. However, the main limitation of this formulation was the rapid elimination of the liposomes (within 1 hour) from the blood after administration.

The creation of PEGylated liposomes allowed the development of long-circulating thermosensitive liposomes. Enhanced delivery of doxorubicin to colon carcinoma tumor subjected to local hyperthermia was achieved by using long-circulating, thermosensitive liposomes composed of DPPC and DSPC (9:1, m/m)

and 3 mol% PEG (Unezaki et al., 1994). Inclusion of PEG resulted in decreased RES uptake, consequently prolongation of circulation time and increased doxorubicin blood levels. Mice treated with thermosensitive liposomes (5 mg doxorubicin/kg) in combination with local hyperthermia (42°C for 5 min) delayed tumor growth and increased survival time compared to both free doxorubicin and thermosensitive liposomes without local hyperthermia.

Incorporating lysolipids, such as MPPC and MSCP, into PEGylated DPPC liposomes promoted more rapid drug release compared to traditional DPPC based thermosensitive liposomes. Lysolipid-containing thermosensitive liposomes composed of DPPC: MPPC: DSPE-PEG-2000 in the molar ratio of 90:10:4 reduced the phase transition temperature and enhanced doxorubicin release rate under mild hyperthermia compared with DPPC liposome without MPPC (Needham, Anyarambhatla, Kong, & Dewhirst, 2000). The lysolipid-containing liposomes released approximately 45% of the doxorubicin contents in 20 s when exposed to 42°C, compared with 20% over 1 h for DPPC liposomes. For the DPPC liposomes, the triggered release temperature occurred between 41°C to 43°C. On the other hand, MPPC-containing liposomes triggered release temperature was lowered by 2°C, to between 39°C and 40°C. *In vivo* study in a human squamous cell carcinoma tumor xenograft model (FaDu) showed that MPPC-containing thermosensitive liposomes were more effective than free drug, DPPC based liposomes, and non-thermosensitive liposomes in reducing tumor growth. Doxorubicin extracted from tumors was significantly higher in animals administered both lysolipid-containing thermosensitive liposomes and mild

hyperthermia. Lysolipids tend to form highly curved micelles that conserve defects formed in the membrane bilayer when phase transition temperature is approached.

A novel formulation of thermosensitive liposomes based on phosphatidyloligoglycerol (DPPGOG) prolonged doxorubicin half-life *in vivo* without the use of PEG and enhanced the drug release rate (Lindner et al., 2004). Doxorubicin was efficiently encapsulated in DPPC/DSPC/DPPGOG 50:20:30 (m/m) and almost completely released within 120 s at 42°C. In addition, the formulation showed improved stability at 37°C in serum compared to the PEGylated DPPC/P-lyso-PC/DSPE-PEG2000 90:10:4 (m/m) thermosensitive liposomes. DPPGOG is similar to the natural lipid DPPG. DPPGOG contains an additional glycerol molecule attached to the glycerol head group via an ether bond. Incorporation of hydrogenated soy phosphatidylcholine (HSPC) lipid increases the transition temperature because it altered the thermotropic phase behavior of liposomes membrane and changes its rigidity. Thermosensitive liposomes formulated with HSPC and loaded with cisplatin improved *in vivo* stability of liposomes in blood. DPPC/HSPC /MSPC /PEG2000-DSPE (60:30:10:4) liposomes greatly decreased cisplatin leakage at 37°C. However, upon exposure to mild hyperthermia the formulation showed notable thermal-sensitivity *in vitro* and improved the survival of animals *in vivo* (Alavizadeh et al., 2017).

Another method for sensitizing non-thermosensitive liposomes or existing heat-responsive liposomes to temperature is by incorporating synthetic polymers that cause membrane disruption in response to mild hyperthermia. Temperature-sensitive polymers are soluble in water and tend to take a coil structure below their lower critical solution temperature since hydrogen bonding between the polymer chains and water molecules is sufficient to solubilize and maintain them in a hydrated coil state. However, when the temperature approaches their lower critical solution temperature, hydrogen bonding is no longer sufficient to solubilize the polymers. As a result, polymers become water-insoluble and tend to take a dehydrated (hydrophobic) globule state that destabilizes liposomes and allows release of the payloads (Kono, 2001) (Figure 1.7).

Poly (N-isopropylacrylamide) (NIPAAm) is one of the most studied temperature-sensitive polymers. However, its lower critical solution temperature 32°C makes employing this polymer alone not clinically practical. Designing NIPAAm polymer with a lower critical solution temperature in the range of physiological temperature is possible if the polymer is co-polymerized with monomers, e.g. hydrophilic acrylamide (AAm). Copolymerization of NIPAAm with various molar concentrations of AAm increases NIPAAm lower critical solution temperature in a proportional manner to AAm concentrations (Hayashi, Kono, & Takagishi, 1999). For instance, Copolymers of 17% AAm will increase the lower critical solution temperature from 32°C to 47°C, whereas 25% AAm demonstrated lower critical solution temperature of 40°C. Han *et al*. examined the use of NIPAAm-AAM (83:17 mol:mol with lower critical solution temperature

of 40°C) on the release profile of doxorubicin (Han, Shin, & Choi, 2006). A liposomal formulation composed of DPPC:HSPC:CHOL:DSPE-PEG-2000 (100:50:30:6) and conjugated with NIPAAm-AAM (83:17) at a final concentration of 10 mg/ml released about 62% of encapsulated doxorubicin at 40°C. Unmodified PEGylated DPPC thermosensitive liposomes released approximately 40% of encapsulated doxorubicin at 40°C. The results demonstrated the synergistic effects of combining the polymer to liposomes. The major disadvantage of NIPAAm polymer is the risk for side effects associated with polymer accumulation in the body since it is not biodegradable. Poly (N-(2-hydroxypropyl) methacrylamide) polymers (p(HPMA)) have been widely studied as carriers for anticancer drugs since they are biodegradable and their thermosensitivity can be adjusted (Kopecek, Kopeckova, Minko, & Lu, 2000). Polymer-coated liposomal formulation composed of DPPC/cholesterol (100:42.5) and coated with 5 mol% p(HPMA) mono/dilactate (monolactate/dilactate ratio was 49/51) triggered calcein release at a higher rate compared to the same formulation not coated with polymer (Paasonen et al., 2007). Liposome formulation coated with 5 mol% polymer released more than 50% of the encapsulated calcein at 43-45°C while uncoated formulation releases about 15-20%.

Similar to NIPAAm copolymers, poly (N-vinylethers) polymers derive their thermosensitive features from the dehydration of polymer chains near their lower critical solution temperature. Besides, they must be synthesized with various monomers in order to produce a polymer with lower critical solution temperature

within the range of physiological temperature (Kono et al., 2005). Poly [2-(2-ethoxy) ethoxyethyl vinyl ether] (EOEOVE), which has a lower critical solution temperature around 40°C, copolymer-modified PEGyated liposomes encapsulated with doxorubicin was fabricated by Kono *et al* to enhance antitumor activity against mouse colon carcinoma #26. The liposomal formulation consisting of EYPC/Chol/PEG-PE (50:45:4) and modified with EOEOVE 2 mol% significantly enhanced the release of doxorubicin above 40°C and caused complete release within 1 min at 45°C (Kono et al., 2010). *In vivo* studies demonstrated that doxorubicin retained tightly inside the liposomes. However, upon applying mild heat, the drug effectively released and suppressed tumor growth in mice compared to the same liposomal formulation without polymer, which exhibited limited degree of tumor suppression.

Poloxamers (Figure 1.8) are nonionic triblock copolymers composed of a hydrophobic block (polypropylene oxide) flanked by two hydrophilic end blocks (polyethylene oxide). These display a distinctive temperature-sensitive mechanism (Bodratti & Alexandridis, 2018). Poloxamers remain as individual non-associated copolymers in aqueous solution since the temperature falls below their critical micellar temperature. However, if the temperature is raised above the critical micellar temperature, the polymers become more hydrophobic and form micelles. Once the polymers form micelles with the hydrophobic core, they will associate with the liposomes membrane initiating defects and disrupting of lipid bilayers, resulting in release of encapsulated drug (Chandaroy, Sen, & Hui, 2001). Thermosensitive liposomes formulation modified with poloxamer (P188)

exhibited excellent stability at body temperature and rapid release of the encapsulated oxaliplatin at the trigger temperature (Zeng et al., 2016). Oxaliplatin thermosensitive liposomes composed of DPPC, MSPC, poloxamer 188 and DSPE-PEG2000 (85:9.5:0.5:5, molar %) accelerated the release of oxaliplatin significantly when the triggered temperature was around 42°C, the cumulative release of oxaliplatin reached 90% at 10 min. The anti-tumor activity of thermosensitive liposomes (2.5 mg/kg) was equal to those of oxaliplatin injection and non-thermosensitive liposomes at 5 mg/kg. Besides, significant improvement of tumor growth inhibition was observed in thermosensitive liposomes compared with the free drug and non-thermosensitive liposomes at the same dose. In another study, doxorubicin was loaded into thermosensitive liposomal formulation composed of DPPC/P188 (3:0.4 molar ratio) and its cytotoxic effects toward A549 cells was examined after applying mild hyperthermia. Incorporation of P188 in DPPC liposomes enhanced the release of doxorubicin at 42°C and exhibited more cytotoxic effects toward A549 cell line comparable with free doxorubicin solution (Tagami, Kubota, & Ozeki, 2015).

DSPE-mPEG2000 in PEGylated thermosensitive liposomes can be replaced by non-ionic surfactants that contain PEGylated acyl chains such as stearyl ether (Brij78) to reduce opsonization and improve pharmacokinetics. Thermosensitive formulation, composed of DPPC and 16 mol% Brij78, enhanced the release of doxorubicin around 42°C and improved its stability in serum at 37^{o}C. Doxorubicin released completely in 15–40 s around 42°C (Tagami, May, Ernsting, & Li, 2012). *In vivo* pharmacokinetics of doxorubicin exhibited a 2.5-fold

increased area under the curve and 2-fold prolonged circulation half-life compared to lyso-lipid temperature-sensitive liposomes formulation composed of DPPC/MSPC/DSPE-PEG2000 (86:10:4). However, Brij78 could impair the bilayer stability of liposomes since the membrane of liposomes can only accommodate Brij78 to a certain amount. For example, incorporation of 24 mol% of Brij78 decreased the bilayer stability and induced significant drug loss (more than 20%).

Researchers also have examined thermosensitive liposomes containing NH_4HCO_3 decompose to generate CO_2 effervescence when exposed to mild hyperthermia (Guo, Yu, Wang, Tan, & Li, 2015). Thermosensitive liposomes modified with copolymers of NIPAAm and N-acryloylpyrrolidine (Kono, Nakai, Morimoto, & Takagishi, 1999), and with elastin-like polypeptide as a heat-triggered component (Park et al., 2014) were also prepared.

1.6.3 Enzyme Responsive Liposomes

Several enzymes in the tumor area are over-expressed, which can be exploited as endogenous triggers to achieve site-specific drug delivery in cancer chemotherapy. Several enzymes within the protease and lipase families are typically over-expressed by cancer cells. Enzymes, including matrix metalloproteinase phospholipase A_2, alkaline phosphatase, transglutaminase and phosphatidylinositol-specific phospholipase C, overexpressed in tumor tissues (Bremer, Tung, & Weissleder, 2001). Enzymes overexpression in the tumor vasculature has been employed as triggers to achieve site-specific drug delivery by designing liposomes that release the encapsulated drug at the tumor

site upon enzymatic activation. Another approach is engineering enzyme-sensitive liposomes with a linker that will cleave off in the presence of overexpressed enzymes, exposing hidden drugs or other functionalities (Arias, 2011). Enzyme responsive liposomes have the advantage of being stable in the extracellular environment until activated at the site of interest by a specific enzyme.

Matrix metalloproteinases (MMPs), a of protease that breaks down components of the extracellular matrix, are often overexpressed in the tumor microenvironment and facilitate the metastasis of cancer cells (Egeblad & Werb, 2002). Among the MMP family, MMP2 and MMP9 are the most targeted for drug delivery since they are involved in the metastasis of several tumors, including, colorectal, breast, lung, prostate, and ovarian (Roomi, Monterrey, Kalinovsky, Rath, & Niedzwiecki, 2009). MMP-sensitive substrates might include proteins, peptides and polymers. Multifunctional liposomal nanocarrier containing MMP2-cleavable octapeptide (Gly-Pro-Leu-Gly-Ile-Ala-Gly-Gln) and cell penetration function (TATp) exhibited higher cellular internalization of labeled liposomes in mouse breast cancer cells (4T1) compared to non-treated controls (Zhu, Kate, & Torchilin, 2012). The authors suggested that when liposomes reached the tumor microenvironment, the peptide was cleaved by MMP2, leading to the exposure of TATp and increased intracellular penetration. PEGylated liposomes synthesized with MMP-9-cleavable, collagen mimetic lipopeptide and loaded with gemcitabine decreased the pancreatic ductal carcinoma cells (PANC-1) tumor volumes effectively compared to liposomes without the MMP-9 substrate. Moreover, *in*

vitro release studies also confirmed the rapid release of liposomes content in response to added MMP9, indicating that lipopeptide was effectively hydrolyzed by MMP9 (Kulkarni et al., 2014). Docetaxel loaded liposomal delivery system, which has both reduction- and enzyme-sensitive properties, was designed to enhance docetaxel release and anti-tumor activity (P. Xu et al., 2015). Methoxy polyethylene glycol-peptide-vitamin E succinate, a MMP9 sensitive copolymer, and methoxy polyethylene glycol-s-s-vitamin E succinate, reduction sensitive, were employed in a liposome delivery system. Complete docetaxel release was achieved in the simulated tumor microenvironment with MMPs and reductive glutathione (50 nM MMP-9 and 10 mM GSH after 10 h). In addition, docetaxel loaded liposomal delivery system exhibited much greater antitumor efficacy and antimetastatic effect against 4T1 breast cancer cells compared to free drug.

Certain lipases are also overexpressed in the tumor microenvironment, which can be exploited for liposomes activation as well. For instance, phospholipase A2 (PLA_2) is up-regulated in the extracellular matrix of cancerous tissue, including breast, lung and liver cancer (Abe et al., 1997). Most prodrugs are attached at the *sn*-1 position since PLA_2 enzymes hydrolyze the fatty ester group at the *sn*-2 position of glycerophospholipids. An enzymatically activated liposome drug delivery system to mask antitumor ether lipids (AELs), which hemotoxicity side effect limits its use, has been investigated (Andresen, Davidsen, Begtrup, Mouritsen, & Jorgensen, 2004). Prodrugs of AELs (proAELs) have been designed using phospholipids with an ether bond at *sn*-1 position and are hydrolyzed to AELs by PLA_2. *In vitro* experiments demonstrated that proAELs

liposomes reduced hemolytic effect compared to the free AELs. PLA_2 susceptible liposomes contained 1-O-stearyl-2-RAR-C6-sn-glycero-3-phosphoglycerol (C6-RAR) as a prodrug of RAR, 4-(4-octylphenyl)-benzoic acid was developed to improve liposomes performance *in vivo* (Arouri & Mouritsen, 2012). The RAR compound exhibited anti-tumor effect against a wide variety of cancer, including breast and colon cancer (Pedersen et al., 2010). In the presence of PLA_2 IC_{50} of C6-RAR prodrug against MT-3 breast carcinoma cell line decreased to 10 μM compared to 110 μM without $sPLA_2$.

Increased extracellular elastase activity has been utilized to develop enzymatically-triggered liposomal delivery systems. Elastase has been correlated with tumor progression and development. It has specificity for uncharged amino acid side chains, mainly alanine or valine. Covalent linkage of DOPE to an elastase substrate (N-acetyl-ala-ala) resulted in a cleavable peptide-lipid (N-Ac-AA-DOPE) and formation of bilayer liposome. Linking Ala-Ala with DOPE changed its shape from an inverted cone to cylindrical. Cleavage of peptide-lipid (N-Ac-AA-DOPE) by elastase led to destabilization and fusion of the liposomes because DOPE returned to its original inverted cone structure (Pak, Ali, Janoff, & Meers, 1998).

Researchers also have investigated several enzymatically-triggered liposomes including glutathione reductase (Chandrawati et al., 2011), glucose oxidase (Jo, Lee, & Kim, 2009), and phospholipase C (Nieva, Goni, & Alonso, 1989).

1.6.4 Redox Responsive Liposomes

In a tumor mass, glutathione (GSH) concentration is significantly higher (100-1000 fold) than the extracellular concentration in normal tissue (V. Torchilin, 2009). The difference in redox potential between normal and tumor tissues has been exploited to develop targeted cancer therapies. The disulfide bond has been commonly used due to the disulfide-to-thiol reduction reaction. Disulfide linkages within amphiphile, such as dithiothreitol, that can be disrupted by thiolytic reducing agents are commonly used. Redox responsive liposomes are destabilized by changes in charge and/or hydrophilicity of the incorporated reducing agents. In some instances, reduction reaction will initiate phase transitions of the lipid system as it removes cross-links (McCarley, 2012).

Redox-responsive liposomes composed of disulfide-linked PEG and cell-penetrating peptides (CPPs) enhanced the antitumor activity of paclitaxel (Fu et al., 2015). Detaching of disulfide-linked PEG by the reducing agent (GSH) exposed CPPs from the liposomes, allowing a higher cellular uptake of the drug. Disulfide-linked PEG-CPP-liposomes with paclitaxel strongly inhibited the proliferation of murine melanoma B16F1 tumor cells *in vitro* and *in vivo*. Compared to non-cleavable liposomes (paclitaxel-PEG-CPP), disulfide-linked PEG-CPP-liposomes reduced tumor volumes in mice by 34.3%. Acid/redox dual-responsive liposomes contain functional lipid 2-[2-(2-carboxylcyclohexylformamido)-3,12-dioxy-1-(1H-imidazolyl-4)-7,8-dithio-4,11-diazapentadecylamide]-glutaric acid ditetradecanol-diester (HH-SS-E2C_{14}) enhanced antitumor efficacy of doxorubicin (X. Xu et al., 2015). A disulfde bond

was incorporated as a redox-sensitive linkage between the hydrophilic block (histidine and acid-cleavable group hexahydrobenzoic amide) and the hydrophobic block (two tetradecyl alkane chains). After incubation with 10 mM GSH at pH 7.4 and 5.5 for 4 h, the cumulative amount of doxorubicin released was about 70%, indicating that higher GSH level caused the disulfide linkage in HH-SS-E2C_{14} to cleave, leading to a prompt release of doxorubicin. HH-SS-E2C_{14} system loaded with doxorubicin exhibited a 2-fold increase in the total apoptotic ratio toward human hepatic carcinoma (HepG2) cells compared to the formulation without disulfde bond.

Redox-responsive liposomes have been used for siRNA delivery (Sun et al., 2015), transfection agent delivery using bis(11 ferrocenylundecyl)dimethylammonium bromide as redox-active lipids (Aytar et al., 2012) and cell penetrating peptide (Wang et al., 2018).

1.7 Conclusion

In addition to the need for extended blood circulation, nanocarriers must release their content effectively at the tumor site. Stimuli-sensitive nanopreparations have exhibited a superior ability to control both the location and time of drug release compared to conventional drug delivery systems. Stimuli-sensitive nanopreparations are specifically designed to target the tumor site and respond to externally applied stimuli, such as mild hyperthermia, or local stimuli, such as pH, or different combinations of the stimuli. Although stimulus-sensitive drug delivery systems improve targeting, delivery and site-specific release of several drugs, further advances are required to take these

developments to clinical reality.

1.8 References

Abe, T., Sakamoto, K., Kamohara, H., Hirano, Y., Kuwahara, N., & Ogawa, M. (1997). Group II phospholipase A2 is increased in peritoneal and pleural effusions in patients with various types of cancer. *Int J Cancer, 74*(3), 245-250. doi: 10.1002/(sici)1097-0215(19970620)74:3<245::aid-ijc2>3.0.co;2-z

Al-Ahmady, Z., & Kostarelos, K. (2016). Chemical Components for the Design of Temperature-Responsive Vesicles as Cancer Therapeutics. *Chem Rev, 116*(6), 3883-3918. doi: 10.1021/acs.chemrev.5b00578

Alavizadeh, S. H., Gheybi, F., Nikpoor, A. R., Badiee, A., Golmohammadzadeh, S., & Jaafari, M. R. (2017). Therapeutic Efficacy of Cisplatin Thermosensitive Liposomes upon Mild Hyperthermia in C26 Tumor Bearing BALB/c Mice. *Mol Pharm, 14*(3), 712-721. doi: 10.1021/acs.molpharmaceut.6b01006

Allen, T. M. (1997). Liposomes. Opportunities in drug delivery. *Drugs, 54 Suppl 4*, 8-14. doi: 10.2165/00003495-199700544-00004

Allen, T. M., Hansen, C., Martin, F., Redemann, C., & Yau-Young, A. (1991). Liposomes containing synthetic lipid derivatives of poly(ethylene glycol) show prolonged circulation half-lives in vivo. *Biochim Biophys Acta, 1066*(1), 29-36.

Andresen, T. L., Davidsen, J., Begtrup, M., Mouritsen, O. G., & Jorgensen, K. (2004). Enzymatic release of antitumor ether lipids by specific phospholipase A2 activation of liposome-forming prodrugs. *J Med Chem, 47*(7), 1694-1703. doi: 10.1021/jm031029r

Arias, J. L. (2011). Drug targeting strategies in cancer treatment: an overview. *Mini Rev Med Chem, 11*(1), 1-17.

Arouri, A., & Mouritsen, O. G. (2012). Phospholipase A(2)-susceptible liposomes of anticancer double lipid-prodrugs. *Eur J Pharm Sci, 45*(4), 408-420. doi: 10.1016/j.ejps.2011.09.013

Aytar, B. S., Muller, J. P., Golan, S., Kondo, Y., Talmon, Y., Abbott, N. L., & Lynn, D. M. (2012). Chemical oxidation of a redox-active, ferrocene-containing cationic lipid: influence on interactions with DNA and characterization in the context of cell transfection. *J Colloid Interface Sci, 387*(1), 56-64. doi: 10.1016/j.jcis.2012.07.083

Bersani, S., Vila-Caballer, M., Brazzale, C., Barattin, M., & Salmaso, S. (2014). pH-sensitive stearoyl-PEG-poly(methacryloyl sulfadimethoxine) decorated liposomes for the delivery of gemcitabine to cancer cells. *Eur J Pharm Biopharm, 88*(3), 670-682. doi: 10.1016/j.ejpb.2014.08.005

Bodratti, A. M., & Alexandridis, P. (2018). Formulation of Poloxamers for Drug Delivery. *J Funct Biomater, 9*(1). doi: 10.3390/jfb9010011

Bregoli, L., Movia, D., Gavigan-Imedio, J. D., Lysaght, J., Reynolds, J., & Prina-Mello, A. (2016). Nanomedicine applied to translational oncology: A future perspective on cancer treatment. *Nanomedicine (Lond), 12*(1), 81-103. doi: 10.1016/j.nano.2015.08.006

Bremer, C., Tung, C. H., & Weissleder, R. (2001). In vivo molecular target assessment of matrix metalloproteinase inhibition. *Nat Med, 7*(6), 743-748. doi: 10.1038/89126

Byrne, J. D., Betancourt, T., & Brannon-Peppas, L. (2008). Active targeting schemes for nanoparticle systems in cancer therapeutics. *Adv Drug Deliv Rev, 60*(15), 1615-1626. doi: 10.1016/j.addr.2008.08.005

Casado, A., Sagrista, M. L., & Mora, M. (2014). Formulation and in vitro characterization of thermosensitive liposomes for the delivery of irinotecan. *J Pharm Sci, 103*(10), 3127-3138. doi: 10.1002/jps.24097

Chandaroy, P., Sen, A., & Hui, S. W. (2001). Temperature-controlled content release from liposomes encapsulating Pluronic F127. *J Control Release, 76*(1-2), 27-37.

Chandrawati, R., Odermatt, P. D., Chong, S. F., Price, A. D., Stadler, B., & Caruso, F. (2011). Triggered cargo release by encapsulated enzymatic catalysis in capsosomes. *Nano Lett, 11*(11), 4958-4963. doi: 10.1021/nl202906j

Chen, D., Liu, W., Shen, Y., Mu, H., Zhang, Y., Liang, R., . . . Fu, F. (2011). Effects of a novel pH-sensitive liposome with cleavable esterase-catalyzed and pH-responsive double smart mPEG lipid derivative on ABC phenomenon. *Int J Nanomedicine, 6*, 2053-2061. doi: 10.2147/IJN.S24344

Chen, D. B., Yang, T. Z., Lu, W. L., & Zhang, Q. (2001). In vitro and in vivo study of two types of long-circulating solid lipid nanoparticles containing paclitaxel. *Chem Pharm Bull (Tokyo), 49*(11), 1444-1447.

Chen, L., Alrbyawi, H., Poudel, I., Arnold, R. D., & Babu, R. J. (2019). Co-delivery of Doxorubicin and Ceramide in a Liposomal Formulation Enhances Cytotoxicity in Murine B16BL6 Melanoma Cell Lines. *AAPS PharmSciTech, 20*(3), 99. doi: 10.1208/s12249-019-1316-0

Chiang, Y. T., Lyu, S. Y., Wen, Y. H., & Lo, C. L. (2018). Preparation and Characterization of Electrostatically Crosslinked Polymer(-)Liposomes in Anticancer Therapy. *Int J Mol Sci, 19*(6). doi: 10.3390/ijms19061615

Cullis, P. R., Chonn, A., & Semple, S. C. (1998). Interactions of liposomes and lipid-based carrier systems with blood proteins: Relation to clearance behaviour in vivo. *Adv Drug Deliv Rev, 32*(1-2), 3-17.

Danhier, F., Feron, O., & Preat, V. (2010). To exploit the tumor microenvironment: Passive and active tumor targeting of nanocarriers for anti-cancer drug delivery. *J Control Release, 148*(2), 135-146. doi: 10.1016/j.jconrel.2010.08.027

Deshpande, P. P., Biswas, S., & Torchilin, V. P. (2013). Current trends in the use of liposomes for tumor targeting. *Nanomedicine (Lond), 8*(9), 1509-1528. doi: 10.2217/nnm.13.118

Drummond, D. C., Noble, C. O., Hayes, M. E., Park, J. W., & Kirpotin, D. B. (2008). Pharmacokinetics and in vivo drug release rates in liposomal nanocarrier development. *J Pharm Sci, 97*(11), 4696-4740. doi: 10.1002/jps.21358

Du, J., Lane, L. A., & Nie, S. (2015). Stimuli-responsive nanoparticles for targeting the tumor microenvironment. *J Control Release, 219*, 205-214. doi: 10.1016/j.jconrel.2015.08.050

Duzgunes, N., Straubinger, R. M., Baldwin, P. A., Friend, D. S., & Papahadjopoulos, D. (1985). Proton-induced fusion of oleic acid-phosphatidylethanolamine liposomes. *Biochemistry, 24*(13), 3091-3098. doi: 10.1021/bi00334a004

Egeblad, M., & Werb, Z. (2002). New functions for the matrix metalloproteinases in cancer progression. *Nat Rev Cancer, 2*(3), 161-174. doi: 10.1038/nrc745

Felber, A. E., Dufresne, M. H., & Leroux, J. C. (2012). pH-sensitive vesicles, polymeric micelles, and nanospheres prepared with polycarboxylates. *Adv Drug Deliv Rev, 64*(11), 979-992. doi: 10.1016/j.addr.2011.09.006

Ferreira Ddos, S., Faria, S. D., Lopes, S. C., Teixeira, C. S., Malachias, A., Magalhaes-Paniago, R., . . . Oliveira, M. C. (2016). Development of a bone-targeted pH-sensitive liposomal formulation containing doxorubicin: physicochemical characterization, cytotoxicity, and biodistribution evaluation in a mouse model of bone metastasis. *Int J Nanomedicine, 11*, 3737-3751. doi: 10.2147/IJN.S109966

Ferreira Ddos, S., Lopes, S. C., Franco, M. S., & Oliveira, M. C. (2013). pH-sensitive liposomes for drug delivery in cancer treatment. *Ther Deliv, 4*(9), 1099-1123. doi: 10.4155/tde.13.80

Fleige, E., Quadir, M. A., & Haag, R. (2012). Stimuli-responsive polymeric nanocarriers for the controlled transport of active compounds: concepts and applications. *Adv Drug Deliv Rev, 64*(9), 866-884. doi: 10.1016/j.addr.2012.01.020

Fu, H., Shi, K., Hu, G., Yang, Y., Kuang, Q., Lu, L., . . . He, Q. (2015). Tumor-targeted paclitaxel delivery and enhanced penetration using TAT-decorated liposomes comprising redox-responsive poly(ethylene glycol). *J Pharm Sci, 104*(3), 1160-1173. doi: 10.1002/jps.24291

Gabizon, A., Shmeeda, H., & Barenholz, Y. (2003). Pharmacokinetics of pegylated liposomal Doxorubicin: review of animal and human studies. *Clin Pharmacokinet, 42*(5), 419-436. doi: 10.2165/00003088-200342050-00002

Gulati, V., & Wallace, R. (2012). Rafts, Nanoparticles and Neural Disease. *Nanomaterials (Basel), 2*(3), 217-250. doi: 10.3390/nano2030217

Guo, F., Yu, M., Wang, J., Tan, F., & Li, N. (2015). Smart IR780 Theranostic Nanocarrier for Tumor-Specific Therapy: Hyperthermia-Mediated Bubble-Generating and Folate-Targeted Liposomes. *ACS Appl Mater Interfaces, 7*(37), 20556-20567. doi: 10.1021/acsami.5b06552

Han, H. D., Shin, B. C., & Choi, H. S. (2006). Doxorubicin-encapsulated thermosensitive liposomes modified with poly(N-isopropylacrylamide-co-acrylamide): drug release behavior and stability in the presence of serum. *Eur J Pharm Biopharm, 62*(1), 110-116. doi: 10.1016/j.ejpb.2005.07.006

Hayashi, H., Kono, K., & Takagishi, T. (1999). Temperature sensitization of liposomes using copolymers of N-isopropylacrylamide. *Bioconjug Chem, 10*(3), 412-418. doi: 10.1021/bc980111b

Hooper, L., Anderson, A. S., Birch, J., Forster, A. S., Rosenberg, G., Bauld, L., & Vohra, J. (2018). Public awareness and healthcare professional advice for obesity as a risk factor for cancer in the UK: a cross-sectional survey. *J Public Health (Oxf), 40*(4), 797-805. doi: 10.1093/pubmed/fdx145

Huang, S. K., Stauffer, P. R., Hong, K., Guo, J. W., Phillips, T. L., Huang, A., & Papahadjopoulos, D. (1994). Liposomes and hyperthermia in mice: increased tumor uptake and therapeutic efficacy of doxorubicin in sterically stabilized liposomes. *Cancer Res, 54*(8), 2186-2191.

Huwyler, J., Drewe, J., & Krahenbuhl, S. (2008). Tumor targeting using liposomal antineoplastic drugs. *Int J Nanomedicine, 3*(1), 21-29.

Ishida, T., Kirchmeier, M. J., Moase, E. H., Zalipsky, S., & Allen, T. M. (2001). Targeted delivery and triggered release of liposomal doxorubicin enhances cytotoxicity against human B lymphoma cells. *Biochim Biophys Acta, 1515*(2), 144-158. doi: 10.1016/s0005-2736(01)00409-6

Ishida, T., Okada, Y., Kobayashi, T., & Kiwada, H. (2006). Development of pH-sensitive liposomes that efficiently retain encapsulated doxorubicin (DXR) in blood. *Int J Pharm, 309*(1-2), 94-100. doi: 10.1016/j.ijpharm.2005.11.010

Jo, S. M., Lee, H. Y., & Kim, J. C. (2009). Glucose-sensitivity of liposomes incorporating conjugates of glucose oxidase and poly(N-isopropylacrylamide-co-methacrylic acid-co-octadecylacrylate). *Int J Biol Macromol, 45*(4), 421-426. doi: 10.1016/j.ijbiomac.2009.06.008

Kalia, J., & Raines, R. T. (2008). Hydrolytic stability of hydrazones and oximes. *Angew Chem Int Ed Engl, 47*(39), 7523-7526. doi: 10.1002/anie.200802651

Khawar, I. A., Kim, J. H., & Kuh, H. J. (2015). Improving drug delivery to solid tumors: priming the tumor microenvironment. *J Control Release, 201*, 78-89. doi: 10.1016/j.jconrel.2014.12.018

Kim, H. K., Van den Bossche, J., Hyun, S. H., & Thompson, D. H. (2012). Acid-triggered release via dePEGylation of fusogenic liposomes mediated by heterobifunctional phenyl-substituted vinyl ethers with tunable pH-sensitivity. *Bioconjug Chem, 23*(10), 2071-2077. doi: 10.1021/bc300266y

Kim, J. W., & Dang, C. V. (2006). Cancer's molecular sweet tooth and the Warburg effect. *Cancer Res, 66*(18), 8927-8930. doi: 10.1158/0008-5472.CAN-06-1501

Kim, S. M., Faix, P. H., & Schnitzer, J. E. (2017). Overcoming key biological barriers to cancer drug delivery and efficacy. *J Control Release, 267*, 15-30. doi: 10.1016/j.jconrel.2017.09.016

Kong, G., Braun, R. D., & Dewhirst, M. W. (2000). Hyperthermia enables tumor-specific nanoparticle delivery: effect of particle size. *Cancer Res, 60*(16), 4440-4445.

Kono, K. (2001). Thermosensitive polymer-modified liposomes. *Adv Drug Deliv Rev, 53*(3), 307-319.

Kono, K., Murakami, T., Yoshida, T., Haba, Y., Kanaoka, S., Takagishi, T., & Aoshima, S. (2005). Temperature sensitization of liposomes by use of thermosensitive block copolymers synthesized by living cationic polymerization: effect of copolymer chain length. *Bioconjug Chem, 16*(6), 1367-1374. doi: 10.1021/bc050004z

Kono, K., Nakai, R., Morimoto, K., & Takagishi, T. (1999). Thermosensitive polymer-modified liposomes that release contents around physiological temperature. *Biochim Biophys Acta, 1416*(1-2), 239-250. doi: 10.1016/s0005-2736(98)00226-0

Kono, K., Ozawa, T., Yoshida, T., Ozaki, F., Ishizaka, Y., Maruyama, K., . . . Aoshima, S. (2010). Highly temperature-sensitive liposomes based on a thermosensitive block copolymer for tumor-specific chemotherapy. *Biomaterials, 31*(27), 7096-7105. doi: 10.1016/j.biomaterials.2010.05.045

Kopecek, J., Kopeckova, P., Minko, T., & Lu, Z. (2000). HPMA copolymer-anticancer drug conjugates: design, activity, and mechanism of action. *Eur J Pharm Biopharm, 50*(1), 61-81.

Kulkarni, P. S., Haldar, M. K., Nahire, R. R., Katti, P., Ambre, A. H., Muhonen, W. W., . . . Mallik, S. (2014). Mmp-9 responsive PEG cleavable nanovesicles for efficient delivery of chemotherapeutics to pancreatic cancer. *Mol Pharm, 11*(7), 2390-2399. doi: 10.1021/mp500108p

Kumar, A., Chen, F., Mozhi, A., Zhang, X., Zhao, Y., Xue, X., . . . Liang, X. J. (2013). Innovative pharmaceutical development based on unique properties of nanoscale delivery formulation. *Nanoscale, 5*(18), 8307-8325. doi: 10.1039/c3nr01525d

Kumari, P., Ghosh, B., & Biswas, S. (2016). Nanocarriers for cancer-targeted drug delivery. *J Drug Target, 24*(3), 179-191. doi: 10.3109/1061186X.2015.1051049

Laginha, K. M., Verwoert, S., Charrois, G. J., & Allen, T. M. (2005). Determination of doxorubicin levels in whole tumor and tumor nuclei in murine breast cancer tumors. *Clin Cancer Res, 11*(19 Pt 1), 6944-6949. doi: 10.1158/1078-0432.CCR-05-0343

Lee, S. M., Chen, H., O'Halloran, T. V., & Nguyen, S. T. (2009). "Clickable" polymer-caged nanobins as a modular drug delivery platform. *J Am Chem Soc, 131*(26), 9311-9320. doi: 10.1021/ja9017336

Lee, Y., & Thompson, D. H. (2017). Stimuli-responsive liposomes for drug delivery. *Wiley Interdiscip Rev Nanomed Nanobiotechnol, 9*(5). doi: 10.1002/wnan.1450

Li, L., ten Hagen, T. L., Haeri, A., Soullie, T., Scholten, C., Seynhaeve, A. L., . . . Koning, G. A. (2014). A novel two-step mild hyperthermia for advanced liposomal chemotherapy. *J Control Release, 174*, 202-208. doi: 10.1016/j.jconrel.2013.11.012

Lindner, L. H., Eichhorn, M. E., Eibl, H., Teichert, N., Schmitt-Sody, M., Issels, R. D., & Dellian, M. (2004). Novel temperature-sensitive liposomes with prolonged circulation time. *Clin Cancer Res, 10*(6), 2168-2178.

Linton, S. S., Sherwood, S. G., Drews, K. C., & Kester, M. (2016). Targeting cancer cells in the tumor microenvironment: opportunities and challenges in combinatorial nanomedicine. *Wiley Interdiscip Rev Nanomed Nanobiotechnol, 8*(2), 208-222. doi: 10.1002/wnan.1358

Liu, J., Ma, H., Wei, T., & Liang, X. J. (2012). CO^2 gas induced drug release from pH-sensitive liposome to circumvent doxorubicin resistant cells. *Chem Commun (Camb), 48*(40), 4869-4871. doi: 10.1039/c2cc31697h

Lu, T., & Ten Hagen, T. L. M. (2017). Inhomogeneous crystal grain formation in DPPC-DSPC based thermosensitive liposomes determines content release kinetics. *J Control Release, 247*, 64-72. doi: 10.1016/j.jconrel.2016.12.030

Matsuo, H., Wakasugi, M., Takanaga, H., Ohtani, H., Naito, M., Tsuruo, T., & Sawada, Y. (2001). Possibility of the reversal of multidrug resistance and the avoidance of side effects by liposomes modified with MRK-16, a monoclonal antibody to P-glycoprotein. *J Control Release, 77*(1-2), 77-86.

Mayer, L. D., Bally, M. B., & Cullis, P. R. (1986). Uptake of adriamycin into large unilamellar vesicles in response to a pH gradient. *Biochim Biophys Acta, 857*(1), 123-126. doi: 10.1016/0005-2736(86)90105-7

McCarley, R. L. (2012). Redox-responsive delivery systems. *Annu Rev Anal Chem (Palo Alto Calif), 5*, 391-411. doi: 10.1146/annurev-anchem-062011-143157

Miyazaki, M., Yuba, E., Hayashi, H., Harada, A., & Kono, K. (2018). Hyaluronic Acid-Based pH-Sensitive Polymer-Modified Liposomes for Cell-Specific Intracellular Drug Delivery Systems. *Bioconjug Chem, 29*(1), 44-55. doi: 10.1021/acs.bioconjchem.7b00551

Mohan, A., Narayanan, S., Sethuraman, S., & Krishnan, U. M. (2014). Novel resveratrol and 5-fluorouracil coencapsulated in PEGylated nanoliposomes improve chemotherapeutic efficacy of combination against head and neck squamous cell carcinoma. *Biomed Res Int, 2014*, 424239. doi: 10.1155/2014/424239

Monteiro, N., Martins, A., Reis, R. L., & Neves, N. M. (2014). Liposomes in tissue engineering and regenerative medicine. *J R Soc Interface, 11*(101), 20140459. doi: 10.1098/rsif.2014.0459

Movahedi, F., Hu, R. G., Becker, D. L., & Xu, C. (2015). Stimuli-responsive liposomes for the delivery of nucleic acid therapeutics. *Nanomedicine (Lond), 11*(6), 1575-1584. doi: 10.1016/j.nano.2015.03.006

Nag, O. K., & Awasthi, V. (2013). Surface engineering of liposomes for stealth behavior. *Pharmaceutics, 5*(4), 542-569. doi: 10.3390/pharmaceutics5040542

Needham, D., Anyarambhatla, G., Kong, G., & Dewhirst, M. W. (2000). A new temperature-sensitive liposome for use with mild hyperthermia: characterization and testing in a human tumor xenograft model. *Cancer Res, 60*(5), 1197-1201.

Nieva, J. L., Goni, F. M., & Alonso, A. (1989). Liposome fusion catalytically induced by phospholipase C. *Biochemistry, 28*(18), 7364-7367. doi: 10.1021/bi00444a032

Nishimura, Y., Ono, K., Hiraoka, M., Masunaga, S., Jo, S., Shibamoto, Y., . . . Ogawa, Y. (1990). Treatment of murine SCC VII tumors with localized hyperthermia and temperature-sensitive liposomes containing cisplatin. *Radiat Res, 122*(2), 161-167.

Ong, S. G., Ming, L. C., Lee, K. S., & Yuen, K. H. (2016). Influence of the Encapsulation Efficiency and Size of Liposome on the Oral Bioavailability of Griseofulvin-Loaded Liposomes. *Pharmaceutics, 8*(3). doi: 10.3390/pharmaceutics8030025

Parra Ortiz, E. (2013). *Effects of pulmonary surfactant proteins SP-B and SP-C on the Physical properties of Biological membranes* (Ph.D.), Complutense University, Madrid, Spain. Retrieved from https://eprints.ucm.es/23506/

Paasonen, L., Romberg, B., Storm, G., Yliperttula, M., Urtti, A., & Hennink, W. E. (2007). Temperature-sensitive poly(N-(2-hydroxypropyl)methacrylamide mono/dilactate)-coated liposomes for triggered contents release. *Bioconjug Chem, 18*(6), 2131-2136. doi: 10.1021/bc700245p

Pacheco-Torres, J., Mukherjee, N., Walko, M., Lopez-Larrubia, P., Ballesteros, P., Cerdan, S., & Kocer, A. (2015). Image guided drug release from pH-sensitive Ion channel-functionalized stealth liposomes into an in vivo glioblastoma model. *Nanomedicine (Lond), 11*(6), 1345-1354. doi: 10.1016/j.nano.2015.03.014

Pak, C. C., Ali, S., Janoff, A. S., & Meers, P. (1998). Triggerable liposomal fusion by enzyme cleavage of a novel peptide-lipid conjugate. *Biochim Biophys Acta, 1372*(1), 13-27. doi: 10.1016/s0005-2736(98)00041-8

Park, S. M., Cha, J. M., Nam, J., Kim, M. S., Park, S. J., Park, E. S., . . . Kim, H. R. (2014). Formulation optimization and in vivo proof-of-concept study of thermosensitive liposomes balanced by phospholipid, elastin-like polypeptide, and cholesterol. *PLoS One, 9*(7), e103116. doi: 10.1371/journal.pone.0103116

Pedersen, P. J., Adolph, S. K., Subramanian, A. K., Arouri, A., Andresen, T. L., Mouritsen, O. G., . . . Clausen, M. H. (2010). Liposomal formulation of retinoids designed for enzyme triggered release. *J Med Chem, 53*(9), 3782-3792. doi: 10.1021/jm100190c

Raj, R., Mongia, P., Kumar Sahu, S., & Ram, A. (2016). Nanocarriers Based Anticancer Drugs: Current Scenario and Future Perceptions. *Curr Drug Targets, 17*(2), 206-228.

Riemann, A., Schneider, B., Gundel, D., Stock, C., Gekle, M., & Thews, O. (2016). Acidosis Promotes Metastasis Formation by Enhancing Tumor Cell Motility. *Adv Exp Med Biol, 876*, 215-220. doi: 10.1007/978-1-4939-3023-4_27

Roomi, M. W., Monterrey, J. C., Kalinovsky, T., Rath, M., & Niedzwiecki, A. (2009). Patterns of MMP-2 and MMP-9 expression in human cancer cell lines. *Oncol Rep, 21*(5), 1323-1333. doi: 10.3892/or_00000358

Samoshina, N. M., Liu, X., Brazdova, B., Franz, A. H., Samoshin, V. V., & Guo, X. (2011). Fliposomes: pH-Sensitive Liposomes Containing a trans-2-morpholinocyclohexanol-Based Lipid That Performs a Conformational Flip and Triggers an Instant Cargo Release in Acidic Medium. *Pharmaceutics, 3*(3), 379-405. doi: 10.3390/pharmaceutics3030379

Sawant, R. R., & Torchilin, V. P. (2012). Challenges in development of targeted liposomal therapeutics. *AAPS J, 14*(2), 303-315. doi: 10.1208/s12248-012-9330-0

Seddon, J. M., Cevc, G., & Marsh, D. (1983). Calorimetric studies of the gel-fluid (L beta-L alpha) and lamellar-inverted hexagonal (L alpha-HII) phase transitions in dialkyl- and diacylphosphatidylethanolamines. *Biochemistry, 22*(5), 1280-1289. doi: 10.1021/bi00274a045

Stylianopoulos, T., Poh, M. Z., Insin, N., Bawendi, M. G., Fukumura, D., Munn, L. L., & Jain, R. K. (2010). Diffusion of particles in the extracellular matrix: the effect of repulsive electrostatic interactions. *Biophys J, 99*(5), 1342-1349. doi: 10.1016/j.bpj.2010.06.016

Sun, Q., Kang, Z., Xue, L., Shang, Y., Su, Z., Sun, H., . . . Zhang, C. (2015). A Collaborative Assembly Strategy for Tumor-Targeted siRNA Delivery. *J Am Chem Soc, 137*(18), 6000-6010. doi: 10.1021/jacs.5b01435

Tagami, T., Kubota, M., & Ozeki, T. (2015). Effective Remote Loading of Doxorubicin into DPPC/Poloxamer 188 Hybrid Liposome to Retain Thermosensitive Property and the Assessment of Carrier-Based Acute Cytotoxicity for Pulmonary Administration. *J Pharm Sci, 104*(11), 3824-3832. doi: 10.1002/jps.24593

Tagami, T., May, J. P., Ernsting, M. J., & Li, S. D. (2012). A thermosensitive liposome prepared with a Cu(2)(+) gradient demonstrates improved pharmacokinetics, drug delivery and antitumor efficacy. *J Control Release, 161*(1), 142-149. doi: 10.1016/j.jconrel.2012.03.023

Takechi-Haraya, Y., Goda, Y., & Sakai-Kato, K. (2017). Control of Liposomal Penetration into Three-Dimensional Multicellular Tumor Spheroids by Modulating Liposomal Membrane Rigidity. *Mol Pharm, 14*(6), 2158-2165. doi: 10.1021/acs.molpharmaceut.7b00051

Torchilin, V. (2009). Multifunctional and stimuli-sensitive pharmaceutical nanocarriers. *Eur J Pharm Biopharm, 71*(3), 431-444. doi: 10.1016/j.ejpb.2008.09.026

Torchilin, V. P. (2007). Targeted pharmaceutical nanocarriers for cancer therapy and imaging. *AAPS J, 9*(2), E128-147. doi: 10.1208/aapsj0902015

Torchilin, V. P., Klibanov, A. L., Huang, L., O'Donnell, S., Nossiff, N. D., & Khaw, B. A. (1992). Targeted accumulation of polyethylene glycol-coated immunoliposomes in infarcted rabbit myocardium. *FASEB J, 6*(9), 2716-2719. doi: 10.1096/fasebj.6.9.1612296

Unezaki, S., Maruyama, K., Takahashi, N., Koyama, M., Yuda, T., Suginaka, A., & Iwatsuru, M. (1994). Enhanced delivery and antitumor activity of doxorubicin using long-circulating thermosensitive liposomes containing amphipathic polyethylene glycol in combination with local hyperthermia. *Pharm Res, 11*(8), 1180-1185.

Van Vlerken, L. E., Vyas, T. K., & Amiji, M. M. (2007). Poly(ethylene glycol)-modified nanocarriers for tumor-targeted and intracellular delivery. *Pharm Res, 24*(8), 1405-1414. doi: 10.1007/s11095-007-9284-6

Wang, H., Sun, M., Li, D., Yang, X., Han, C., & Pan, W. (2018). Redox sensitive PEG controlled octaarginine and targeting peptide co-modified nanostructured lipid carriers for enhanced tumour penetrating and targeting in vitro and in vivo. *Artif Cells Nanomed Biotechnol, 46*(2), 313-322. doi: 10.1080/21691401.2017.1307214

Weinstein, J. N., Magin, R. L., Yatvin, M. B., & Zaharko, D. S. (1979). Liposomes and local hyperthermia: selective delivery of methotrexate to heated tumors. *Science, 204*(4389), 188-191. doi: 10.1126/science.432641

Wicki, A., Witzigmann, D., Balasubramanian, V., & Huwyler, J. (2015). Nanomedicine in cancer therapy: challenges, opportunities, and clinical applications. *J Control Release, 200*, 138-157. doi: 10.1016/j.jconrel.2014.12.030

Wust, P., Hildebrandt, B., Sreenivasa, G., Rau, B., Gellermann, J., Riess, H., . . . Schlag, P. M. (2002). Hyperthermia in combined treatment of cancer. *Lancet Oncol, 3*(8), 487-497.

Xu, P., Meng, Q., Sun, H., Yin, Q., Yu, H., Zhang, Z., . . . Li, Y. (2015). Shrapnel nanoparticles loading docetaxel inhibit metastasis and growth of breast cancer. *Biomaterials, 64*, 10-20. doi: 10.1016/j.biomaterials.2015.06.017

Xu, X., Zhang, L., Assanhou, A. G., Wang, L., Zhang, Y., Li, W., . . . Zhang, A. C. (2015). Acid/redox dual-activated liposomes for tumortargeted drug delivery and enhanced therapeutic efficacy. *RSC Advances*(5), 67803–67808. doi: 10.1039/c5ra06445g

Yang, L. V. (2017). Tumor Microenvironment and Metabolism. *Int J Mol Sci, 18*(12). doi: 10.3390/ijms18122729

Ye, P., Zhang, W., Yang, T., Lu, Y., Lu, M., Gai, Y., . . . Xiang, G. (2014). Folate receptor-targeted liposomes enhanced the antitumor potency of imatinib through the combination of active targeting and molecular targeting. *Int J Nanomedicine, 9*, 2167-2178. doi: 10.2147/IJN.S60178

Zaorsky, N. G., Churilla, T. M., Egleston, B. L., Fisher, S. G., Ridge, J. A., Horwitz, E. M., & Meyer, J. E. (2017). Causes of death among cancer patients. *Ann Oncol, 28*(2), 400-407. doi: 10.1093/annonc/mdw604

Zeng, C., Yu, F., Yang, Y., Cheng, X., Liu, Y., Zhang, H., . . . Mei, X. (2016). Preparation and Evaluation of Oxaliplatin Thermosensitive Liposomes with Rapid Release and High Stability. *PLoS One, 11*(7), e0158517. doi: 10.1371/journal.pone.0158517

Zhai, G., Wu, J., Yu, B., Guo, C., Yang, X., & Lee, R. J. (2010). A transferrin receptor-targeted liposomal formulation for docetaxel. *J Nanosci Nanotechnol, 10*(8), 5129-5136.

Zhang, H., Li, R. Y., Lu, X., Mou, Z. Z., & Lin, G. M. (2012). Docetaxel-loaded liposomes: preparation, pH sensitivity, pharmacokinetics, and tissue distribution. *J Zhejiang Univ Sci B, 13*(12), 981-989. doi: 10.1631/jzus.B1200098

Zhang, Q., Weber, C., Schubert, U. S., & Hoogenboom, R. (2017). Thermoresponsive polymers with lower critical solution temperature: from fundamental aspects and measuring techniques to recommended turbidimetry conditions. *Materials Horizons, 4*(2), 109-116. doi: 10.1039/C7MH00016B

Zhang, Y., Zhai, M., Chen, Z., Han, X., Yu, F., Li, Z., . . . Mei, X. (2017). Dual-modified liposome codelivery of doxorubicin and vincristine improve targeting and therapeutic efficacy of glioma. *Drug Deliv, 24*(1), 1045-1055. doi: 10.1080/10717544.2017.1344334

Zhao, W., Zhuang, S., & Qi, X. R. (2011). Comparative study of the in vitro and in vivo characteristics of cationic and neutral liposomes. *Int J Nanomedicine, 6*, 3087-3098. doi: 10.2147/IJN.S25399

Zhigaltsev, I. V., Winters, G., Srinivasulu, M., Crawford, J., Wong, M., Amankwa, L., . . . Maurer, N. (2010). Development of a weak-base docetaxel derivative that can be loaded into lipid nanoparticles. *J Control Release, 144*(3), 332-340. doi: 10.1016/j.jconrel.2010.02.029

Zhu, L., Kate, P., & Torchilin, V. P. (2012). Matrix metalloprotease 2-responsive multifunctional liposomal nanocarrier for enhanced tumor targeting. *ACS Nano, 6*(4), 3491-3498. doi: 10.1021/nn300524f

Zhu, L., & Torchilin, V. P. (2013). Stimulus-responsive nanopreparations for tumor targeting. *Integr Biol (Camb), 5*(1), 96-107. doi: 10.1039/c2ib20135f

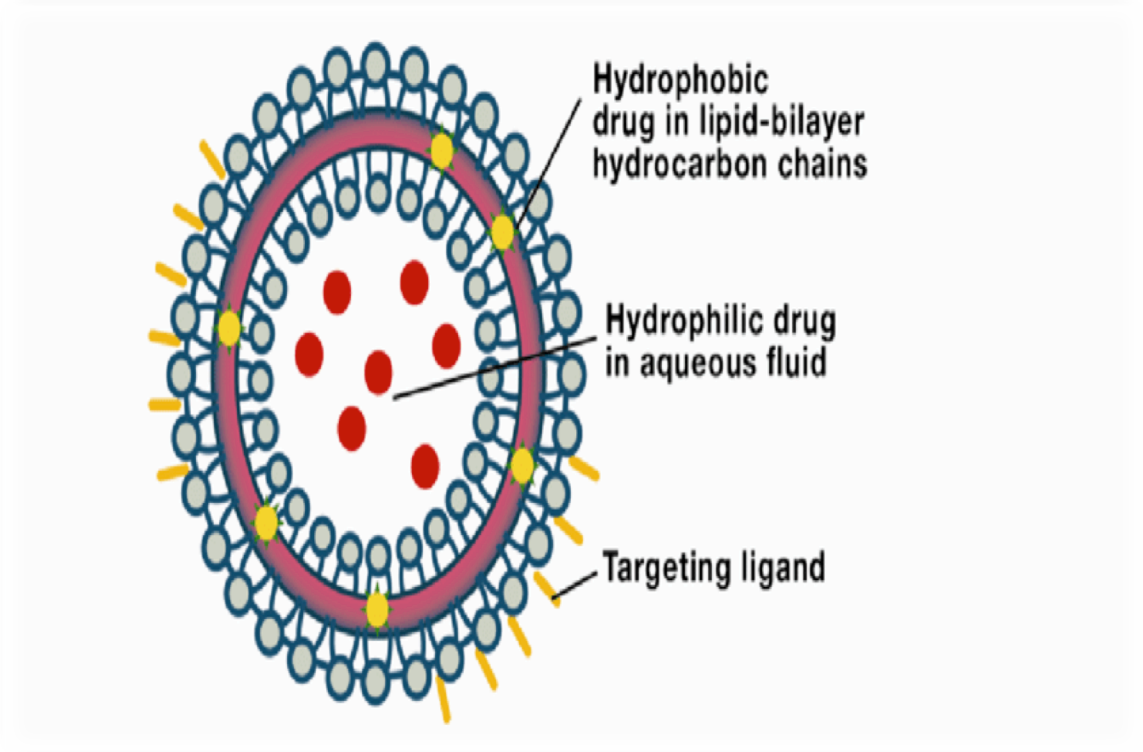

Figure 1.1: Hydrophilic and hydrophobic drugs encapsulated within liposomes (Gulati & Wallace, 2012)

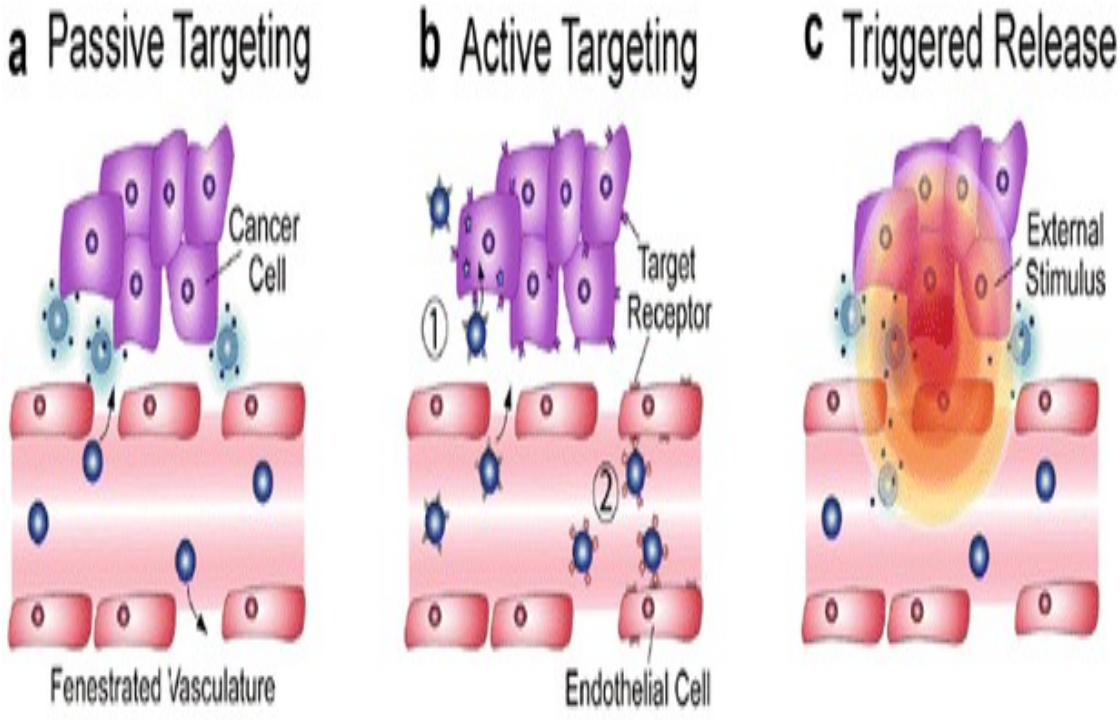

Figure 1.2: Types of targeting for nanoparticle delivery to tumor tissue (Wicki et al., 2015)

Table 1.1: Some compounds used for the preparation of pH-sensitive liposomes

Lipid/polymer /moiety/introduced for pH-sensitive character	Liposomal composition	Reference
DOPE	DOPE/ CHEMS /DSPE-PEG (5.7:3.8:0.5)	(Ferreira Ddos et al., 2016)
CHEMS	DOPE/HSPC/CHEMS/CHOL/mPEG(2000)-DSPE (4:2:2:2:0.3)	(Ishida et al., 2006)
POPC	POPC/PEG-ceramide (50:4:5)	(Samoshina et al., 2011)
hydrazone	S100PC/Chol/ mPEG2000-Hz-CHEMS (90:10:3)	(D. Chen et al., 2011)
Thiol cleavable PEG-derivative	DOPE/CHEMS/ mPEG-S-S-DSPE/Mal-PEG-DSPE (6:4:0.24:0.06)	(Ishida et al., 2001)
PIVE	PEG-PIVE/ DOPE (2:98, 5:95, and 12:88 mPEG-PIVE /DOPE)	(H. K. Kim et al., 2012)
PAA	DPPC/ DOPG/ cholesterol (18.048:1.152:12.8 µmol) + 10 mol% of Chol-PAA	(S. M. Lee et al., 2009)
MGlu & CHex	EYPC/ MGlu & Chex/ EYPC (lipids/polymer 7:3, w/w)	(Miyazaki et al., 2018)
OA	PE/CHOL/OA (3:2:3 w/w)	(H. Zhang et al., 2012)

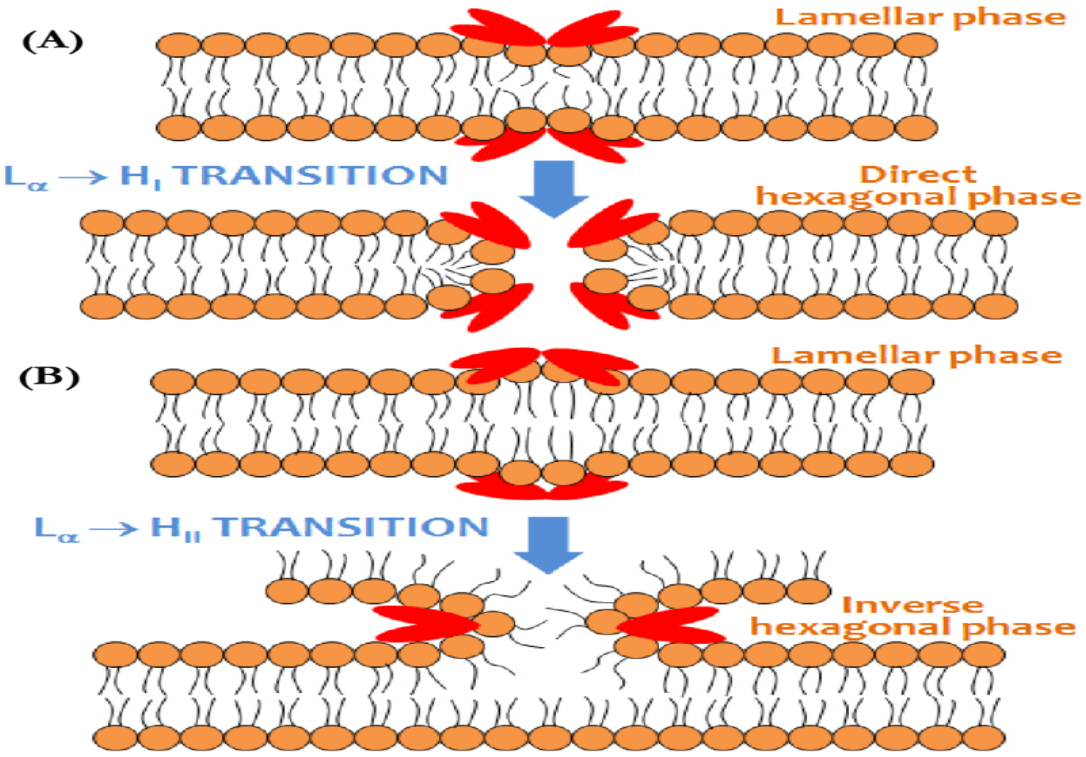

Figure 1.3: Schematic representation of (A) direct hexagonal phase H_I (B) inverse hexagonal phase H_{II} (Parra Ortiz, 2013)

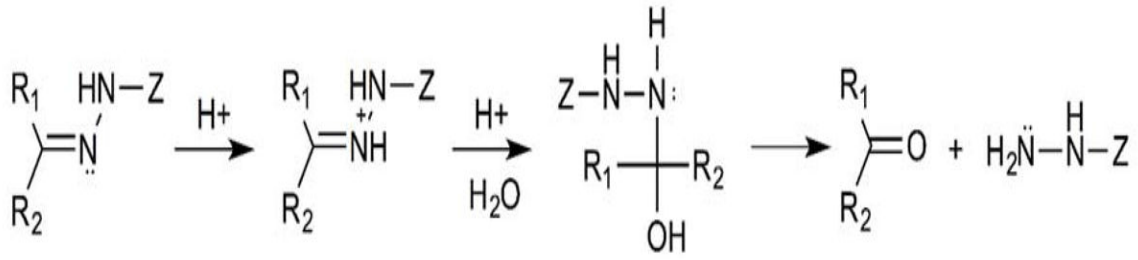

(A)

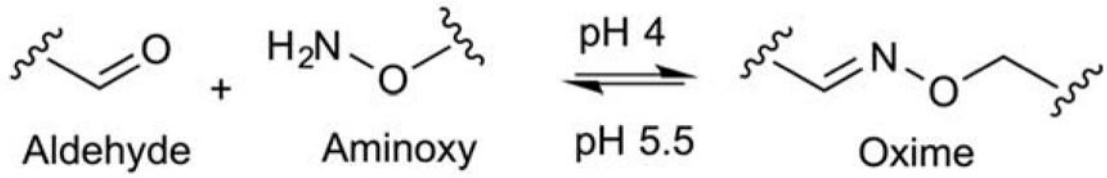

(B)

Figure 1.4: Schematic representation of (A) Hydrazone bond hydrolysis mechanism. (B) Oxime bond hydrolysis mechanism (Y. Lee & Thompson, 2017)

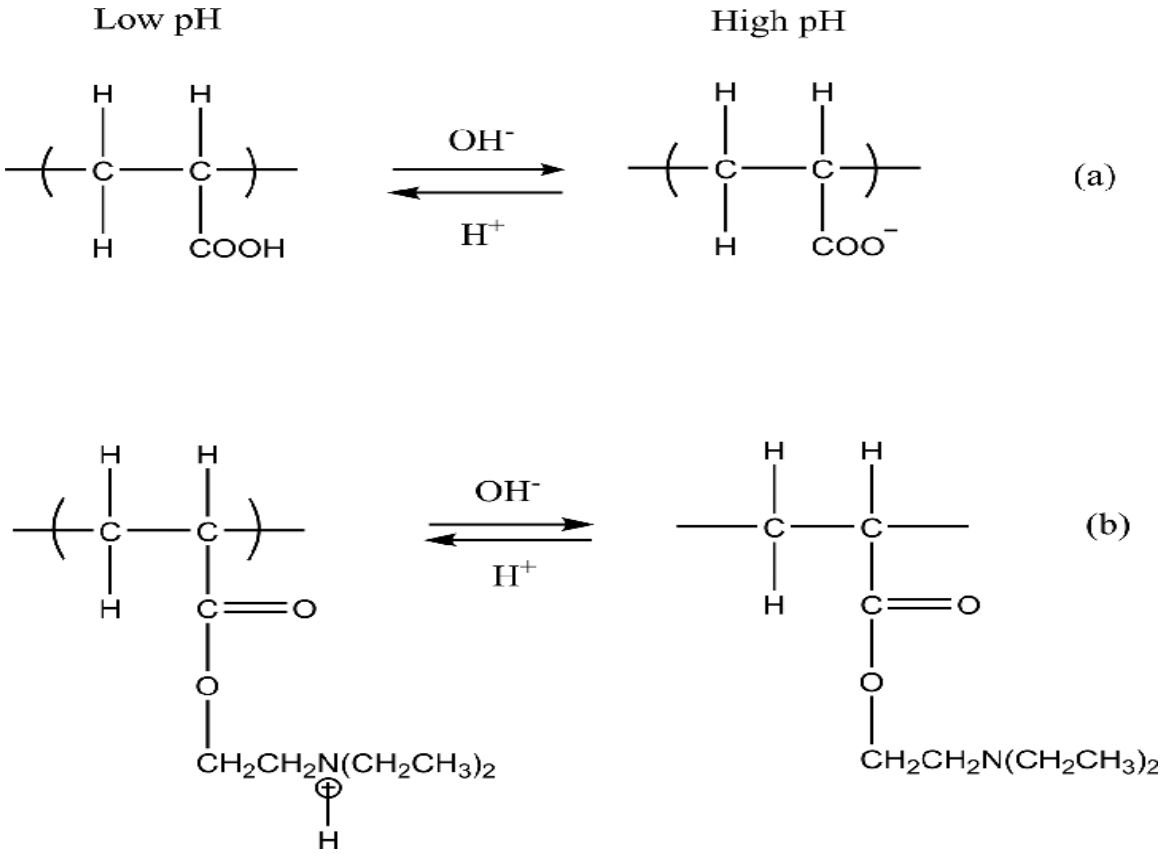

Figure 1.5: pH-dependent ionization of membrane-destabilizing polymers. (a) Poly (acrylic acid) and (b) poly (N,N'-diethylaminoethyl methacrylate)

Table 1.2: Some compounds used for the preparation of thermosensitive liposomes

Material	Formulation molar ratio	Drug	Phase transition temperature (Tm)	Reference
DPPC	DPPC:DSPC, 7:3	Methotrexate	42°C	(Weinstein et al., 1979)
DPPC	DPPC:DSPC, 9:1+ 3 mol% PEG	Doxorubicin	42°C	PEG (Unezaki et al., 1994)
MPPC	DPPC: MPPC: DSPE-PEG-2000 ,90:10:4	Doxorubicin	39 - 40°C	(Needham et al., 2000).
DPPGOG	DPPC/DSPC/DPPGOG 50:20:30	Doxorubicin	42°C	(Lindner et al., 2004)
NIPAAm-AAM	DPPC:HSPC:CHOL:DSPE-PEG-2000 (100:50:30:6) with NIPAAm-AAM (83:17) 10 mg/ml	Doxorubicin	40°C	(Han et al., 2006)
EOEOVE	EYPC/Chol/PEG-PE (50:45:4)+ EOEOVE 2 mol%	Doxorubicin	45°C	(Kono et al., 2010)
poloxamer 188	DPPC:MSPC: poloxamer 188:DSPE-PEG2000 (85:9.5:0.5:5, molar %)	Oxaliplatin	42°C	(Zeng et al., 2016)
Brij78	DPPC and 16 mol% Brij78	Doxorubicin	40 - 42°C	(Tagami et al., 2012)

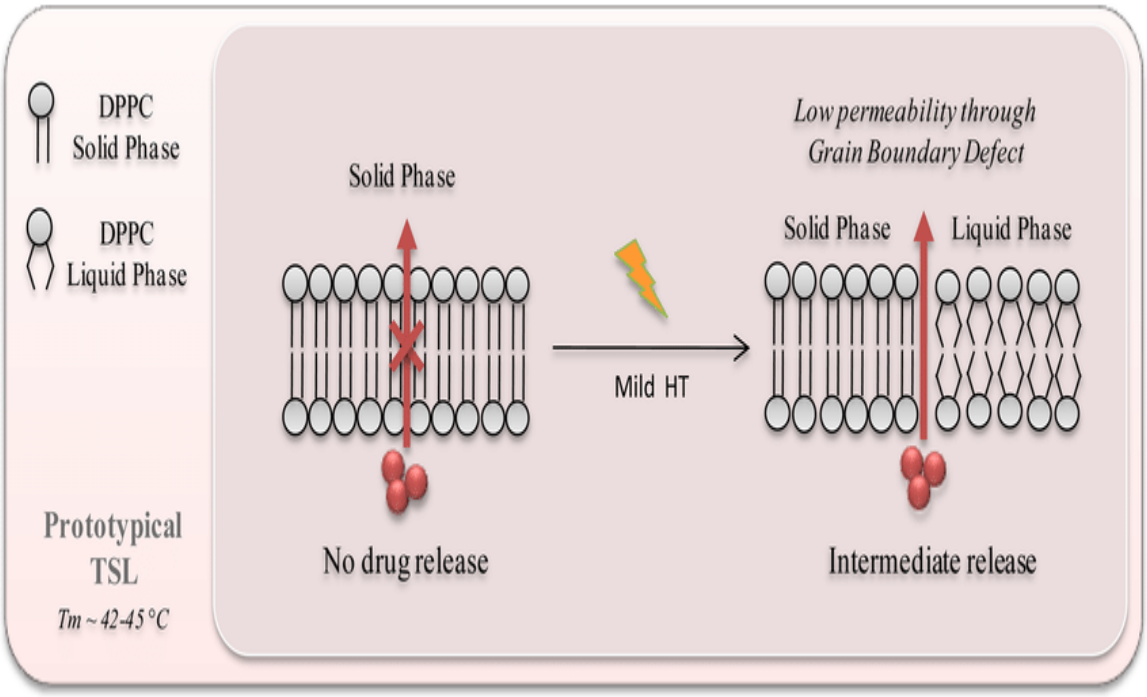

Figure 1.6: Phase transition behavior of thermosensitive liposomes (Al-Ahmady & Kostarelos, 2016)

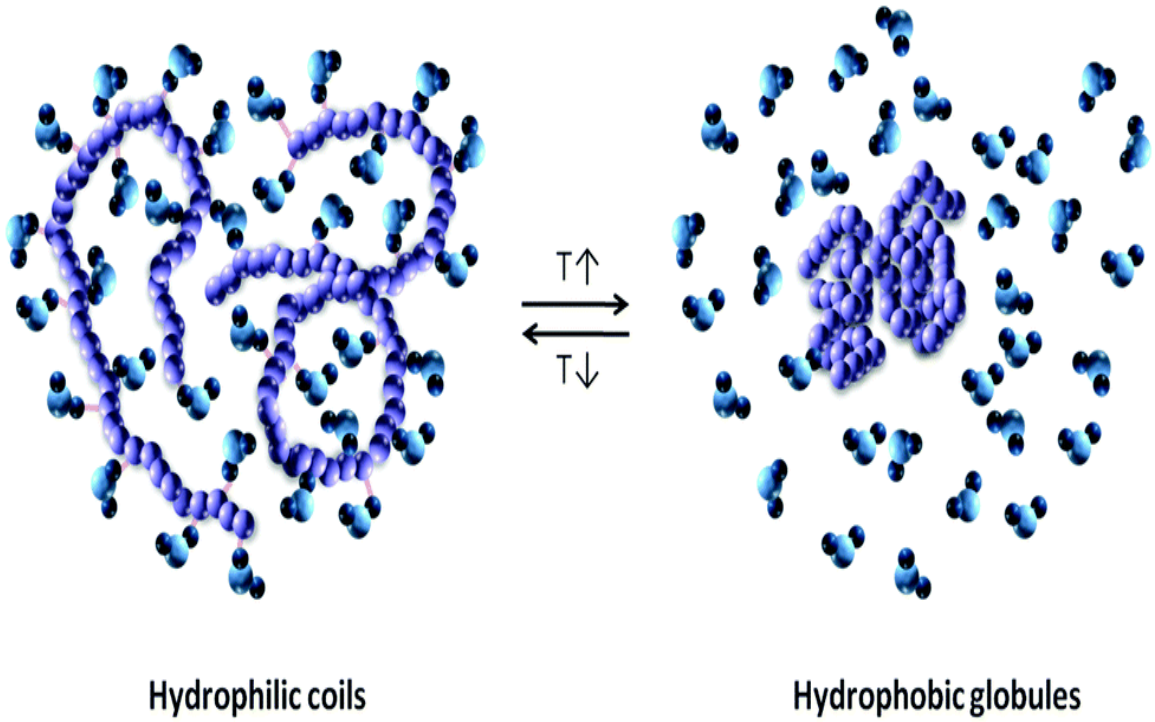

Figure 1.7: Temperature-sensitive polymers are soluble in water and tend to take a coil structure below their lower critical solution temperature. Polymers become water-insoluble and tend to take a dehydrated (hydrophobic) globule state above their lower critical solution temperature (Zhang, Weber, Schubert, & Hoogenboom, 2017)

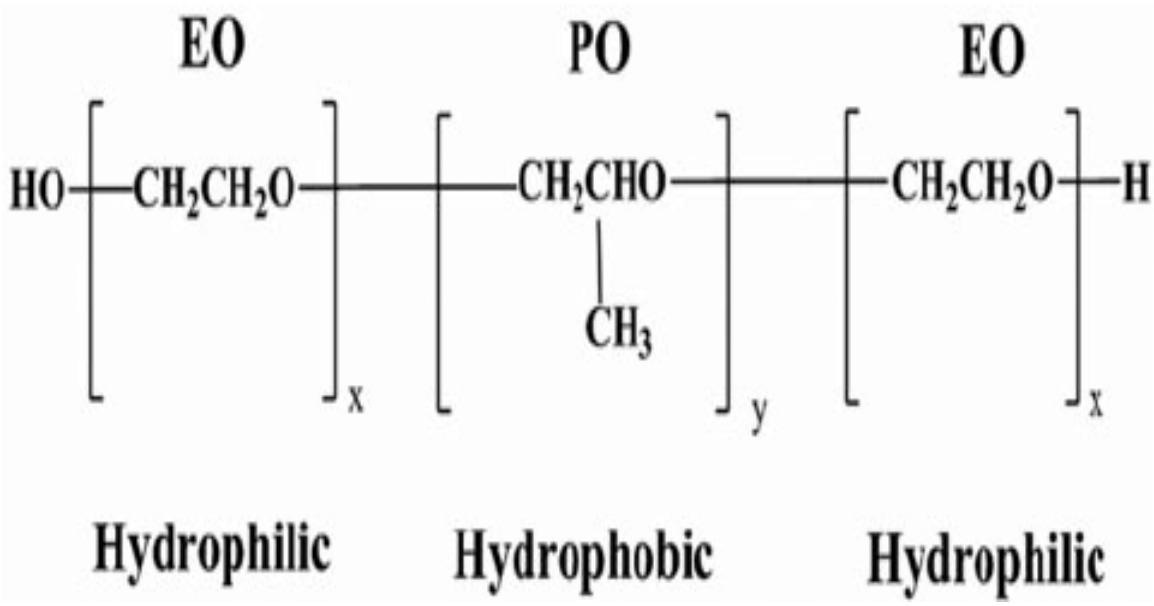

Figure 1.8: Poloxamers are nonionic triblock copolymers composed of a hydrophobic block (polypropylene oxide) flanked by two hydrophilic end blocks (polyethylene oxide)

Chapter 2. Short-Chain Ceramide for Enhanced Cellular Uptake and Cytotoxicity of Liposome-Encapsulated Daunorubicin in Melanoma (B16-BL6) Cell lines

2.1 Abstract

Co-delivery of daunorubicin (DNR) and C6-ceramide (C6-Cer) using a liposomal system in B16-BL6 melanoma cell lines for enhanced cytotoxic effects was investigated. DNR was encapsulated within liposomes and (C6-Cer) was a component of the lipid bilayer. PEGylated liposomes, containing C6-Cer, were prepared (45:33:5:17 mol% of DSPC/ cholesterol/PEG2000-DSPE/C6-Cer) using the lipid film hydration method and loaded with DNR (drug:lipid ratio 1:5). DNR liposomes enriched with C6-Cer exhibited high drug encapsulation efficiency (>90%), small size (~100 nm), narrow size distribution (~0.2) and good release and stability profiles. Liposomal DNR enriched with C6-Cer exhibited the highest cytotoxicity against B16-BL6 cells, resulting in about 10-fold higher cytotoxicity compared to the standard DNR solution ($p < 0.001$). The IC_{50} was 0.05 uM and 0.5 uM for DNR-C6-Cer and DNR solution, respectively. DNR liposomes enriched with C6-Cer also displayed a significant increase in cytotoxicity compared to the commercially available liposome formulation (DSPC/cholesterol/DNR). The IC_{50} was 0.05 uM and 0.3 uM for DNR-C6-Cer and the commercially available liposome formulation, respectively. This study provides a basis for developing a co-delivery system of DNR and ceramide liposomes for melanoma treatment.

2.2 Introduction

Malignant melanoma represents a public health concern in the United States as its incidence has increased regularly over the past 30 years and statistical data estimate the doubling of occurrence every 10-20 years (Sandru, Voinea, Panaitescu, & Blidaru, 2014). Malignant melanoma is fatal and highly metastatic with a 5-year or less survival rate (Tas, 2012). However, the alarming rise of incidence is not the only factor that contributes to the severity of the problem, but also the inefficiency of the currently used systemic treatments. Further, malignant melanoma shows a high relapse rates. Thus, the current scenario warrants developing novel delivery systems to provide targeted delivery and prevent further relapse. This can be achieved when the delivery system is able to provide complete remission of cancer cells at the target site to prevent future recurrence. Systemic therapy is the mainstay of treatment for most patients with stage IV melanoma. Systemic therapies might include cytotoxic chemotherapy, immunotherapy, or a combination therapy called bio-chemotherapy (Bhatia, Tykodi, & Thompson, 2009).

The current treatment methods of chemotherapy (including alkylating agents such as dacarbazine, temozolomide, the platinum analogs, and the microtubular toxins) are not able to prevent relapse and also suffer from systemic adverse effects such as cardiac toxicity, neuropathy, neutropenia, kidney failure, myelosuppression, alopecia, etc. (Luke & Schwartz, 2013). Furthermore, the modest antitumor activity of the chemotherapeutic agents led to the investigation of combinations of these agents to improve outcomes, which include an increase

in the response rate and possibly survival. Thus, targeted therapy that can carry multiple components, such as a targeting agent and anticancer agent, has been sought to prevent the systemic toxic effects of chemotherapeutic drugs and increase the response rate and possibly survival (Fielding, 1991).

Strategies to improve drug delivery for enhanced tumor therapy include nanoparticulate drug carriers, such as liposomes, polymeric and solid lipid nanoparticles (Roy Chaudhuri et al., 2012). Liposomes (Figure 2.1) are spherical lipid vesicles that are made upon hydration of different lipids (Samad, Sultana, & Aqil, 2007). They consist of a lipid bilayer with an aqueous phase inside (Akbarzadeh et al., 2013). Hydrophobic molecules can be localized into the bilayer membrane, and hydrophilic molecules can be entrapped in the aqueous core (Sercombe et al., 2015). Liposomes are considered one approach to entrap poor-soluble molecules, increase circulation time, modify tissue distribution of therapeutic agents, increase cellular uptake and decrease drug toxicity toward healthy cells (Abu Lila & Ishida, 2017).

Daunorubicin (DNR) is an antineoplastic in the anthracycline class that possesses an antitumor effect against a wide spectrum of tumors (Figure 2.2). DNR interacts and forms complexes with DNA by intercalation between base pairs. Besides, it inhibits topoisomerase II activity by stabilizing the DNA-topoisomerase II complex; as a result, preventing the religation portion of the ligation-religation reaction that topoisomerase II catalyzes (Crivellari, Lombardi, Spazzapan, Veronesi, & Toffoli, 2004). DNR has been used primarily in the acute leukemias; however, it displays broader activity against a variety of solid tumors.

The clinical use of DNR is limited by its toxicity to healthy tissues. The main acute dose-limiting toxicities are bone marrow depression and stomatitis (Childhood Acute Lymphoblastic Leukaemia Collaborative, 2009). Irreversible cardiomyopathy represents another significant side effect that limits the cumulative dose used of DNR over time (McGowan et al., 2017). The development of resistance to the anthracycline DNR represents one of the major obstacles that limits therapy with this agent (Nielsen, Maare, & Skovsgaard, 1996). Studies directed at the elucidation of mechanisms of anticancer drug resistance have shown that mammalian cell lines can develop multiple drug resistance (MDR). When these cell lines are continuously exposed to gradually increasing doses of anthracycline antibiotics drug-resistant can be developed. The drug resistance phenotype is characterized by decreased drug accumulation as a result of active drug efflux (Larsen, Escargueil, & Skladanowski, 2000). Nanocarriers loaded with anthracycline agents enhance the efficacy of these agents against different types of cancer including melanoma, targeted delivery to the tumor site, minimized systemic toxicity and overcoming drug resistance (Ma & Mumper, 2013).

Ceramides play an essential role as a cell-signaling mediator in cell differentiation, cell cycle arrest and apoptosis (Figure 2.3). These processes involve P13K/Akt signaling pathway (Oskouian & Saba, 2010). Furthermore, ceramides are known to induce transbilayer movement of lipids in the cell membrane and to alter the bilayer asymmetry across the cell membrane (Paulusma & Oude Elferink, 2006). The increasing intracellular level of

ceramides has been linked to cell apoptosis (Zhou, Summers, Birnbaum, & Pittman, 1998). The lipids composition distribution across the plasma membrane is asymmetrical among the inner and the outer layers. The outer layer is mainly composed of sphingolipids, such as sphingomyelin and glycosphingolipids. Using lipids analog to those located in outer membrane, like C6-Ceramide and C8-Ceramide, enhanced the membrane permeability and increased the cellular uptake of chemotherapeutic medications by cancer cells (van Lummel et al., 2011). Besides, short-chain ceramides are easily metabolized because they are similar to the components of the plasma membrane (Fenske, Chonn, & Cullis, 2008).

The objective of this study was to determine the cytotoxicity and cellular uptake of DNR liposomal formulation enriched with ceramides (C6-Cer). Ceramides have anti-tumor activity *in vitro* and *in vivo* (Kolesnick & Kronke, 1998). Ceramides target the PI3K/Akt pathway through dephosphorylation of Akt, leading to increased cytotoxicity and cell apoptosis and they act synergistically when in combination with other chemotherapeutics (Zhou et al., 1998). Furthermore, ceramide could facilitate the transmembrane diffusion of DNR, leading to increased cytotoxicity and apoptosis against B16-BL6 melanoma cancer cells. We hypothesized that co-delivery of ceramide and DNR in a liposomal formulation would potentiate the cytotoxicity and cellular uptake of DNR. Ceramide and PEGylated liposomes were formulated and characterized for size, size distribution, DNR release, cellular uptake and cytotoxicity.

2.3 Experimental Methods

2.3.1 Materials

1,2-distearoyl-*sn*-glycero-3-phosphocholine (DSPC), 1,2-distearoyl-*sn*-glycero-3-phosphoethanolamine-N-[methoxy(polyethyleneglycol)-2000] (ammonium salt) (DSPE-mPEG (2000)), C6-Ceramide (C6-Cer) were purchased from Avanti Polar Lipids Inc (Alabaster, AL). Cholesterol and Ammonium sulfate were purchased from JT Baker (Phillipsburg, NJ). Fetal bovine serum, Dulbecco's Modified Eagle's Medium (DMEM) and other reagents for cell culture were purchased from Mediatech (Manassas, VA). Daunorubicin was purchased from AvaChem Scientific (San Antonio, TX). 2′,7′-Dichlorofluorescin diacetate and Phosphate Buffered Saline (PBS pH7.4) were purchased from Sigma-Aldrich (St. Louis, MO). Bicinchoninic acid protein kit was purchased from Thermo Scientific (IL, USA). 3-(4,5-Dimethyl-2-thiazolyl)-2,5-diphenyl-2H-tetrazolium bromide (MTT) was purchased from Calbiochem (Darmstadt, Germany). Polycarbonate membrane (0.08 μm) was purchased from Whatman (Maidstone, UK). Melanoma (B16-BL6) cancer cells were obtained from American Type Culture Collection (Manassas, VA).

2.3.2 Liposomes Preparation

Liposomes were prepared by lipid film hydration using a rotary vacuum evaporator. Briefly, DSPC, cholesterol, C6-Cer, and DSPE-mPEG (2000) 10 mg/ml solutions were prepared in chloroform. The solutions were mixed at a molar ratio of 45:33:5:17 for DSPC/cholesterol/DSPE-mPEG(2000)/ C6-Cer, and flash evaporated on a rotavapor (Rotavapor, Büchi, Germany) set at 25 mmHg

vacuum and 65°C. The lipid film formed on the wall of the flask was further dried under a stream of nitrogen for 1h, followed by vacuum desiccation for 2 h. The dry lipid film was then hydrated in 250 mM ammonium sulfate solution (pH 5.5). This mixture was then placed in a water-bath incubator (65°C) for 1 h to form coarse liposomes. These were subjected to seven liquid nitrogen freeze–thaw cycles above the phase transition temperature of the primary lipid (DSPC) before extrusion. The liposome mixture was then extruded through 80 nm (10 passes) polycarbonate filter using Lipex® 100 ml barrel extruders (Transferra Nanosciences Inc, Burnaby, BC. Canada). The free ammonium sulfate outside the liposomes was removed by dialysis (using 12, 000 to 14,000 Daltons molecular weight cut off dialysis tubing) against sucrose solution (10% w/v, 250 ml) at 4°C. Sucrose solution was discarded and replaced with fresh solution at 1,4,8 h intervals and then left overnight. The total phospholipid concentration of each formulation was quantified following acid hydrolysis and inorganic phosphate assay (Bartlett, 1959). Liposomal formulation similar to DaunoXome®, composed of DSPC/cholesterol/daunorubicin (in a 10:5:1 molar ratio), was prepared by the same method; however, citrate was used instead of ammonium sulfate to hydrate the lipid film. Table 2.1 summarizes the different formulations prepared.

2.3.3 Drug Encapsulation in Liposomes (Active Loading)

DNR solution was prepared by dissolving the required quantities of drug in the PBS; the pH was adjusted to 8 with 0.1N NaOH solution. The drug solution was added to the lipid solution in 1:5 drug-to-lipid ratios. Excess DNR was then

removed by dialysis against sucrose solution (10%) at 4^{o}C. Based on initial results of drug loading efficiency, a 1:5 drug-to-lipid ratio was found to be optimum, and this ratio was used for all formulations.

2.3.4 Encapsulation Efficiency (EE%) and Drug Loading (DL%) Measurement

The amount of DNR entrapped into liposomes (EE% and DL%) was determined fluorometrically at 480 nm (excitation) and 590 nm (emission) using a microplate reader 142 (Fluostar, BMG labtechnologies, Germany). Briefly, Triton X-100 (1%) was added to break the liposome bilayer and release the entrapped DNR. Liposomal drug concentration was calculated by absorbance based on a standard curve of DNR. All the experiments were run in triplicate and mean data were presented.

The EE% was calculated as follows:

$$\text{Encapsulation Efficiency (\%)} = \frac{\text{amount of liposomal drug}}{\text{total amount of drug}} \times 100$$

The DL % was calculated as follows:

$$\text{Drug Loading (\%)} = \frac{\text{amount of liposomal drug}}{\text{total amount of drug added} + \text{amount of excipients added}} \times 100$$

2.3.5 Particle Size Determination of Liposomal Formulations

The particle size distribution of the liposomal formulations was performed by the dynamic light scattering method using Nicomp 380 ZLS particle size analyzer (Particle Sizing Systems, Santa Barbara, CA). Mean particle size and polydispersity index of the formulations after appropriate dilutions were calculated.

2.3.6 Determination of Zeta Potential

Measurements of liposome zeta potential were carried out by photon correlation spectroscopy (PCS, Zetatrac, Largo, FL, USA). For the analyses, formulations were diluted in an aqueous medium. All determinations were performed in triplicate at room temperature (25°C).

2.3.7 *In Vitro* Release Studies

The release profile of DNR from liposome formulations was determined by the dialysis method. PBS (pH 7.4), filled in 250 ml conical flask, was used as a receptor phase. Regenerated cellulose dialysis tubing (12,000 to 14,000 Daltons molecular weight cut off), 30 mm × 25 mm release area, pre-soaked in buffer solution for one hour, was used. 1 ml of the formulation or DNR solution was placed in the dialysis tubing while immersed in the receptor phase. All flasks were incubated at 37^{o}C in a rotary shaker set at 150 rpm. Samples (1 ml) were collected at different time intervals, and the sample volumes were replenished with fresh buffer immediately. The concentration of DNR in the receptor buffer (dialysate) was analyzed fluorometrically at 480 nm (excitation) and 590 nm (emission) using a microplate reader. The cumulative percent of DNR released versus time (h) was plotted. All experiments were run in triplicate and mean data was presented.

2.3.8 Stability Studies

Short-term stability was conducted to monitor the physical stability of the liposomes. All liposomal formulations were stored at 4^{o}C under N_2 and protected

from light for one month. Dialysis was performed to remove non-capsulated drug and all parameters were measured again.

2.3.9 Cell Culture

Melanoma (B16-BL6) cells were cultured in Dulbecco's Modified Eagle's Medium (DMEM). The medium was supplemented with 10% fetal bovine serum (FBS), 100 U/ml penicillin, and 100 µg/ml streptomycin at 37°C in a humidified atmosphere containing 5% CO_2. All experiments were performed at a confluence of 90 to 95%.

2.3.10 Measurement of Cell Viability by MTT Assay

B16-BL6 cells were cultured in flat-bottom 96-well plates for 24 hours. The cell density in the wells was around 8×10^3 cells/well. The cells received treatments of various liposomal formulations (0.01 µM, 0.05 µM, 0.1 µM, 0.5 µM, and 1 µM) for 48 h prior to MTT assay. After experimental treatments, 10 µl of 3-[4, 5-dimethylthiazol-2-yl]-2, 5-diphenyl tetrazolium bromide (MTT) was added to each well and the cells were incubated at 37^{o}C for an additional 2 hours. Finally, the medium was aspirated and 200 µl dimethylsulfoxide (DMSO) was added to each well to solubilize the dye remaining in the plates. The absorbance was measured using a microplate reader (spectramax M5, molecular devices, Sunnyvale, CA, USA) at 544 nm. All the experiments were run in triplicate and mean data were presented.

2.3.11 Flow Cytometry Analysis of Cellular Uptake of Daunorubicin

B16-BL6 cells were plated in 24-well plates at a concentration of 50×10^3 cells per well. Cells were washed twice in PBS and incubated with free DNR

or liposomal formulation with equivalent DNR. Following incubation, the cells were washed twice with PBS and then re-suspended in a fresh medium. Fluorescence histograms were then recorded with a BD FACS Calibur flow cytometer (Beckton Dickinson, U.S.A.). 30,000 events were collected per sample.

2.3.11 Measurement of Oxidative Stress

The determination of intracellular reactive oxidant species generated by DNR was based on the oxidation of 2',7'-dichlorodihydrofluorescein diacetate to the fluorescent product, 2',7'-dichlorofluorescein. B16-BL6 cells were cultured in flat-bottom 24-well plates for 24 hours. At 90% of confluence, cells were exposed to 14 μM of different liposomal formulations or free DNR for 24 hours. Following treatment with various formulations, medium was aspirated, and the cells were washed three times with PBS before being placed into 1 ml of cell culture medium without FBS. 2',7'-dichlorodihydrofluorescein diacetate was added to a final concentration of 10 μM, and cells were incubated for 20 min. The cells were again washed twice with PBS and maintained in 1 ml of culture medium. Intracellular fluorescence was measured at wavelengths of 480nm (excitation) and 535 nm (emission) using a microplate reader (Spectramax M5, molecular devices, Sunnyvale, CA USA). Each study was repeated three times and the mean fluorescence was presented.

2.3.12 Fluorescence Microscopy

B16-BL6 cells were seeded in a flat-bottom 24-well plate for 24 hours. After exposure to liposomal DNR or free DNR for 16 hours, cells were washed

and fixed (15 min in 4% (w/v) paraformaldehyde in phosphate-buffered saline). All samples were examined using a fluorescence microscope (EVOS fl, ZP-PKGA-0494 REV A, USA) and photographed at 20X magnifications.

2.3.13 Statistical Analysis

All data were presented as mean ± standard deviation. GraphPad Prism software was used to determine the standard deviation and statistical levels of significance. All data were subjected to one-way analysis of variance (ANOVA) to determine the statistical levels of significance. P-value of less than 0.05 was considered to be statistically significant.

2.4 Results and Discussion

2.4.1 Formulation Preparation

The liposomes prepared with and without ceramide were evaluated for EE% and DL%. To obtain liposomes with desirable EE%, DNR was mixed with lipid (DNR:lipid) at a ratio of 1:5.. As shown in Table 2.2, the EE% and DL% of the formulations were above 90 and 15, respectively. Our preliminary studies showed a 1:5 drug-to-lipid ratio demonstrated higher EE and DL%, hence this ratio was used for all liposomal formulations.

The mechanism by which the drug-to-lipid ratio influences the EE is of particular interest. An inverse relationship was noticed between EE and the concentration of drug. The EE% decreases with increased drug concentration (Mayer et al., 1990). The existence of drug precipitate in the liposome interior may explain the inverse relationship between EE and drug concentration. Increasing drug-to-lipid ratio (above 1) will cause the drug to precipitate inside

the liposomes leading to significant disruption of the liposomal membrane, which causes leakage of encapsulated drug from liposomes (Johnston, Edwards, Karlsson, & Cullis, 2008).

High EE of amphipathic weak bases, such as DNR, might be achieved by a transmembrane ammonium sulfate gradient in and out of liposomes (active loading) (Wei et al., 2018). Similar to most drugs, DNR was not efficiently entrapped into the aqueous phase of the liposome without a pH gradient (Plourde et al., 2017). In the case of active loading, liposomes are initially prepared in an acidic environment. After vesicle self-assembly, the core of the liposome remains acidic while the extravesicular pH level is similar to physiological conditions (Hood, Vreeland, & DeVoe, 2014). Remote loading of uncharged drug allows molecules to diffuse into the liposomal intravesicular interior where they become protonated. The positively charged drug can no longer cross the bilayer membrane and is trapped inside the liposomes cavity (Deamer, Prince, & Crofts, 1972).

Insertion of PEG on the surface of liposomes is a common strategy to enhance the hydrophilicity of the particle surface, as the liver preferentially takes up particles with a hydrophobic surface (Otsuka, Nagasaki, & Kataoka, 2003). It is important to mention that mole% PEG can significantly affect the percentage of drug encapsulated inside liposomes. An inverse relationship was noticed between mole% of PEG and EE of drugs because PEG, in addition to its steric effect, might occupy some space in the core of the liposomes (Nicholas, Scott, Kennedy, & Jones, 2000). Mole% of PEG used in our formulation does not affect

DNR EE of liposomes. There is no statistically significant difference in EE between the liposomal formulations with and without PEG liposomes ($p > 0.05$).

2.4.2 Characterization of NP Formulations

The average particle size, PI, and zeta potential values for different liposomal formulations are listed in Table 2.2. The average particle size was less than 100 nm, and the PI values were small (< 0.27) indicating uniform size distribution of liposomal formulations. The zeta-potential of PEG-liposomes was negative because PEG-DSPE lipid imparts a negative charge (Nag, Yadav, Hedrick, & Awasthi, 2013). On the other hand, the zeta-potential of non-PEGylated-liposomes was close to zero suggesting a neutral charge.

As shown in Table 2.2, there is no significant difference in particle size between liposomes formulations with (F1) or without (F2) ceramide, indicating that the addition of short-chain ceramide (C6-Cer) does not affect particle size ($p > 0.05$). Particle size is an essential parameter that plays a pivotal role in the pharmacokinetic profile of the drug. Liposomes with large size are usually taken up by liver, spleen and other parts of the reticuloendothelial system (RES) (Rothkopf, Fahr, Fricker, Scherphof, & Kamps, 2005). Liposomes with particle size below 100 nm and a narrow size distribution are preferred for tumor targeting (Immordino, Dosio, & Cattel, 2006). The present study provides DNR liposomes with particle sizes below 100 nm, high entrapment efficiency (> 90%) and a homogenous size distribution (PI < 0.27).

2.4.3 Drug Release *In Vitro*

Figure 2.4 shows DNR release from the dialysis studies for free DNR, F1, F2 and F3. Free DNR as a solution diffused rapidly and showed a complete 100 % release within one h; DNR-liposome (F1 and F2) significantly slowed the DNR release. Liposomes similar to DaunoXome® (F3) released DNR fairly rapidly compared to other liposomes (F1 and F2). The *in vitro* results consist with the *in vivo* results DaunoXome® showed a relatively short plasma half-life (~4 h) (Bellott et al., 2001). In contrast, F1 and F2 had a longer *in vitro* release time due to the steric barrier provided by the surface-grafted PEG, compared to F3.

Modification of liposomes surface with PEG reduced the release of encapsulated drugs and demonstrated a better, sustained-release performance as it sterically inhibits both non-specific and specific protein interaction on the surface of liposomes (Nag & Awasthi, 2013). PEG moiety located on the surface of the liposome eliminates the faster uptake of liposome by the RES by forming a protective layer “steric effect” that minimizes protein binding (opsonins binding) to liposomes and subsequent uptake by macrophage (Yang et al., 2007) (Drummond, Meyer, Hong, Kirpotin, & Papahadjopoulos, 1999).

Another rationale for the use of PEGylated liposomes is to reduce the toxicity profile of DNR (such as cardiotoxicity) with a decrease in acute adverse effects (such as nausea and vomiting). Low peak plasma concentrations of free drug (anthracycline doxorubicin) and decreased cardiotoxicity was observed after administration of PEGylated liposomes compared with free drug due to reduced

tendency of the liposomal drug to accumulate in cardiac tissue (Gabizon, Shmeeda, & Barenholz, 2003).

Incorporation of short-chain ceramide into the liposomal bilayer did not enhance DNR leakage ($p > 0.05$) compared to the same formulation without ceramide. Apparently, incorporation of sphingolipid (C6-Cer) did not affect DNR diffusion through the liposomal bilayer.

A higher drug: lipid ratio in liposomes lead to reduced release of encapsulated drugs that precipitate in the liposome interior because drug release from liposome is not governed by the usual Fick's law relationship (Johnston et al., 2006). In other words, the percent of drug released over time is dependent on the initial interior drug concentration. The release of drugs from liposomal formulations follows Fick's law of diffusion only if they do not precipitate in the liposome interior as in ciprofloxacin (Johnston et al., 2008).

The release of anthracycline drugs such as doxorubicin and DNR from liposomes is highly dependent on the drug: lipid ratio because they encapsulated as precipitates in the liposome interior (Abraham et al., 2004). The release rate is proportional to the concentration of dissolved drug, which will remain constant until all of the precipitated form has dissolved. As a result, the time required for drug release will be directly proportional to the amount of drug in the precipitated form (Johnston et al., 2008). A higher drug: lipid ratio in liposomes is most likely to cause zero order slow release of the encapsulated anthracycline drugs since they will mainly exist in nanocrystal form, which has low tendency to donate its proton to the ammonium internalized in liposomes (Wei et al., 2018).

Formulations with a drug: lipid ratio between 0.1 and 0.6 exhibit optimized release properties (Johnston et al., 2006); however, the EE must be considered as well when selecting the drug: lipid ratio. Drug: lipid ratio of 1:5 used in our formulations did not reduce the release of DNR from liposomes relative to time to a significant extent, in which case, the formulations would have little therapeutic value because of complete drug retention. RES will ultimately take liposomes even if they are formulated as stealth liposomes (S. D. Li & Huang, 2009).

2.4.4 Cytotoxicity of Liposomal Formulations *In Vitro*

To investigate if DNR-C6-Cer has improved anti-proliferation activity, the B16-BL6 cells were treated with DNR formulations at different concentrations (0.01-1 uM). As is shown in Figure 2.5A, liposome with C6-Cer (F1) exhibited the highest cytotoxicity compared to other liposomal formulations (F2 and F3).

As shown in Figure 2.5B, the cell toxicity (0.05 uM, 48 hours) due to liposomes with C6-Cer (F1), F2, F3, and free DNR was 51, 70, 69.6 and 81%, respectively. The IC_{50} of F1 was about 10-fold lower than DNR solution (0.05 uM compared to 0.5 uM) ($p < 0.001$). The IC_{50} of F1 was about 4-fold lower than F2 and F3 liposomes (0.05 uM compared to 0.2 uM) ($p < 0.01$). There was no significant difference in cytotoxicity between F2 and F3.

Low specificity of conventional anti-cancer drugs, which cause several toxic side effects, usually limit the increase in the dose required for eradicating the cancerous growth (Nurgali, Jagoe, & Abalo, 2018). One of the most evolved strategies developed in the last two decades was the enhancement of the tumor-specific delivery of the chemotherapeutic agents.

Liposomal drug formulations have been used to enhance the therapeutic efficacy and significantly reduce the toxic effect of anticancer agents on healthy tissues, including the anthracycline drug DNR. Furthermore, they impact the pharmacokinetics and tissue distribution of the incorporated anticancer agent (Olusanya, Haj Ahmad, Ibegbu, Smith, & Elkordy, 2018).

Anthracyclines, such as DNR and doxorubicin, are the mainstay of therapy for different cancers like acute myeloid leukemia (AML) and metastatic breast cancer. However, their use has been limited by the associated toxicities, including myelosuppression, alopecia, stomatitis, and most importantly, cardiotoxicity (Watts, 1991).

Liposome based anthracyclines drugs were developed to enhance tumor targeting in order to lower their systemic side effects. However, those formulations have demonstrated similar efficacy to conventional therapy while improving the safety profile (Rivera, 2003). Liposomal doxorubicin was not absorbed rapidly by MCF7 cells and exhibited no superior efficacy towards the doxorubicin-resistant strain (MCF7-adr). Hence, various chemical modifications of liposomal formulations have been made (e.g. active targeting) to improve their uptake rate and, consequently, their antitumor activity (W. Wang et al., 2017).

In our study, we altered the membrane permeability of the tumor cells by using C6-Cer. The distribution of lipids across the plasma membrane is asymmetrical among the inner and outer layers. The outer layer is predominantly composed of sphingolipids, e.g., sphingomyelin and glycosphingolipids. Using of

a lipid analog to those located in the outer membrane, like C6-Cer, enhanced the membrane permeability and increased the cellular uptake of chemotherapeutic drugs by cancer cells (Chen, Alrbyawi, Poudel, Arnold, & Babu, 2019; van Lummel et al., 2011). Short-chain ceramides, such as C6-Cer, modify the permeability of the tumor cell membrane through channel formation (Elrick, Fluss, & Colombini, 2006). Such membrane voids might enhance membrane permeability of DNR.

In the present study, we demonstrated *in vitro* a strong enhancement of DNR delivery into B16-BL6 tumor cells. Liposomal formulation enriched with C6-Cer resulted in strong cytotoxic activity *in vitro* compared to the same formulation without ceramide. Incorporation of C6-Cer in liposomal formulations reduced the IC_{50} approximately 4-fold, from 0.05 to 0.2 uM, compared to the same formulation without ceramide. A blank liposomal formulation (no drug) containing C6-Cer did not exhibit any effect on cell survival. This indicates that the increased efficacy is most likely due to enhanced DNR uptake as a result of the incorporation of C6-Cer.

2.4.5 Cellular Uptake Studies

The cellular uptake of free DNR, F1 and F3 was also measured in B16-BL6 cell lines. After 16 h incubation at 14 uM concentration, the cellular uptake of different formulations was measured using flow cytometry analysis. The results show that the uptake of F1 was 3–fold higher than that of F2 and 2–fold higher than that of the free DNR. This further confirmed that the addition of C6-Cer to liposomal formulation significantly enhanced the cellular uptake of DNR (Figure

2.6A and 2.6B).

The main challenge in liposomal delivery to tumor tissue is lack of rapid cellular accumulation; as a result, liposomes are washed out before incorporation of encapsulated drug in the target cells (Hatakeyama et al., 2007). F1 showed much higher DNR fluorescence within cells compared to F2 ($p < 0.001$). This indicates that the addition of C6-Cer increased the cellular uptake of DNR. It should be noted that the activity of a drug, like DNR, depends mainly upon its intracellular concentration, which is primarily determined by the kinetics of its influx and efflux across the cell membrane (Ma et al., 2009).

The mechanism by which C6-Cer enhances the cellular uptake, hence the cytotoxic effect, of DNR is not fully understood; however, it was proposed that ceramides, when incorporated into the liposomal bilayer, facilitate drug trans-membrane diffusion by making the plasma membrane more permeable through damage to the bilayer asymmetry across the cell membrane (Veldman et al., 2005). Ceramide creates channels through the cell membrane and these channels have prolonged open lifetimes and large diameters, in excess of 10 nm (Siskind, Fluss, Bui, & Colombini, 2005)

Following 16 hours of incubation (14 μM DNR), the fluorescence levels were consistently higher in F1, intermediate in F2 and F3 and low in free DNR (Figure 2.7A). These data are in agreement with our flow cytometry data that C6-Cer enhanced the delivery of DNR into tumor cells.

C6-Cer enriched liposomes increased the nuclear accumulation of DNR to a greater extent. C6-Cer could change the physical properties of plasma membrane such as thickness and permeability through creating channels (Veldman, Zerp, van Blitterswijk, & Verheij, 2004). The channels within the lipid bilayer could facilitate DNR accumulation in the cells.

In order to investigate the interaction of C6-Cer with the cellular membrane, we incorporated fluorescent C6-Cer into the liposomal formulation encapsulated with DNR. Furthermore, we made a blank liposomal formulation with fluorescent C6-Cer. As shows in Figure 2.7B, C6-Cer interacted with the membrane bilayer allowing more DNR to accumulate in the nucleus. It is important to note that short-chain ceramides like C6-Cer are more effective than long-chain ceramides (C16-Cer and C24-Cer), which are unable to alter cell membranes structure due to their long and hydrophobic acyl chain that decrease fluidity and stabilize the membrane (Kim et al., 2016).

2.4.6 Reactive Oxygen Species (ROS)

Anthracycline drugs such as DNR could elevate the intracellular production of reactive oxygen species like hydrogen peroxide (S. Wang et al., 2004). There is a direct relationship between the drug concentration inside cells and ROS generation.

F1 exhibited the highest ROS production compared to F2, F3 and free DNR ($p < 0.01$) (Figure 2.8). On the other hand, there is no statistical significant difference between F2 and F3 ($p > 0.05$).

Anthracycline drugs are reduced by cancer cells to semiquinone, a free radical that produces O_2 •- in the presence of Oxygen. O_2 •- could be ultimately converted to hydrogen peroxide H_2O_2 (Wagner, Evig, Reszka, Buettner, & Burns, 2005). DNR induced ROS production in tumor cells and that was proportional to drug accumulation in tumor cells (Heasman, Zaitseva, Bowles, Rushworth, & Macewan, 2011).

ROS results in B16-BL6 cell line are correlated well with cellular uptake results, suggesting C6-Cer liposomes enhance DNR uptake by the tumor cells. Since the liposomal formulation with C6-Cer showed much higher ROS production in B16-BL6 cells after 24 hours incubation compared to the same formulation without C6-Cer ($p < 0.01$), such finding indicates that the addition of C6-Cer has increased the cellular uptake of DNR in tumor cells.

2.4.7 Short-Term Stability of Liposomal Formulations

Physical stability of different PEGylated liposomes during storage (4°C for one month) was followed by measuring time-dependent changes in liposome size, EE%, DL%, zeta potential and polydispersity index (Table 2.3). There were no significant changes in any parameter during the stability study compared to the data to that of the initial analysis.

Ceramide stabilizes lipid rafts; as a result, long-term storage instability of PEGylated liposomes in the presence of ceramide is unlikely (Zolnik et al., 2008). Furthermore, the introduction of cholesterol, less than 50%, decreased the fluidity of the lipid bilayer, leading to higher physical stability (Love, Amos, Kellaway, & Williams, 1990). It is important to mention that the drug: lipid ratio can greatly

affect liposomal stability. Since anthracycline drugs precipitate as fibrous-bundle aggregates in liposomes (X. Li et al., 1998), high drug: lipid ratio might cause liposomal deformation. Drug: lipid ratio of 1:5 used in our formulations did not cause liposomal membrane deformation, which explains good stability profiles of liposomal formulations, especially in terms of EE.

2.5 Conclusions

Liposomes were prepared at a 1:5 molar ratio of drug to lipid, with a narrow particle size distribution, high EE% and desirable DNR release kinetics. The optimum liposome formulation had 45:33:5:17 molar ratio for lipid/ cholesterol/DSPE-mPEG(2000)/ ceramide. This formulation exhibited high drug encapsulation efficiency (>90%), small size (~100 nm), a narrow size distribution (~0.2) and good release and stability profiles. Furthermore, the formulation exhibited a higher cellular uptake and cytotoxic effect on the B16-BL6 cell line than free DNR or liposomes with no ceramide. Therefore, this formulation appears to be a promising delivery system for the treatment of melanoma.

2.6 References

Abraham, S. A., Edwards, K., Karlsson, G., Hudon, N., Mayer, L. D., & Bally, M. B. (2004). An evaluation of transmembrane ion gradient-mediated encapsulation of topotecan within liposomes. *J Control Release, 96*(3), 449-461. doi: 10.1016/j.jconrel.2004.02.017

Abu Lila, A. S., & Ishida, T. (2017). Liposomal Delivery Systems: Design Optimization and Current Applications. *Biol Pharm Bull, 40*(1), 1-10. doi: 10.1248/bpb.b16-00624

Ait-Oudhia, S., Mager, D. E., & Straubinger, R. M. (2014). Application of pharmacokinetic and pharmacodynamic analysis to the development of liposomal formulations for oncology. *Pharmaceutics, 6*(1), 137-174. doi: 10.3390/pharmaceutics6010137

Akbarzadeh, A., Rezaei-Sadabady, R., Davaran, S., Joo, S. W., Zarghami, N., Hanifehpour, Y., . . . Nejati-Koshki, K. (2013). Liposome: classification, preparation, and applications. *Nanoscale Res Lett, 8*(1), 102. doi: 10.1186/1556-276X-8-102

Bartlett, G. R. (1959). Phosphorus assay in column chromatography. *J Biol Chem, 234*(3), 466-468.

Bellott, R., Auvrignon, A., Leblanc, T., Perel, Y., Gandemer, V., Bertrand, Y., . . . Robert, J. (2001). Pharmacokinetics of liposomal daunorubicin (DaunoXome) during a phase I-II study in children with relapsed acute lymphoblastic leukaemia. *Cancer Chemother Pharmacol, 47*(1), 15-21. doi: 10.1007/s002800000206

Bhatia, S., Tykodi, S. S., & Thompson, J. A. (2009). Treatment of metastatic melanoma: an overview. *Oncology (Williston Park), 23*(6), 488-496.

Chen, L., Alrbyawi, H., Poudel, I., Arnold, R. D., & Babu, R. J. (2019). Co-delivery of Doxorubicin and Ceramide in a Liposomal Formulation Enhances Cytotoxicity in Murine B16BL6 Melanoma Cell Lines. *AAPS PharmSciTech, 20*(3), 99. doi: 10.1208/s12249-019-1316-0

Childhood Acute Lymphoblastic Leukaemia Collaborative, G. (2009). Beneficial and harmful effects of anthracyclines in the treatment of childhood acute lymphoblastic leukaemia: a systematic review and meta-analysis. *Br J Haematol, 145*(3), 376-388. doi: 10.1111/j.1365-2141.2009.07624.x

Crivellari, D., Lombardi, D., Spazzapan, S., Veronesi, A., & Toffoli, G. (2004). New oral drugs in older patients: a review of idarubicin in elderly patients. *Crit Rev Oncol Hematol, 49*(2), 153-163. doi: 10.1016/S1040-8428(03)00120-3

Deamer, D. W., Prince, R. C., & Crofts, A. R. (1972). The response of fluorescent amines to pH gradients across liposome membranes. *Biochim Biophys Acta, 274*(2), 323-335.

Drummond, D. C., Meyer, O., Hong, K., Kirpotin, D. B., & Papahadjopoulos, D. (1999). Optimizing liposomes for delivery of chemotherapeutic agents to solid tumors. *Pharmacol Rev, 51*(4), 691-743.

Elrick, M. J., Fluss, S., & Colombini, M. (2006). Sphingosine, a product of ceramide hydrolysis, influences the formation of ceramide channels. *Biophys J, 91*(5), 1749-1756. doi: 10.1529/biophysj.106.088443

Fenske, D. B., Chonn, A., & Cullis, P. R. (2008). Liposomal nanomedicines: an emerging field. *Toxicol Pathol, 36*(1), 21-29. doi: 10.1177/0192623307310960

Fielding, R. M. (1991). Liposomal drug delivery. Advantages and limitations from a clinical pharmacokinetic and therapeutic perspective. *Clin Pharmacokinet, 21*(3), 155-164. doi: 10.2165/00003088-199121030-00001

Gabizon, A., Shmeeda, H., & Barenholz, Y. (2003). Pharmacokinetics of pegylated liposomal Doxorubicin: review of animal and human studies. *Clin Pharmacokinet, 42*(5), 419-436. doi: 10.2165/00003088-200342050-00002

Hatakeyama, H., Akita, H., Kogure, K., Oishi, M., Nagasaki, Y., Kihira, Y., . . . Harashima, H. (2007). Development of a novel systemic gene delivery system for cancer therapy with a tumor-specific cleavable PEG-lipid. *Gene Ther, 14*(1), 68-77. doi: 10.1038/sj.gt.3302843

Heasman, S. A., Zaitseva, L., Bowles, K. M., Rushworth, S. A., & Macewan, D. J. (2011). Protection of acute myeloid leukaemia cells from apoptosis induced by front-line chemotherapeutics is mediated by haem oxygenase-1. *Oncotarget, 2*(9), 658-668. doi: 10.18632/oncotarget.321

Hood, R. R., Vreeland, W. N., & DeVoe, D. L. (2014). Microfluidic remote loading for rapid single-step liposomal drug preparation. *Lab Chip, 14*(17), 3359-3367. doi: 10.1039/c4lc00390j

Immordino, M. L., Dosio, F., & Cattel, L. (2006). Stealth liposomes: review of the basic science, rationale, and clinical applications, existing and potential. *Int J Nanomedicine, 1*(3), 297-315.

Johnston, M. J., Edwards, K., Karlsson, G., & Cullis, P. R. (2008). Influence of drug-to-lipid ratio on drug release properties and liposome integrity in liposomal doxorubicin formulations. *J Liposome Res, 18*(2), 145-157. doi: 10.1080/08982100802129372

Johnston, M. J., Semple, S. C., Klimuk, S. K., Edwards, K., Eisenhardt, M. L., Leng, E. C., . . . Cullis, P. R. (2006). Therapeutically optimized rates of drug release can be achieved by varying the drug-to-lipid ratio in liposomal vincristine formulations. *Biochim Biophys Acta, 1758*(1), 55-64. doi: 10.1016/j.bbamem.2006.01.009

Kim, Y. A., Day, J., Lirette, C. A., Costain, W. J., Johnston, L. J., & Bittman, R. (2016). Synthesis and photochemical properties of PEGylated coumarin-caged ceramides for cell studies. *Chem Phys Lipids, 194*, 117-124. doi: 10.1016/j.chemphyslip.2015.07.006

Kolesnick, R. N., & Kronke, M. (1998). Regulation of ceramide production and apoptosis. *Annu Rev Physiol, 60*, 643-665. doi: 10.1146/annurev.physiol.60.1.643

Larsen, A. K., Escargueil, A. E., & Skladanowski, A. (2000). Resistance mechanisms associated with altered intracellular distribution of anticancer agents. *Pharmacol Ther, 85*(3), 217-229.

Li, S. D., & Huang, L. (2009). Nanoparticles evading the reticuloendothelial system: role of the supported bilayer. *Biochim Biophys Acta, 1788*(10), 2259-2266. doi: 10.1016/j.bbamem.2009.06.022

Li, X., Hirsh, D. J., Cabral-Lilly, D., Zirkel, A., Gruner, S. M., Janoff, A. S., & Perkins, W. R. (1998). Doxorubicin physical state in solution and inside liposomes loaded via a pH gradient. *Biochim Biophys Acta, 1415*(1), 23-40.

Li, Y., Li, S., Qin, X., Hou, W., Dong, H., Yao, L., & Xiong, L. (2014). The pleiotropic roles of sphingolipid signaling in autophagy. *Cell Death Dis, 5*, e1245. doi: 10.1038/cddis.2014.215

Love, W. G., Amos, N., Kellaway, I. W., & Williams, B. D. (1990). Specific accumulation of cholesterol-rich liposomes in the inflammatory tissue of rats with adjuvant arthritis. *Ann Rheum Dis, 49*(8), 611-614.

Luke, J. J., & Schwartz, G. K. (2013). Chemotherapy in the management of advanced cutaneous malignant melanoma. *Clin Dermatol, 31*(3), 290-297. doi: 10.1016/j.clindermatol.2012.08.016

Ma, P., Dong, X., Swadley, C. L., Gupte, A., Leggas, M., Ledebur, H. C., & Mumper, R. J. (2009). Development of idarubicin and doxorubicin solid lipid nanoparticles to overcome Pgp-mediated multiple drug resistance in leukemia. *J Biomed Nanotechnol, 5*(2), 151-161.

Ma, P., & Mumper, R. J. (2013). Anthracycline Nano-Delivery Systems to Overcome Multiple Drug Resistance: A Comprehensive Review. *Nano Today, 8*(3), 313-331. doi: 10.1016/j.nantod.2013.04.006

Mayer, L. D., Tai, L. C., Bally, M. B., Mitilenes, G. N., Ginsberg, R. S., & Cullis, P. R. (1990). Characterization of liposomal systems containing doxorubicin entrapped in response to pH gradients. *Biochim Biophys Acta, 1025*(2), 143-151.

McGowan, J. V., Chung, R., Maulik, A., Piotrowska, I., Walker, J. M., & Yellon, D. M. (2017). Anthracycline Chemotherapy and Cardiotoxicity. *Cardiovasc Drugs Ther, 31*(1), 63-75. doi: 10.1007/s10557-016-6711-0

Nag, O. K., & Awasthi, V. (2013). Surface engineering of liposomes for stealth behavior. *Pharmaceutics, 5*(4), 542-569. doi: 10.3390/pharmaceutics5040542

Nag, O. K., Yadav, V. R., Hedrick, A., & Awasthi, V. (2013). Post-modification of preformed liposomes with novel non-phospholipid poly(ethylene glycol)-conjugated hexadecylcarbamoylmethyl hexadecanoic acid for enhanced circulation persistence in vivo. *Int J Pharm, 446*(1-2), 119-129. doi: 10.1016/j.ijpharm.2013.02.026

Nicholas, A. R., Scott, M. J., Kennedy, N. I., & Jones, M. N. (2000). Effect of grafted polyethylene glycol (PEG) on the size, encapsulation efficiency and permeability of vesicles. *Biochim Biophys Acta, 1463*(1), 167-178.

Nielsen, D., Maare, C., & Skovsgaard, T. (1996). Cellular resistance to anthracyclines. *Gen Pharmacol, 27*(2), 251-255.

Nurgali, K., Jagoe, R. T., & Abalo, R. (2018). Editorial: Adverse Effects of Cancer Chemotherapy: Anything New to Improve Tolerance and Reduce Sequelae? *Front Pharmacol, 9*, 245. doi: 10.3389/fphar.2018.00245

Olusanya, T. O. B., Haj Ahmad, R. R., Ibegbu, D. M., Smith, J. R., & Elkordy, A. A. (2018). Liposomal Drug Delivery Systems and Anticancer Drugs. *Molecules, 23*(4). doi: 10.3390/molecules23040907

Oskouian, B., & Saba, J. D. (2010). Cancer treatment strategies targeting sphingolipid metabolism. *Adv Exp Med Biol, 688*, 185-205.

Otsuka, H., Nagasaki, Y., & Kataoka, K. (2003). PEGylated nanoparticles for biological and pharmaceutical applications. *Adv Drug Deliv Rev, 55*(3), 403-419.

Paulusma, C. C., & Oude Elferink, R. P. (2006). Diseases of intramembranous lipid transport. *FEBS Lett, 580*(23), 5500-5509. doi: 10.1016/j.febslet.2006.06.067

Plourde, K., Derbali, R. M., Desrosiers, A., Dubath, C., Vallee-Belisle, A., & Leblond, J. (2017). Aptamer-based liposomes improve specific drug loading and release. *J Control Release, 251*, 82-91. doi: 10.1016/j.jconrel.2017.02.026

Rivera, E. (2003). Liposomal anthracyclines in metastatic breast cancer: clinical update. *Oncologist, 8 Suppl 2*, 3-9.

Rothkopf, C., Fahr, A., Fricker, G., Scherphof, G. L., & Kamps, J. A. (2005). Uptake of phosphatidylserine-containing liposomes by liver sinusoidal endothelial cells in the serum-free perfused rat liver. *Biochim Biophys Acta, 1668*(1), 10-16. doi: 10.1016/j.bbamem.2004.10.013

Roy Chaudhuri, T., Arnold, R. D., Yang, J., Turowski, S. G., Qu, Y., Spernyak, J. A., . . . Straubinger, R. M. (2012). Mechanisms of tumor vascular priming by a nanoparticulate doxorubicin formulation. *Pharm Res, 29*(12), 3312-3324. doi: 10.1007/s11095-012-0823-4

Samad, A., Sultana, Y., & Aqil, M. (2007). Liposomal drug delivery systems: an update review. *Curr Drug Deliv, 4*(4), 297-305.

Sandru, A., Voinea, S., Panaitescu, E., & Blidaru, A. (2014). Survival rates of patients with metastatic malignant melanoma. *J Med Life, 7*(4), 572-576.

Sercombe, L., Veerati, T., Moheimani, F., Wu, S. Y., Sood, A. K., & Hua, S. (2015). Advances and Challenges of Liposome Assisted Drug Delivery. *Front Pharmacol, 6*, 286. doi: 10.3389/fphar.2015.00286

Siskind, L. J., Fluss, S., Bui, M., & Colombini, M. (2005). Sphingosine forms channels in membranes that differ greatly from those formed by ceramide. *J Bioenerg Biomembr, 37*(4), 227-236. doi: 10.1007/s10863-005-6632-2

Tas, F. (2012). Metastatic behavior in melanoma: timing, pattern, survival, and influencing factors. *J Oncol, 2012*, 647684. doi: 10.1155/2012/647684

van Lummel, M., van Blitterswijk, W. J., Vink, S. R., Veldman, R. J., van der Valk, M. A., Schipper, D., . . . Koning, G. A. (2011). Enriching lipid nanovesicles with short-chain glucosylceramide improves doxorubicin delivery and efficacy in solid tumors. *FASEB J, 25*(1), 280-289. doi: 10.1096/fj.10-163709

Veldman, R. J., Koning, G. A., van Hell, A., Zerp, S., Vink, S. R., Storm, G., . . . van Blitterswijk, W. J. (2005). Coformulated N-octanoyl-glucosylceramide improves cellular delivery and cytotoxicity of liposomal doxorubicin. *J Pharmacol Exp Ther, 315*(2), 704-710. doi: 10.1124/jpet.105.087486

Veldman, R. J., Zerp, S., van Blitterswijk, W. J., & Verheij, M. (2004). N-hexanoyl-sphingomyelin potentiates in vitro doxorubicin cytotoxicity by enhancing its cellular influx. *Br J Cancer, 90*(4), 917-925. doi: 10.1038/sj.bjc.6601581

Wagner, B. A., Evig, C. B., Reszka, K. J., Buettner, G. R., & Burns, C. P. (2005). Doxorubicin increases intracellular hydrogen peroxide in PC3 prostate cancer cells. *Arch Biochem Biophys, 440*(2), 181-190. doi: 10.1016/j.abb.2005.06.015

Wang, S., Konorev, E. A., Kotamraju, S., Joseph, J., Kalivendi, S., & Kalyanaraman, B. (2004). Doxorubicin induces apoptosis in normal and tumor cells via distinctly different mechanisms. intermediacy of H(2)O(2)- and p53-dependent pathways. *J Biol Chem, 279*(24), 25535-25543. doi: 10.1074/jbc.M400944200

Wang, W., Shao, A., Zhang, N., Fang, J., Ruan, J. J., & Ruan, B. H. (2017). Cationic Polymethacrylate-Modified Liposomes Significantly Enhanced Doxorubicin Delivery and Antitumor Activity. *Sci Rep, 7*, 43036. doi: 10.1038/srep43036

Watts, R. G. (1991). Severe and fatal anthracycline cardiotoxicity at cumulative doses below 400 mg/m^2: evidence for enhanced toxicity with multiagent chemotherapy. *Am J Hematol, 36*(3), 217-218.

Wei, X., Shamrakov, D., Nudelman, S., Peretz-Damari, S., Nativ-Roth, E., Regev, O., & Barenholz, Y. (2018). Cardinal Role of Intraliposome Doxorubicin-Sulfate Nanorod Crystal in Doxil Properties and Performance. *ACS Omega, 3*(3), 2508-2517. doi: 10.1021/acsomega.7b01235

Yang, T., Cui, F. D., Choi, M. K., Cho, J. W., Chung, S. J., Shim, C. K., & Kim, D. D. (2007). Enhanced solubility and stability of PEGylated liposomal paclitaxel: in vitro and in vivo evaluation. *Int J Pharm, 338*(1-2), 317-326. doi: 10.1016/j.ijpharm.2007.02.011

Zhou, H., Summers, S. A., Birnbaum, M. J., & Pittman, R. N. (1998). Inhibition of Akt kinase by cell-permeable ceramide and its implications for ceramide-induced apoptosis. *J Biol Chem, 273*(26), 16568-16575.

Zolnik, B. S., Stern, S. T., Kaiser, J. M., Heakal, Y., Clogston, J. D., Kester, M., & McNeil, S. E. (2008). Rapid distribution of liposomal short-chain ceramide in vitro and in vivo. *Drug Metab Dispos, 36*(8), 1709-1715. doi: 10.1124/dmd.107.019679

Table 2.1: Composition and molar ratio of liposomal formulations

Ingredients	**F1**	**F2**	**F3***	**F4**
DSPC	45	45	10	45
Cholesterol	33	33	5	33
DSPE-mPEG (2000)	5	5	-	5
C6-Cer	17	-	-	17
DNR:lipid ratio	1:5	1:5	1:10:5	-

* Liposomal formulation similar to DaunoXome®
1:10:5 is the molar ratio of daunorubicin:DSPC:cholesterol
1:5 is the molar ratio of daunorubicin:total lipids

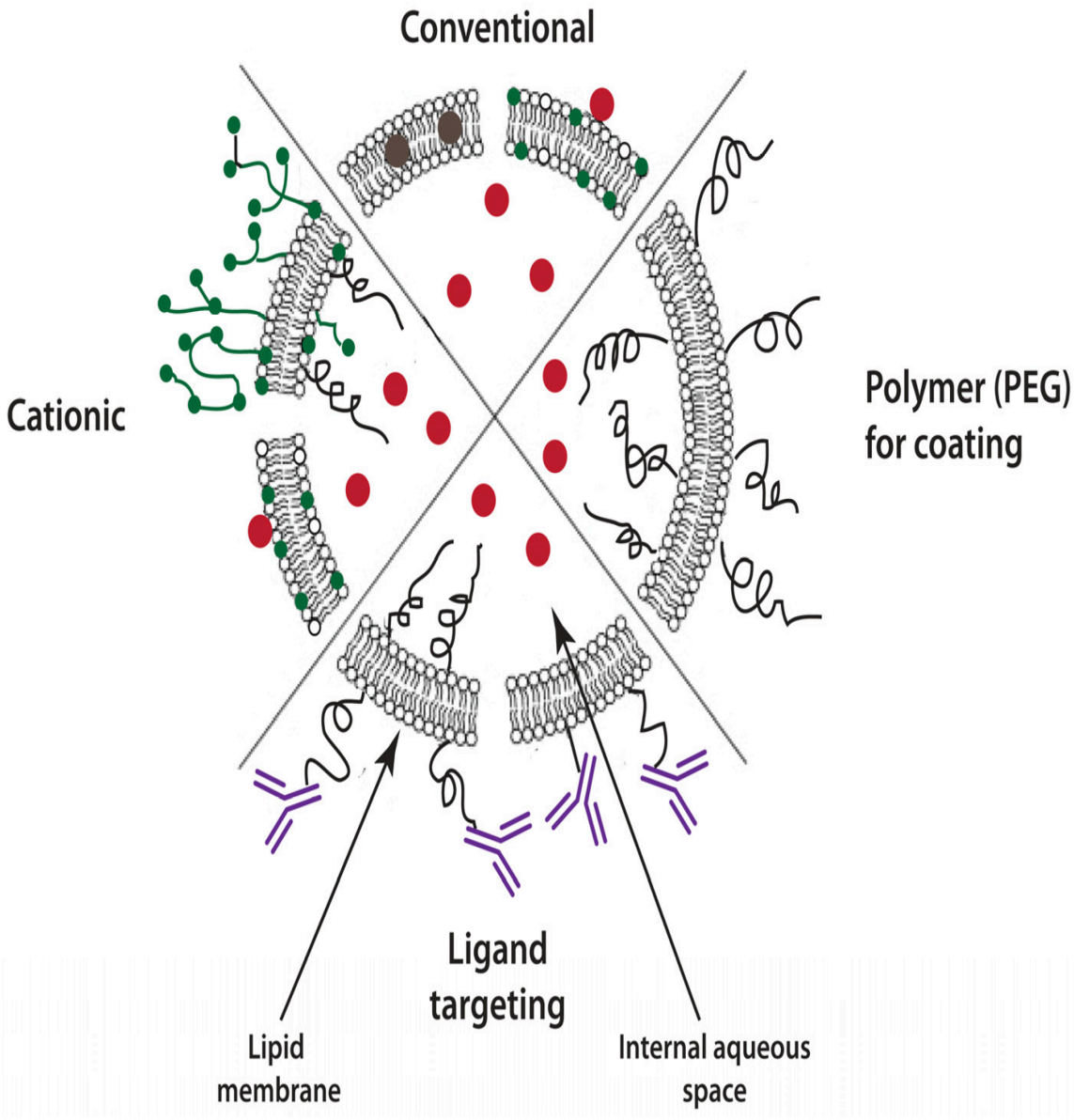

Figure 2.1: Sterically stabilized liposomes versus conventional liposomes (Ait-Oudhia, Mager, & Straubinger, 2014)

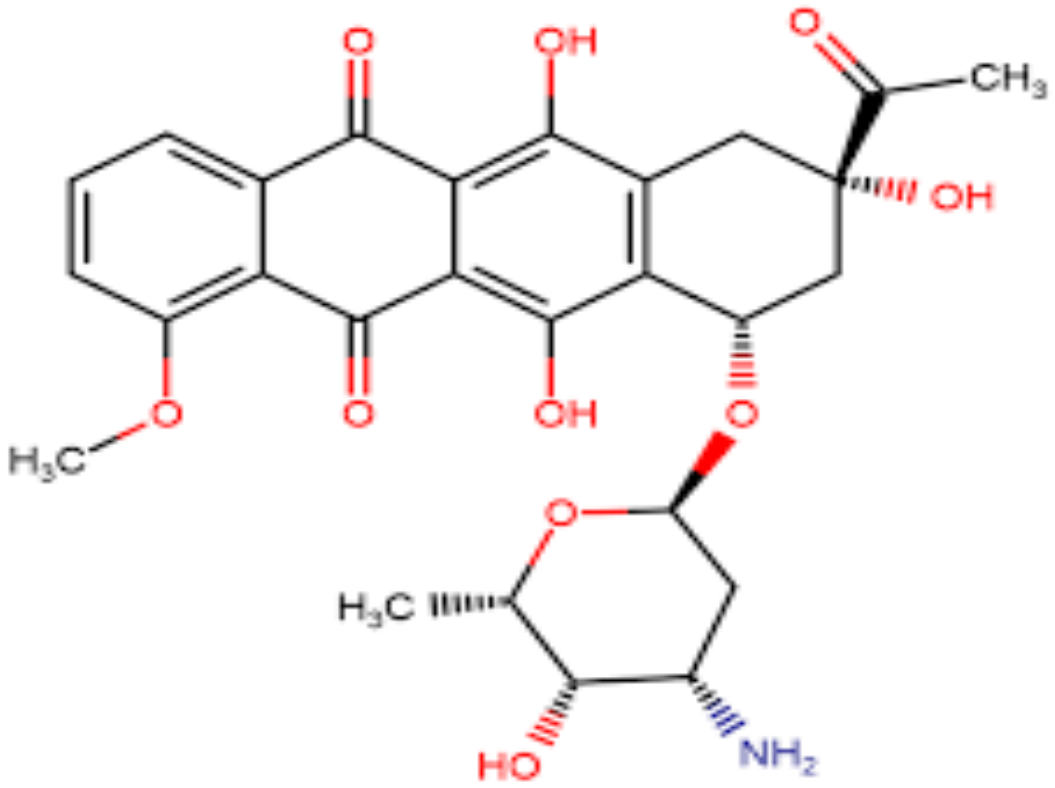

Figure 2.2: Chemical structure of daunorubicin

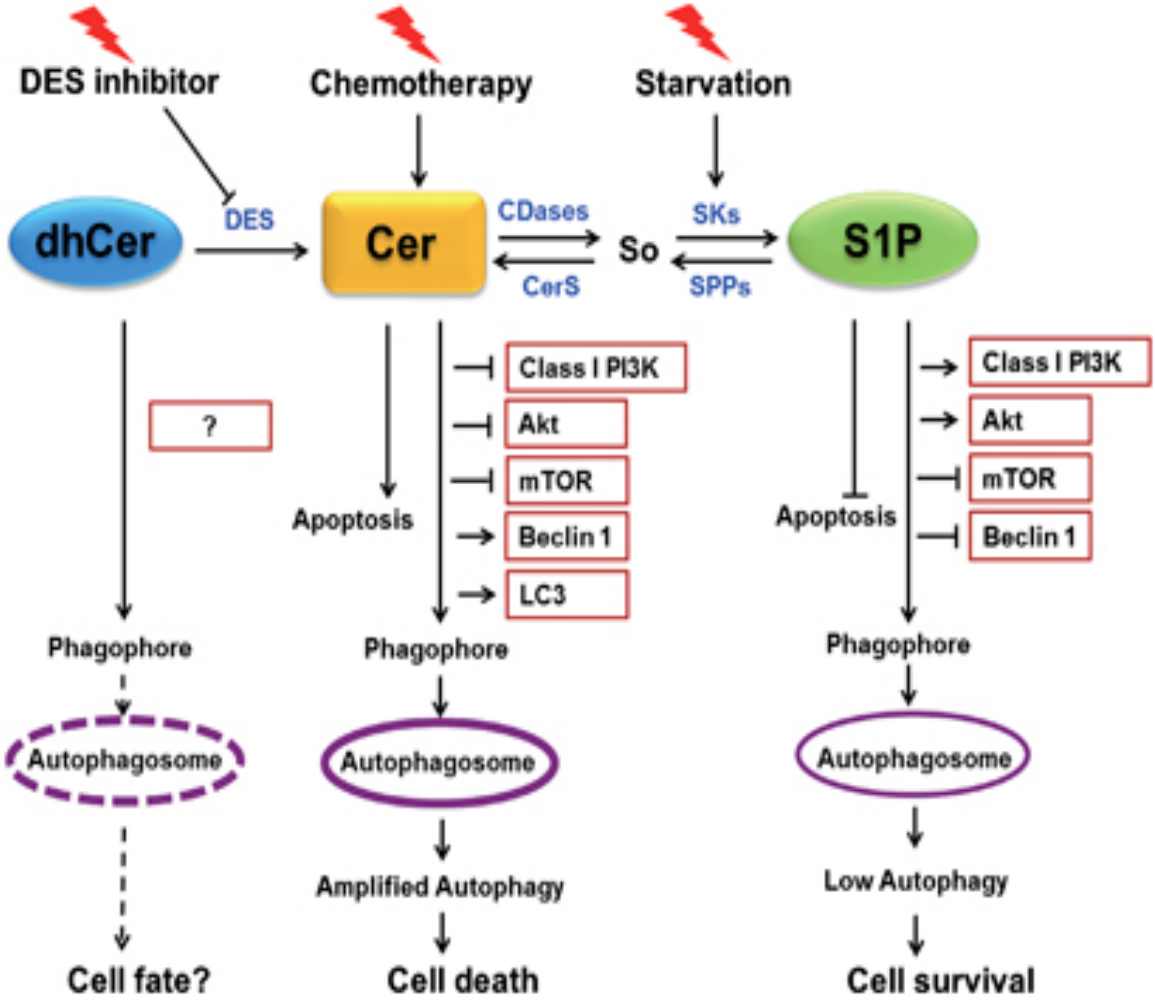

Figure 2.3: Ceramide inhibits Akt activation through a PI3K–dependent mechanism (Y. Li et al., 2014)

Table 2.2: Physicochemical characteristics of liposome formulations. (Mean ± standard deviation, n = 3)

DNR Liposomal Formulation	Encapsulation Efficiency %	Drug Loading (%)	Particle Size (nm)	PI	Zeta Potential (mV)
F1	91.0 ± 2.5	15.3 ± 0.71	103.0 ± 2.6	0.20 ± 0.015	-17.2 ± 1.4
F2	91.0 ± 2.0	15.3 ± 0.69	91.0 ± 2.0	0.26 ± 0.015	-28.1 ± 0.7
F3	95.0 ± 0.57	17.0 ± 0.57	81.0 ± 1.1	0.16 ± 0.010	-3.0 ± 1.3

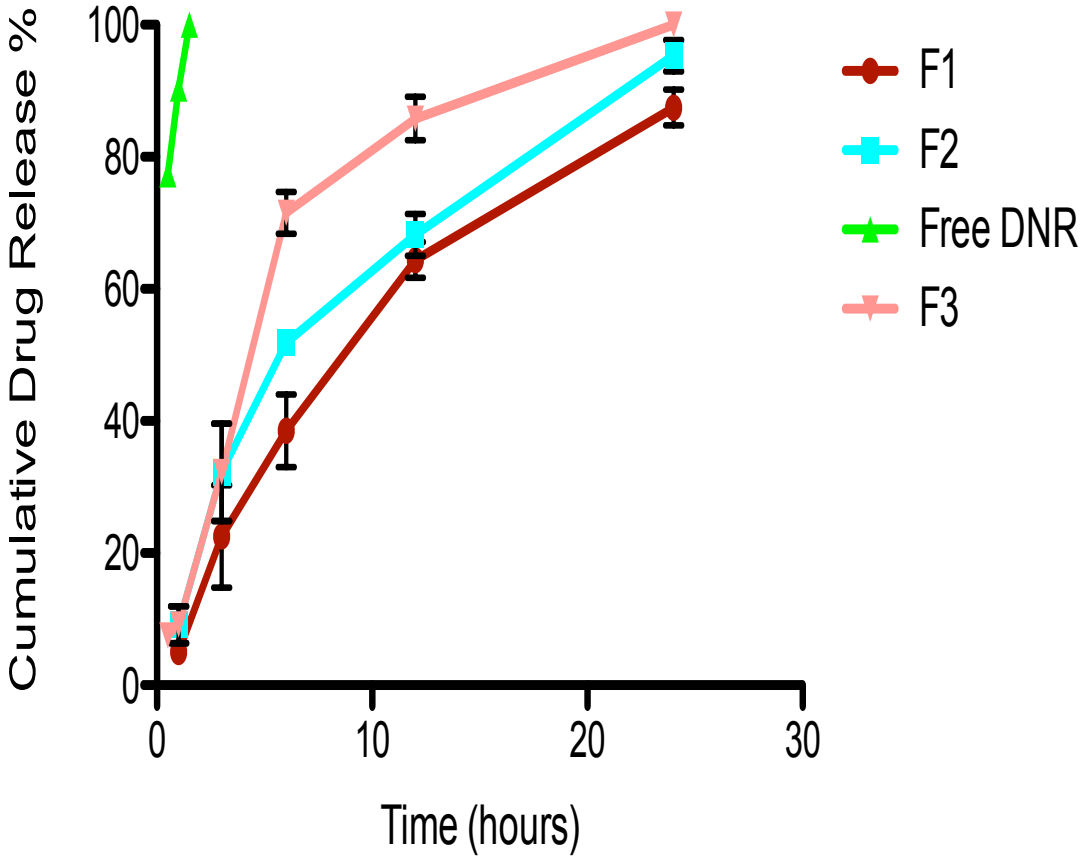

Figure 2.4: *In vitro* release profiles of DNR encapsulated liposomes in PBS (pH 7.4). Values represent Mean ± SD, n = 3

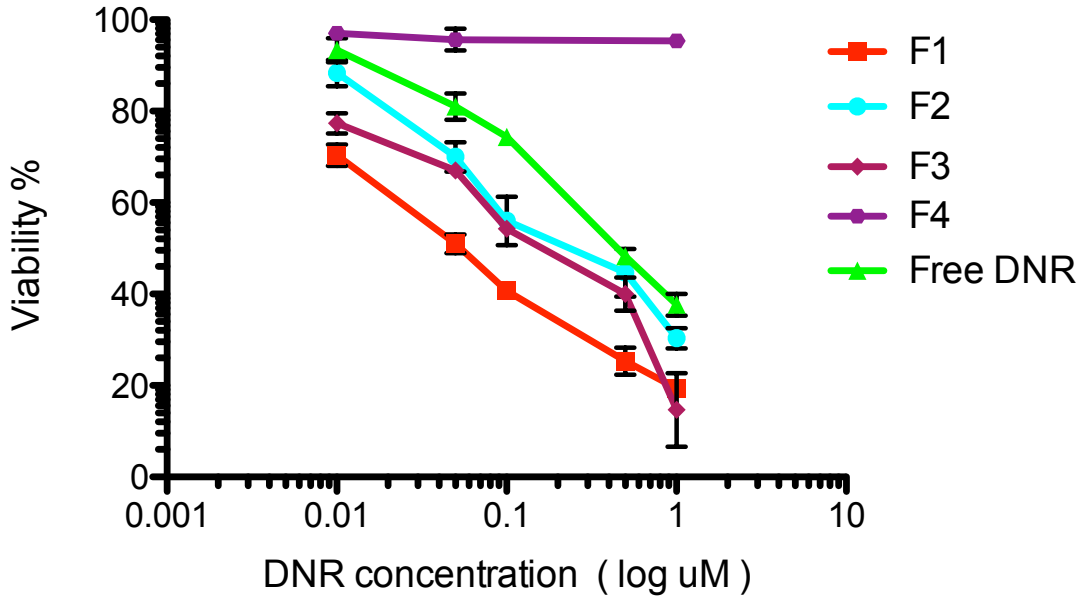

Figure 2.5A: Cytotoxic effect of DNR against B16-BL6 cell lines. All data are expressed as mean percentages (n=3) to untreated control cells

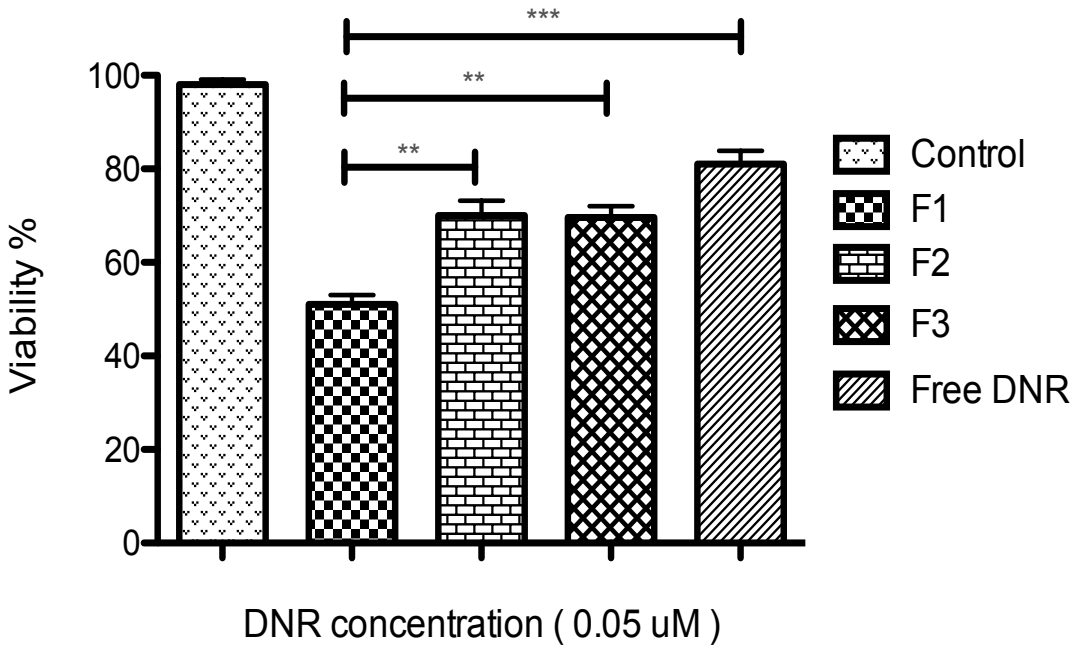

Figure 2.5B: *In vitro* cytotoxicity of liposomal formulations in B16-BL6 cell lines. ** indicates $p < 0.01$, and *** indicates $P < 0.001$. Mean ± SD of n = 3

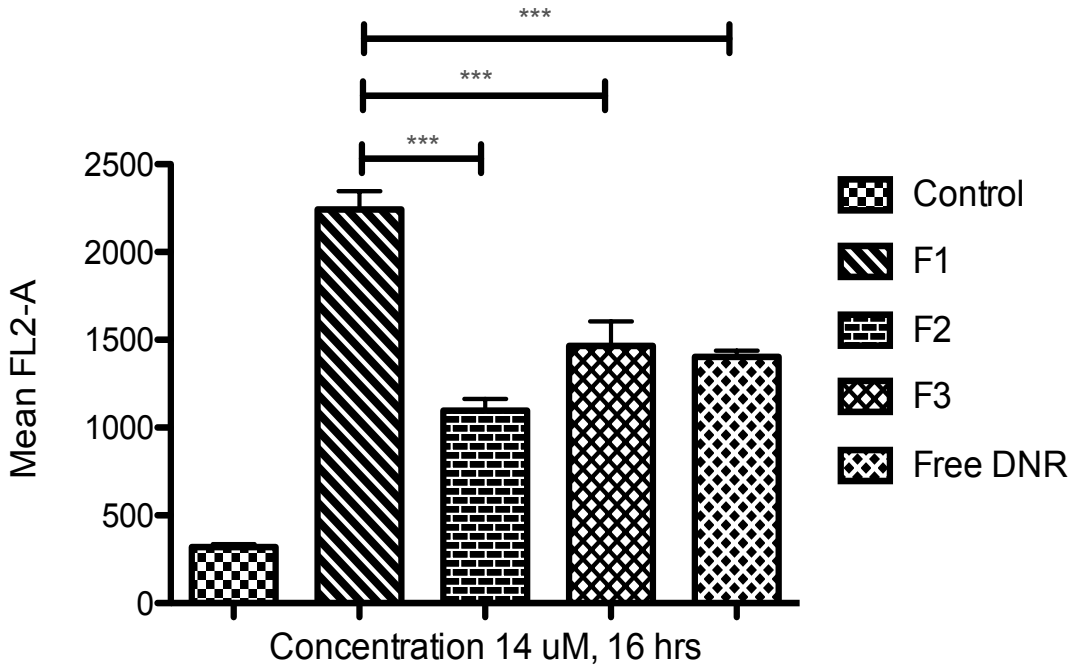

Figure 2.6A: DNR cellular uptake from liposome formulations analyzed by flow cytometry (EX 480 nm and EM 590 nm). 30,000 events were collected per sample. *** indicates $p < 0.001$. Mean ± SD of n = 3

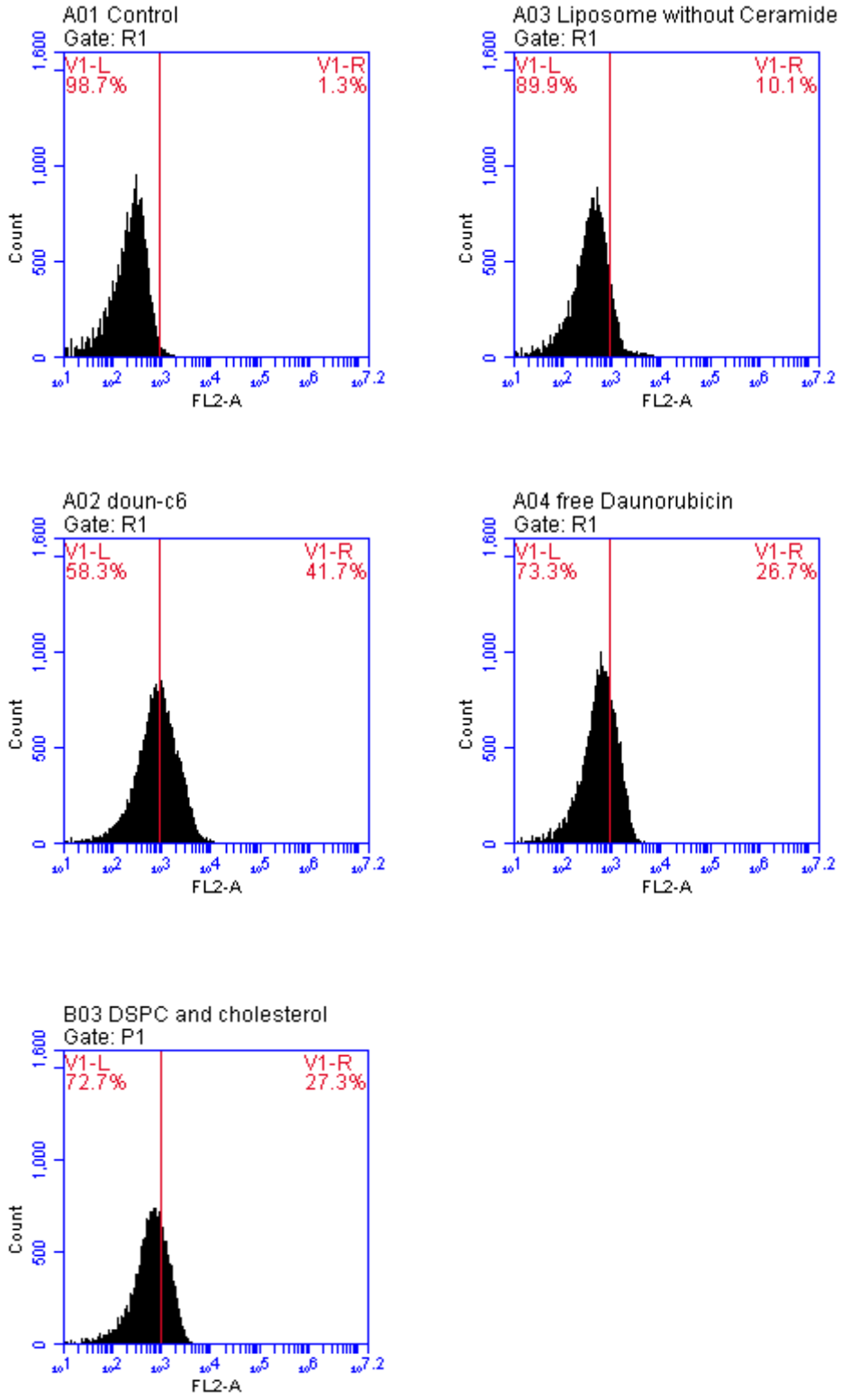

Figure 2.6B: DNR uptake studies on liposomal formulations analyzed by flow cytometry (EX 480 nm and EM 590 nm)

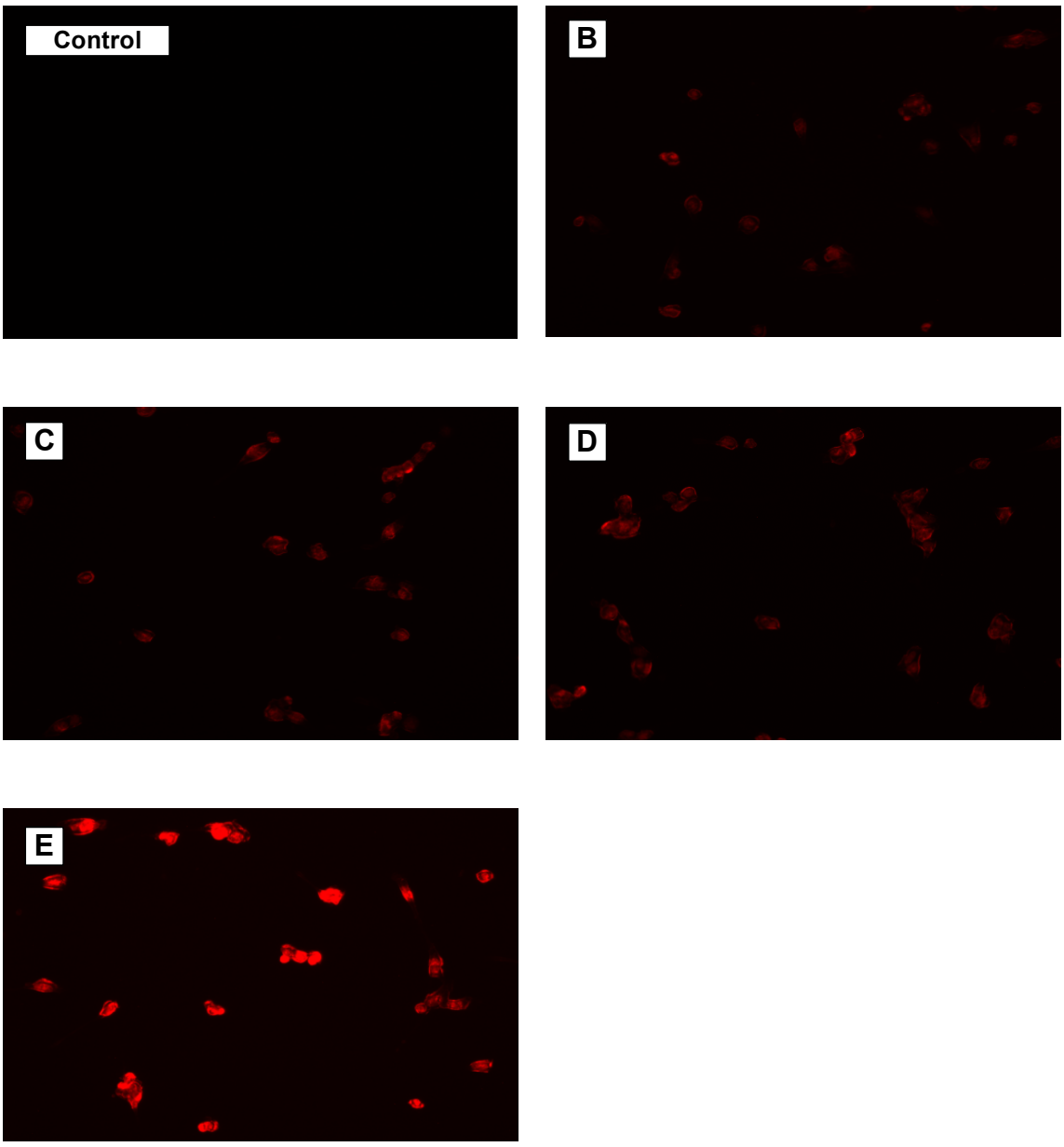

Figure 2.7A: Fluorescence microscopy showing C6-Cer enhanced DNR uptake from liposomes. B16-BL6 cells were treated with free DNR (B), or F3 (C), or F2 (D), or F1 (E). Final liposomal DNR concentrations were 14 uM

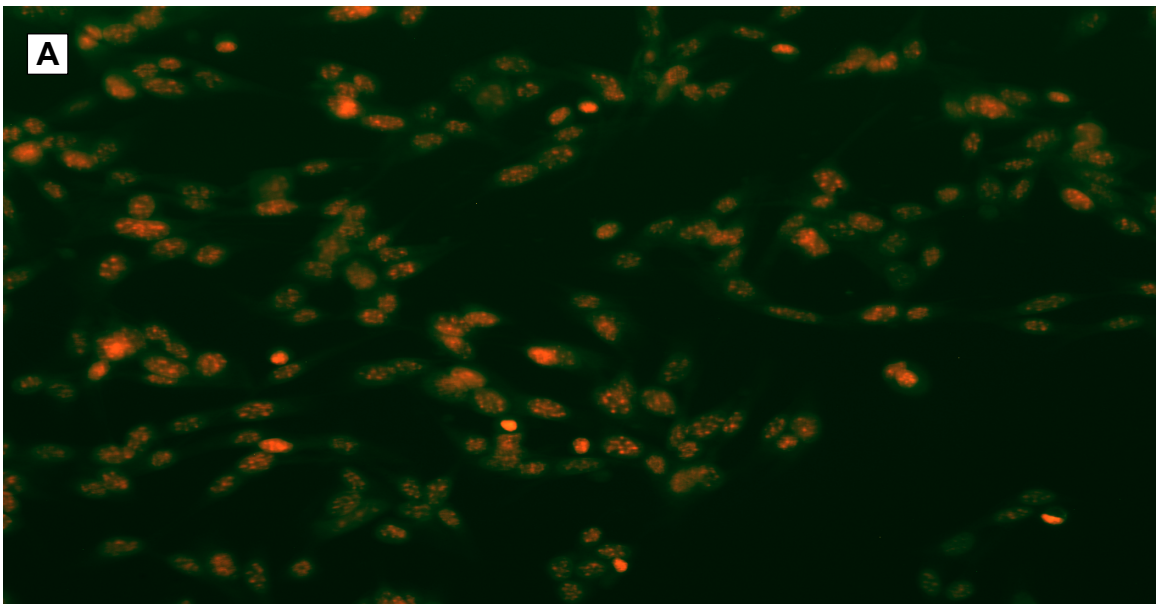

Red color represents DNR while green color represents fluorescent C6-Cer

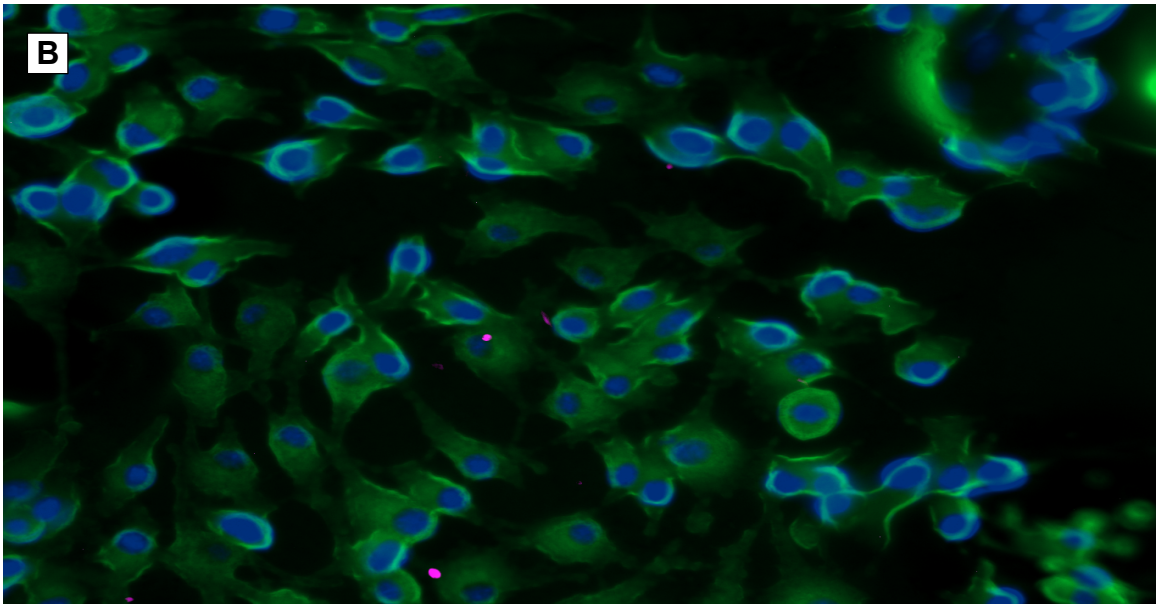

Figure 2.7B: Fluorescence microscopy showing C6-Cer interacting with the cellular membrane (A) fluorescent C6-Cer liposomal formulation encapsulated with DRN (B) fluorescent C6-Cer liposomal formulation. Final liposomal DNR concentrations were 14 uM

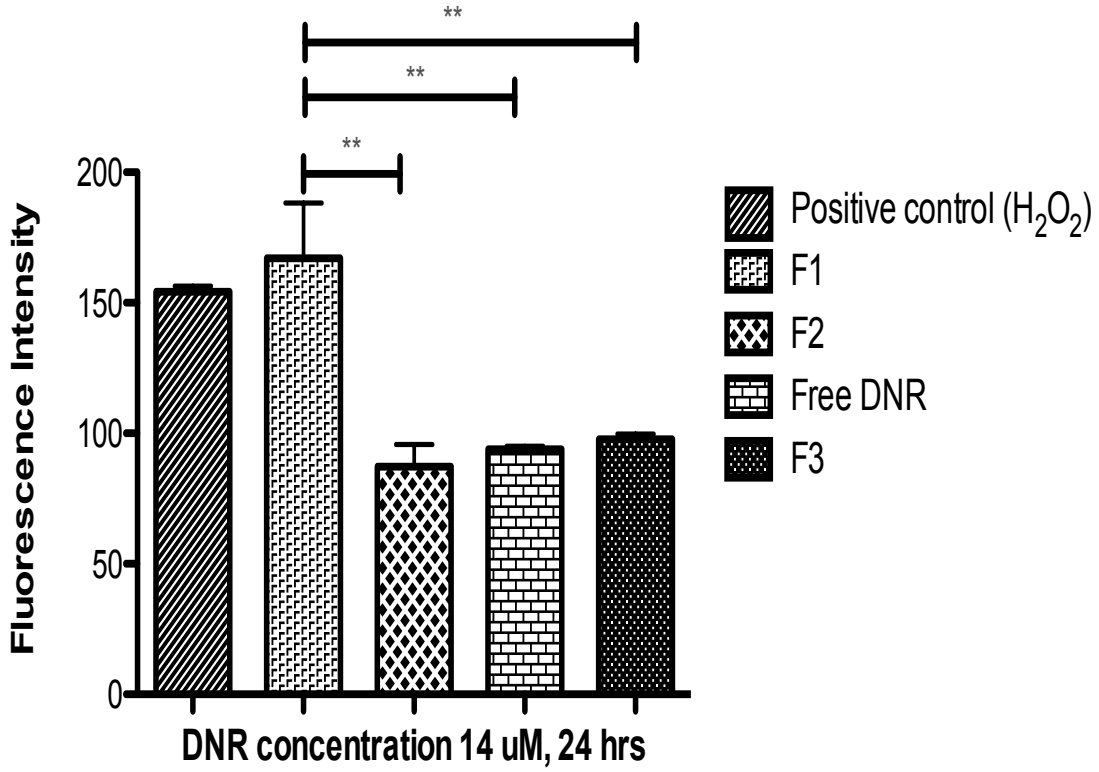

Figure 2.8: DNR-induced ROS generation in B16-BL6 cell lines. Cells were treated for 24 h with free and liposomal DNR (14 uM) and H_2O_2 (0.01%) as a positive control. Data corrected for cellular protein content and represented as means ± SD of three independent experiments. ** indicates $p < 0.01$

Table 2.3: Stability study of liposome formulations. Values represented as mean ± SD, n = 3

	Fresh formulation			After 1 month		
Formulation	F1	F2	F3	F1	F2	F3
Particle Size (nm)	103.0 ± 2.6	91.0 ± 2.0	81.0 ± 1.1	111.0 ± 1.3	98.0 ± 2.9	83.0 ± 2.2
PI	0.20 ± 0.02	0.26 ± 0.02	0.16 ± 0.01	0.22 ± 0.03	0.27 ± 0.03	0.19 ± 0.04
E.E %	91.0 ± 2.5	91.0 ± 2.0	95.0 ± 0.57	89.0 ± 2.7	90.0 ± 3.7	93.0 ± 1.9
D.L %	15.3 ± 0.71	15.3 ± 0.69	17.0 ± 0.57	14.7 ± 0.54	14.9 ± 1.3	16.0 ± 0.67
Zeta Potential (mV)	-17.2 ± 1.4	-28.1 ± 0.7	-3.0 ± 1.3	-15.1 ± 2.4	-24.6 ± 3.4	-5.0 ± 2.4

PI= Polydispersity Index; EE%= Encapsulation Efficiency; DL%= Drug Loading

Chapter 3. Cardiolipin Based pH-Sensitive Liposomes for Enhanced Cellular Uptake and Cytotoxicity of Daunorubicin in Melanoma (B16-BL6) Cell Lines

3.1 Abstract

Daunorubicin (DNR) and cardiolipin (CL) were co-delivered using a pH-sensitive liposomal system in B16-BL6 melanoma cell lines for enhanced cytotoxic effects. CL decreases the mechanical stability of the cell membrane by a decrease in lipid packing and formation of nonlamellar structures. DNR was encapsulated within liposomes and CL as a component of the lipid bilayer. PEGylated pH-sensitive liposomes, containing CL, were prepared in the molar ratio 40:30:5:17:8 for DOPE/cholesterol/DSPE-mPEG (2000)/CL using the lipid film hydration method and loaded with DNR (drug:lipid ratio 1:5). The CL liposomes exhibited high drug encapsulation efficiency (>90%), a small size (~94 nm), narrow size distribution (polydispersity index ~0.16) and a rapid release profile at acidic pH (within 1 h). Furthermore, the CL liposomes exhibited 12.5 and 5-fold higher cytotoxicity compared to DNR or liposomes similar to DaunoXome®. This study provides a basis for developing a co-delivery system of DNR and CL encapsulating liposomes for melanoma treatment.

3.2 Introduction

The American Cancer Society predicted that 96,480 new cases of melanoma would occur in 2019 (7% of all cancer cases). Of those cases, 7,230 patients are expected to die, predominantly because of widespread metastases (Siegel, Miller, & Jemal, 2019). Patients with stage IV disease, where cancer has metastases in distant visceral sites, have a 1-year survival rate of 41% (Zbytek et al., 2008).

Although treatment of primary cutaneous melanoma by surgery yields a high survival rate, advanced metastatic melanoma cannot be treated by surgery alone and, thus, requires better therapeutic methods (Liu & Sheikh, 2014). Since radiation therapy alone has also proven to be ineffective for treating metastatic melanoma, chemotherapeutic drugs such as dacarbazine and temozolomide are being used to medically manage metastatic melanomas (Barker & Lee, 2012).

Chemotherapeutic agents have been used for the treatment of metastatic melanoma for over three decades. However, The modest antitumor activity of the cytotoxic drugs led to investigation of combinations of these agents to improve therapeutic outcomes (Del Prete, Maurer, O'Donnell, Forcier, & LeMarbre, 1984). Combinations of cytotoxic drugs may yield higher response rates than monotherapy, but are associated with more significant side effects such as hematologic, gastrointestinal and cutaneous toxicities (Hamm et al., 2008). Targeted drug delivery devices typically are more effective than conventional treatments and usually exhibit fewer side effects and less systemic toxicity (Bahrami et al., 2017). These devices usually carry multiple components, such as

targeting agents, imaging agents and anticancer drugs, for optimized functions such as drug targeting to the tumor site and easy diagnosis.

The use of liposomes as drug delivery systems was highly successful due to their ability to enhance the solubility of poorly soluble drugs and to encapsulate a wide range of drugs. Besides, their efficiency, biocompatibility and nonimmunogenicity have increased their use as drug delivery systems (Deshpande, Biswas, & Torchilin, 2013).

Liposomes consist of a lipid bilayer with an aqueous phase where hydrophilic moieties can be entrapped while hydrophobic moieties can be localized into the bilayer membrane (Sercombe et al., 2015). Liposomes properties differ considerably with lipid composition since the lipid bilayer components determines their rigidity, size, release rate and surface charge. For instance, saturated phospholipids with long acyl chains (for example, DPPC) form a rigid and more stable bilayer structure compared to unsaturated phosphatidylcholine types. Incorporation of DSPE-PEG lipid into liposomes bilayer is critical for the prolongation of liposome circulation time in the blood stream (Gabizon, Goren, Cohen, & Barenholz, 1998). Another rationale for the use of PEGylated liposomes for DNR is to reduce cardiotoxicity and to decrease gastrointestinal side effects such as nausea and vomiting. PEGylated liposomes decreased cardiotoxicity due to the targeted delivery of anthracycline drugs and reduced tendency to accumulate in the cardiac tissue (Gabizon, Shmeeda, & Barenholz, 2003). Major obstacles to liposomal drug delivery are slow drug

release and the absence of fusogenic activity after internalization into the endosomal compartment (Sudimack, Guo, Tjarks, & Lee, 2002).

The development of pH-sensitive liposomes is a very promising strategy for cancer treatment. The concept is based on the fact that tumors usually have a lower pH than healthy tissue, and stimuli-sensitive liposomes can be prepared to release the incorporated drug only when subjected to this unique tumor condition (Torchilin, 2007). pH-sensitive liposomes have been designed to be stable at physiological pH, but to be destabilized upon acidification by tumor microenvironment, thereby promoting the release of their encapsulated contents (Y. Lee & Thompson, 2017).

Acidic extracellular pH is a major characteristic of tumor tissue (Figure 3.1), largely considered to be due to lactic acid secretion from anaerobic glycolysis in hypoxia and an excess amount of CO_2 production (Kato et al., 2013; Yoneda, Hiasa, Nagata, Okui, & White, 2015). In tumor microenvironment, a local pH range from 5.5 to 7.0 is not unusual (Gatenby & Gillies, 2004).

1,2-dioleoyl-sn-glycero-3-phosphoethanolamine (DOPE) is one of the critical components of pH-sensitive liposomes. When liposomes containing DOPE are incubated in acidic pH, they undergo destabilization. This effect is facilitated by low hydration of the polar head group of DOPE, which is converted to a hexagonal inverted phase causing the formation of non-lamellar structures that trigger destabilization of liposomes bilayers at acidic pH (Paliwal, Paliwal, & Vyas, 2015). pH-sensitive lipid DOPE has a strong propensity to form a nonbilayer structure at acidic pH, causing liposomes to release their contents in

response to acidic pH in the tumor microenvironment while remaining stable in plasma, thus enhancing the cytoplasmic delivery of different agents (Fattal, Couvreur, & Dubernet, 2004).

Non-bilayer lipids such as DOPE, which have a cone shape and will not form the bilayer alone, but can be stabilized in a bilayer structure by incorporation of bilayer preferring lipids such as phosphatidylserine (PS) or a weakly acidic amphiphile such as cholesteryl hemisuccinate (CHEMS) (Momekova, Rangelov, & Lambov, 2010). The incorporation of stabilizing lipids causes liposomal formulations to be stable at neutral pH. Under acidic conditions, the stabilizing lipid becomes partially protonated and loses its ability to stabilize the bilayer structure. Reducing stabilizing effect as a result of protonation of the stabilizing lipid will allow DOPE molecules to revert into their inverted hexagonal phase (Cullis & de Kruijff, 1979), thus destruction of liposomal bilayer organization and payload release (Figure 3.2).

Among phospholipid classes, Cardiolipin (CL) has an interesting chemical structure (Figure 3.3), being highly acid and having a head group (glycerol) that is esterified to two phosphatidylglyceride backbone fragments instead of one, forming a dimeric structure (Paradies, Paradies, De Benedictis, Ruggiero, & Petrosillo, 2014). CL lipid is crucial for both mitochondrial bioenergetics and many cellular processes outside of the mitochondria such as cell apoptosis and cell wall biogenesis (Shen, Ye, McCain, & Greenberg, 2015). Due to its unique structure, CL can have a nonbilayer propensity in the context of biomembranes, promoting local regions of high curvature because it forms inverted hexagonal

structures in isolation under certain conditions such as low pH (Malhotra et al., 2017). CL increases the bilayer fluidity as its presence introduces a higher unsaturation degree to the membrane bilayer (Unsay, Cosentino, Subburaj, & Garcia-Saez, 2013). Furthermore, when CL interacts with calcium across the membrane, it leads to changes in lipid packing and structure, increasing flip-flop motion of lipids (Gerritsen, de Kruijff, Verkleij, de Gier, & van Deenen, 1980). CL has some effects on the mechanical properties of the membrane. CL decreases the mechanical stability of the membrane due to a decrease in lipid packing and formation of nonlamellar structures, resulting in deformation of biological membrane (Sennato et al., 2005).

Daunorubicin (DNR), an anthracycline derivative, is a potent chemotherapy drug that exhibits broad-spectrum anti-tumor activity against a wide range of cancers, including blood malignant cancers (such as leukaemia and lymphoma), many types of solid (carcinoma), and soft (sarcomas) tissue tumors (Zunino, Giuliani, Savi, Dasdia, & Gambetta, 1982). It produces its anti-tumor activity by blocking topoisomerase 2, an enzyme that cancer cells need in order to divide and grow (Tacar, Sriamornsak, & Dass, 2013). Due to poor targeting efficiency, DNR has many side effects such as cardiotoxicity, acute vomiting and nausea, gastrointestinal problems, baldness, and disturbances to the neurological system (Hortobagyi, 1997). Compared with conventional anthracyclines, liposomal formulations of anthracyclines exhibit less toxicity because injected liposomes cannot pass the vascular space in sites that have tight capillary junctions, such as the heart muscle (Rafiyath et al., 2012). Due to

their ability to deliver drugs to their intended site of action, liposomal formulations antitumor efficacy is better or at least comparable to that of the conventional formulations (Sercombe et al., 2015).

The objective of this study is to determine the cytotoxicity and cellular uptake of pH-sensitive DNR liposomal formulation enriched with CL. It has been proposed that CL is involved in the regulation of programmed cell death. CL allows specific targeting of truncated Bid (tBid) to the mitochondria and facilitates its binding with interaction partners such as Bcl-xL (Garcia-Saez, Ries, Orzaez, Perez-Paya, & Schwille, 2009; Lutter et al., 2000). As a result, Bax, a pro-apoptotic pore-forming protein is activated, which is assumed to be involved in the permeabilization of the outer mitochondrial membrane causing the release of apoptotic factors (Kuwana et al., 2002). Most importantly, many model membrane studies determined that the incorporation of CL leads to conformational changes in the membrane structure, making the membrane structurally deformed and more permeable (Unsay et al., 2013).

3.3 Experimental Methods

3.3.1 Materials

1,2-dioleoyl-sn-glycero-3-phosphoethanolamine (DOPE), 1,2-distearoyl-*sn*-glycero-3-phosphoethanolamine-N-[methoxy(polyethylene glycol)-2000] (ammonium salt) (DSPE-mPEG (2000)), cardiolipin (CL), 1,1',2,2'-tetraoleoyl cardiolipin[4-(dipyrromethene boron difluoride)butanoyl] (ammonium salt), TopFluor® CL, cholesteryl hemisuccinate (CHEMS) were purchased from Avanti Polar Lipids Inc (Alabaster, AL). Stearylamine (SA) was purchased from Sigma-

Aldrich (St.Louis, MO). Cholesterol and ammonium sulfate were purchased from JT Baker (Phillipsburg, NJ). Fetal bovine serum (FBS), Dulbecco's Modified Eagle's Medium (DMEM), Earle's Balanced Salt Solution (EBSS) and other reagents for cell culture were purchased from Mediatech (Manassas, VA). Daunorubicin was purchased from AvaChem Scientific (San Antonio, TX). 2′,7′-Dichlorofluorescin diacetate and Phosphate Buffered Saline (PBS) were purchased from Sigma-Aldrich (St. Louis, MO). Bicinchoninic acid protein kit was purchased from Thermo Scientific (IL, USA). 3-(4,5-Dimethyl-2-thiazolyl)-2,5-diphenyl-2H-tetrazolium bromide (MTT) was purchased from Calbiochem (Darmstadt, Germany). Polycarbonate membrane (0.08 μm) was purchased from Whatman Maidstone, UK). Melanoma (B16BL6) cancer cells were obtained from American Type Culture Collection (Manassas, VA).

3.3.2 Liposomes Preparation

Liposomes were prepared by the lipid film hydration technique using a rotary vacuum evaporator. Briefly, DOPE, cholesterol, DSPE-mPEG, CL and SA were prepared as at 10 mg/ml solution individually in chloroform. These solutions were mixed at a molar ratio of 40:30:5:17:8 for DOPE/cholesterol/DSPE-mPEG (2000)/CL and SA. The mixture was flash evaporated on a (Rotavapor, Büchi, Germany) by applying about 25 mmHg vacuum at 65^{o}C water bath temperature. The lipid film deposited on the wall of the flask was further dried under a stream of nitrogen for 1h, followed by vacuum desiccation for 2 h. The dry lipid film was then hydrated in 250 mM ammonium sulfate solution (pH 5.5). This mixture was then placed in a water-bath incubator (65^{o}C) for 1 h to form coarse liposomes.

This mixture was then subjected to seven liquid nitrogen freeze–thaw cycles above the phase transition temperature of the different lipids before extrusion. The liposome mixture was then extruded through 80 nm (10 passes) polycarbonate filter using Lipex® 100 ml barrel extruder (Transferra Nanosciences Inc, Burnaby, BC. Canada). The free ammonium sulfate outside the liposomes was removed by dialysis (using 12, 000 to 14,000 Daltons molecular weight cut off dialysis tubing) against sucrose solution (10% w/v, 250 ml) at 4^{o}C. The solution medium was then discarded and replaced with fresh solution at 1,4,8 h intervals and then left overnight. The phospholipid concentration of each formulation was quantified following acid hydrolysis and inorganic phosphate assay (Bartlett, 1959). Liposomal formulation similar to DaunoXome®, composed of DSPC/cholesterol/daunorubicin (in a 10:5:1 molar ratio), was prepared by the same method; however, citrate was used instead of ammonium sulfate to hydrate the lipid film. Table 3.1 summarizes the different formulations prepared.

3.3.3 Drug Encapsulation in Liposomes (Active Loading)

DNR solution of an appropriate concentration was prepared by adding the required quantities of drug in the PBS and this drug solution, after adjusting the pH to 8 with 0.1N NaOH, was added to the lipid solution at appropriate drug-to-lipid ratios (1:5). Excess DNR was then removed by dialysis against sucrose solution (10%) at 4^{o}C. Based on initial results of drug loading efficiency, 1:5 drug-to-lipid ratio was found to be optimum and this ratio was used for all formulations.

3.3.4 Encapsulation Efficiency (EE%) and Drug Loading (DL%) Measurement

The amount of DNR entrapped into liposomes (EE% and DL%) was determined fluorometrically at 480 nm (excitation) and 590 nm (emission) using a microplate reader 142 (Fluostar, BMG Labtechnologies, Germany). Briefly, Triton X-100 (1%) was added to liposomal DNR to break the liposome bilayer and release the entrapped DNR. The liposomal drug concentration was calculated from a DNR standard curve. All experiments were run in triplicate and mean data were presented.

The EE% was calculated as follows:

$$\text{Encapsulation Efficiency (\%)} = \frac{\text{amount of liposomal drug}}{\text{total amount of drug}} \times 100$$

The DL % was calculated as follows:

$$\text{Drug Loading (\%)} = \frac{\text{amount of liposomal drug}}{\text{total amount of drug added} + \text{amount of excipients added}} \times 100$$

3.3.5 Particle Size Determination of Liposomal Formulations

The particle size distribution of the liposomal formulations was carried out by the dynamic light scattering method using a Nicomp 380 ZLS particle size analyzer (Particle Sizing Systems, Santa Barbara, CA). Mean particle size and polydispersity index of the formulations after appropriate dilutions were calculated.

3.3.6 Determination of Zeta Potential

Measurements of liposome zeta potential were carried out by photon correlation spectroscopy (PCS, Zetatrac, Largo, FL, USA). For the analyses,

formulations were diluted in an aqueous medium. All determinations were performed in triplicate at room temperature (25°C).

3.3.7 In Vitro Release studies

The release of DNR from liposome formulations was determined by the dialysis method. PBS (pH =7.4) and PBS (pH =5.5,) filled in 250 ml conical flasks were used as a receptor phase. Regenerated cellulose dialysis tubing (12,000 to 14,000 Daltons molecular weight cut off), 30 mm × 25 mm release area, pre-soaked in buffer solution for one hour, was used. 1 ml of the formulation or DNR solution was placed in the dialysis tubing, which was immersed in the receptor phase. All flasks were incubated at 37^{o}C in a rotary shaker set at 150 rpm. Samples (1 ml) were collected at different time intervals and the sample volumes were replenished with fresh buffer immediately. The concentration of DNR in the receptor buffer (dialysate) was analyzed fluorometrically at 480 nm (excitation) and 590 nm (emission) using a microplate reader 142 (Fluostar, BMG Labtechnologies, Germany). The cumulative amount of DNR released versus time was plotted. Experiments were run in triplicate and mean data was presented.

3.3.8 Stability Studies

Short-term stability was conducted to monitor the physical stability of the liposomes. All liposomal formulations were stored at 4^{o}C under N_2 and protected from light for up to one month and EE, particle size, zeta potential and polydispersity were determined after performing dialysis to remove non-capsulated drug.

3.3.9 Cell Culture

Melanoma (B16-BL6) cells were cultured in Dulbecco's Modified Eagle's Medium (DMEM). The medium was supplemented with 10% fetal bovine serum (FBS), 100 U/ml penicillin, and 100 µg/ml streptomycin at 37°C in a humidified atmosphere containing 5% CO_2. All experiments were performed at a confluence of 90 to 95%. The pH of the cell culture medium was measured to determine the pH of the extracellular fluid.

3.3.10 Measurement of Cell Viability by MTT Assay

B16-BL6 cells were cultured in flat-bottom 96-well plates for 24 hours. The cell density in the wells was around 8×10^3 cells/well. The cells received treatments of various liposomal formulations (0.01 µM, 0.05 µM, 0.1 µM, 0.5 µM, 1 µM and 2 µM) for 48 h prior to MTT assay. After treatments, 10 µl of 3-[4, 5-dimethylthiazol-2-yl]-2, 5-diphenyl tetrazolium bromide (MTT) was added to each well and the cells were incubated at 37^oC for an additional 2 hours. Finally, the medium was aspirated and 200 µl dimethylsulfoxide (DMSO) was added to each well to solubilize the dye remaining in the plates. The absorbance was measured using a microplate reader (Spectramax M5, molecular devices, Sunnyvale, CA, USA) at 544 nm. All the experiments were run in triplicate and mean data were presented.

3.3.11 Cellular Daunorubicin Uptake

B16-BL6 cells were cultured in flat-bottom 24-well plates. At optimum confluence, the cells were exposed to 14 µM liposomal DNR or free DNR for 4,8 and 12 hours. After extensive washing with PBS, cells were lysed in 100 µl of 1%

Triton X-100. DNR fluorescence was then measured by a microplate reader (spectramax M5, molecular devices, Sunnyvale, CA, USA) at 480 and 590 nm for excitation and emission, respectively. Cellular DNR contents were calculated and corrected for any differences in protein content, as determined with the bicinchoninic acid assay (Smith et al., 1985). All values were corrected for background fluorescence. All experiments were run in triplicate and mean data were presented.

3.3.12.Daunorubicin Retention Studies

To evaluate cellular DNR accumulation by cancer cells after the drug efflux period, cells grown in 24-well plates were loaded with DNR in the form of free DNR solution or liposomal-DNR (14 μM) for four h. The supernatant was removed at the end of treatment, and cells were washed with ice-cold PBS. The wells were refilled with fresh drug-free EBSS, and cells were incubated at 37°C to facilitate cellular drug efflux. At predetermined time intervals (1,2 and 4h), supernatant containing the effluxed drug was removed. Cells were washed and lysed, and the amount of DNR retained by the cells was measured with a microplate fluorometer as described above.

3.3.13 Fluorescence Microscopy

B16-BL6 cells were seeded in a flat-bottom 24-well plate for 24 hours. After exposure to liposomal DNR or free DNR for 14 hours, cells were washed and fixed [15 min in 4% (w/v) paraformaldehyde in phosphate-buffered saline]. All samples were examined with a fluorescence microscope (EVOS fl, ZP-PKGA-0494 REV A, USA) and photographed at 20X magnification.

3.3.14 Statistical Analysis

All the data were presented as mean ± standard deviation. GraphPad Prism software was used to determine the standard deviation and statistical levels of significance. All data were subjected to one-way analysis of variance (ANOVA) to determine the statistical levels of significance. A P-value less than 0.05 was considered to be statistically significant.

3.4 Results and Discussion

3.4.1 Formulation Preparation

The liposomes prepared with CL were evaluated for EE% and DL%. To obtain liposomes with desirable EE%, DNR was mixed with lipid (DNR:lipid) at a ratio of 1:5. DNR was loaded into the aqueous phase of liposome by active loading, using ammonium sulfate 250 mM. As shown in Table 3.2, the EE% and DL% of the formulations were above 90 and 15, respectively. Our preliminary studies showed that a 1:5 drug-to-lipid ratio demonstrated a higher EE% and DL%, hence this ratio was used for all liposomal formulation.

The drug-to-lipid ratio has a significant influence on the EE of DNR. An indirect relationship has been observed between EE% and drug concentration. The EE% decreases with increased drug concentration (Mayer et al., 1990). The existence of drug precipitate in the liposome interior may explain the inverse relationship between EE and drug concentration. Increasing drug-to-lipid ratio beyond 1:5 causes the drug to precipitate inside the liposomes leading to significant disruption of the liposomal membrane, which causes leakage of

encapsulated drug from liposomes (Johnston, Edwards, Karlsson, & Cullis, 2008).

High EE% of amphipathic weak bases, such as DNR, might be achieved by a transmembrane ammonium sulfate gradient in and out of liposomes (active loading) (Haran, Cohen, Bar, & Barenholz, 1993) (Wei et al., 2018). Similar to most drugs, DNR was not efficiently entrapped in the aqueous phase of the liposome without a pH gradient (Plourde et al., 2017). In the active loading method, liposomes are initially prepared in an acidic environment. After vesicle self-assembly, the core of the liposome remains acidic while the extravesicular pH level is similar to physiological conditions (Hood, Vreeland, & DeVoe, 2014). Remote loading of the uncharged drug allows molecules to diffuse into the liposomal intravesicular interior where they become protonated. The positively charged drug can no longer cross the bilayer membrane and is trapped inside the liposomes cavity (Deamer, Prince, & Crofts, 1972).

To increase the percentage of drug encapsulated inside liposomes, we replaced cholesterol with CHEMS. DOPE lipid by itself with these structural aspects (inverted hexagonal phase) cannot form lipid bilayers at neutral pH, so it must be combined with amphiphilic molecules containing a protonatable acidic group such as CHEMS to form bilayers (Straubinger, 1993). Insertion of PEG on the surface of liposomes is a common strategy to enhance the hydrophilicity of the particle surface, as the reticuloendothelial system (RES) preferentially takes up particles with a hydrophobic surface (Otsuka, Nagasaki, & Kataoka, 2003). It is important to mention that mole% PEG can significantly affect the percentage of

drug encapsulated inside liposomes. An inverse relationship was noticed between mole% of PEG and EE of drugs since PEG might occupy space in the core of the liposomes (Nicholas, Scott, Kennedy, & Jones, 2000). Mole % of PEG used in our formulation does not affect DNR EE. There is no statistically significant difference in EE between F1 and F2 ($p > 0.05$).

3.4.2 Characterization of NP Formulations

The particle size of F1 was about 94 nm with a polydispersity of 0.2, indicating uniform and dispersed liposomal formulations (Table 3.2). The zeta potential of F1 was negative because CL is a quadruple-chained anionic amphiphile lipid composed of two 1,2-diacyl phosphatidate moieties esterified to the 1- and 3-hydroxyl groups of a single glycerol molecule. Under physiological conditions, phosphodiester moieties should both be negatively charged (Lewis & McElhaney, 2009) . Besides, PEG-DSPE lipid, incorporated into liposomes to extend the circulation time, imparts a negative charge (Nag, Yadav, Hedrick, & Awasthi, 2013). The zeta-potential of F2 was in the neutral range since it is composed of neutral lipids.

As shown in Table 3.2, there is no significant difference in particle size between liposomes formulations with or without CL indicating that the addition of CL does not affect particle size ($p > 0.05$). Particle size is a significant parameter that plays crucial roles in the pharmacokinetics of drug distribution. The liver, spleen and other parts of the RES usually take up liposomes larger than 200 nm (Rothkopf, Fahr, Fricker, Scherphof, & Kamps, 2005). Therefore, liposomes less than 200 nm in diameter and of uniform size are preferred for tumor targeting

(Immordino, Dosio, & Cattel, 2006). The liposome preparation method allowed instantaneous and reproducible formation of DNR-CL liposomes with mean particle size below 100 nm in size and high entrapment efficiency (> 90%).

3.4.3 Drug Release *in vitro*

Figure 3.4 shows DNR release from the dialysis studies on free DNR, F1, and F2 at pH 5.5 as well as pH 7.4. Free DNR as a solution diffused rapidly and completely (100%) release 1-2 h. At pH 7.4, F1 liposomes showed only 50% DNR release within 24 h while F2 liposomes released DNR fairly rapidly (50% of DNR was released within 5 h). There was no significant change in the release profile for both free DNR and F2 liposomes at pH 5.5 as compared to pH 7.4. However, DNR release from pH-sensitive liposomes (F1) was significantly faster at pH 5.5 (50% of DNR was released within 8 h). At pH 7.4, F1 formulation had a longer release time due to the steric barrier provided by the surface-grafted PEG (Nag & Awasthi, 2013).

Liposomes that exhibit triggered release features have potentially important applications in drug delivery. Liposomes can be formulated to make them sensitive to a variety of physical and chemical conditions, such as temperature, light, or pH (Heidarli, Dadashzadeh, & Haeri, 2017). pH-sensitive liposomes have been designed to trigger and promote fast and efficient release of entrapped molecules in response to an acidic environment. The acidosis in the extracellular microenvironment of tumor tissue can be attributed to the poor organization and dysfunctional vasculature, heterogeneous blood flow, and insufficient nutrient delivery (Helmlinger, Yuan, Dellian, & Jain, 1997).

DOPE-based, pH-sensitive, liposome drug-delivery system has been widely developed for targeted cancer therapy. Under physiological conditions (pH 7.4), pH-sensitive liposomes exhibit excellent stability; however, in acidic pH (5-5-6.5) DOPE undergoes a phase transition from a lamellar phase to an inverted hexagonal phase (H_{II}), leading to the loss of the spherical structure of the liposomes, and consequently, releasing of encapsulated molecules (Litzinger & Huang, 1992). Lipids components and molar ratios of liposomes (40 mol% DOPE and 5 mol% PEG) in our study achieved the desired release profile consistent with literature data. The leakage of DOX from different pH-sensitive formulations, containing DOPE and CHEMS, was examined with different mol% of DOPE at different pH (Ishida, Okada, Kobayashi, & Kiwada, 2006). Generally, pH-sensitivity improved with increasing mol% DOPE. After incubation for one hour at pH 5.5, liposomal formulation containing 40 mol% DOPE exhibited pH-sensitivity and enhanced drug release but exhibited good drug retention at pH 7.4. Inclusion of PEG at mol% similar to our formulation (5%) is not expected to significantly decrease drug release in response to the low pH (Slepushkin et al., 1997). As a result, effective release of contents can be achieved by pH-sensitive liposomes while preventing rapid clearance by the RES system.

When we developed the pH-sensitive liposomal DNR formulation, we Incorporated CHEMS instead of cholesterol into liposomes in order to obtain the most optimal release profile. CHEMS is an acidic cholesterol ester that self-assembles into bilayers in alkaline and neutral aqueous media. It is commonly used with DOPE to prepare pH-sensitive liposomes as it stabilizes DOPE at

neutral pH and produces intense bilayer deformation when the pH decreases (Ferreira Ddos, Lopes, Franco, & Oliveira, 2013). At neutral pH the electrostatic repulsion between deprotonated carboxylate groups of CHEMS and phosphate groups of DOPE allows the formation of bilayer structures. However, at acidic pH, destabilization of liposomes is facilitated by the protonation of carboxylate groups, eliminating charge repulsion in the bilayer, and subsequently resulting in the reversion of DOPE molecules into their original inverted hexagonal phase (Kanamala, Wilson, Yang, Palmer, & Wu, 2016).

3.4.4 Cytotoxicity of DNR-CL-DOPE Liposomes to B16-BL6 Cells

As shown in Figure 3.5A, the IC_{50} of F1 was about 12.5-fold lower than DNR solution and about 5-fold lower than F2. Lack of specificity of conventional anti-cancer drug dosage forms increases the dose required to reach the target organs to inhibit tumor growth, which explains the high dose of DNR solution required to achieve 50% inhibition (Nurgali, Jagoe, & Abalo, 2018).

Liposomal drug formulations have been employed to improve the therapeutic efficacy and significantly decrease the toxic effect of anticancer agents, including anthracycline DNR. Furthermore, they impact the pharmacokinetics and tissue distribution of the incorporated anticancer agent (Olusanya, Haj Ahmad, Ibegbu, Smith, & Elkordy, 2018).

Liposomal anthracyclines were developed to enhance tumor targeting of conventional anthracyclines to reduce their side effects. Liposomal anthracycline formulations have demonstrated similar efficacy to conventional therapy while improving the safety profile (Rivera, 2003). Various chemical modifications of

liposomal formulations have been made (e.g. active targeting) to improve their uptake rate; consequently, their antitumor activity. The concept of pH-sensitive liposomes emerged from the reality that tumors exhibit an acidic environment as compared with healthy tissues. These liposomes are stable at physiological pH (pH 7.4) but undergo destabilization under acidic conditions, thus leading to the release of their contents.

Many studies have reported that nanoparticles formulations of anthracycline yield less effective *in vitro* cytotoxicity (i.e., higher IC_{50}) than free drug because nano-particles must release their entrapped drug (Kratz et al., 2002; C. C. Lee et al., 2006). In our study, the pH of the extracellular fluid of B16-BL6 cell lines ranged between 6.2-6.4. *In vitro* cytotoxic activity of F1 was significantly higher than that of the free solution and F2 ($p < 0.001$). There was no significant difference in cytotoxicity between free DNR solutions and F2 (Figure 3.5B).

In addition to increasing the release rate of the encapsulated DNR, we altered the permeability of the tumor cell membrane (by using CL) to enhance the therapeutic effect. Remodeling of cell membrane structure, which comprises both proteins and lipids, is controlled by interactions between specific proteins and lipids. A unique property of CL lipid is its ability to disturb the packing of the membrane and decrease its mechanical stability. 5% CL can promote the formation of flowerlike domains that grew with time leading to membrane structure remodeling, deformation, and permeabilization (Unsay et al., 2013). In our study, we believe that such physical changes induced by CL might enhance

membrane permeability of DNR, and therefore, its cytotoxic effect. Liposomal formulation enriched with CL resulted in a strong cytotoxic activity *in vitro* because enhancing membrane permeability will increase cellular uptake of chemotherapeutic drugs by cancer cells. In our study, liposomal formulation enriched with CL exhibited enhanced antitumor activity compared to liposomal formulation without CL. Also, empty liposomal formulation containing CL did not show any effect on cell survival. Thus, CL might contribute to enhance intracellular DNR delivery. Also, rapid destabilization of pH-sensitive liposomes under acidic pH, in addition to increasing DNR release, might facilitate CL interaction with the membrane.

3.4.5 Enhanced DNR Uptake by Liposomes Enriched with CL in B16-BL6 Cells

Figure 3.6A, presents the 12-h time profiles of DNR uptake by tumor cells treated with 14 μM. DNR formulations. Cellular DNR levels of DNR solution reached a plateau within 4 h, whereas F1 cellular DNR levels continued to increase up to 12 h. When treated with DNR solution and F2, B16-BL6 cells accumulated 58% and 44% less DNR at 8 h, respectively, compared to F1 (Figure 3.6B). There was no significant difference between F2 and free DNR ($p > 0.05$).

Several chemotherapeutic drugs target intracellular organelles, like the nucleus, to achieve their anticancer activities. For instance, DNR may intercalate between the DNA bases and disrupt the action of topoisomerase II (Fukushima, Ueda, Uchida, & Nakamura, 1993). As a result, effective chemotherapy requires a reasonably high level of drug molecules to accumulate within the cancer cells.

Anthracycline drugs enter cells by passive diffusion (Speelmans, Staffhorst, de Kruijff, & de Wolf, 1994), so their anti-tumor effect can be enhanced either by increasing cellular uptake or increasing cellular retention (Lei et al., 2011). In our study, pH-sensitive CL liposomes promoted rapid release of DNR; however, they exhibited more cellular uptake compared to free DNR. This indicates that incorporating CL plays an important role in increasing cellular uptake. Besides, F1 accumulated higher DNR levels than with F2, which strengthen our hypothesis that CL has an essential role regarding enhancing cellular uptake.

3.4.6 DNR Cellular Retention Studies

Figure 3.7A demonstrates the effects of F1 on cellular DNR retention in the tumor cells. The decline in the cellular DNR levels, as a result of drug efflux into fresh EBSS medium, is presented as a function of time up to 4 h. The F1 liposomes demonstrated enhanced DNR cellular retention compared with DNR solution and F2 ($p<0.05$). After 2 h, F1 enhanced DNR retention by 3-fold and 2.2-fold compared with DNR solution and F2, respectively (Figure 3.7B). There was no significant difference in the retention between F2 and free DNR ($p >0.05$).

Limited availability of anthracycline drugs due to their insufficient distribution in solid tumors in association with efflux by the P-gp pump, increases sequestration in endosomes and tumor cell packing density (Wong et al., 2006). Anthracycline DOX retention was significantly greater when more DOX accumulated inside cancer cells because the P-gp pump is saturated by high drug concentration (J. H. Lee, Na, Song, Lee, & Kuh, 2012). In our study, the higher cellular retention of DNR was due to an increase in passive drug diffusion.

Since CL increases the membrane fluidity and affects its mechanical properties, it allows more DNR to accumulate inside tumor cells, which causes saturation of the P-gp pump and decreases drug efflux. Furthermore, DNR accumulation in a large amount inside tumor cells will limit the drug ability to move outside cells across the destabilized membrane. DNR will accumulate strongly in the nucleus and in acid vesicles (more intracellular DNR store). Such strong binding will decrease the efflux rate and cause a low diffusion coefficient (Wielinga, Westerhoff, & Lankelma, 2000).

3.4.7 Visualization of Cellular Internalization of CL Liposomes

We visualized the uptake of DNR and liposomal formulations by fluorescence imaging. Figure 3.8A shows that F1 displayed significantly higher DNR accumulation. After 6 hours of incubation (14 μM DNR), the fluorescence levels were consistently higher in the formulation enriched with CL compared with F2 and free DNR. The results correlate with both cytotoxicity and cellular uptake results. Fluorescence microscopy results demonstrated that CL enhanced the delivery of DNR into tumor cells through changes in the physical properties of the cell membrane such as thickness and permeability. To investigate the interaction of CL with the cellular membrane, we incorporated fluorescent CL into the liposomal formulation encapsulated with DRN. Furthermore, we made a blank liposomal formulation with fluorescent CL. As shown in Figure 3.8B, CL interacted with the membrane bilayer allowing more DNR to accumulate in the nucleus.

3.4.8 Short-Term Stability of Liposomal Formulations

Physical stability of different liposomes during storage (4°C for one month) was followed by measuring time-dependent changes in liposome size, EE%, DL%, zeta potential, and polydispersity index (Table 3.3). There were no significant changes in any parameters during the stability study.

In order to develop stable pH-sensitive liposome formulations, cholesterol was added to the lipid composition to increase the membrane rigidity. It is usually found that between 20 and 50 mol% of cholesterol is required to maintain bilayer stability when mixed with HII preferring lipids such as DOPE (Briuglia, Rotella, McFarlane, & Lamprou, 2015). Besides, incorporation of PEG-PE to the membrane of pH-sensitive liposomes imports steric stability to these liposomes (Edwards, Johnsson, Karlsson, & Silvander, 1997). Since anthracycline drugs precipitate as fibrous-bundle aggregates in the liposomes (Li et al., 1998), high drug: lipid ratio might cause liposomal deformation. Drug: lipid ratio of 1:5 used in our formulations did not cause liposomal membrane deformation, which explains the good stability profiles of liposome formulation especially in term of EE.

3.5 Conclusions

The optimum liposome formulation had 40:30:5:17:8 molar ratio for DOPE/ cholesterol/DSPE-mPEG (2000)/ CL and SA. The liposomes were prepared at a 1:5 molar ratio of drug-to-lipid exhibited high drug encapsulation efficiency (>90%), small size (~94 nm), and narrow size distribution (~0.16). DNR was rapidly released from pH–sensitive liposomes under acidic environment (within 1 h) while under physiological pH, liposomes, exhibited a good stability profile. CL

enriched liposomes exhibited a higher cytotoxic and DNR cellular uptake effect on B16-BL6 cell lines than liposomes similar to DaunoXome® and free DNR, suggesting that CL changes the physical properties of the plasma membrane leading to more diffusion of DNR into cancer cells. Therefore, this formulation appears to be a promising delivery system for the treatment of melanoma.

3.6 References

Bahrami, B., Hojjat-Farsangi, M., Mohammadi, H., Anvari, E., Ghalamfarsa, G., Yousefi, M., & Jadidi-Niaragh, F. (2017). Nanoparticles and targeted drug delivery in cancer therapy. *Immunol Lett, 190*, 64-83. doi: 10.1016/j.imlet.2017.07.015

Barker, C. A., & Lee, N. Y. (2012). Radiation therapy for cutaneous melanoma. *Dermatol Clin, 30*(3), 525-533. doi: 10.1016/j.det.2012.04.011

Bartlett, G. R. (1959). Phosphorus assay in column chromatography. *J Biol Chem, 234*(3), 466-468.

Briuglia, M. L., Rotella, C., McFarlane, A., & Lamprou, D. A. (2015). Influence of cholesterol on liposome stability and on in vitro drug release. *Drug Deliv Transl Res, 5*(3), 231-242. doi: 10.1007/s13346-015-0220-8

Cullis, P. R., & de Kruijff, B. (1979). Lipid polymorphism and the functional roles of lipids in biological membranes. *Biochim Biophys Acta, 559*(4), 399-420.

Deamer, D. W., Prince, R. C., & Crofts, A. R. (1972). The response of fluorescent amines to pH gradients across liposome membranes. *Biochim Biophys Acta, 274*(2), 323-335.

Del Prete, S. A., Maurer, L. H., O'Donnell, J., Forcier, R. J., & LeMarbre, P. (1984). Combination chemotherapy with cisplatin, carmustine, dacarbazine, and tamoxifen in metastatic melanoma. *Cancer Treat Rep, 68*(11), 1403-1405.

Deshpande, P. P., Biswas, S., & Torchilin, V. P. (2013). Current trends in the use of liposomes for tumor targeting. *Nanomedicine (Lond), 8*(9), 1509-1528. doi: 10.2217/nnm.13.118

Edwards, K., Johnsson, M., Karlsson, G., & Silvander, M. (1997). Effect of polyethyleneglycol-phospholipids on aggregate structure in preparations of small unilamellar liposomes. *Biophys J, 73*(1), 258-266. doi: 10.1016/S0006-3495(97)78066-4

Fan, Y., Chen, C., Huang, Y., Zhang, F., & Lin, G. (2017). Study of the pH-sensitive mechanism of tumor-targeting liposomes. *Colloids Surf B Biointerfaces, 151*, 19-25. doi: 10.1016/j.colsurfb.2016.11.042

Fattal, E., Couvreur, P., & Dubernet, C. (2004). "Smart" delivery of antisense oligonucleotides by anionic pH-sensitive liposomes. *Adv Drug Deliv Rev, 56*(7), 931-946. doi: 10.1016/j.addr.2003.10.037

Ferreira Ddos, S., Lopes, S. C., Franco, M. S., & Oliveira, M. C. (2013). pH-sensitive liposomes for drug delivery in cancer treatment. *Ther Deliv, 4*(9), 1099-1123. doi: 10.4155/tde.13.80

Fukushima, T., Ueda, T., Uchida, M., & Nakamura, T. (1993). Action mechanism of idarubicin (4-demethoxydaunorubicin) as compared with daunorubicin in leukemic cells. *Int J Hematol, 57*(2), 121-130.

Gabizon, A., Goren, D., Cohen, R., & Barenholz, Y. (1998). Development of liposomal anthracyclines: from basics to clinical applications. *J Control Release, 53*(1-3), 275-279.

Gabizon, A., Shmeeda, H., & Barenholz, Y. (2003). Pharmacokinetics of pegylated liposomal Doxorubicin: review of animal and human studies. *Clin Pharmacokinet, 42*(5), 419-436. doi: 10.2165/00003088-200342050-00002

Garcia-Saez, A. J., Ries, J., Orzaez, M., Perez-Paya, E., & Schwille, P. (2009). Membrane promotes tBID interaction with BCL(XL). *Nat Struct Mol Biol, 16*(11), 1178-1185. doi: 10.1038/nsmb.1671

Gatenby, R. A., & Gillies, R. J. (2004). Why do cancers have high aerobic glycolysis? *Nat Rev Cancer, 4*(11), 891-899. doi: 10.1038/nrc1478

Gerritsen, W. J., de Kruijff, B., Verkleij, A. J., de Gier, J., & van Deenen, L. L. (1980). Ca2+-induced isotropic motion and phosphatidylcholine flip-flop in phosphatidylcholine-cardiolipin bilayers. *Biochim Biophys Acta, 598*(3), 554-560.

Hamm, C., Verma, S., Petrella, T., Bak, K., Charette, M., & Melanoma Disease Site Group of Cancer Care Ontario's Program in Evidence-based, C. (2008). Biochemotherapy for the treatment of metastatic malignant melanoma: a systematic review. *Cancer Treat Rev, 34*(2), 145-156. doi: 10.1016/j.ctrv.2007.10.003

Haran, G., Cohen, R., Bar, L. K., & Barenholz, Y. (1993). Transmembrane ammonium sulfate gradients in liposomes produce efficient and stable entrapment of amphipathic weak bases. *Biochim Biophys Acta, 1151*(2), 201-215.

Heidarli, E., Dadashzadeh, S., & Haeri, A. (2017). State of the Art of Stimuli-Responsive Liposomes for Cancer Therapy. *Iran J Pharm Res, 16*(4), 1273-1304.

Helmlinger, G., Yuan, F., Dellian, M., & Jain, R. K. (1997). Interstitial pH and pO2 gradients in solid tumors in vivo: high-resolution measurements reveal a lack of correlation. *Nat Med, 3*(2), 177-182.

Hood, R. R., Vreeland, W. N., & DeVoe, D. L. (2014). Microfluidic remote loading for rapid single-step liposomal drug preparation. *Lab Chip, 14*(17), 3359-3367. doi: 10.1039/c4lc00390j

Hortobagyi, G. N. (1997). Anthracyclines in the treatment of cancer. An overview. *Drugs, 54 Suppl 4*, 1-7. doi: 10.2165/00003495-199700544-00003

Huber, V., Camisaschi, C., Berzi, A., Ferro, S., Lugini, L., Triulzi, T., . . . Rivoltini, L. (2017). Cancer acidity: An ultimate frontier of tumor immune escape and a novel target of immunomodulation. *Semin Cancer Biol, 43*, 74-89. doi: 10.1016/j.semcancer.2017.03.001

Immordino, M. L., Dosio, F., & Cattel, L. (2006). Stealth liposomes: review of the basic science, rationale, and clinical applications, existing and potential. *Int J Nanomedicine, 1*(3), 297-315.

Ishida, T., Okada, Y., Kobayashi, T., & Kiwada, H. (2006). Development of pH-sensitive liposomes that efficiently retain encapsulated doxorubicin (DXR) in blood. *Int J Pharm, 309*(1-2), 94-100. doi: 10.1016/j.ijpharm.2005.11.010

Johnston, M. J., Edwards, K., Karlsson, G., & Cullis, P. R. (2008). Influence of drug-to-lipid ratio on drug release properties and liposome integrity in liposomal doxorubicin formulations. *J Liposome Res, 18*(2), 145-157. doi: 10.1080/08982100802129372

Kanamala, M., Wilson, W. R., Yang, M., Palmer, B. D., & Wu, Z. (2016). Mechanisms and biomaterials in pH-responsive tumour targeted drug delivery: A review. *Biomaterials, 85*, 152-167. doi: 10.1016/j.biomaterials.2016.01.061

Kato, Y., Ozawa, S., Miyamoto, C., Maehata, Y., Suzuki, A., Maeda, T., & Baba, Y. (2013). Acidic extracellular microenvironment and cancer. *Cancer Cell Int, 13*(1), 89. doi: 10.1186/1475-2867-13-89

Kratz, F., Warnecke, A., Scheuermann, K., Stockmar, C., Schwab, J., Lazar, P., . . . Unger, C. (2002). Probing the cysteine-34 position of endogenous serum albumin with thiol-binding doxorubicin derivatives. Improved efficacy of an acid-sensitive doxorubicin derivative with specific albumin-binding properties compared to that of the parent compound. *J Med Chem, 45*(25), 5523-5533.

Kuwana, T., Mackey, M. R., Perkins, G., Ellisman, M. H., Latterich, M., Schneiter, R., . . . Newmeyer, D. D. (2002). Bid, Bax, and lipids cooperate to form supramolecular openings in the outer mitochondrial membrane. *Cell, 111*(3), 331-342.

Lee, C. C., Gillies, E. R., Fox, M. E., Guillaudeu, S. J., Frechet, J. M., Dy, E. E., & Szoka, F. C. (2006). A single dose of doxorubicin-functionalized bow-tie dendrimer cures mice bearing C-26 colon carcinomas. *Proc Natl Acad Sci U S A, 103*(45), 16649-16654. doi: 10.1073/pnas.0607705103

Lee, J. H., Na, K., Song, S. C., Lee, J., & Kuh, H. J. (2012). The distribution and retention of paclitaxel and doxorubicin in multicellular layer cultures. *Oncol Rep, 27*(4), 995-1002. doi: 10.3892/or.2012.1650

Lee, Y., & Thompson, D. H. (2017). Stimuli-responsive liposomes for drug delivery. *Wiley Interdiscip Rev Nanomed Nanobiotechnol, 9*(5). doi: 10.1002/wnan.1450

Lei, T., Srinivasan, S., Tang, Y., Manchanda, R., Nagesetti, A., Fernandez-Fernandez, A., & McGoron, A. J. (2011). Comparing cellular uptake and cytotoxicity of targeted drug carriers in cancer cell lines with different drug resistance mechanisms. *Nanomedicine (Lond), 7*(3), 324-332. doi: 10.1016/j.nano.2010.11.004

Lewis, R. N., & McElhaney, R. N. (2009). The physicochemical properties of cardiolipin bilayers and cardiolipin-containing lipid membranes. *Biochim Biophys Acta, 1788*(10), 2069-2079. doi: 10.1016/j.bbamem.2009.03.014

Li, X., Hirsh, D. J., Cabral-Lilly, D., Zirkel, A., Gruner, S. M., Janoff, A. S., & Perkins, W. R. (1998). Doxorubicin physical state in solution and inside liposomes loaded via a pH gradient. *Biochim Biophys Acta, 1415*(1), 23-40.

Litzinger, D. C., & Huang, L. (1992). Phosphatidylethanolamine liposomes: drug delivery, gene transfer and immunodiagnostic applications. *Biochim Biophys Acta, 1113*(2), 201-227.

Liu, Y., & Sheikh, M. S. (2014). Melanoma: Molecular Pathogenesis and Therapeutic Management. *Mol Cell Pharmacol, 6*(3), 228.

Lutter, M., Fang, M., Luo, X., Nishijima, M., Xie, X., & Wang, X. (2000). Cardiolipin provides specificity for targeting of tBid to mitochondria. *Nat Cell Biol, 2*(10), 754-761. doi: 10.1038/35036395

Malhotra, K., Modak, A., Nangia, S., Daman, T. H., Gunsel, U., Robinson, V. L., . . . Alder, N. N. (2017). Cardiolipin mediates membrane and channel interactions of the mitochondrial TIM23 protein import complex receptor Tim50. *Sci Adv, 3*(9), e1700532. doi: 10.1126/sciadv.1700532

Mayer, L. D., Tai, L. C., Bally, M. B., Mitilenes, G. N., Ginsberg, R. S., & Cullis, P. R. (1990). Characterization of liposomal systems containing doxorubicin entrapped in response to pH gradients. *Biochim Biophys Acta, 1025*(2), 143-151.

Momekova, D., Rangelov, S., & Lambov, N. (2010). Long-circulating, pH-sensitive liposomes. *Methods Mol Biol, 605*, 527-544. doi: 10.1007/978-1-60327-360-2_35

Nag, O. K., & Awasthi, V. (2013). Surface engineering of liposomes for stealth behavior. *Pharmaceutics, 5*(4), 542-569. doi: 10.3390/pharmaceutics5040542

Nag, O. K., Yadav, V. R., Hedrick, A., & Awasthi, V. (2013). Post-modification of preformed liposomes with novel non-phospholipid poly(ethylene glycol)-conjugated hexadecylcarbamoylmethyl hexadecanoic acid for enhanced circulation persistence in vivo. *Int J Pharm, 446*(1-2), 119-129. doi: 10.1016/j.ijpharm.2013.02.026

Nicholas, A. R., Scott, M. J., Kennedy, N. I., & Jones, M. N. (2000). Effect of grafted polyethylene glycol (PEG) on the size, encapsulation efficiency and permeability of vesicles. *Biochim Biophys Acta, 1463*(1), 167-178.

Nurgali, K., Jagoe, R. T., & Abalo, R. (2018). Editorial: Adverse Effects of Cancer Chemotherapy: Anything New to Improve Tolerance and Reduce Sequelae? *Front Pharmacol, 9*, 245. doi: 10.3389/fphar.2018.00245

Olusanya, T. O. B., Haj Ahmad, R. R., Ibegbu, D. M., Smith, J. R., & Elkordy, A. A. (2018). Liposomal Drug Delivery Systems and Anticancer Drugs. *Molecules, 23*(4). doi: 10.3390/molecules23040907

Otsuka, H., Nagasaki, Y., & Kataoka, K. (2003). PEGylated nanoparticles for biological and pharmaceutical applications. *Adv Drug Deliv Rev, 55*(3), 403-419.

Paliwal, S. R., Paliwal, R., & Vyas, S. P. (2015). A review of mechanistic insight and application of pH-sensitive liposomes in drug delivery. *Drug Deliv, 22*(3), 231-242. doi: 10.3109/10717544.2014.882469

Paradies, G., Paradies, V., De Benedictis, V., Ruggiero, F. M., & Petrosillo, G. (2014). Functional role of cardiolipin in mitochondrial bioenergetics. *Biochim Biophys Acta, 1837*(4), 408-417. doi: 10.1016/j.bbabio.2013.10.006

Plourde, K., Derbali, R. M., Desrosiers, A., Dubath, C., Vallee-Belisle, A., & Leblond, J. (2017). Aptamer-based liposomes improve specific drug loading and release. *J Control Release, 251*, 82-91. doi: 10.1016/j.jconrel.2017.02.026

Rafiyath, S. M., Rasul, M., Lee, B., Wei, G., Lamba, G., & Liu, D. (2012). Comparison of safety and toxicity of liposomal doxorubicin vs. conventional anthracyclines: a meta-analysis. *Exp Hematol Oncol, 1*(1), 10. doi: 10.1186/2162-3619-1-10

Rivera, E. (2003). Liposomal anthracyclines in metastatic breast cancer: clinical update. *Oncologist, 8 Suppl 2*, 3-9.

Rothkopf, C., Fahr, A., Fricker, G., Scherphof, G. L., & Kamps, J. A. (2005). Uptake of phosphatidylserine-containing liposomes by liver sinusoidal endothelial cells in the serum-free perfused rat liver. *Biochim Biophys Acta, 1668*(1), 10-16. doi: 10.1016/j.bbamem.2004.10.013

Sennato, S., Bordi, F., Cametti, C., Coluzza, C., Desideri, A., & Rufini, S. (2005). Evidence of domain formation in cardiolipin-glycerophospholipid mixed monolayers. A thermodynamic and AFM study. *J Phys Chem B, 109*(33), 15950-15957. doi: 10.1021/jp051893q

Sercombe, L., Veerati, T., Moheimani, F., Wu, S. Y., Sood, A. K., & Hua, S. (2015). Advances and Challenges of Liposome Assisted Drug Delivery. *Front Pharmacol, 6*, 286. doi: 10.3389/fphar.2015.00286

Shen, Z., Ye, C., McCain, K., & Greenberg, M. L. (2015). The Role of Cardiolipin in Cardiovascular Health. *Biomed Res Int, 2015*, 891707. doi: 10.1155/2015/891707

Siegel, R. L., Miller, K. D., & Jemal, A. (2019). Cancer statistics, 2019. *CA Cancer J Clin, 69*(1), 7-34. doi: 10.3322/caac.21551

Slepushkin, V. A., Simoes, S., Dazin, P., Newman, M. S., Guo, L. S., Pedroso de Lima, M. C., & Duzgunes, N. (1997). Sterically stabilized pH-sensitive liposomes. Intracellular delivery of aqueous contents and prolonged circulation in vivo. *J Biol Chem, 272*(4), 2382-2388.

Smith, P. K., Krohn, R. I., Hermanson, G. T., Mallia, A. K., Gartner, F. H., Provenzano, M. D., . . . Klenk, D. C. (1985). Measurement of protein using bicinchoninic acid. *Anal Biochem, 150*(1), 76-85.

Speelmans, G., Staffhorst, R. W., de Kruijff, B., & de Wolf, F. A. (1994). Transport studies of doxorubicin in model membranes indicate a difference in passive diffusion across and binding at the outer and inner leaflets of the plasma membrane. *Biochemistry, 33*(46), 13761-13768.

Straubinger, R. M. (1993). pH-sensitive liposomes for delivery of macromolecules into cytoplasm of cultured cells. *Methods Enzymol, 221*, 361-376.

Sudimack, J. J., Guo, W., Tjarks, W., & Lee, R. J. (2002). A novel pH-sensitive liposome formulation containing oleyl alcohol. *Biochim Biophys Acta, 1564*(1), 31-37.

Tacar, O., Sriamornsak, P., & Dass, C. R. (2013). Doxorubicin: an update on anticancer molecular action, toxicity and novel drug delivery systems. *J Pharm Pharmacol, 65*(2), 157-170. doi: 10.1111/j.2042-7158.2012.01567.x

Torchilin, V. P. (2007). Targeted pharmaceutical nanocarriers for cancer therapy and imaging. *AAPS J, 9*(2), E128-147. doi: 10.1208/aapsj0902015

Unsay, J. D., Cosentino, K., Subburaj, Y., & Garcia-Saez, A. J. (2013). Cardiolipin effects on membrane structure and dynamics. *Langmuir, 29*(51), 15878-15887. doi: 10.1021/la402669z

Wei, X., Shamrakov, D., Nudelman, S., Peretz-Damari, S., Nativ-Roth, E., Regev, O., & Barenholz, Y. (2018). Cardinal Role of Intraliposome Doxorubicin-Sulfate Nanorod Crystal in Doxil Properties and Performance. *ACS Omega, 3*(3), 2508-2517. doi: 10.1021/acsomega.7b01235

Wielinga, P. R., Westerhoff, H. V., & Lankelma, J. (2000). The relative importance of passive and P-glycoprotein mediated anthracycline efflux from multidrug-resistant cells. *Eur J Biochem, 267*(3), 649-657. doi: 10.1046/j.1432-1327.2000.01030.x

Wong, H. L., Bendayan, R., Rauth, A. M., Xue, H. Y., Babakhanian, K., & Wu, X. Y. (2006). A mechanistic study of enhanced doxorubicin uptake and retention in multidrug resistant breast cancer cells using a polymer-lipid hybrid

nanoparticle system. *J Pharmacol Exp Ther, 317*(3), 1372-1381. doi: 10.1124/jpet.106.101154

Yoneda, T., Hiasa, M., Nagata, Y., Okui, T., & White, F. (2015). Contribution of acidic extracellular microenvironment of cancer-colonized bone to bone pain. *Biochim Biophys Acta, 1848*(10 Pt B), 2677-2684. doi: 10.1016/j.bbamem.2015.02.004

Zbytek, B., Carlson, J. A., Granese, J., Ross, J., Mihm, M. C., Jr., & Slominski, A. (2008). Current concepts of metastasis in melanoma. *Expert Rev Dermatol, 3*(5), 569-585. doi: 10.1586/17469872.3.5.569

Zunino, F., Giuliani, F., Savi, G., Dasdia, T., & Gambetta, R. (1982). Anti-tumor activity of daunorubicin linked to poly-L-aspartic acid. *Int J Cancer, 30*(4), 465-470.

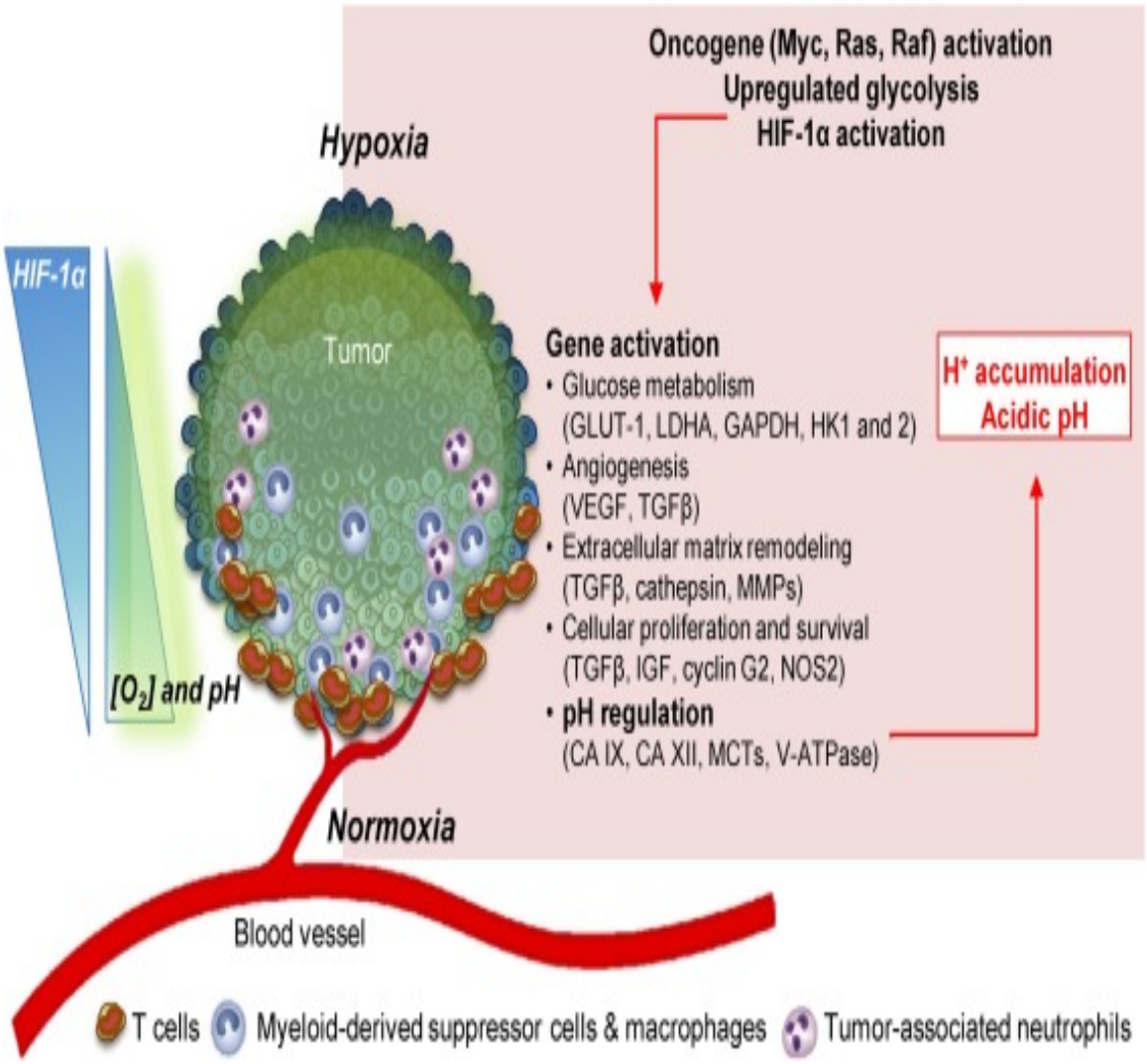

Figure 3.1: Mechanisms contributing to low pH in the tumor microenvironment (TME). Accumulation of protons as a result of low oxygen supply and activation of oncogenes that upregulate glycolysis cause acidification of TME (Huber et al., 2017)

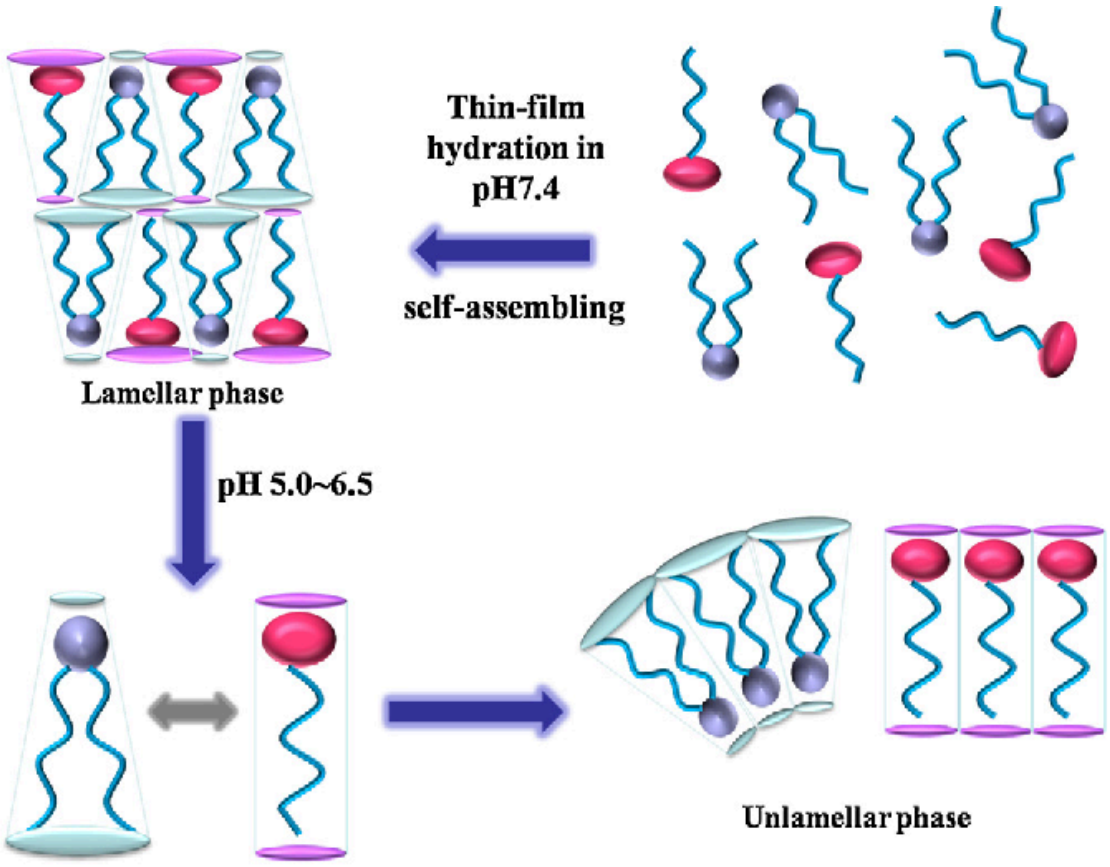

Figure 3.2: Under acidic conditions, the stabilizing lipid becomes partially protonated and loses its ability to stabilize the bilayer structure (Fan, Chen, Huang, Zhang, & Lin, 2017)

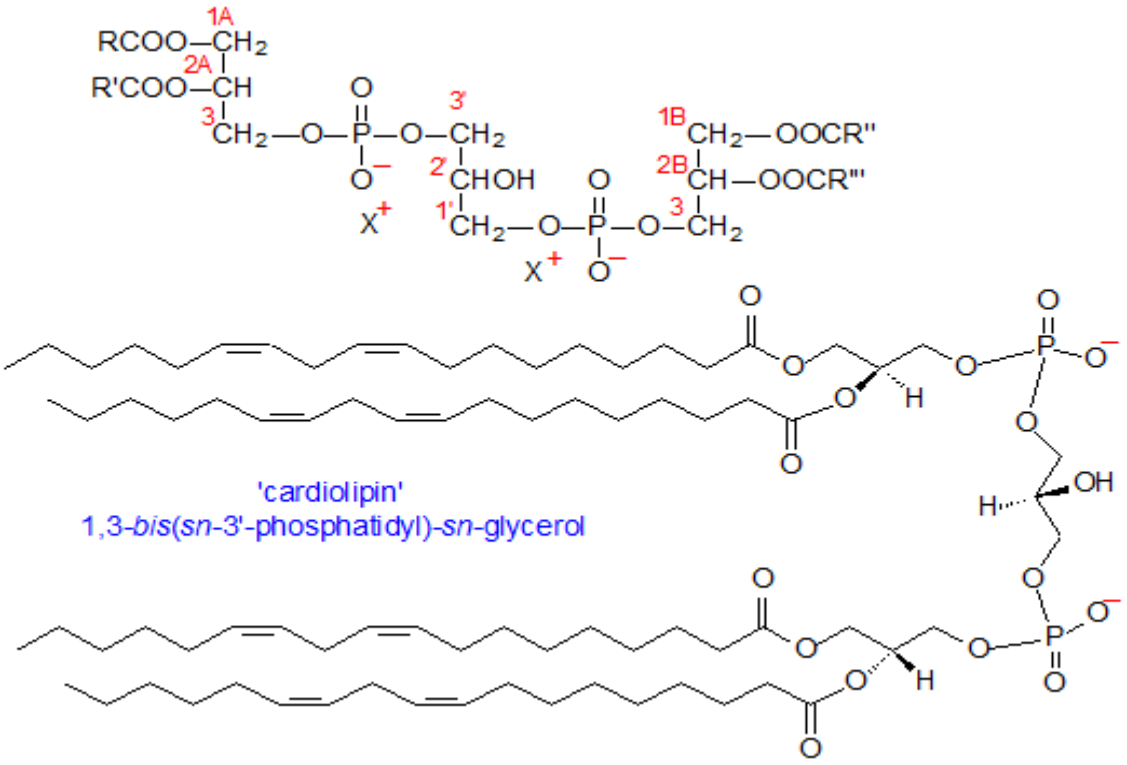

Figure 3.3: Cardiolipin structure

Table 3.1: Composition and molar ratio of various liposomal formulations

Ingredients	**F1**	**F2***	**F3**
DOPE	40	-	40
CHEMS	30		30
DSPE-mPEG (2000)	5	-	5
DSPC	-	10	-
Cholesterol	-	5	-
CL	17	-	17
SA	8	-	8
DNR:lipid ratio	1:5	1:10:5	-

* Liposomal formulation similar to DaunoXome®
1:10:5 is the molar ratio of daunorubicin:DSPC:cholesterol
1:5 is the molar ratio of daunorubicin:total lipids

Table 3.2: Physicochemical characteristics of different liposome formulations. Values are expressed as mean ± SD, n = 3

DNR Liposomal Formulation	Encapsulation Efficiency %	Drug Loading (%)	Particle Size (nm)	PI	Zeta Potential (mV)
F1	95.0 ± 3.7	15.8 ± 0.6	94.0 ± 3.7	0.16 ± 0.03	-39.1 ± 3.1
F2	94.0 ± 0.5	15.8 ± 0.4	83.0 ± 3.1	0.18 ± 0.07	-5.0 ± 1.8

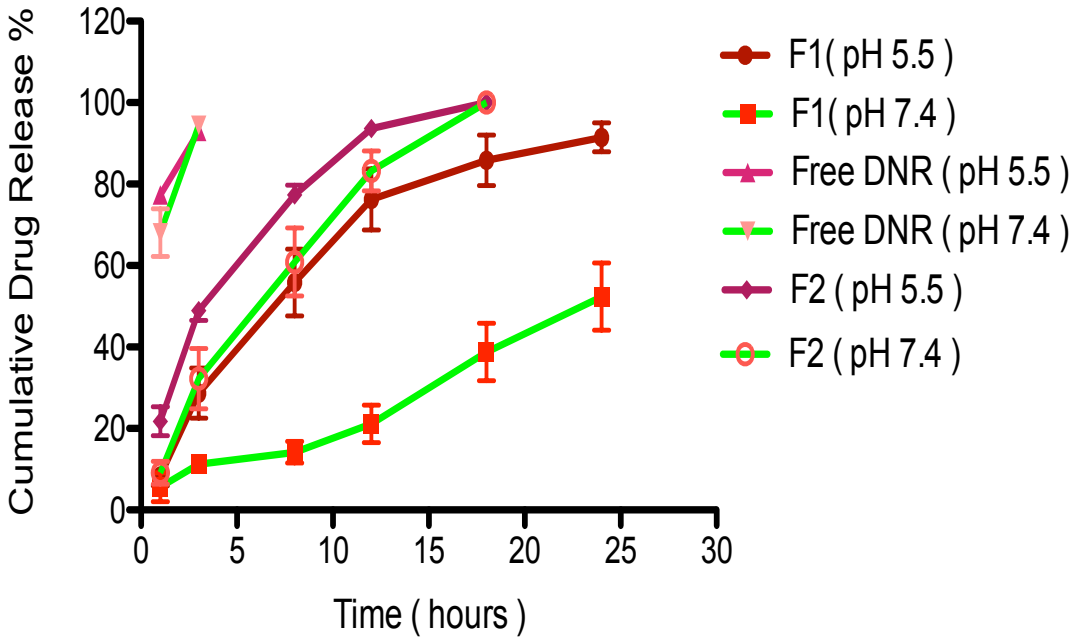

Figure 3.4: *In vitro* release profiles of DNR encapsulated liposomes. Values represented as mean ± SD, n = 3

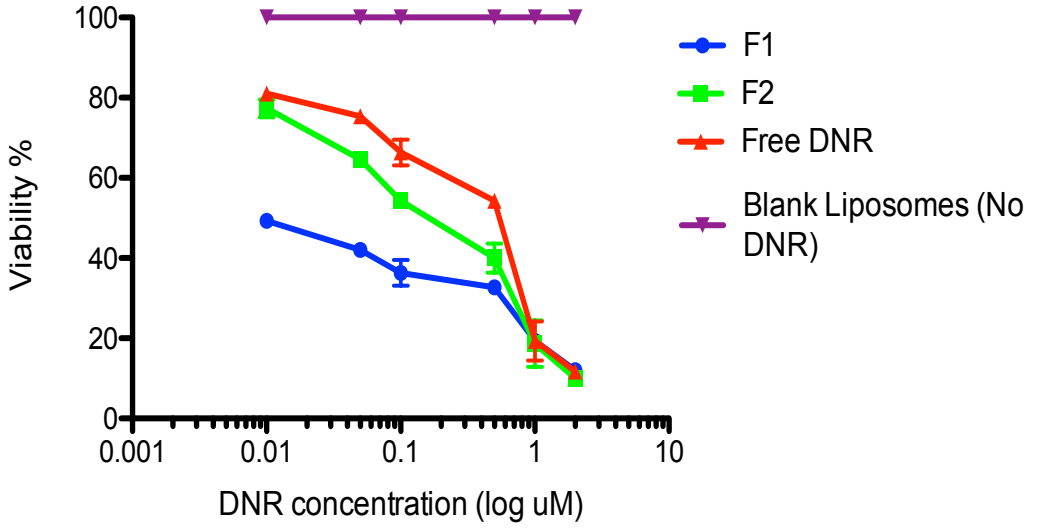

Figure 3.5A: CL potentiates the cytotoxic effect of DNR pH-sensitive liposomes against B16-BL6 cell lines. All data are expressed as mean percentages (n=3) to untreated control cells

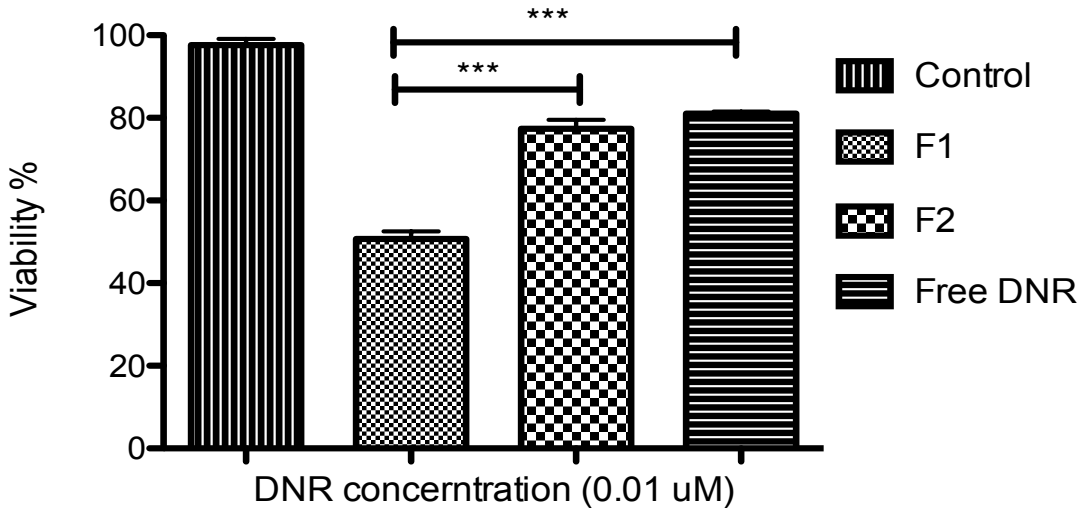

Figure 3.5B: *In vitro* cytotoxicity of different formulations in B16-BL6 cell lines. *** indicates $p < 0.001$. Values represented as mean ± SD, n = 3

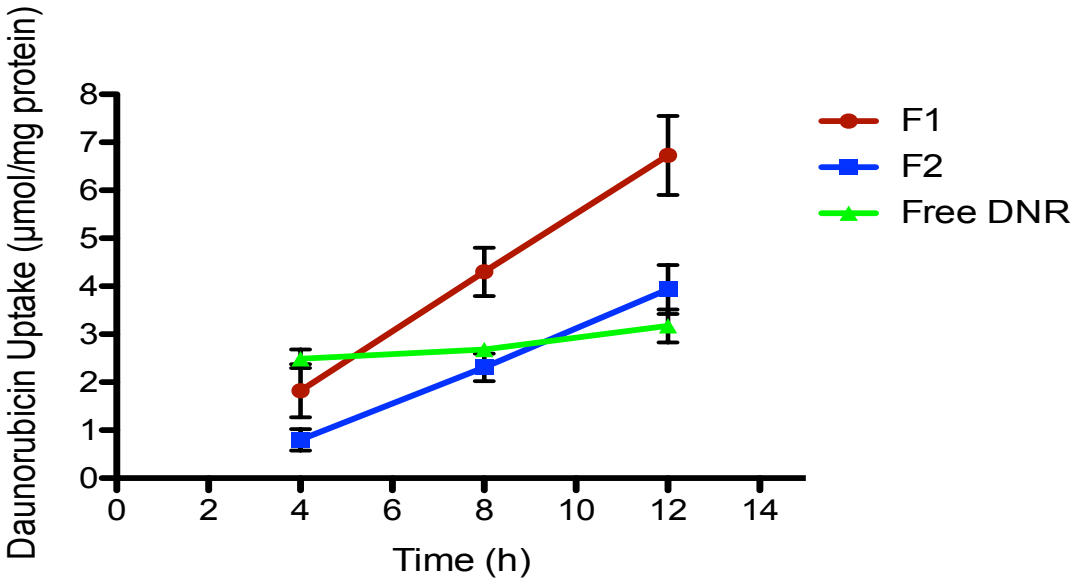

Figure 3.6A: Effect of pH-sensitive liposomes enriched with CL on DNR uptake by B16-BL6 cancer cell lines. Values represented as mean ± SD, n = 3

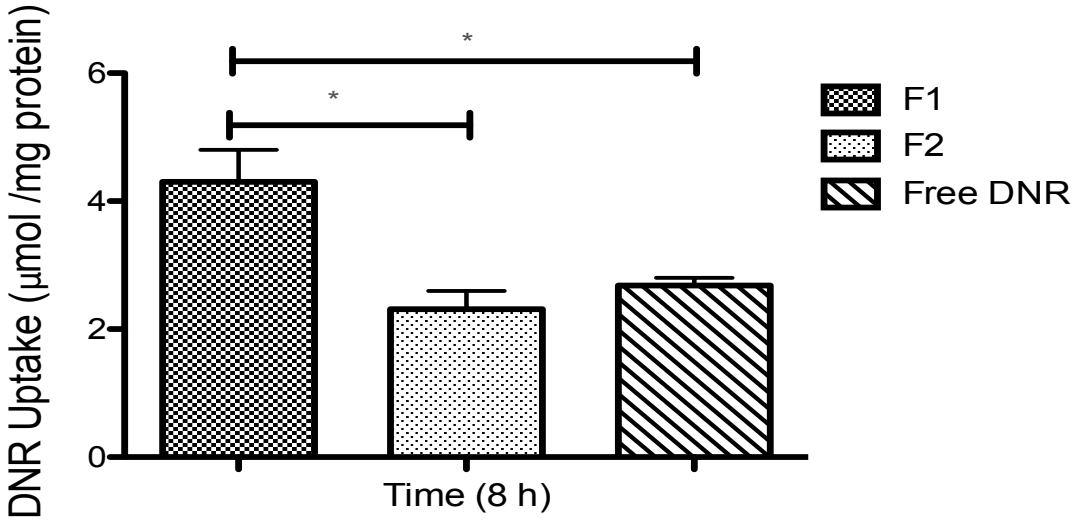

Figure 3.6B: Effect of pH-sensitive liposomes enriched with CL on DNR uptake by B16-BL6 cancer cell lines. * indicates $p < 0.05$. Values represented as mean ± SD, n = 3

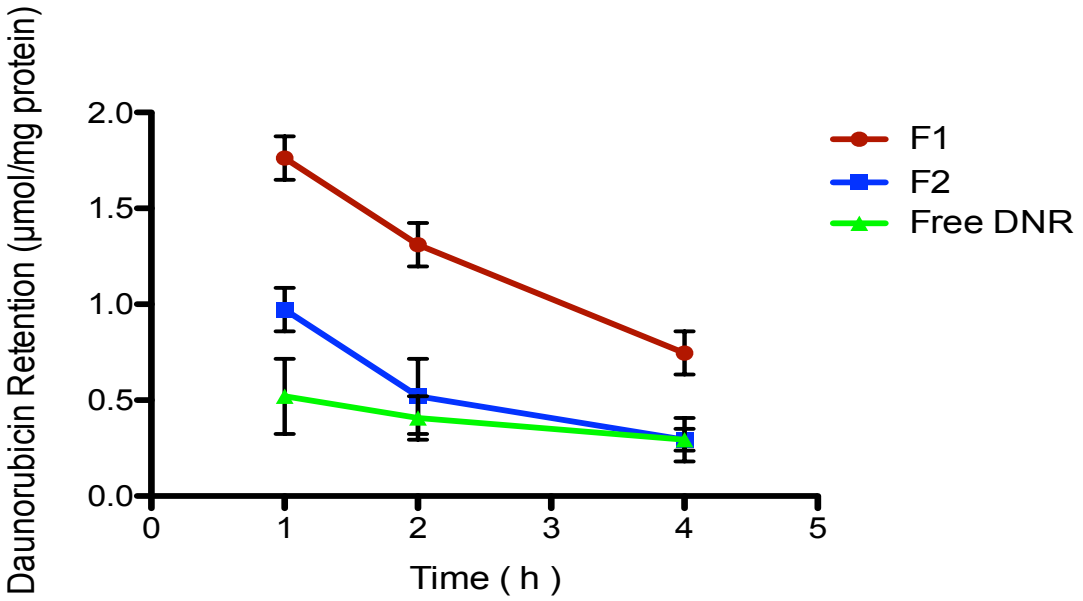

Figure 3.7A: Effect of pH-sensitive liposomes enriched with CL on the amount of DNR retained by B16-BL6 cancer cell lines. Values represented as mean ± SD, n = 3

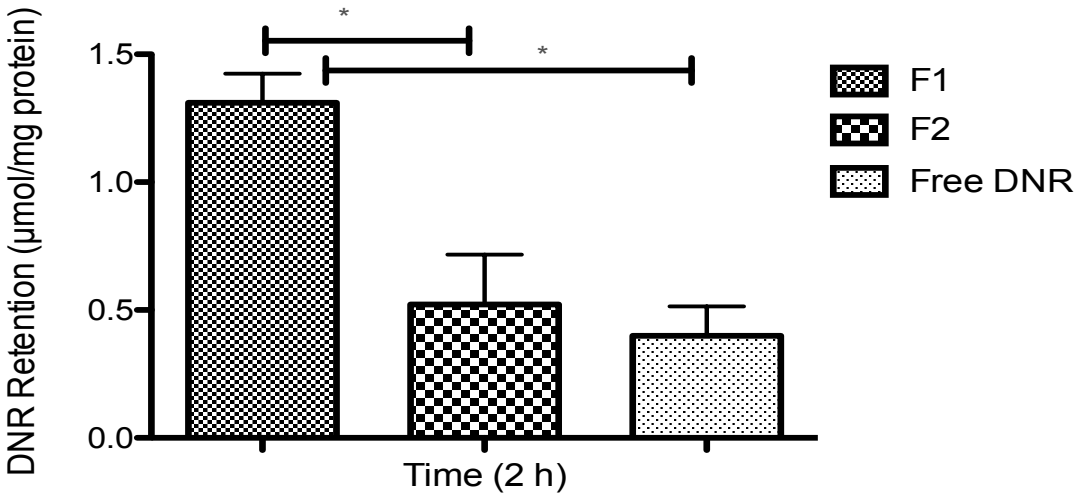

Figure 3.7B: Effect of pH-sensitive liposomes enriched with CL on the amount of DNR retained by B16-BL6 cancer cell lines. * indicates $p < 0.05$. Values represented as mean ± SD, n = 3

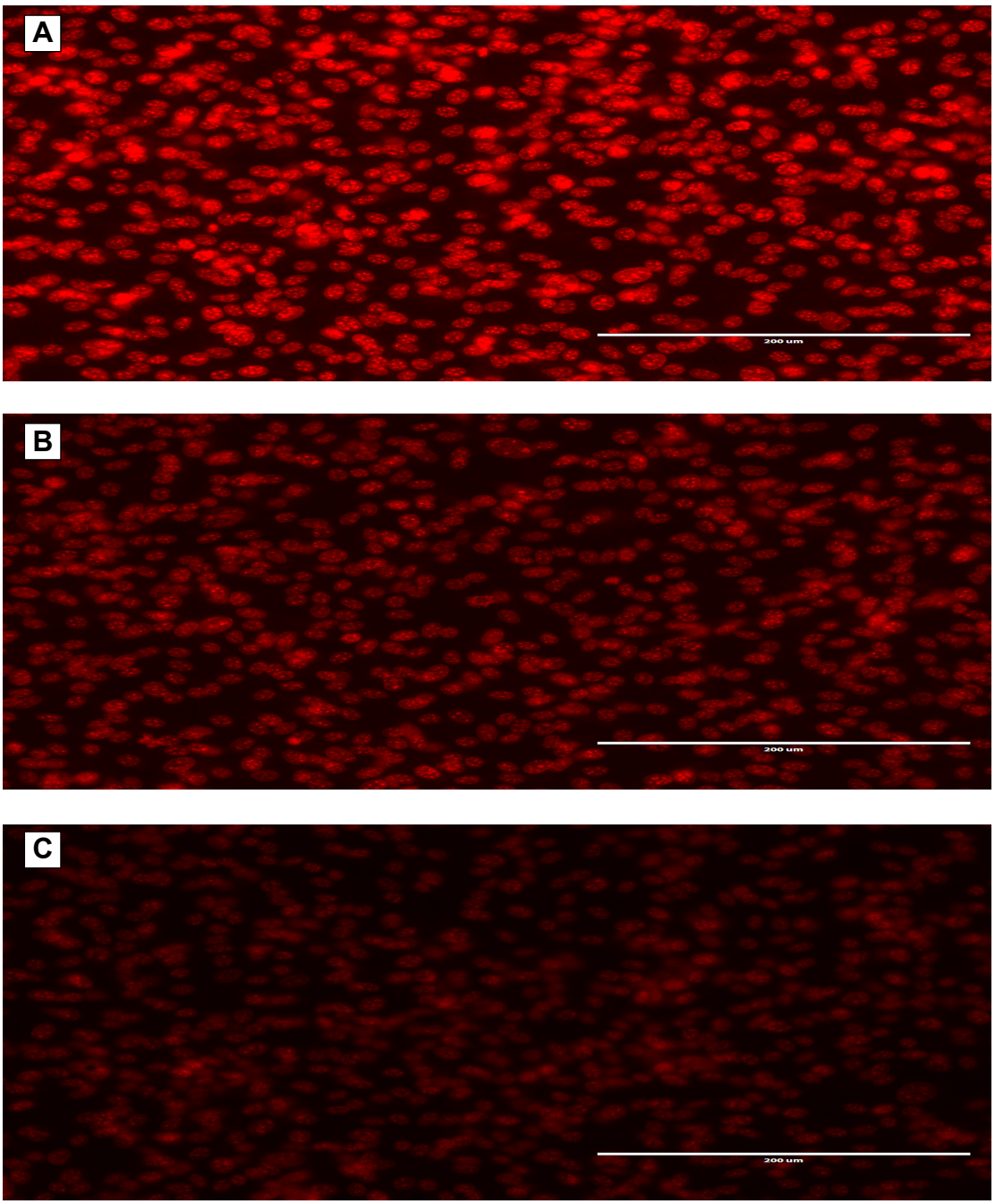

Figure 3.8A: Fluorescence microscopy showing CL enhanced DNR uptake from liposomes. F1 (A), F2 (B), free DNR (C)

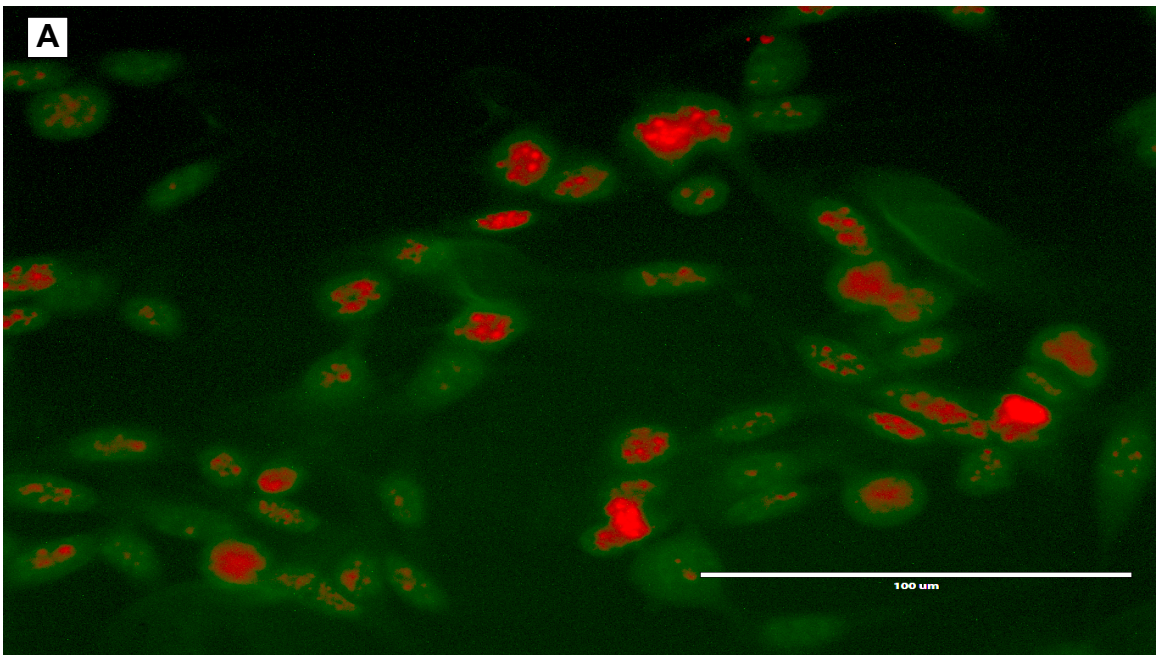

Red color represents DNR while green color represents fluorescent CL

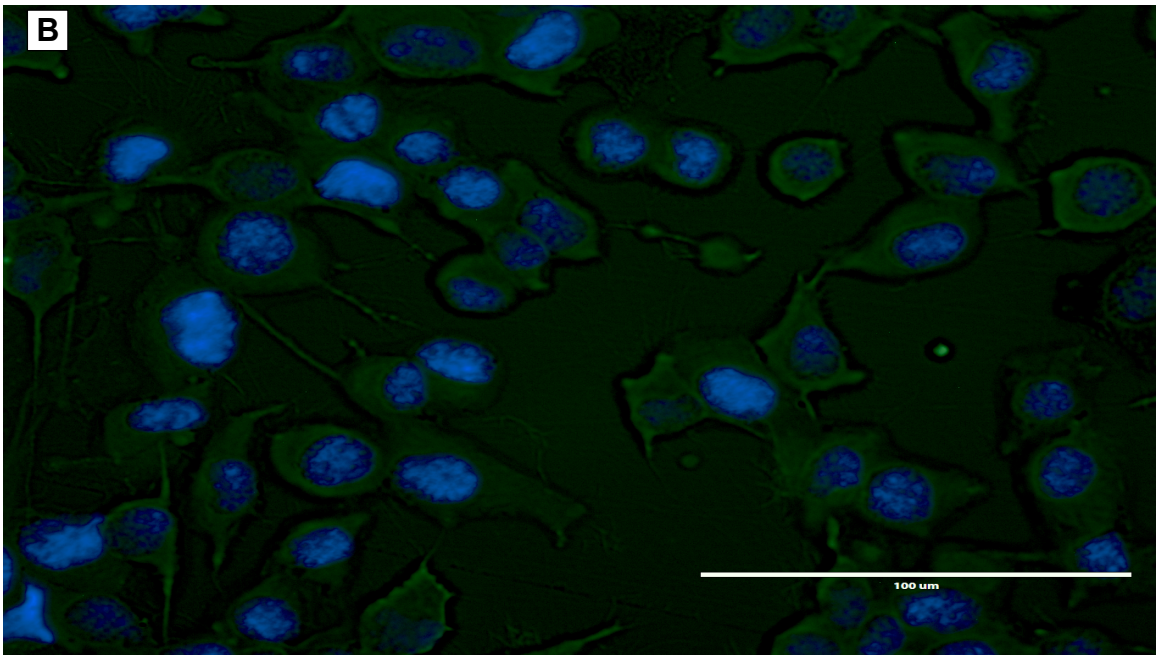

Blue color represents nuclei of cells stained with DAPI while green color represents fluorescent CL

Figure 3.8B: Fluorescence microscopy showing CL interacting with the cellular membrane. Fluorescent CL liposomal formulation encapsulated with DNR (A) or no DNR (B)

Table 3.3: Stability of formulations stored at 4^{o}C under N_2 and protected from light for 1 month. Values represented as mean ± SD, n = 3

	F1		F2	
Formulation	t= 0	t= 1 month	t= 0	t= 1 month
Size Particle Size (nm)	94.0 ± 3.7	112.3 ± 4.2	83.0 ± 3.1	86.0 ± 3.2
PI	0.16 ± 0.03	0.18 ± 0.01	0.18 ± 0.07	0.23 ± 0.07
E.E %	95.0 ± 3.7	86.0 ± 4.4	94.0 ± 0.5	92.0 ± 2.7
D.L %	15.8 ± 0.6	14.7 ± 0.8	15.8 ± 0.4	16 .6 ± 0.3
Zeta Potential (mV)	-39.1 ± 3.1	-15.1 ± 2.4	-5.0 ± 1.8	-4.0 ± 1.9

PI= Polydispersity Index; EE%= Encapsulation Efficiency; DL%= Drug Loading

Chapter 4. Cardiolipin for Enhanced Cellular Uptake and Cytotoxicity of Thermosensitive Liposome-Encapsulated Daunorubicin Toward Breast Cancer (MDA-MB-231) Cell Lines

4.1 Abstract

Daunorubicin (DNR) and cardiolipin (CL) were co-delivered using thermosensitive liposomes (TSLs). DPPC, MSPC, cholesterol, DSPE-mPEG (2000) and CL at a molar ratio of 57:40:30:3:20, respectively, were used in the formulation of liposomes. CL forms raft-like microdomains that may relocate and change lipids organization of both mitochondria outer and inner membrane. Such transbilayer lipid movement eventually leads to membrane permeabilization. TSLs were prepared using lipid film hydration (drug:lipid ratio 1:5) where DNR was encapsulated within liposomes and CL acted as a component of the lipid bilayer. The liposomes exhibited high drug encapsulation efficiency (>90%), small size (~115 nm), narrow size distribution (polydispersity index ~0.12) and a rapid release profile under the influence of mild hyperthermia. The liposomes also exhibited ~4-fold higher cytotoxicity against MDA-MB-231 cells compared to DNR or liposomes similar to DaunoXome®. This study provides a basis for developing a co-delivery system of DNR and CL encapsulating liposomes for breast cancer treatment.

4.2 Introduction

Breast cancer is one of the leading causes of cancer mortality among women worldwide (Yun et al., 2014). In the United States alone, more than 266,120 new breast cancer cases were diagnosed and 41,400 women died as the result of the disease in 2018 (Margolis et al., 2019). Based on the most recent data, the 5–year mortality rate for women diagnosed with breast cancer is 53% (Hendrick, Baker, & Helvie, 2019). Surgery with or without radiotherapy achieves local control of cancer; however, when there is metastasis, systemic treatment is used in the form of hormonal therapy, chemotherapy, targeted therapy, or any combination of these (Cain et al., 2019; Mahvi, Liu, Grinstaff, Colson, & Raut, 2018). Using chemotherapy for breast cancer treatment, in many patients, becomes ineffective and does not improve life expectancy as only a few patients with metastatic disease are cured, and treatments frequently cause significant adverse effects (Roy, Singh, Upadhyay, & Bhaskar, 2013).

Chemotherapy is commonly administered if the tumor reaches a high grade and/or node-positive (Lovitt, Shelper, & Avery, 2018). Docetaxel, doxorubicin, cyclophosphamide, paclitaxel and 5-fluorouracil are the most active cytotoxic agents for both early and advanced-stage breast cancer. Anthracyclines and taxanes drugs in combination with fluorouracil and cyclophosphamide are current therapeutics for breast cancer treatment (Hernandez-Aya & Gonzalez-Angulo, 2013). Generally, cytotoxic drugs are highly toxic, nonspecific, and do not differentiate between healthy and cancerous cells.

Chemotherapy-induced toxicities, such as neurotoxicity, cardiotoxicity and bone marrow suppression, represent a major challenge for health care providers and have a significant impact on therapeutic decisions. In addition, cytotoxic agents impair the immune system, which has a critical role against cancers (Corti et al., 2012). As a result, targeted delivery systems, such as drug-loaded liposomes and nanoparticles, have been developed for specific delivery to tumor cells with minimal systemic exposure.

The anthracycline drugs class are one of the most active single cytotoxic agents in metastatic breast cancer. The major actions of anthracyclines are DNA intercalation, inhibition of topoisomerase II and the formation of free radicals (Tacar, Sriamornsak, & Dass, 2013). Daunorubicin (DNR) is a non-specific anthracycline antibiotic and has been used in treating a wide range of cancers, including breast cancer (Weiss, 1992). Clinical use of DNR is limited by two major problems, systemic toxicity, mainly cardiotoxicity, and drug resistance (Zucchi & Danesi, 2003).

Liposomes are well recognized for drug and gene delivery with clinical evidence of efficacy. Liposomes are lipid vesicles that allow delivery of hydrophilic molecules in the aqueous compartment and lipophilic molecules in the lipid bilayer (Allen & Cullis, 2013). Liposomes have several advantages for drug delivery of chemotherapeutic drugs. They have a role increasing drug solubility, providing targeted drug delivery, reducing the toxic effect of drugs, extending circulation half-life (Allen, 1994), being effective in overcoming multidrug resistance and enhancing the therapeutic index (Matsuo et al., 2001).

Although PEGylation improves circulation half-life by reducing RES uptake, it decreases targeted liposomal accumulation and drug release by steric hindrance effect (Immordino, Dosio, & Cattel, 2006). As a result, new liposomes where the release is promoted at the tumor's vicinity by physiological stimuli (such as pH) or physical external stimuli (such as heat) have been prepared (Figure 4.1). Thermosensitive liposomes (TSLs) are a distinctive class of triggerable liposomes as they promote drug release into the tumor vasculature and interstitial space under the influence of mild hyperthermia (Huang et al., 1994). Inclusion of lipids with transition temperatures (40–45^{o}C) closer to physiological body temperature into liposomes allows generating a high intravascular drug concentration and a significant increase of anthracycline release into the tumor tissue after external localized heating (L. Li et al., 2013). Typically, TSLs consist of DPPC (T_m = 41.4°C) alone or with MSPC (T_m = 40°C) (Liu & Conboy, 2004) (Figure 4.2). TSLs are stable in circulating blood (at 37°C); however, they release their contents rapidly when exposed to a mildly hyperthermic temperature (at 42°C) because vesicles fuse and form planar bilayers, allowing rapid release of encapsulated molecules (Attwood, Choi, & Leonenko, 2013; Leonenko, Finot, Ma, Dahms, & Cramb, 2004). Hence, increasing their concentration into the tumor tissue.

Cardiolipin (CL) that differs from other glycerophospholipids because it is composed of four fatty acyl chains and three glycerol moieties, resulting in a negatively charged, cone-shaped structure (Ikon, Su, Hsu, Forte, & Ryan, 2015). CL plays a role in various cellular functions and signaling pathways inside and

outside of mitochondria. CL can trigger apoptosis because it induces a structural defect of the inner mitochondrial membrane (Castedo et al., 1995). CL forms raft-like microdomains that may relocate and change lipids organization of both mitochondria outer and inner membrane. Such transbilayer lipid movement eventually leads to membrane permeabilization and cell death (Manganelli et al., 2015). Interestingly, CL also promotes extramitochondria membrane permeabilization. CL alters the mechanical stability of the membrane due to a decrease in lipid packing and formation of nonlamellar structures, resulting in deformation of the biological membrane (Sennato et al., 2005).

The objective of this study was to determine the cytotoxicity and cellular uptake of thermosensitive DNR liposomal formulation enriched with CL. It has been proposed that CL plays an important role in the regulation of programmed cell death. CL permeabilization of the outer mitochondrial membrane initiates the release of apoptotic factors (Kuwana et al., 2002) because it allows specific targeting of truncated Bid (tBid) to the mitochondria (Lutter et al., 2000) and facilitates its binding with Bcl-xL (Garcia-Saez, Ries, Orzaez, Perez-Paya, & Schwille, 2009). As a result, BAK and Bax, pro-apoptotic pore-forming proteins are activated, which are assumed to be responsible for permeabilization of mitochondrial membrane. Interestingly, numerous model membrane studies determined that the incorporation of CL, besides disturbing the mitochondrial membrane, triggers structural changes in the cell membrane, making the membrane structurally deformed and more permeable (Unsay, Cosentino, Subburaj, & Garcia-Saez, 2013).

4.3 Experimental Methods

4.3.1 Materials

1,2-dipalmitoyl-*sn*-glycero-3-phosphocholine (DPPC), 1-myristoyl-2-stearoyl-*sn*-glycero-3-phosphocholine (MSPC), 1,2-distearoyl-*sn*-glycero-3-phosphoethanolamine-N-[methoxy(polyethylene glycol)-2000] (ammonium salt) (DSPE-mPEG (2000)), cardiolipin (CL), 1,1',2,2'-tetraoleoyl cardiolipin[4-(dipyrromethene boron difluoride)butanoyl] (ammonium salt), TopFluor® CL were purchased from Avanti Polar Lipids Inc (Alabaster, AL). Cholesterol and ammonium sulfate were purchased from JT Baker (Phillipsburg, NJ). Fetal bovine serum (FBS), Dulbecco's Modified Eagle's Medium (DMEM) and other reagents for cell culture were purchased from Mediatech (Manassas, VA). Daunorubicin was purchased from AvaChem Scientific (San Antonio, TX). Phosphate Buffered Saline (PBS) was purchased from Sigma-Aldrich (St. Louis, MO). Bicinchoninic acid protein kit was purchased from Thermo Scientific (IL, USA). 3-(4,5-Dimethyl-2-thiazolyl)-2,5-diphenyl-2H-tetrazolium bromide (MTT) was purchased from Calbiochem (Darmstadt, Germany). Polycarbonate membrane (0.08 μm) was purchased from Whatman Maidstone, UK). MDA-MB-231 breast cancer cells were obtained from American Type Culture Collection (Manassas, VA).

4.3.2 Liposomes Preparation

Liposomes were prepared by lipid film hydration technique using rotary vacuum evaporator. Briefly, DPPC. MSPC, cholesterol, DSPE-mPEG (2000) and CL were prepared as 10 mg/ml solution individually in chloroform. These

solutions were mixed at a molar ratio of 57:40:30:3:20 for DPPC/ MSPC/cholesterol/DSPE-mPEG (2000)/ and CL. The mixture was flash evaporated on a rotavapor (Rotavapor, Büchi, Germany) by applying a vacuum of about 25mmHg at 65^{o}C, until it forms a thin film on the inner wall of the flask. The lipid film was further dried under a stream of nitrogen for 1h, followed by vacuum desiccation for 2 h. The dry lipid film was then hydrated in 250 mM ammonium sulfate solution (pH 5.5). This mixture was then placed in a water-bath incubator (65^{o}C) for 1 h to form coarse liposomes and underwent seven liquid nitrogen freeze–thaw cycles above the phase transition temperature of the primary lipid. The liposome mixture was then extruded (10 passes) through 80 nm polycarbonate filter using Lipex® 100 ml barrel extruder (Transferra Nanosciences Inc, Burnaby, BC. Canada). The free ammonium sulfate outside the liposomes was removed by dialysis (12, 000 to 14,000 Daltons molecular weight cut off dialysis tubing) against sucrose solution (10% w/v, 250 ml) at 4^{o}C. Sucrose solution was discarded and replaced with fresh solution after 1,4,8 h intervals and then left overnight. The total phospholipid concentration of each formulation was quantified using an assay for inorganic phosphate following acid hydrolysis (Bartlett, 1959). Liposomal formulation similar to DaunoXome®, composed of DSPC/cholesterol/DNR (in a 10:5:1 molar ratio), was prepared by the same method; however, citrate was used instead of ammonium sulfate to hydrate the lipid film. Table 4.1 summarizes the different formulations prepared.

4.3.3 Drug Encapsulation in Liposomes (Active Loading)

DNR solution of an appropriate concentration was prepared by adding the required quantities of the drug in PBS. This solution, after adjusting the pH to 8, was added to the liposomes at appropriate drug-to-lipid ratios (0.2:1). Excess DNR was then removed by dialysis against sucrose solution (10%) at 4^{o}C. Based on initial results of drug loading efficiency, 1:5 drug-to-lipid ratio was found to be optimum and was used for all formulations.

4.3.4 Encapsulation Efficiency (EE%) and Drug Loading (DL%) Measurement

The amount of DNR entrapped into liposomes (EE% and DL%) was determined fluorometrically at 480 nm (excitation) and 590 nm (emission) using a microplate reader 142 (Fluostar, BMG Labtechnologies, Germany). Briefly, Triton X-100 (1%) was added to different liposomal DNR to break the liposome bilayer and release the entrapped DNR. Liposomal drug concentration was calculated from the DNR standard curve. All experiments were run in triplicate and mean data were presented.

The EE% was calculated as:

$$\text{Encapsulation Efficiency } (\%) = \frac{\text{amount of liposomal drug}}{\text{total amount of drug}} \times 100$$

The DL % was calculated as:

$$\text{Drug Loading } (\%) = \frac{\text{amount of liposomal drug}}{\text{total amount of drug added } + \text{ amount of excipients added}} \times 100$$

4.3.5 Particle Size Determination of Liposomal Formulations

The particle size distribution of the liposomal formulations was carried out by the dynamic light scattering method using Nicomp 380 ZLS particle size analyzer (Particle Sizing Systems, Santa Barbara, CA). Mean particle size and polydispersity index of the formulations after appropriate dilutions were calculated.

4.3.6 Determination of Zeta Potential

Measurements of liposome zeta potential were carried out by photon correlation spectroscopy (PCS, Zetatrac, Largo, FL, USA). For the analyses, formulations were diluted in an aqueous medium. All determinations were performed in triplicate at room temperature (25°C).

4.3.7 Determination of Osmolarity

Osmolarity of the formulations was analyzed by a vapor pressure osmometer (model K-7000 Knauer, Berlin, Germany). Before performing the analyses, the osmometer was calibrated with a solution of NaCl (400 mOsm). The determinations were made in triplicate at 25°C.

4.3.8 *In Vitro* Release Studies

The release profile of DNR from liposome formulations was determined by the dialysis method. PBS (pH 7.4) in 250 ml conical flasks was used as a receptor phase. Regenerated dialysis tubing (12,000 to 14,000 Daltons molecular weight cut off), 30 mm × 25 mm release area, pre-soaked in buffer solution for one hour, was used. 1 ml of the formulation or DNR solution was placed in the dialysis tubing while immersed in the receptor phase. All flasks were incubated at

37^{o}C or 42^{o}C in a rotary shaker set at 150 rpm. Samples (1 ml) were collected at different time intervals and the sample volumes were replenished with fresh buffer immediately. The concentration of DNR in the receptor buffer (dialysate) was analyzed fluorometrically (480 nm excitation and 590 nm emission) using a microplate reader. The cumulative amount of DNR released versus time was plotted. All experiments were run in triplicate and mean data were presented.

4.3.9 Stability Studies

Short-term physical stability was on the liposomes. All liposomal formulations were stored at 4^{o}C under N_2 and protected from light for one month and particle size, polydispersity, zeta potential and osmolarity were determined.

4.3.10 Cell Culture

MDA-MB-231 cells were cultured in Dulbecco's Modified Eagle's Medium (DMEM). The medium was supplemented with 10% fetal bovine serum (FBS), 100 U/ml penicillin, and 100 µg/ml streptomycin at 37°C in a humidified atmosphere containing 5% CO_2. All experiments were performed at a confluence of 90 to 95%.

4.3.11 Measurement of Cell Viability by MTT Assay

MDA-MB-231 cells were cultured in flat-bottom 96-well plates for 24 hours. The cell density in the wells was around 8 × 10^3 cells/well. The cells received treatments of various liposomal formulations (0.01 µM, 0.05 µM, 0.1 µM, 0.5 µM, 1 µM, 2 µM and 3 µM) for 48 h prior to MTT assay. TSL treated cells were heated by placing the well plates in precision-controlled incubator at 42^{o}C for 10 min (after the incubator has reached thermal equilibrium), then returned back to 37^{o}C

or only incubated at 37^{o}C. After treatments, 10 µl of 3-[4, 5-dimethylthiazol-2-yl]-2, 5-diphenyl tetrazolium bromide (MTT) was added to each well and the cells were incubated at 37^{o}C for an additional 2 hours. Finally, the medium was aspirated and 200 µl dimethylsulfoxide (DMSO) was added to each well to solubilize the dye remaining in the plates. The absorbance was measured using a microplate reader (Spectramax M5, molecular devices, Sunnyvale, CA, USA) at 544 nm. All experiments were run in triplicate and mean data were presented.

4.3.12 Cellular Daunorubicin Uptake

MDA-MB-231 cells were cultured in flat-bottom 24-well plates. At confluence, cells were exposed to 14 µM of liposomal DNR or free DNR for 0.5 and 4 hours at different temperature (37^{o}C and 42^{o}C). TSL treated cells were heated by placing the well plates in precision-controlled incubator at 42^{o}C for 10 min (after the incubator has reached thermal equilibrium), then returned to 37^{o}C. After extensive washing with PBS, cells were lysed in 100 µl of 1% Triton X-100. DNR fluorescence was measured by a microplate reader at 480- and 590-nm for excitation and emission, respectively. After calculating cellular DNR contents with a standard curve, all contents were corrected for any differences in protein content using the bicinchoninic acid assay (Smith et al., 1985). In addition, all values were corrected for background fluorescence. All the experiments were run in triplicate and mean data were presented.

4.3.13.Fluorescence Microscopy

MDA-MB-231 cells were seeded in a flat-bottom 24-well plate for 24 hours. After exposure to liposomal DNR or free DNR 14 µM for 0.5 and 6 hours

at 37^{o}C or 42^{o}C (TSL treated cells were heated at 42^{o}C for 10 min then returned to 37^{o}C), cells were washed and fixed [15 min in 4% (w/v) paraformaldehyde in phosphate-buffered saline]. All samples were examined with a fluorescence microscope (EVOS fl, ZP-PKGA-0494 REV A, USA) and photographed through at 20X magnification.

4.3.14 Statistical Analysis

The DNR % released from liposomes was plotted as a function of time (h). All data were presented as mean ± standard deviation. GraphPad Prism software was used to determine the standard deviation and statistical levels of significance. All data were subjected to one-way analysis of variance (ANOVA) to determine the statistical levels of significance. P-value less than 0.05 was considered to be statistically significant.

4.4 Results and Discussion

4.4.1 Formulation Preparation

The liposomes prepared with CL were evaluated for EE and DL%. As shown in Table 4.2, the EE% and DL% for the formulations were above 90 and 15, respectively. DNR was entrapped inside liposomes by the active loading method. This is one of the best approaches to attain a high EE%. Anthracycline drugs have been loaded into TSL successfully by this strategy (Gubernator et al., 2010). The high EE% of amphipathic weak bases, such as DNR, is achieved by a transmembrane ammonium sulfate gradient in and out of liposomes (active loading) (Wei et al., 2018). Similar to most drugs, DNR was not efficiently entrapped into the aqueous phase of the liposome without a pH gradient

(Plourde et al., 2017). In active loading, liposomes are initially prepared in an acidic environment. After vesicle self-assembly, the core of the liposome remains acidic while the extravesicular pH level is similar to physiological conditions (Hood, Vreeland, & DeVoe, 2014). Remote loading of the uncharged drug allows molecules to diffuse into the liposomal intravesicular interior where they become protonated. The positively charged drug can no longer cross the bilayer membrane and is trapped inside the liposomes (Deamer, Prince, & Crofts, 1972).

Mole% PEG can significantly affect the EE%. An inverse relationship existed between mole% of PEG and EE of drugs since PEG might occupy some space in the core of the liposomes (Nicholas, Scott, Kennedy, & Jones, 2000). Mole% of PEG used in our formulation does not affect DNR EE%. There is no significant difference in EE% between liposomal formulations with PEG (F1) and F3 (without PEG) ($p > 0.05$). In addition, DNR:lipid at a ratio of 1:5 used in our TSL formulations obtained the desirable EE (above 90%). Drug-to-lipid ratio has a great influence on the EE% of anthracycline drugs such as DOX and DNR. The EE% decreases with increased anthracycline drug concentration (Mayer et al., 1990). Increasing drug-to-lipid ratio (above 20%) will cause the drug to precipitate inside the liposomes leading to significant disruption of the liposomal membrane, which causes leakage of encapsulated drug (Johnston, Edwards, Karlsson, & Cullis, 2008).

4.4.2 Characterization of NP Formulations

Two types of TSLs, with and without CL, were fabricated via the film evaporation/ extrusion method. As showing in Table 4.2, the particle size of F1

was about 115 nm with a polydispersity of 0.12, indicating uniform and dispersed liposomes. The particle size of F2 was about 123 nm with a polydispersity of 0.11. The zeta potential of F1 was negative (~27) due to (1) CL is a quadruple-chained anionic amphiphile lipid composed of two 1,2-diacyl phosphatidate moieties esterified to the 1- and 3-hydroxyl groups of a single glycerol molecule. Under physiological conditions, phosphodiester moieties should both be negatively charged (Lewis & McElhaney, 2009). (2) PEG-DSPE lipid, incorporated into liposomes to extend the circulation time, imparts a negative charge (Nag, Yadav, Hedrick, & Awasthi, 2013). The zeta-potential of F2 was less negative than F1 due to the absence of CL. The zeta-potential of F3 proved to be around neutral.

As shown in Table 4.2, there is no significant difference in particle size between TSL formulations prepared with or without CL ($p > 0.05$). Particle size is a very important parameter in the pharmacokinetics of the entrapped drug. Liposomes that have particles between 70-120 nm theoretically can pass through large fenestrations, sinusoidal capillaries as an example, and at the same time provide a greater carrying capacity than smaller liposomes (Gabizon & Papahadjopoulos, 1988). Liposomes with diameters larger than 200 nm have high RES uptake (Sun et al., 2017) while smaller particles diminish the uptake by RES and are preferred for tumor targeting (Immordino et al., 2006). Liposome preparation of F1 allowed reproducible liposome formation with diameters below 100, small PI (< 0.2) and high entrapment efficiency (> 90%).

4.4.3 Temperature Triggered Release *In Vitro*

The release of DNR from different liposomal formulation at 37^{o}C and 42^{o}C is depicted in Figure 4.3. As expected, the release of DNR was very slow (no more than 5% DNR at one hour) from both F1 and F2 TSLs at 37°C. However, the release of DNR significantly accelerated when the temperature was above DPPC and MSPC transition temperatures (42^{o}C). The cumulative release of DNR reached 90% within one hour. Regarding non-TSL formulation (F3), temperature had almost no effect on the release of DNR.

Development of drug delivery nanocarriers with controllable drug retention and release characteristics is a challenge. The therapeutic efficacy of regular liposomal anthracycline is not considerably enhanced because of inadequate drug release at the site of action. However, long-circulation time and reduction of drug-associated toxicity were observed (Koukourakis et al., 2000; Soloman & Gabizon, 2008). Typically, liposomes release their contents by passive diffusion or liposome degradation, which is not favorable for non-cell cycle specific anthracycline drugs because the therapeutic concentration might not achieved (Bandak, Goren, Horowitz, Tzemach, & Gabizon, 1999). Thus, to optimize the amount of drug release, development of liposomal systems that release drug at the target site in response to a specific stimulus, such as pH or mild hyperthermia, have been developed.

The first TSLs were formulated by Yatvin *et al*, in 1978. The formulation was composed of DPPC and DSPC lipids (Yatvin, Weinstein, Dennis, & Blumenthal, 1978). Since then, TSLs have been further developed. The idea is

that liposomes have lipids that undergo phase transitions in response to heating(Blok, van Deenen, & De Gier, 1976). Below their transition temperature, lipids exist in gel phase and are well ordered and packed; however, when temperature is elevated to approach their transition temperature, the mobility of lipid increases and liposome bilayers changes from a solid gel phase to a liquid crystalline phase (Ta & Porter, 2013) (Figure 4.4). This makes the membrane more permeable to water and encapsulated drugs (Kneidl, Peller, Winter, Lindner, & Hossann, 2014; Ta & Porter, 2013). DPPC lipid (T_m = 41.4°C) is a key component in most TSL formulations and is usually used with other lipids such as MSPC (T_m = 40°C) or MPPC (T_m = 44°C), and DSPE-PEG to increase the circulation time (Gaber et al., 1996).

Several TSLs have been designed to enhance anthracycline drugs release in response to mild hyperthermia. A liposomal formulation composed of DPPC/HSPC/cholesterol/DPPE-PEG 50:25:15:3 (mol/mol) exhibited fast release of DOX (60% released within 30 minutes) when incubated at 42°C (Gaber, Hong, Huang, & Papahadjopoulos, 1995). Another lysolecithin-containing thermosensitive formulation composed of DPPC:MPPC:DSPE-PEG-2000 in the molar ratio of 90:10:4 accelerated the release rate of DOX from liposomes at 41.3°C (80% of DOX released in 20 seconds) (Needham, Anyarambhatla, Kong, & Dewhirst, 2000).

TSL formulations in our study exhibited a slow release profile at 37°C. There was no significant difference in the release profile between F1 and F2, indicating that the addition of CL has no effect on drug release ($p > 0.05$). Under

the influence of mild hyperthermia, both F1 and F2 completely released DNR within an hour. There was no significant difference in the release profile between F1 and F2, indicating that the addition of CL did not slow DNR release. Extended exposure to mild hyperthermia is not necessary. After decreasing the temperature below the transition temperature, the membrane will not solidify homogenously since solid domains will be formed within the membrane (Landon, Park, Needham, & Dewhirst, 2011).

4.4.4 Cytotoxicity of DNR-loaded TSLs

From the dose-response curves for cells incubated with various formulations for 48 hours, the IC_{50} values were determined. The IC_{50} values for free DNR, F3, F2 and F1 are 1.9 ± 0.15 μM, 2.1 ± 0.4 μM, 2 μM ± 0.31 and 0.5 μM ± 0.15, respectively (Figure 4.5A). Thus, the IC_{50} of F1 was about 3.8-fold lower than DNR solution. Furthermore, The IC_{50} F1 was about 4-fold lower than F2.

Anthracycline DNR is an antineoplastic drug that exhibits antitumor activity against a wide variety of cancer including breast cancer cells and cancer stem cells (Guo et al., 2010). However, its use is limited by the development of haematotoxicity, nephrotoxicity, peripheral neuropathy and cardiomyopathy (Klimtova et al., 2002). Encapsulating chemotherapy drugs in a biocompatible material that can deliver them to their intended site of action might provide a solution to this problem (Akbarzadeh et al., 2013). Liposomes are considered one of the most successful drug delivery systems applying nanotechnology to increase circulation time and reduce toxicities of conventional

drugs by a change in drug distribution in the body (Lammers, Hennink, & Storm, 2008). Despite the fast release and targeting the tumor site, the efficacy of therapeutic molecules is often limited by the insufficient accumulation in target tissues (Pisco, Jackson, & Huang, 2014).

Herein, we report the development of a CL thermosensitive liposomal formulation composed of DPPC /MSPC/ DSPE-mPEG (2000) /CL, to enhance both the release and uptake of DNR against MDA-MB-231 breast cancer cells. Our *in vitro* cytotoxic data provided clear evidence to support DNR TSLs with CL (F1) as more effective in breast cancer cell growth inhibition compared with TSLs without CL (F2) and free DNR (Figure 4.5B).

We did not observe any significant cell damage to MDA-MB-231 when 10 min mild hyperthermia was applied. 10 min was enough to release DNR. A positive impact on the amount and rate of DNR released in the presence of multiple types of lipids resulted from an increase in packing incompatibility and, hence, increased permeability when mild hyperthermia was applied (Bassett, Anderson, & Tacker, 1986). Furthermore, we did not observe any significant enhancement in cellular toxicity between free DNR and F2, indicating complete drug release from TSLs. In addition, empty liposomal formulation containing CL (F4) did not exhibit any effect on cell survival. Thus, the increased efficacy of F1 might contribute to enhance intracellular DNR delivery.

This is a strong indication that CL lipid affected the membrane permeability since anthracycline drugs enter cells by passive diffusion (Speelmans, Staffhorst, de Kruijff, & de Wolf, 1994), and the anti-tumor effect is

enhanced by increasing cellular uptake (Lei et al., 2011). CL has the capability to form domains on the cell membrane that ultimately change membrane physical stability allowing more drugs to enter into cells (Sennato et al., 2005).

Besides triggering drug release from the TSLs, mild hyperthermia can increase tumor vascular permeability and, thus, accumulation of liposomes in the tumor site (Huang et al., 1994). We conducted cell viability assay using a high concentration of DNR without exposure of cells to mild hyperthermia to assure that TSLs will not release DNR unless exposed to mild hyperthermia and to assure that CL has no effect on cell viability at 37°C. As shown in Figure 4.6, after a prolonged incubation time (24 and 48 h) at 37°C, no significant reduction in cell viability was observed from TSLs due to lack of drug release. Our TSLs enriched with CL were stable in physiological environments; however, they were versatile by modulation of temperature as intended.

4.4.5 DNR Accumulation Into MDA-MB-231 Cell Lines

The DNR uptake by tumor cells treated with different DNR formulations, all containing 14 μM, were evaluated at 37°C and 42°C. As shown in Figure 4.7A, after 0.5 h at 37°C free DNR showed the highest uptake and TSL uptake showed the lowest. However, after 4 h, F3 showed a higher uptake compared with free DNR while TSLs still did not exhibit any significant uptake. In Figure 4.7B, mild hyperthermia enhanced DNR uptake significantly, especially at 4 h. When treated with F1 for 4 h, DNR accumulated 240%, 256% and 152% compared to F2, free DNR, and F3, respectively.

PEGylation of liposomes significantly reduces cellular uptakes and efficacious drug release of the liposomes, which interferes with the antitumor efficacy of liposome-encapsulated drugs (Y. Li et al., 2015). However, PEGylation is still very important as it increases liposomes circulation time by decreasing RES uptake. Liposomes without PEG are taken easily by endocytic process and their uptake is time and concentration-dependent (Cui, Wan, Yang, Ren, & Guo, 2017). Several stimuli-responsive liposomes, such as light, enzyme, pH, temperature-sensitive liposomes, have been formulated to increase drugs release from liposomes at tumor site.

At 37°C, free DNR exhibited the highest cellular uptake in early-stage (0.5 h) because drug solution could be easily diffused through the lipid bilayer of cells; however, after 4 h, F3 exhibited more intracellular accumulation of DNR because this formulation was not grafted with PEG and can be taken more effectively by endocytosis. TSLs either with or without CL had good stability and did not release DNR. When applying mild hyperthermia, rapid release of DNR was observed from our TSLs formulation. At 4 h, we observed the enhanced effect of CL on DNR accumulations as more DNR accumulated within cells in case of F1 compared to other formulations. Enrichment of TSLs with CL enhanced the cellular uptake might due to the ability of CL to form domains on cell membrane that eventually change its physical stability, fluidity, mechanical structure, allowing more drug to accumulate into cells. Cellular uptake results are consistent with both release cytotoxicity results.

4.4.6 DNR Internalized Efficiently From CL-TSLs in MDA-MB-231 Cancer Cells

Confocal fluorescence microscopy was used to observe the intracellular uptake of DNR from TSLs and the standard DNR at 37°C and after exposure to mild hyperthermia. Intracellular incorporation of DNR in MDA-MB-231 revealed no DNR uptake at 37°C for F1 and F2 compared with free DNR and F3 (Figure 4.8A). After exposing cells containing F1 and F2 to mild hyperthermia, a significant and visible increase in DNR uptake was observed (Figure 4.8B).

F1 displayed a significantly higher DNR accumulation in a time-dependent manner. After 6 hours of incubation (14 μM DNR), the fluorescence levels were consistently higher in F1 compared with F3, F2, and free DNR. CL changes the physical properties of cells membrane such as thickness and permeability leading to more DNR accumulation inside cells. To examine the interaction of CL with the cellular membrane, we incorporated fluorescent CL into the liposomal formulation encapsulated with DRN. Furthermore, we made a blank liposomal formulation with fluorescent CL. As shown in Figure 4.9, CL interacted with the cell membrane leading to more DNR accumulation inside cancer cells.

4.4.7 Short -Term Stability Studies

The particle size, EE%, DL%, PI, zeta potential and osmolarity of different formulations kept at 4°C were monitored for one month as shown in Table 4.3. There were no significant changes for any of the indexes, including EE%, suggesting that there was no significant drug leaked from TSLs. Slow leaking and high stability always characterized the most promising liposomal system with desirable efficacy. Stability data indicated that CL did not destabilize the

liposomal membrane. Since anthracycline drugs precipitate as fibrous-bundle aggregates in liposomes (X. Li et al., 1998), high drug: lipid ratio might cause liposomal deformation. Drug: lipid ratio of (1:5) used in our formulations does not cause liposomal membrane deformation, which explains the good stability profile, especially the EE%. In addition, the most stable liposomal formulation was obtained by incorporation of 30 mol% cholesterol (Briuglia, Rotella, McFarlane, & Lamprou, 2015).

4.5 Conclusion

We have designed TSLs by control of DPPC, MSPC, DSPEPEG, cholesterol and CL ratio. The characteristics of selected formulations were investigated *in vitro* for drug release at different temperatures, DNR accumulation, and antitumor efficacy. The results demonstrated that our TSLs with CL released their contents rapidly when exposed to mild hyperthermia for a short time. However, our liposomal system was confirmed to be highly stable in physiological environments and during storage. CL enriched liposomes exhibited a higher cytotoxic and cellular uptake on MDA-MB-231 cell lines than the same formulation without CL, free DNR and liposomes similar to DaunoXome®. Therefore, this formulation appears to be a promising delivery system in the treatment of breast cancer.

4.6 References

Akbarzadeh, A., Rezaei-Sadabady, R., Davaran, S., Joo, S. W., Zarghami, N., Hanifehpour, Y., . . . Nejati-Koshki, K. (2013). Liposome: classification, preparation, and applications. *Nanoscale Res Lett, 8*(1), 102. doi: 10.1186/1556-276X-8-102

Allen, T. M. (1994). Long-circulating (sterically stabilized) liposomes for targeted drug delivery. *Trends Pharmacol Sci, 15*(7), 215-220.

Allen, T. M., & Cullis, P. R. (2013). Liposomal drug delivery systems: from concept to clinical applications. *Adv Drug Deliv Rev, 65*(1), 36-48. doi: 10.1016/j.addr.2012.09.037

Attwood, S. J., Choi, Y., & Leonenko, Z. (2013). Preparation of DOPC and DPPC Supported Planar Lipid Bilayers for Atomic Force Microscopy and Atomic Force Spectroscopy. *Int J Mol Sci, 14*(2), 3514-3539. doi: 10.3390/ijms14023514

Bandak, S., Goren, D., Horowitz, A., Tzemach, D., & Gabizon, A. (1999). Pharmacological studies of cisplatin encapsulated in long-circulating liposomes in mouse tumor models. *Anticancer Drugs, 10*(10), 911-920.

Bartlett, G. R. (1959). Phosphorus assay in column chromatography. *J Biol Chem, 234*(3), 466-468.

Bassett, J. B., Anderson, R. U., & Tacker, J. R. (1986). Use of temperature-sensitive liposomes in the selective delivery of methotrexate and cis-platinum analogues to murine bladder tumor. *J Urol, 135*(3), 612-615.

Blok, M. C., van Deenen, L. L., & De Gier, J. (1976). Effect of the gel to liquid crystalline phase transition on the osmotic behaviour of phosphatidylcholine liposomes. *Biochim Biophys Acta, 433*(1), 1-12.

Briuglia, M. L., Rotella, C., McFarlane, A., & Lamprou, D. A. (2015). Influence of cholesterol on liposome stability and on in vitro drug release. *Drug Deliv Transl Res, 5*(3), 231-242. doi: 10.1007/s13346-015-0220-8

Cain, E. H., Saha, A., Harowicz, M. R., Marks, J. R., Marcom, P. K., & Mazurowski, M. A. (2019). Multivariate machine learning models for prediction of pathologic response to neoadjuvant therapy in breast cancer using MRI features: a study using an independent validation set. *Breast Cancer Res Treat, 173*(2), 455-463. doi: 10.1007/s10549-018-4990-9

Castedo, M., Macho, A., Zamzami, N., Hirsch, T., Marchetti, P., Uriel, J., & Kroemer, G. (1995). Mitochondrial perturbations define lymphocytes undergoing apoptotic depletion in vivo. *Eur J Immunol, 25*(12), 3277-3284. doi: 10.1002/eji.1830251212

Corti, A., Pastorino, F., Curnis, F., Arap, W., Ponzoni, M., & Pasqualini, R. (2012). Targeted drug delivery and penetration into solid tumors. *Med Res Rev, 32*(5), 1078-1091. doi: 10.1002/med.20238

Cui, X., Wan, B., Yang, Y., Ren, X., & Guo, L. H. (2017). Length effects on the dynamic process of cellular uptake and exocytosis of single-walled carbon nanotubes in murine macrophage cells. *Sci Rep, 7*(1), 1518. doi: 10.1038/s41598-017-01746-9

Deamer, D. W., Prince, R. C., & Crofts, A. R. (1972). The response of fluorescent amines to pH gradients across liposome membranes. *Biochim Biophys Acta, 274*(2), 323-335.

Gaber, M. H., Hong, K., Huang, S. K., & Papahadjopoulos, D. (1995). Thermosensitive sterically stabilized liposomes: formulation and in vitro studies on mechanism of doxorubicin release by bovine serum and human plasma. *Pharm Res, 12*(10), 1407-1416.

Gaber, M. H., Wu, N. Z., Hong, K., Huang, S. K., Dewhirst, M. W., & Papahadjopoulos, D. (1996). Thermosensitive liposomes: extravasation and release of contents in tumor microvascular networks. *Int J Radiat Oncol Biol Phys, 36*(5), 1177-1187.

Gabizon, A., & Papahadjopoulos, D. (1988). Liposome formulations with prolonged circulation time in blood and enhanced uptake by tumors. *Proc Natl Acad Sci U S A, 85*(18), 6949-6953.

Garcia-Saez, A. J., Ries, J., Orzaez, M., Perez-Paya, E., & Schwille, P. (2009). Membrane promotes tBID interaction with BCL(XL). *Nat Struct Mol Biol, 16*(11), 1178-1185. doi: 10.1038/nsmb.1671

Gasselhuber, A., Dreher, M. R., Negussie, A., Wood, B. J., Rattay, F., & Haemmerich, D. (2010). Mathematical spatio-temporal model of drug delivery from low temperature sensitive liposomes during radiofrequency tumour ablation. *Int J Hyperthermia, 26*(5), 499-513. doi: 10.3109/02656731003623590

Gubernator, J., Chwastek, G., Korycinska, M., Stasiuk, M., Grynkiewicz, G., Lewrick, F., . . . Kozubek, A. (2010). The encapsulation of idarubicin within liposomes using the novel EDTA ion gradient method ensures improved drug retention in vitro and in vivo. *J Control Release, 146*(1), 68-75. doi: 10.1016/j.jconrel.2010.05.021

Guo, J., Zhou, J., Ying, X., Men, Y., Li, R. J., Zhang, Y., . . . Lu, W. L. (2010). Effects of stealth liposomal daunorubicin plus tamoxifen on the breast cancer and cancer stem cells. *J Pharm Pharm Sci, 13*(2), 136-151.

Hendrick, R. E., Baker, J. A., & Helvie, M. A. (2019). Breast cancer deaths averted over 3 decades. *Cancer*. doi: 10.1002/cncr.31954

Hernandez-Aya, L. F., & Gonzalez-Angulo, A. M. (2013). Adjuvant systemic therapies in breast cancer. *Surg Clin North Am, 93*(2), 473-491. doi: 10.1016/j.suc.2012.12.002

Hongshu, B., Jianxiu, X., Hong, J., Shan, G., Dongjuan, Y., Yan, F., & Kai, S. (2019). Current developments in drug delivery with thermosensitive liposomes Author links open overlay panel. *Asian Journal of Pharmaceutical Sciences, 14*(4), 365-379. doi: https://doi.org/10.1016/j.ajps.2018.07.006

Hood, R. R., Vreeland, W. N., & DeVoe, D. L. (2014). Microfluidic remote loading for rapid single-step liposomal drug preparation. *Lab Chip, 14*(17), 3359-3367. doi: 10.1039/c4lc00390j

Huang, S. K., Stauffer, P. R., Hong, K., Guo, J. W., Phillips, T. L., Huang, A., & Papahadjopoulos, D. (1994). Liposomes and hyperthermia in mice: increased tumor uptake and therapeutic efficacy of doxorubicin in sterically stabilized liposomes. *Cancer Res, 54*(8), 2186-2191.

Ikon, N., Su, B., Hsu, F. F., Forte, T. M., & Ryan, R. O. (2015). Exogenous cardiolipin localizes to mitochondria and prevents TAZ knockdown-induced apoptosis in myeloid progenitor cells. *Biochem Biophys Res Commun, 464*(2), 580-585. doi: 10.1016/j.bbrc.2015.07.012

Immordino, M. L., Dosio, F., & Cattel, L. (2006). Stealth liposomes: review of the basic science, rationale, and clinical applications, existing and potential. *Int J Nanomedicine, 1*(3), 297-315.

Johnston, M. J., Edwards, K., Karlsson, G., & Cullis, P. R. (2008). Influence of drug-to-lipid ratio on drug release properties and liposome integrity in liposomal doxorubicin formulations. *J Liposome Res, 18*(2), 145-157. doi: 10.1080/08982100802129372

Klimtova, I., Simunek, T., Mazurova, Y., Hrdina, R., Gersl, V., & Adamcova, M. (2002). Comparative study of chronic toxic effects of daunorubicin and doxorubicin in rabbits. *Hum Exp Toxicol, 21*(12), 649-657. doi: 10.1191/0960327102ht311oa

Kneidl, B., Peller, M., Winter, G., Lindner, L. H., & Hossann, M. (2014). Thermosensitive liposomal drug delivery systems: state of the art review. *Int J Nanomedicine, 9*, 4387-4398. doi: 10.2147/IJN.S49297

Koukourakis, M. I., Koukouraki, S., Fezoulidis, I., Kelekis, N., Kyrias, G., Archimandritis, S., & Karkavitsas, N. (2000). High intratumoural accumulation of stealth liposomal doxorubicin (Caelyx) in glioblastomas and in metastatic brain tumours. *Br J Cancer, 83*(10), 1281-1286. doi: 10.1054/bjoc.2000.1459

Kuwana, T., Mackey, M. R., Perkins, G., Ellisman, M. H., Latterich, M., Schneiter, R., . . . Newmeyer, D. D. (2002). Bid, Bax, and lipids cooperate to form supramolecular openings in the outer mitochondrial membrane. *Cell, 111*(3), 331-342.

Lammers, T., Hennink, W. E., & Storm, G. (2008). Tumour-targeted nanomedicines: principles and practice. *Br J Cancer, 99*(3), 392-397. doi: 10.1038/sj.bjc.6604483

Landon, C. D., Park, J. Y., Needham, D., & Dewhirst, M. W. (2011). Nanoscale Drug Delivery and Hyperthermia: The Materials Design and Preclinical and Clinical Testing of Low Temperature-Sensitive Liposomes Used in Combination with Mild Hyperthermia in the Treatment of Local Cancer. *Open Nanomed J, 3*, 38-64. doi: 10.2174/1875933501103010038

Lei, T., Srinivasan, S., Tang, Y., Manchanda, R., Nagesetti, A., Fernandez-Fernandez, A., & McGoron, A. J. (2011). Comparing cellular uptake and cytotoxicity of targeted drug carriers in cancer cell lines with different drug resistance mechanisms. *Nanomedicine (Lond), 7*(3), 324-332. doi: 10.1016/j.nano.2010.11.004

Leonenko, Z. V., Finot, E., Ma, H., Dahms, T. E., & Cramb, D. T. (2004). Investigation of temperature-induced phase transitions in DOPC and DPPC phospholipid bilayers using temperature-controlled scanning force microscopy. *Biophys J, 86*(6), 3783-3793. doi: 10.1529/biophysj.103.036681

Lewis, R. N., & McElhaney, R. N. (2009). The physicochemical properties of cardiolipin bilayers and cardiolipin-containing lipid membranes. *Biochim Biophys Acta, 1788*(10), 2069-2079. doi: 10.1016/j.bbamem.2009.03.014

Li, L., ten Hagen, T. L., Hossann, M., Suss, R., van Rhoon, G. C., Eggermont, A. M., . . . Koning, G. A. (2013). Mild hyperthermia triggered doxorubicin release from optimized stealth thermosensitive liposomes improves intratumoral drug delivery and efficacy. *J Control Release, 168*(2), 142-150. doi: 10.1016/j.jconrel.2013.03.011

Li, X., Hirsh, D. J., Cabral-Lilly, D., Zirkel, A., Gruner, S. M., Janoff, A. S., & Perkins, W. R. (1998). Doxorubicin physical state in solution and inside liposomes loaded via a pH gradient. *Biochim Biophys Acta, 1415*(1), 23-40.

Li, Y., Liu, R., Yang, J., Shi, Y., Ma, G., Zhang, Z., & Zhang, X. (2015). Enhanced retention and anti-tumor efficacy of liposomes by changing their cellular uptake and pharmacokinetics behavior. *Biomaterials, 41*, 1-14. doi: 10.1016/j.biomaterials.2014.11.010

Liu, J., & Conboy, J. C. (2004). Phase transition of a single lipid bilayer measured by sum-frequency vibrational spectroscopy. *J Am Chem Soc, 126*(29), 8894-8895. doi: 10.1021/ja031570c

Lovitt, C. J., Shelper, T. B., & Avery, V. M. (2018). Doxorubicin resistance in breast cancer cells is mediated by extracellular matrix proteins. *BMC Cancer, 18*(1), 41. doi: 10.1186/s12885-017-3953-6

Lutter, M., Fang, M., Luo, X., Nishijima, M., Xie, X., & Wang, X. (2000). Cardiolipin provides specificity for targeting of tBid to mitochondria. *Nat Cell Biol, 2*(10), 754-761. doi: 10.1038/35036395

Mahvi, D. A., Liu, R., Grinstaff, M. W., Colson, Y. L., & Raut, C. P. (2018). Local Cancer Recurrence: The Realities, Challenges, and Opportunities for New Therapies. *CA Cancer J Clin, 68*(6), 488-505. doi: 10.3322/caac.21498

Manganelli, V., Capozzi, A., Recalchi, S., Signore, M., Mattei, V., Garofalo, T., . . . Sorice, M. (2015). Altered Traffic of Cardiolipin during Apoptosis: Exposure on the Cell Surface as a Trigger for "Antiphospholipid Antibodies". *J Immunol Res, 2015*, 847985. doi: 10.1155/2015/847985

Margolis, R., Wessner, C., Stanczak, M., Liu, J. B., Li, J., Nam, K., . . . Eisenbrey, J. R. (2019). Monitoring Progression of Ductal Carcinoma In Situ Using Photoacoustics and Contrast-Enhanced Ultrasound. *Transl Oncol, 12*(7), 973-980. doi: 10.1016/j.tranon.2019.04.018

Matsuo, H., Wakasugi, M., Takanaga, H., Ohtani, H., Naito, M., Tsuruo, T., & Sawada, Y. (2001). Possibility of the reversal of multidrug resistance and the avoidance of side effects by liposomes modified with MRK-16, a monoclonal antibody to P-glycoprotein. *J Control Release, 77*(1-2), 77-86.

Mayer, L. D., Tai, L. C., Bally, M. B., Mitilenes, G. N., Ginsberg, R. S., & Cullis, P. R. (1990). Characterization of liposomal systems containing doxorubicin entrapped in response to pH gradients. *Biochim Biophys Acta, 1025*(2), 143-151.

Nag, O. K., Yadav, V. R., Hedrick, A., & Awasthi, V. (2013). Post-modification of preformed liposomes with novel non-phospholipid poly(ethylene glycol)-conjugated hexadecylcarbamoylmethyl hexadecanoic acid for enhanced circulation persistence in vivo. *Int J Pharm, 446*(1-2), 119-129. doi: 10.1016/j.ijpharm.2013.02.026

Needham, D., Anyarambhatla, G., Kong, G., & Dewhirst, M. W. (2000). A new temperature-sensitive liposome for use with mild hyperthermia: characterization and testing in a human tumor xenograft model. *Cancer Res, 60*(5), 1197-1201.

Nicholas, A. R., Scott, M. J., Kennedy, N. I., & Jones, M. N. (2000). Effect of grafted polyethylene glycol (PEG) on the size, encapsulation efficiency and permeability of vesicles. *Biochim Biophys Acta, 1463*(1), 167-178.

Pisco, A. O., Jackson, D. A., & Huang, S. (2014). Reduced Intracellular Drug Accumulation in Drug-Resistant Leukemia Cells is Not Only Solely Due to MDR-Mediated Efflux but also to Decreased Uptake. *Front Oncol, 4*, 306. doi: 10.3389/fonc.2014.00306

Plourde, K., Derbali, R. M., Desrosiers, A., Dubath, C., Vallee-Belisle, A., & Leblond, J. (2017). Aptamer-based liposomes improve specific drug loading and release. *J Control Release, 251*, 82-91. doi: 10.1016/j.jconrel.2017.02.026

Roy, A., Singh, M. S., Upadhyay, P., & Bhaskar, S. (2013). Nanoparticle mediated co-delivery of paclitaxel and a TLR-4 agonist results in tumor regression and enhanced immune response in the tumor microenvironment of a mouse model. *Int J Pharm, 445*(1-2), 171-180. doi: 10.1016/j.ijpharm.2013.01.045

Sennato, S., Bordi, F., Cametti, C., Coluzza, C., Desideri, A., & Rufini, S. (2005). Evidence of domain formation in cardiolipin-glycerophospholipid mixed monolayers. A thermodynamic and AFM study. *J Phys Chem B, 109*(33), 15950-15957. doi: 10.1021/jp051893q

Smith, P. K., Krohn, R. I., Hermanson, G. T., Mallia, A. K., Gartner, F. H., Provenzano, M. D., . . . Klenk, D. C. (1985). Measurement of protein using bicinchoninic acid. *Anal Biochem, 150*(1), 76-85.

Soloman, R., & Gabizon, A. A. (2008). Clinical pharmacology of liposomal anthracyclines: focus on pegylated liposomal Doxorubicin. *Clin Lymphoma Myeloma, 8*(1), 21-32.

Speelmans, G., Staffhorst, R. W., de Kruijff, B., & de Wolf, F. A. (1994). Transport studies of doxorubicin in model membranes indicate a difference in passive diffusion across and binding at the outer and inner leaflets of the plasma membrane. *Biochemistry, 33*(46), 13761-13768.

Sun, X., Yan, X., Jacobson, O., Sun, W., Wang, Z., Tong, X., . . . Chen, X. (2017). Improved Tumor Uptake by Optimizing Liposome Based RES Blockade Strategy. *Theranostics, 7*(2), 319-328. doi: 10.7150/thno.18078

Ta, T., & Porter, T. M. (2013). Thermosensitive liposomes for localized delivery and triggered release of chemotherapy. *J Control Release, 169*(1-2), 112-125. doi: 10.1016/j.jconrel.2013.03.036

Tacar, O., Sriamornsak, P., & Dass, C. R. (2013). Doxorubicin: an update on anticancer molecular action, toxicity and novel drug delivery systems. *J Pharm Pharmacol, 65*(2), 157-170. doi: 10.1111/j.2042-7158.2012.01567.x

Unsay, J. D., Cosentino, K., Subburaj, Y., & Garcia-Saez, A. J. (2013). Cardiolipin effects on membrane structure and dynamics. *Langmuir, 29*(51), 15878-15887. doi: 10.1021/la402669z

Wei, X., Shamrakov, D., Nudelman, S., Peretz-Damari, S., Nativ-Roth, E., Regev, O., & Barenholz, Y. (2018). Cardinal Role of Intraliposome Doxorubicin-Sulfate Nanorod Crystal in Doxil Properties and Performance. *ACS Omega, 3*(3), 2508-2517. doi: 10.1021/acsomega.7b01235

Weiss, R. B. (1992). The anthracyclines: will we ever find a better doxorubicin? *Semin Oncol, 19*(6), 670-686.

Yatvin, M. B., Weinstein, J. N., Dennis, W. H., & Blumenthal, R. (1978). Design of liposomes for enhanced local release of drugs by hyperthermia. *Science, 202*(4374), 1290-1293.

Yun, H., Shi, R., Yang, Q., Zhang, X., Wang, Y., Zhou, X., & Mu, K. (2014). Over expression of hRad9 protein correlates with reduced chemosensitivity in breast cancer with administration of neoadjuvant chemotherapy. *Sci Rep, 4*, 7548. doi: 10.1038/srep07548

Zucchi, R., & Danesi, R. (2003). Cardiac toxicity of antineoplastic anthracyclines. *Curr Med Chem Anticancer Agents, 3*(2), 151-171.

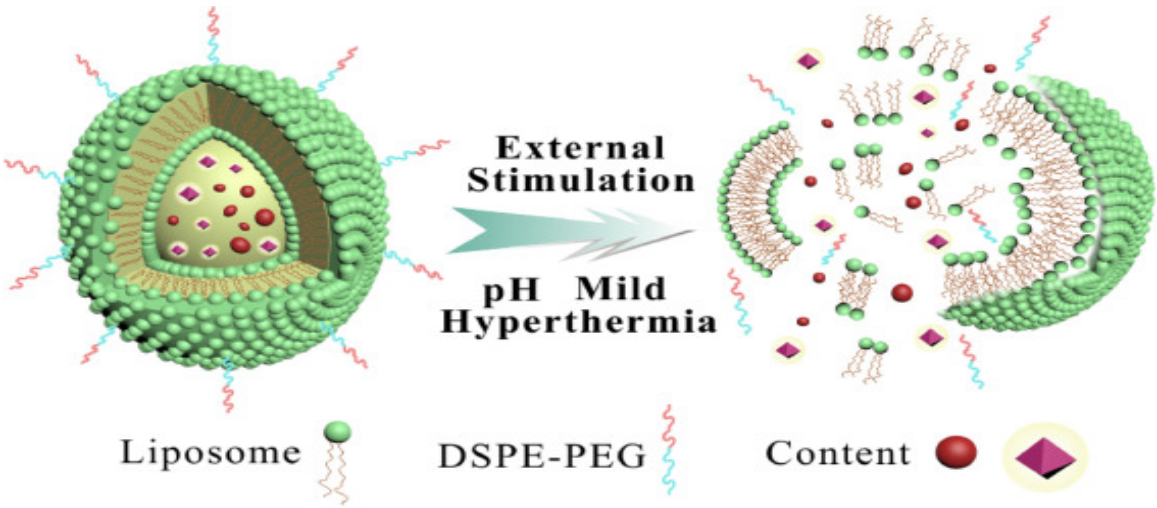

Figure 4.1: Liposomes prepared by multifunctional biomaterials, responding to an external trigger, rapidly releasing their contents (Hongshu et al., 2019)

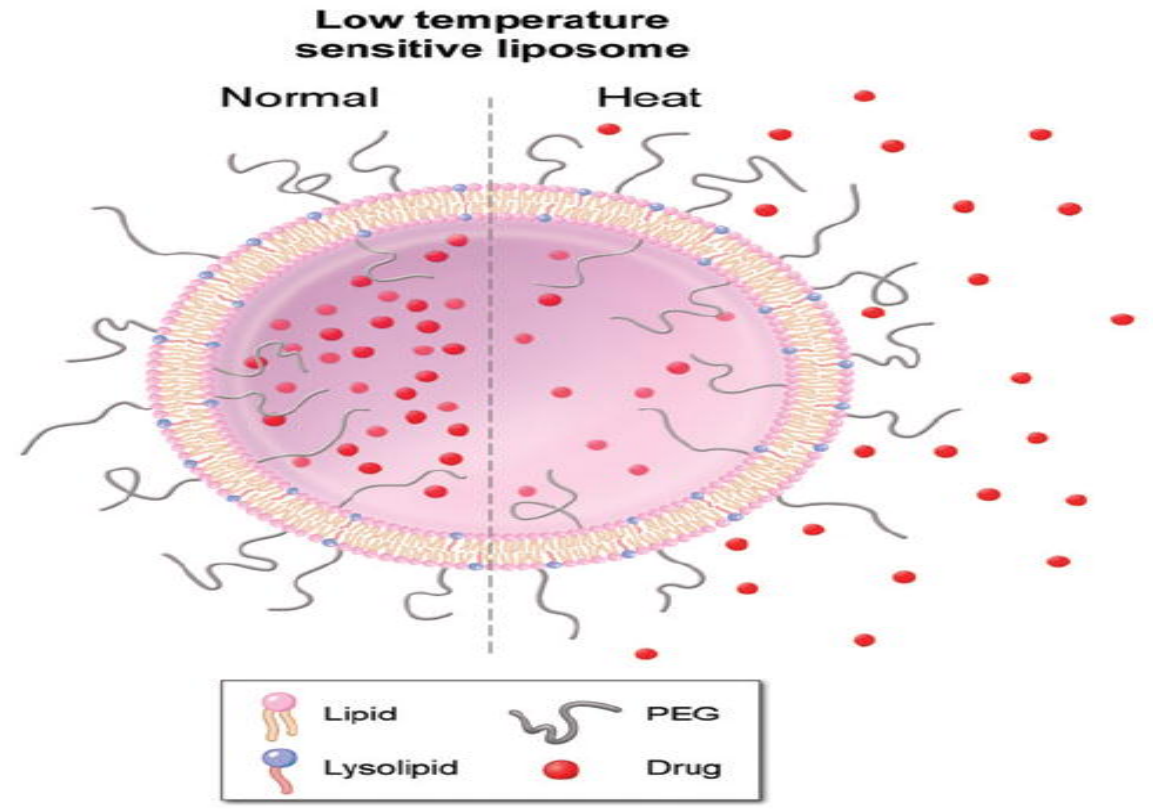

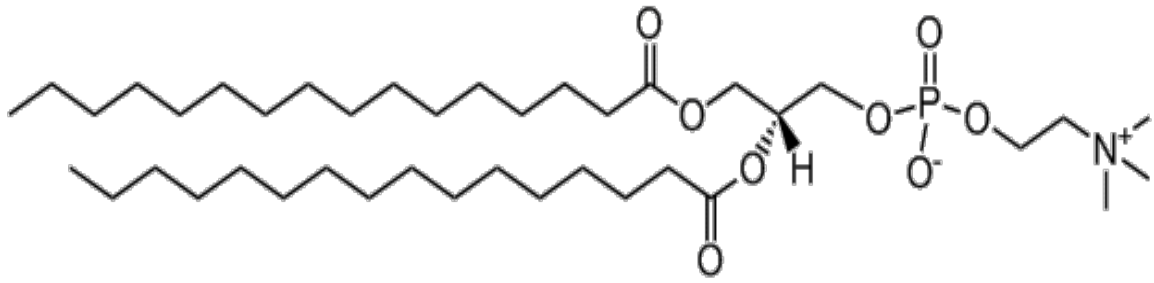

A

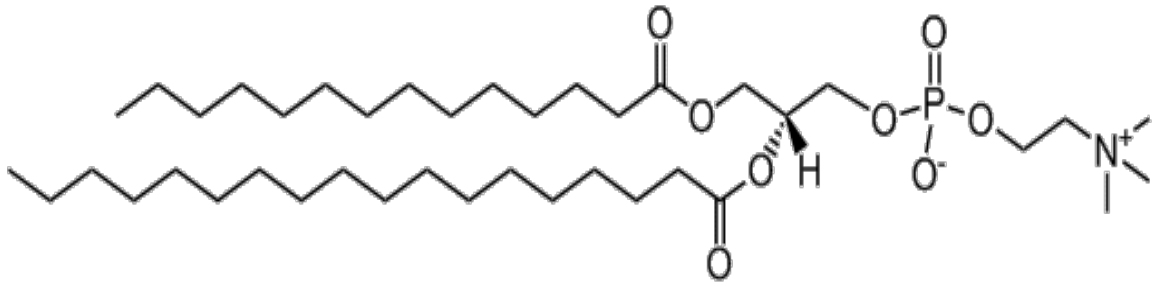

B

Figure 4.2: Lipid bilayer of TSLs contains lysolipids such as DPPC (A) and MSPC (B). They rapidly release their content in response to mild hyperthermia (Gasselhuber et al., 2010)

Table 4.1: Composition and molar ratio of various liposomal formulations

Ingredients	**F1**	**F2**	**F3***	**F4**
DPPC	57	57	-	57
MSPC	40	40	-	40
DSPC	-	-	10	-
Cholesterol	30	30	5	30
DSPE-mPEG (2000)	3	3	-	3
CL	20	-	-	20
DNR:lipid ratio	1:5	1:5	1:10:5	-

* Liposomal formulation similar to DaunoXome®
1:10:5 is the molar ratio of daunorubicin:DSPC:cholesterol
1:5 is the molar ratio of daunorubicin:total lipids

Table 4.2: Physiochemical characteristic of different liposome formulations. Values are expressed as mean ± standard deviation = 3

Formulation	EE %	DL (%)	Particle Size (nm)	PI	Zeta Potential (mV)	Osmolarity (Osm/L)
F1	98.0 ± 0.8	16.2 ± 0.4	115.2 ± 1.3	0.12 ± 0.03	-27.7 ± 1.9	309.0 ± 3.6
F2	96.0 ± 3.6	15.7± 0.7	123.6 ± 1.7	0.11 ± 0.01	-9.7 ± 2.8	299.6 ± 14.9
F3	94.0 ± 3.7	17.0 ± 0.9	85.0 ± 3.4	0.15 ± 0.03	-2.5 ± 2.1	279.6 ± 14.5

EE= Encapsulation Efficiency; DL= Drug Loading; PI= Polydispersity Index

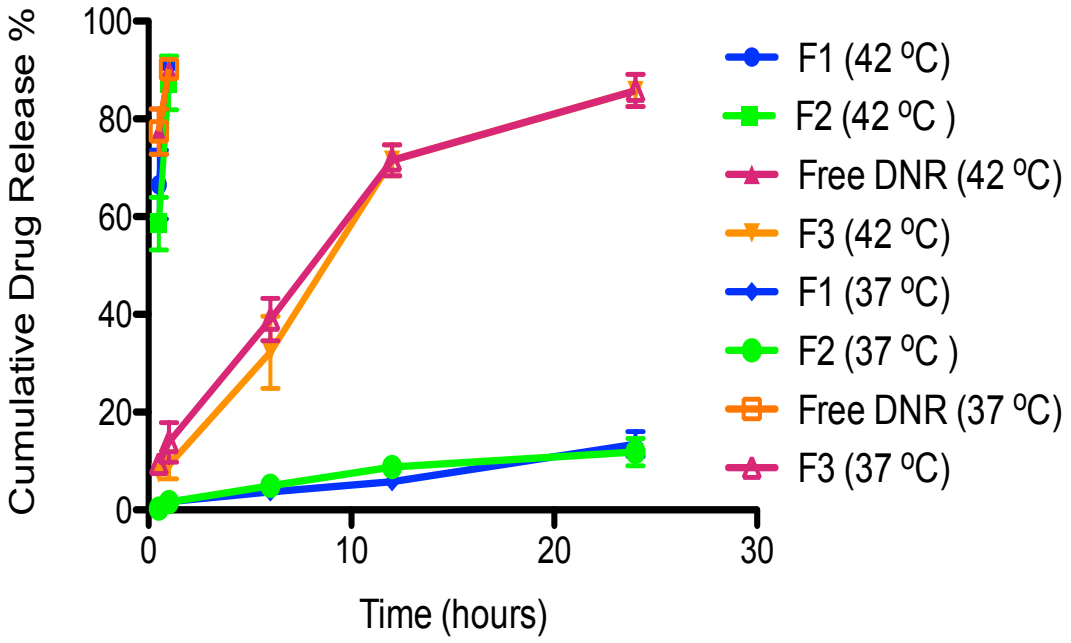

Figure 4.3: Release profiles of DNR from TSL and non-TSL formulations at 37°C and 42°C. Non-TSLs was not influenced by temperature

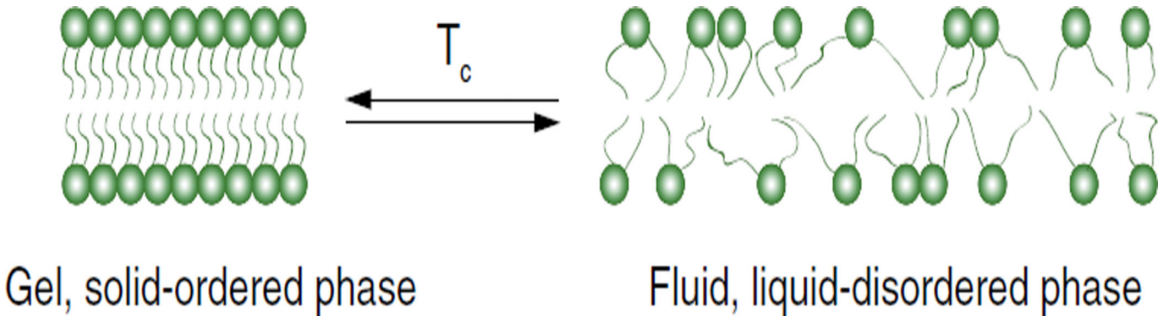

Figure 4.4: Enhancement of lipid bilayer fluidity due to an increase in temperature to a degree above lipids transition temperature can facilitate drug release from liposomes (Ta & Porter, 2013)

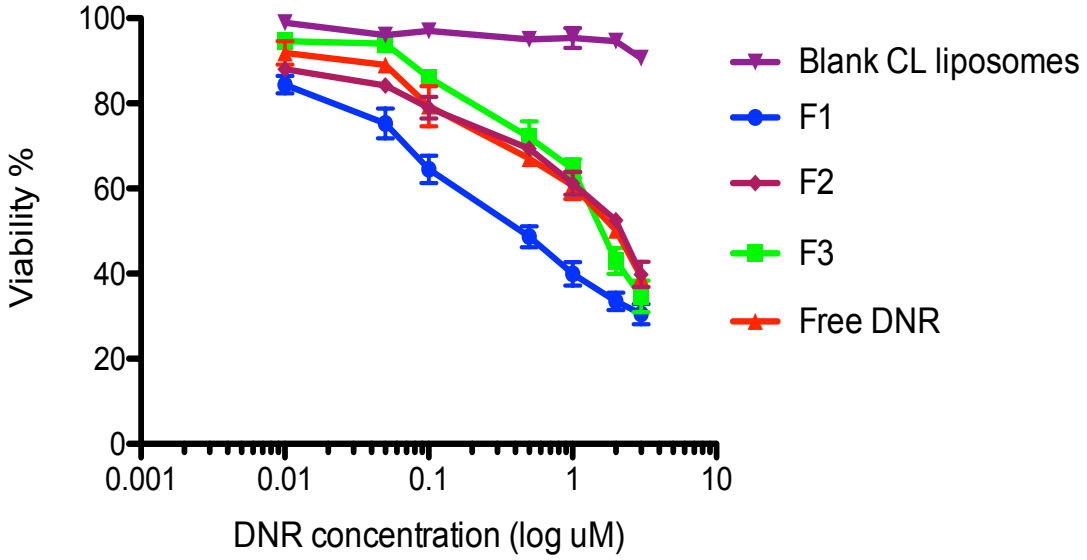

Figure 4.5A: CL potentiates the cytotoxic effect of DNR TSLs against MDA-MB-231 cell lines. Cells incubated at 42°C for 10 min then returned to 37°C. All data are expressed as mean percentages (n=3) to untreated control cells

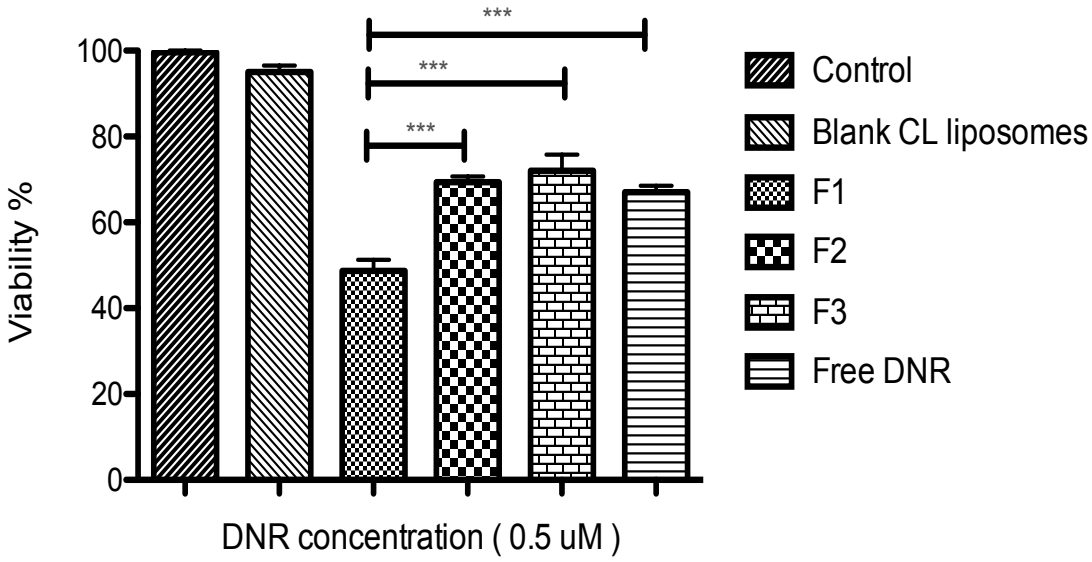

Figure 4.5B: In vitro cytotoxicity of different formulations against MDA-MB-231 breast cancer cells. Cells incubated at 42°C for 10 min then returned to 37°C for 48 hours. *** indicates $p < 0.001$. Mean ± SD of n = 3

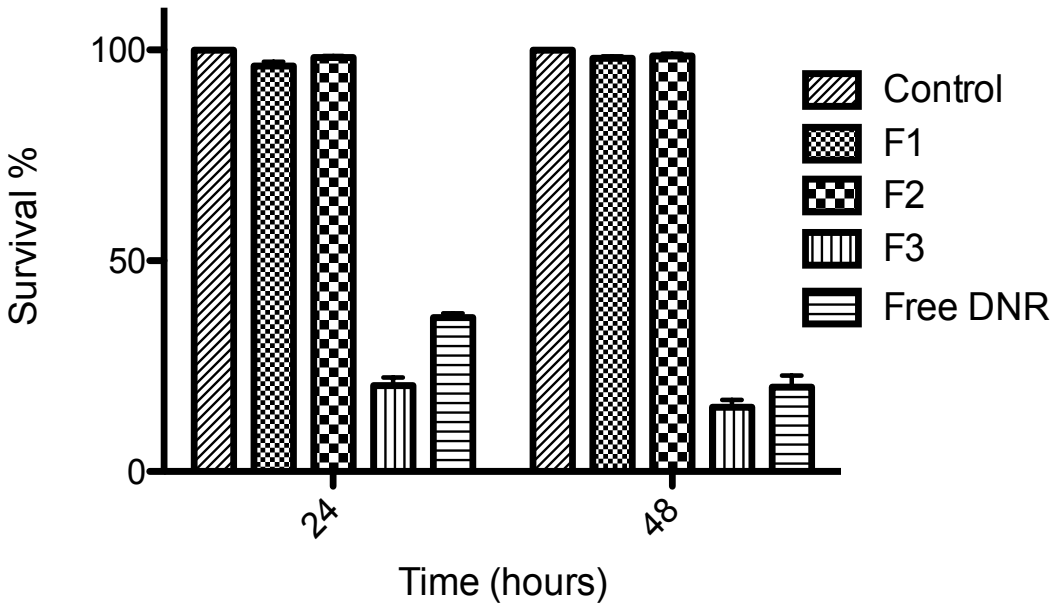

Figure 4.6: Cytotoxic activity (MTT assay) of different types of TSLs (F1 and F2) compared to F3 and free DNR. The cytotoxic activity of DNR loaded TSLs was studied at 14 μM DNR at 37°C on MDA-MB-231cell lines

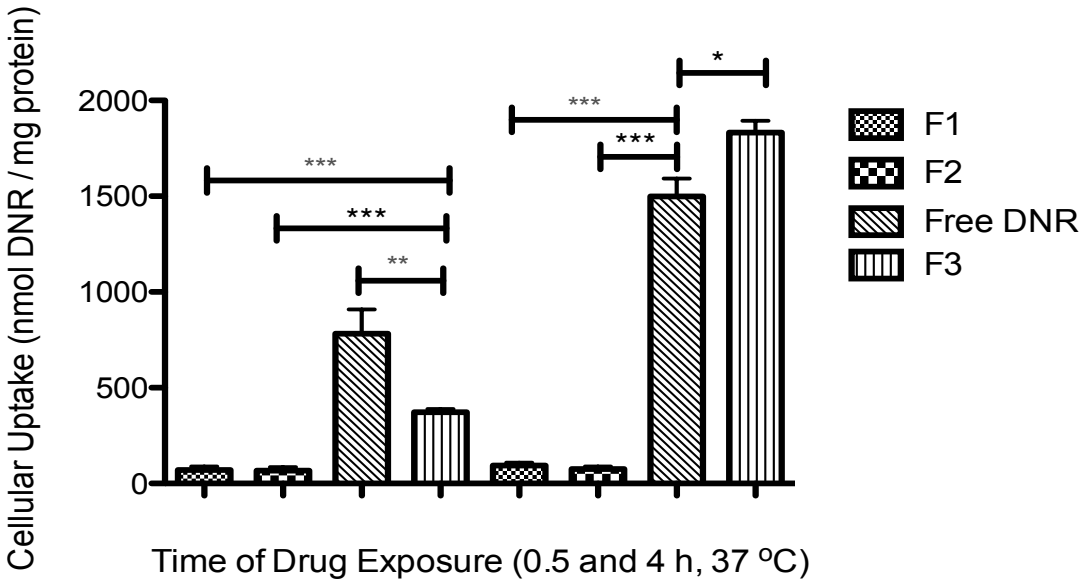

Figure 4.7A: Cellular uptake of TSLs DNR (14 μM) at 37°C by MDA-MB-231 cancer cell lines. * indicates $p < 0.05$, ** indicates $p < 0.01$, and *** indicates $p < 0.001$. Mean ± SD of n = 3

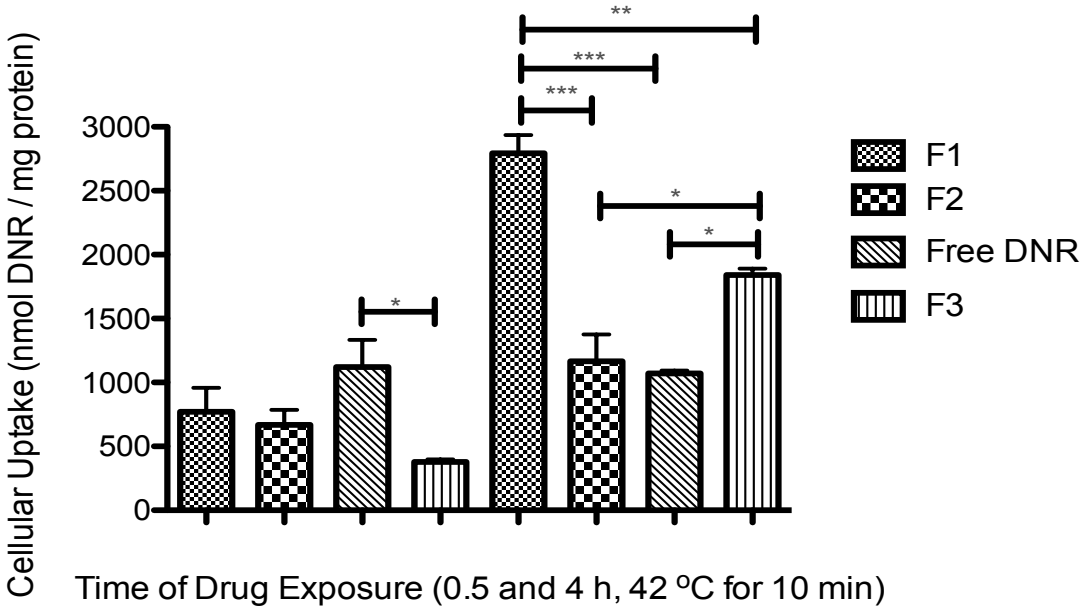

Figure 4.7B: Effect of TSLs enriched with CL on DNR uptake by MDA-MB-231 cancer cell lines after exposure to mild hyperthermia. . * indicates $p < 0.05$, ** indicates $p < 0.01$, and *** indicates $p < 0.001$. Mean ± SD of n = 3

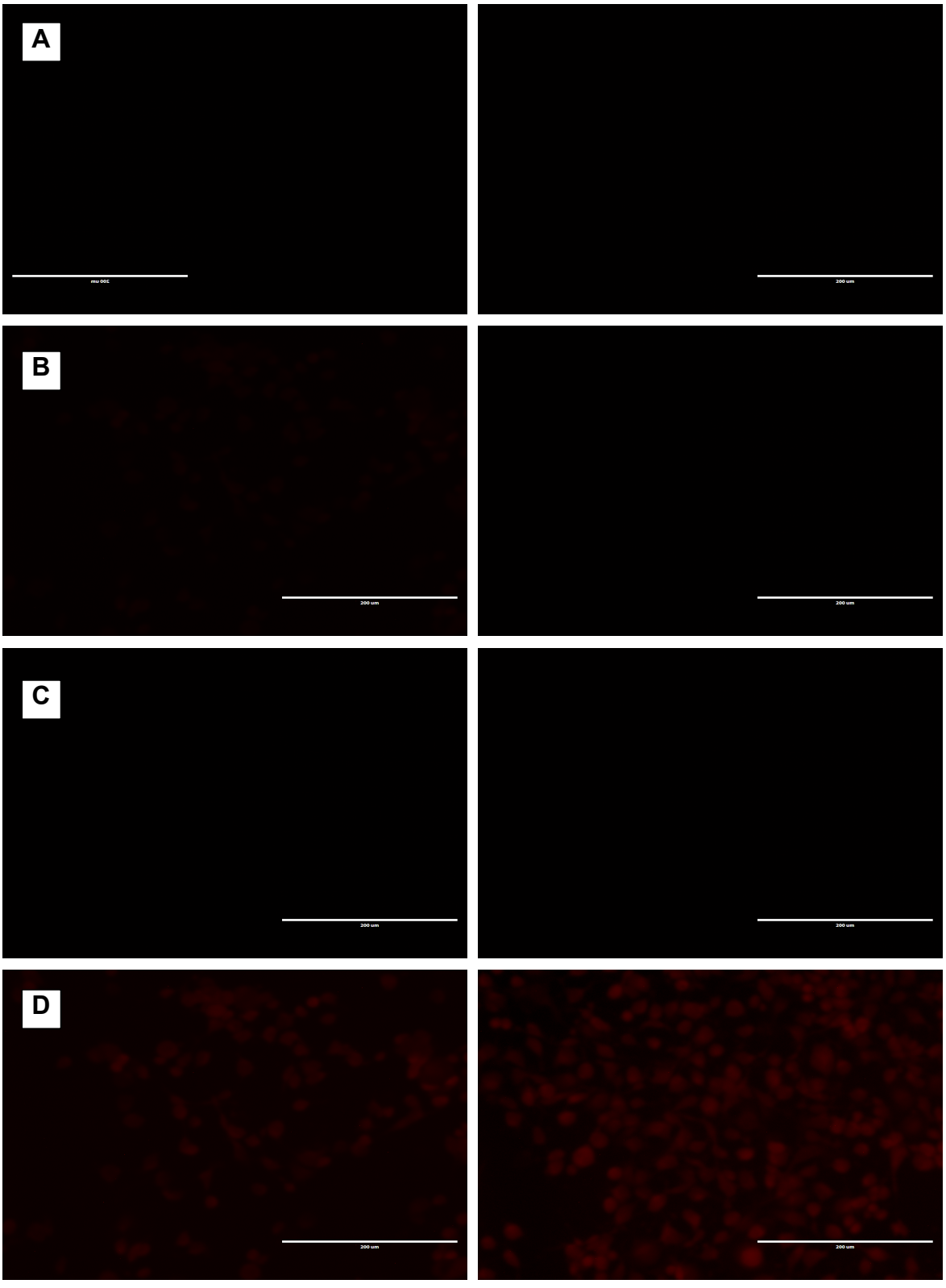
A
200 um
200 um
B
200 um
200 um
C
200 um
200 um
D
200 um
200 um

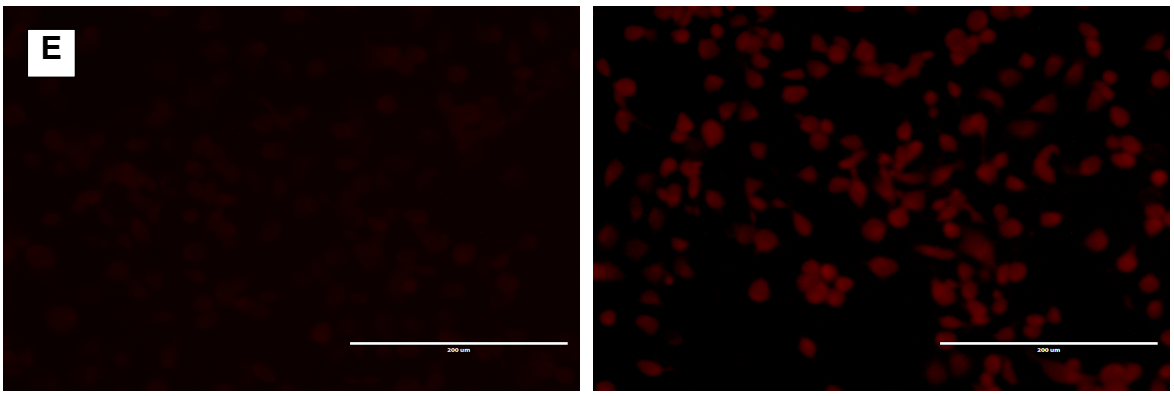

Figure 4.8A: Fluorescence microscopy of different liposomes at 37°C after 0.5 h (left) and 6 h (right). MDA-MB-231 cells were cultured for 24 h (A) and then were treated with F1 (B) F2 (C), free DNR (D) or F3 (E). Final liposomal DNR concentrations were 14 uM

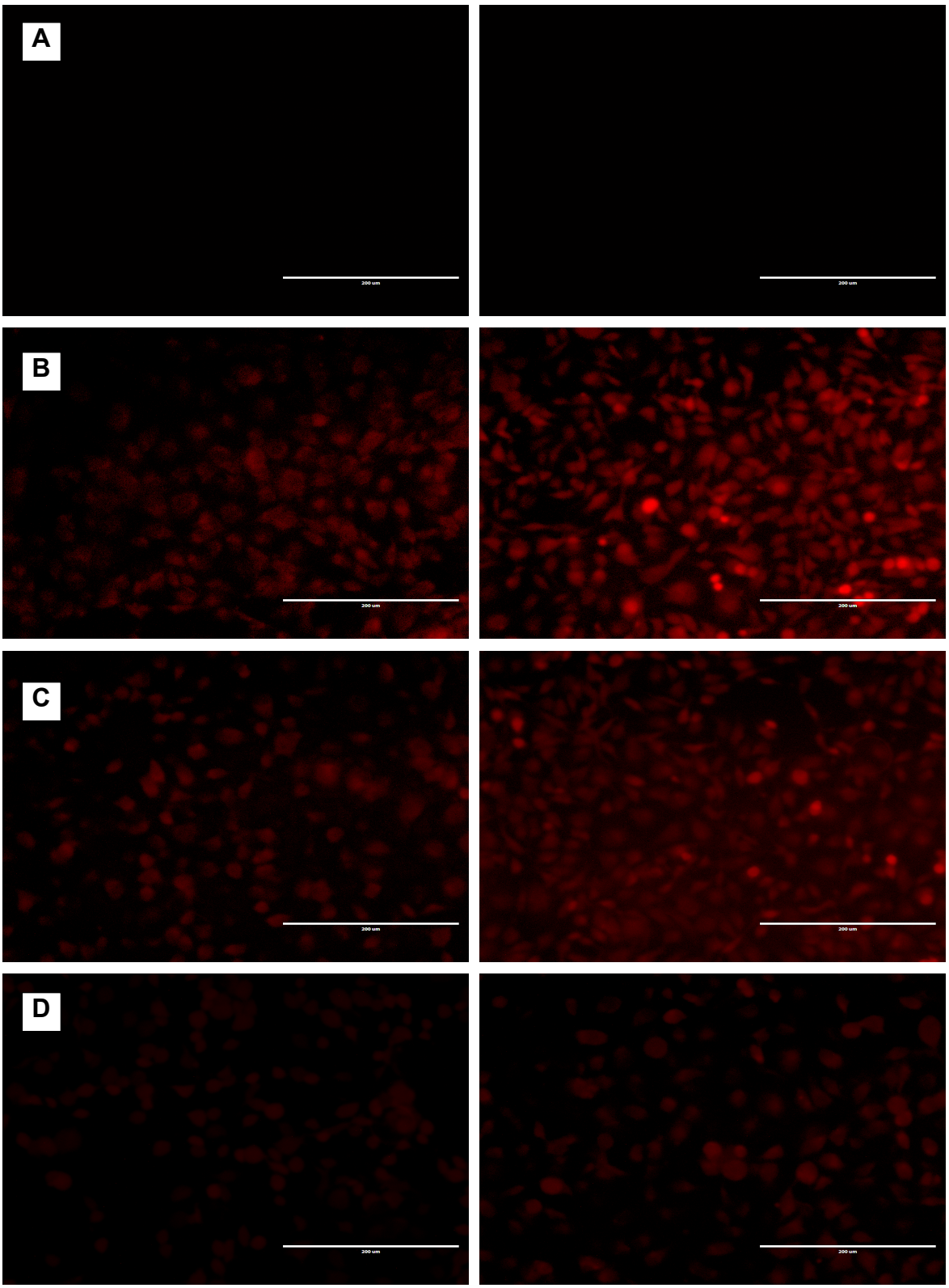
A
200 um
200 um
B
200 um
200 um
C
200 um
200 um
D
200 um
200 um

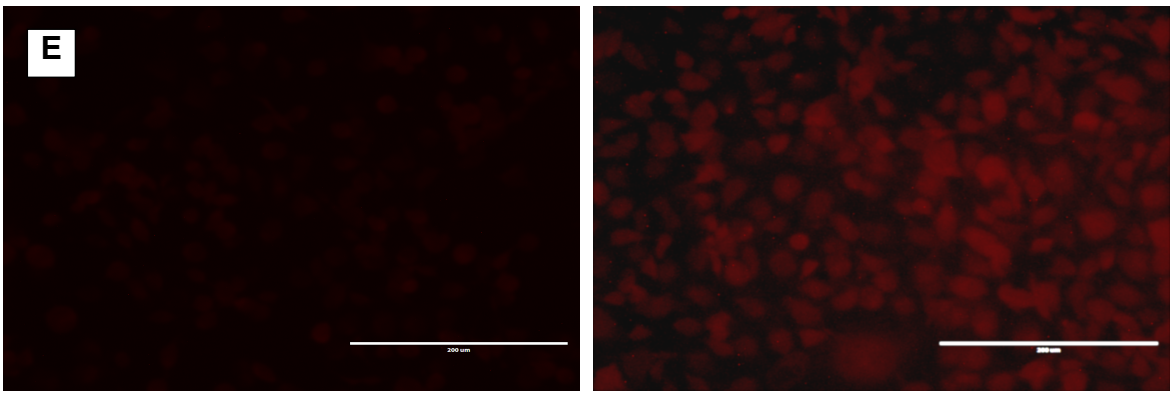

Figure 4.8B: Fluorescence microscopy showing CL enhanced DNR uptake from TSL after exposure to mild hyperthermia (42°C, 10 min) after 0.5 h (left) and 6 h (right). MDA-MB-231 cells were cultured for 24 h (A) and then were treated with F1 (B), F2 (C), free DNR (D) or F3 (E). Final liposomal DNR concentrations were 14 uM

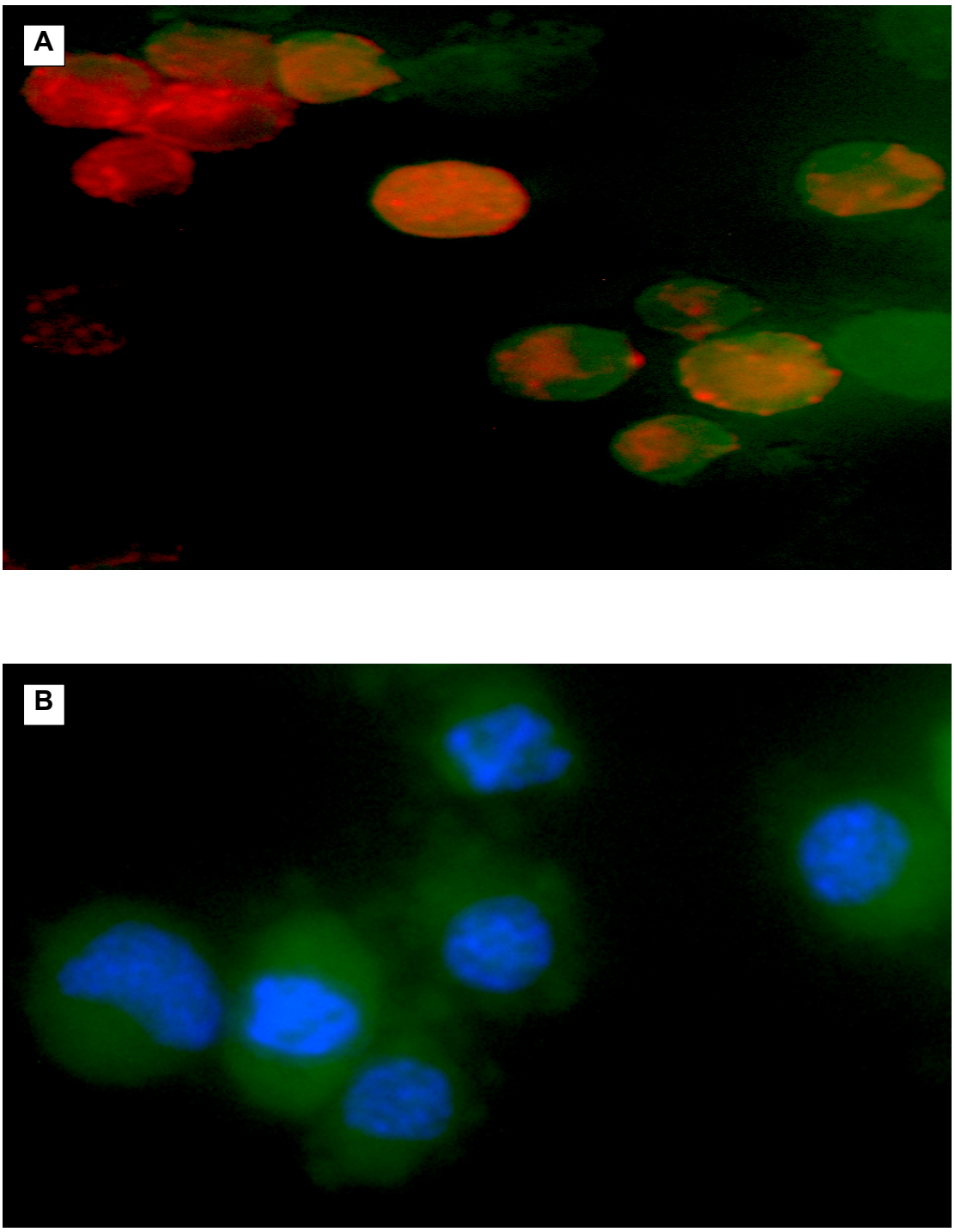

Figure 4.9: Fluorescence microscopy showing CL interacting with the cellular membrane. Fluorescent CL liposomal formulation with DNR (A), and fluorescent CL liposomal formulation with DAPI staining (B). Final liposomal DNR concentrations were 14 uM

Table 4.3: Formulations one month stability at 4^{o}C under N_2 and protected from light. Values represented as mean ± SD, n = 3

	Fresh formulation			After 1 month		
Formulation	F1	F2	F3	F1	F2	F3
Particle Size (nm)	115.2 ± 1.3	123.6 ± 1.7	85.0 ± 3.4	118.6 ± 2.5	124.6 ± 1.4	88.0 ± 2.4
PI	0.12 ± 0.03	0.11 ± 0.01	0.15 ± 0.03	0.22 ±0 .01	0.17 ± 0.06	0.16 ± 0.07
EE %	98.0 ± 0.8	96.0 ± 3.6	94.0 ± 3.7	95.0 ± 2.5	93.0 ± 1.4	92.0 ± 2.1
DL %	16.2 ± 0.4	15.7 ± 0.7	17.0 ± 0.9	15.8 ± 0.4	15.4 ± 0.2	15 .9 ± 0.7
Zeta Potential (mV)	-27.7 ± 1.9	-9.7 ± 2.8	-2.5 ± 2.1	-24.4 ± 1.4	-7.4 ± 2.9	-4.0 ± 2.1
Osmolarity (Osm/L)	309.0 ± 3.6	299.6 ± 14.9	279.6 ± 14.5	311.0 ± 6.7	314.0 ± 2.9	249.0 ± 11.2

PI= Polydispersity Index; EE%= Encapsulation Efficiency; DL%= Drug Loading

Chapter 5: Drug Delivery to the Posterior Segment of the Eye: Challenges and Innovations

5.1 Abstract

The delivery of therapeutic agents to the posterior segment of the eye is challenging, owing to anatomical and physiological barriers of the eye. Conventional dosage forms, such as solutions, suspensions, and ointments, lack long residence time and they can not reach the posterior segment of the eye, choroid, vitreous body and retina. Currently, periocular and intravitreal injection is the common route for the delivery of drugs to treat posterior segment eye diseases due to targeted, localized site of the drug treatment. However, the injections are invasive and can result in pain, formation of cataract, retinal detachment, increased intraocular pressure and endophthalmitis. Hence, noninvasive advanced ophthalmic formulations are required to target the site, sustain drug levels and reduce sides effects associated with the administration. Novel ocular drug delivery systems such as nanoparticles, liposomes, microneedles, and ocular implants are efficient formulation strategies to target and sustain drug levels in the posterior segment of the eye. With current research, efficient delivery systems may be available in the near future to treat various posterior segment diseases in a non-invasive manner.

5.2 Introduction to the Eye

The eye is a complex organ with a unique anatomy and physiology. It is composed of 98% water, 1.8% solid, 0.67% protein, 0.65% sugar, 0.66% NaCl, and 0.79% other mineral elements such as sodium, ammonia and potassium. The structure of eye can be anatomically divided into two main parts: anterior segment (cornea, iris, lens, pupil, ciliary body and, aqueous humor) and posterior segment (vitreous humor, retina, choroid, sclera and the optic nerve) (Figure 5.1). The cornea is the outer transparent structure at the front of the eye that covers the iris, pupil and anterior chamber and it is the eye's primary light-focusing structure. In addition, it provides a protective barrier to the anterior segment (Gaudana, Ananthula, Parenky, & Mitra, 2010). The iris, the colored part of the eye, is responsible for controlling the amount of light permitted to enter the eye by adjusting the diameter and size of the pupil .The lens, the transparent structure inside the eye, focuses the incoming light rays onto the retina. The pupil is the opening in the middle of the iris through which light passes to the back of the eye. The ciliary body is the part of the eye that produces aqueous humor. The aqueous humor, the clear watery fluid in the front of the eyeball, is 98% water and it provides nutrients to the surrounding tissues.

The vitreous humor is a clear jelly-like substance that fills the space between the back of the retina and the surface of the lens and makes up the majority (about 80%) of the volume of the eye. In addition, the vitreous humor contains phagocytic cells that remove blood and other debris that may otherwise interfere with light transmission. The retina is the innermost layer of the eye that

contains photoreceptors (rods and cones) and creates impulses that are sent through the optic nerve to the brain. The sclera is the white visible portion of the eyeball (the outermost layer) where the muscles that move the eyeball are attached. The choroid is a thin blood-rich membrane that lies between the retina and the sclera and it is responsible for supplying blood to the retina. The optic nerve is a bundle of nerve fibers that connect the retina to the area of the brain (the visual cortex), which assembles the signals into images. Diseases affecting the anterior segment include glaucoma, anterior uveitis, allergic conjunctivitis, and cataract. Posterior ocular segment diseases include age-related macular degeneration, diabetic macular edema and diabetic retinopathy.

5.3 Routes of Administration

Ocular drug delivery has met with significant challenges due to the inherent and unique ocular anatomy and physiology. Anatomical and physiological constraints that limit drug delivery to the eye include nasolachrymal drainage, reflex blinking, tear turnover, and decreased permeability across the corneal epithelium (Bachu, Chowdhury, Al-Saedi, Karla, & Boddu, 2018). In ophthalmic formulation development, the first thing to consider is the route of administration since barriers are route specific. Furthermore, the administration route should not interfere with the normal function of the eye. Each route of administration used for ocular drug delivery has its own benefits and challenges, which are summarized in Table 5.1.

5.3.1 Topical Administration

Topical administration, commonly in the form of solutions, suspensions, gels, emulsions, and ointments, is employed to treat anterior segment diseases such as keratitis, uveitis, and conjunctivitis. Topical drug delivery is the most convenient route of administration due to self-administrable, noninvasive, and high patient compliance. However, precorneal factors, such as drainage, blinking, tear film, and induced lacrimation, and anatomical barriers have a negative impact on the bioavailability of topical formulations (Abdelkader & Alany, 2012). Blood flow in the choroid and conjunctival tissues, along with lymphatic flow in the conjunctival tissue and episclera are effective barriers that cause significant drug loss into the systemic circulation, which consequently lowers ocular bioavailability. Topical administration is only ideal for treatment of the anterior segment diseases since anatomical and physiological barriers result in less than 5% delivery to the posterior tissues.

Corneal layers, particularly the stroma and epithelium, are considered the main barriers for ocular drug delivery. The highly hydrated structure of the stroma, which comprises approximately 90% of the corneal thickness, is composed of an extracellular matrix and collagen fibrils. Therefore, stroma poses a major barrier for permeation of lipophilic molecules (Vadlapudi & Mitra, 2013). The corneal epithelium, which is lipophilic in nature, poses a significant barrier for permeation of topically administered hydrophilic molecules. Due to the existence of conjunctival blood capillaries and lymphatics, conjunctival drug absorption is considered to be negligible. Moreover, conjunctival epithelial tight junctions may

limit the passive movement of hydrophilic molecules. Permeability through the sclera is considered to be similar to that of the corneal stroma. The sclera mostly consists of collagen fibers and proteoglycans, a negatively charged matrix. As a result, positively charged molecules exhibit poor permeability through the sclera due to their binding to the negatively charged proteoglycan matrix (Kim, Lutz, Wang, & Robinson, 2007). Additionally, permeability through the cornea and sclera is inversely proportional to the molecules radius (Ban et al., 2017).

5.3.2 Systemic Administration

Due to rapid drainage and poor residence time and absorption across ocular tissues, topical administration is not possible for delivering drugs to the posterior eye tissues. Hence the drugs are systemically delivered by injection. In addition, systemic delivery, either orally or parenterally, may be given for posterior segment treatment and, in some cases, to complement topical treatment for certain anterior segment diseases. Following systemic administration, blood–aqueous barrier is the major barrier for anterior segment ocular drug delivery while blood–retinal barrier is the major barrier for posterior segment ocular drug delivery (Freddo, 2013). Oral delivery might be used in combination with topical delivery to produce therapeutic concentrations in the posterior segment. Compared to the injectable route, oral delivery is preferred, especially for treatment of chronic retinal diseases, as it is noninvasive. However, oral administration requires a high dose, which can result in systemic side effects.

5.3.3 Periocular and Intravitreal Administration

Several injectable routes are employed to overcome low ocular bioavailability of topical delivery, especially when a chronic long-term ocular illness is present. The periocular route of administration includes subconjunctival, subtenon, retrobulbar, and peribulbar (Figure 5.2). Subconjunctival injection enhances permeation of water-soluble drugs since it obviates the conjunctival epithelial barrier. However, the circulation in surrounding tissues can decrease the ocular bioavailability to the targeted location due to rapid drug elimination as formulation is drained into systemic circulation (Kim, Csaky, Wang, & Lutz, 2008). Subtenon injections are used to achieve high drug levels in the vitreous; however, these result in chemosis (swelling of the conjunctiva) and subconjunctival hemorrhage due to the tearing of small blood vessels (Kumar, Eid, & Dodds, 2011). Retrobulbar administration is commonly used to achieve anesthesia for intraocular and orbital surgeries (Ashaye, Ubah, & Sotumbi, 2002). Peribulbar administration involves injection of drugs above and/or below the globe and is a viable route for the delivery of anesthesia, particularly in cataract surgery (Rizzo et al., 2005).

The intravitreal injection is more invasive than the periocular route, however, it offers distinct advantages as drug formulation is directly inserted into the vitreous humor. Administration via this route is associated with adverse effects such as retinal detachment, cataract, hyperemia, hemorrhage and endophthalmitis (Raghava, Hammond, & Kompella, 2004). Intracameral route is

similar to intravitreal injections, but this administration route delivers drug to the anterior chamber.

The eye is a complex organ and drug delivery in the right amounts at the intended sites a very challenging task. Although each route of administration has specific benefits, no single drug delivery administration route is capable of avoiding all of the barriers presented by the eye.

5.4 Ophthalmic Drug Delivery Systems

Various drug delivery strategies have been developed to circumvent different ocular barriers and to achieve desired levels of administrated drugs. The types of ophthalmic drug delivery systems range from the traditional topical formulations (solution, suspension, gel, etc.) to novel drug delivery systems for controlled release and enhanced drug delivery to the posterior segment (microneedles, implants, etc.). The ideal ocular drug delivery system targets and maintains effective drug concentrations at the target site, minimizes systemic exposure, and improves patient compliance.

5.4.1 Conventional Ophthalmic Delivery Systems

For most of the topically applied ophthalmic drugs, the site of action is usually the cornea, conjunctiva, sclera, or the other tissues of the anterior segment. Topical administration is the most widely preferred route to treat the diseases affecting the anterior segment of the eye. For their favorable cost benefit, simplicity of formulation and good patient acceptability, more than 90% of the marketed ophthalmic formulations are in the form of solutions (62.4%), suspensions (8.7%), and ointments (17.4%).

5.4.1.1 Solutions

Topical drops instillations are non-invasive, safe, convenient to the patient and provide an immediate therapeutic effect. However, only about 20% of the administrated dose is retained in the eye due to reflux blinking and tear turnover (Schoenwald, 1990). In addition, less than 5% of the topically applied dose reaches deeper ocular tissues (Alavizadeh et al., 2017). Therefore, to improve ocular bioavailability, different additives, such as viscosity and permeation enhancers, are added. Viscosity enhancers improve drug residence time in the precorneal area. Examples of viscosity enhancers for ocular use include hydroxy methyl cellulose, hydroxy ethyl cellulose, sodium carboxy methyl cellulose, and hydroxypropyl methyl cellulose (Baranowski, Karolewicz, Gajda, & Pluta, 2014). Permeation enhancers improve the permeability of the cornea to drugs by reversibly modifying the corneal barrier integrity. Examples include ethylenediaminetetra acetic acid sodium salt (EDTA), polyoxyethylene lauryl ether, sodium taurocholate and saponins (Moiseev, Morrison, Steele, & Khutoryanskiy, 2019).

Despite being a patient compliant and non-invasive mode of ocular drug administration, topical drops instillation is associated with various side effects such as vision interference, redness and irritation. Also, it is difficult to achieve and maintain a therapeutic drug level in the posterior segment of the eye.

5.4.1.2 Suspensions

Suspensions are another type of non-invasive ocular formulation where finely divided insoluble drugs are dispersed in an aqueous medium containing a

suitable suspending and dispersing agent. Duration of drug action for suspensions is dependent on the particle size of the dispersed drug particles. Large particle size helps retain particles longer in the precornea pocket and causes slow drug dissolution. On the other hand, small particle size facilitates rapid drug absorption into ocular tissues (Schoenwald & Stewart, 1980). Since suspensions formulations contain dispersed insoluble drug particles, they can produce irritation and increased lacrimation upon instillation, which decrease the amount of time that the drug has to dissolve and permeate the sclera or the cornea.

5.4.1.3 Ointments & Gels

Ophthalmic ointments contain a mixture of semisolid and a solid hydrocarbon (paraffin wax). Ophthalmic gels are formulated to produce viscosity-modified solutions. Recently, ophthalmic gels formulated using hydrophilic polymers (hydrogels) along with stimuli responsive polymers (*in situ* gelling systems) have gained growing interest as carrier systems for topical application. Stimuli-responsive gels are liquids that transform into a gel upon contact with the eye through a trigger. Stimuli can be physical (light and temperature), chemical (pH, redox potential, electrolyte) or biological (enzymes). Examples of polymers employed include gellan gum, poloxamer, and cellulose acetate phthalate. Both ointments and gels enhance ocular bioavailability and sustain drug release through increased residence time due to their higher viscosity. However, they can lead to blurred vision and matting of the eyelids.

5.4.1.4 Emulsions

Drug solubility and bioavailability can be enhanced using an emulsion-based formulation. Oil in water (o/w) type emulsion is a commonly used vehicle in ophthalmic drug delivery. Emulsions enhance ocular bioavailability by improving precorneal residence time (compared to solutions) and provide prolonged drug release. However, blurred vision is a limitation.

5.5 Posterior Barriers

In the last few decades, numerous approaches have been utilized for treatment of posterior segment eye diseases. Conventional ocular formulations do not yield therapeutic drug levels in the posterior segment of the eye due to limited drug delivery and targeting (Gaudana, Jwala, Boddu, & Mitra, 2009). Anatomical structure of the eye makes it a highly protected organ and restricts therapeutic agents transport from blood into the posterior segment (Dalkara et al., 2009). The inner limiting membrane and the blood–retinal barrier are the main biological barriers that limit drug transport from the vitreous to the retina (Peynshaert, Devoldere, Minnaert, De Smedt, & Remaut, 2019). Endothelium efflux transporters facilitate a rapid elimination of molecules from the posterior segment of the eye (Hornof, Toropainen, & Urtti, 2005).

Various forms of drug-delivery system have been developed to meet the demand of treating posterior eye diseases. Novel devices and formulations are designed to surpass ocular barriers and help to minimize side effects associated with conventional topical formulations. In addition, novel devices and

formulations are developed to enhance ocular bioavailability as they allow long precorneal residence time and sustain the drug release.

5.6 Novel Ocular Drug Delivery Systems for Posterior Segment

5.6.1 Microneedle

Due to the excellent barrier properties of superficial tissues of sclera and cornea, drugs can not reach the posterior segment of the eye in therapeutic concentrations. In the recent years, microneedles (MNs) have been employed through the transscleral route for drug delivery to posterior ocular tissues. MNs are custom designed to penetrate only hundreds of microns into sclera, so they do not cause damage to the retina. Typically, MNs are 25–2000 μm in height and can be fabricated from a wide variety of materials and in different shapes. MNs are attached to a base support and can create transport pathways of micron dimensions (Kaushik et al., 2001). MNs can be used by different methods. MNs can be applied and removed to create micropores followed by drug administration. For immediate delivery, MNs coated with drugs are applied directly. Some polymeric MNs are fabricated to slowly dissolve over a period of time and deliver the drug within them (Figure 5.3).

MNs drug delivery systems may provide efficient treatment for posterior ocular diseases, such as age related macular degeneration, posterior uveitis and diabetic retinopathy. They may help circumvent blood retinal barrier and deliver therapeutic drug in a sufficient concentration to the posterior segment. MNs help to deposit drug into the sclera or into the suprachoroidal space, a narrow space between the sclera and the choroid, which might facilitate diffusion of drug into

the posterior segment (Jung, Chiang, Grossniklaus, & Prausnitz, 2018). MNs drug transport may be affected by a wide variety of MNs variables such as height, type of material and size.

Hollow MNs were employed to enhance sulforhodamine delivery into the posterior segment of the eye (Jiang, Moore, Edelhauser, & Prausnitz, 2009). Hollow MNs were inserted into human cadaver sclera. After insertion of hollow MNs (720 μm into the sclera), an aqueous solution of sulforhodamine was infused into sclera at constant pressure (15 psi). Each individual microneedle delivered 10 – 35 μl of the solution into the sclera. The volume transported appears to be adequate for several ophthalmic drugs. MNs arrays made of polyvinyl pyrrolidone were designed to surpass the barrier function of ocular tissues to improve ocular drug delivery (Thakur et al., 2016). Fluorescein sodium (MW =70 k) and fluorescein isothiocyanate–dextrans (MW = 150 kDa) were used as model drugs. MNs were able to penetrate the outer layer of the cornea (epithelium with thickness of about 50 μm) and the scleral tissue, resulting in high drug diffusion in the posterior segment. MNs were used to inject particles into the suprachoroidal space of rabbit, pig, and cadaver eyes (Patel, Lin, Edelhauser, & Prausnitz, 2011). MNs successfully delivered sulforhodamine B, nanoparticle, microparticle and suspensions into the suprachoroidal space in all eye models. Applied pressures of 250–300 kPa and needle lengths of 800–1,000 μm delivered volumes up to 35 μL.

5.6.2 Nanocarriers

Nanotechnology based ophthalmic formulations have shown promising results for improving ocular bioavailability to the posterior segment. Nanocarriers may protect the therapeutic compounds from degradation, modify tissue uptake, provide sustained release and minimize ocular irritation (Moshfeghi & Peyman, 2005). Several nanocarriers, such as nanoparticles, liposomes, microspheres, and nanosuspensions have been developed for ocular drug delivery.

Microspheres containing 50% PKC412, a kinase inhibitor, for the treatment of choroidal neovascularization, were examined in a porcine model for delivery to the posterior segment (Saishin et al., 2003). PKC412 was detected in the choroid ten days following periocular injection (100 mg) of 50% PKC412 microspheres. After twenty days, high levels of PKC412 were detected in choroid, vitreous, and retina.

Polylactides, slowly degradable aliphatic polyesters, nanoparticles were developed to target the posterior segment and to provide a prolonged release of the encapsulated compounds (Bourges et al., 2003). They were loaded with two fluorochromes (positively charged) and Nile red (neutral) as labels. Polylactides nanoparticles (2.2 mg/mL) localization within the intraocular tissues was observed after a single (5 µL) intravitreous injection in normal rat eyes. After six hours, nanoparticles diffused and stained the retina and retinal pigment epithelium cells. In addition, nanoparticles was detected within the retinal pigment epithelium cells four months after a single intravitreous injection.

Liposomes have also been explored as a delivering system for ocular drugs to the eye's posterior segment. Liposomes represent an ideal delivery system due to their ability to encapsulate both hydrophilic and hydrophobic drugs, cell membrane like structure and excellent biocompatibility. The behavior of a liposomal delivery system, composed of DSPC and labeled with coumarin-6 as a fluorescence reagent, was examined after it was topically administered to mice via eye drops (Hironaka et al., 2009). They showed higher fluorescence emission in the retina 30 min after administration. Epifluorescence microscopy of the whole eye revealed that the delivery path of liposomes to the posterior segment might be through the tissues trabecular meshwork, iris root and pars plana and not via corneal penetration or systemic delivery, since no fluorescence was detected in the inner endothelium layer of the cornea and the optic nerve.

The current evidence suggests nanoparticles to be of value in targeted and controlled drug delivery for posterior eye diseases. However, some limitations, such as insufficient encapsulation efficacy, control of particle size and stability, have to be overcome before clinical trials for posterior eye diseases.

5.6.3 Implants

Ocular implants are used to obtain therapeutic drug concentrations in the posterior segment. They are surgically placed intravitreally by making a small incision at pars plana, located posterior to the lens and anterior to the retina. They can be fabricated as biodegradable and non-biodegradable drug releasing devices. Generally, they are designed to provide a platform for the sustained release of drugs and to circumvent blood retina barrier (Del Amo & Urtti, 2008).

Non-biodegradable polymeric implants offer long-lasting release, from several months to years. Non-biodegradable implants might be fabricated using EVA, PVA and PCF polymers (Abdelkader & Alany, 2012). Biodegradable implants are not required to be surgically removed and may be fabricated using PGA, PCL, POE and PLGA (Kimura & Ogura, 2001).

Retisert® is an examples of a marketed non-biodegradable implant. It is a sterile PVA implant, which contains 0.59 mg fluocinolone acetonide, approved by FDA for the treatment of chronic uveitis that affects the posterior segment of the eye. It is designed to deliver a sustained release of fluocinolone for up to 2.5 years. The implant had effectively managed inflammation and reduced uveitis recurrences, from 51.4% to 6.1%. Vitrasert® is another controlled release intraocular implant approved by the FDA for the treatment of AIDS-associated cytomegalovirus retinitis. It contains 4.5 mg ganciclovir and PVA/EVA polymers that allow diffusion of drug over an extended period of 5–8 m. The implant prolonged the median time for disease progression compared to IV treatment (196 days vs 71 days, respectively).

A biodegradable intravitreal implant, Ozurdex® (dexamethasone 700 µg) has been approved by the FDA for the treatment of non-infectious uveitis and macular edema secondary to retinal vein occlusion (Banerjee, Bunce, & Charteris, 2013). Ozurdex® contains a PLGA polymer matrix that degrades slowly allowing extended release of dexamethasone up to 6 months (Chin et al., 2017). Clinical trials have confirmed decreased vision loss and improved vision acuity. For 412 eyes treated with Ozurdex®, 30% gained at least 15 letters in

Best Corrected Visual Acuity (BCVA) after 60 days (Haller et al., 2011). Surodex™ is another biodegradable implant approved by FDA for the treatment of intraocular inflammation and macular edema. It is composed of PLGA and hydroxypropyl methylcellulose and is used to achieve a sustained dexamethasone release for a period of 7–10 days (Chang & Wong, 1999). Surodex™ has an anti-inflammatory effect comparable to topical steroid administration (Tan, Chee, Lim, & Lim, 1999).

Implants can provide sustained drug release, reduced side effects and circumvent blood retina barrier. However, implantation is an invasive procedure. In addition, it might cause some adverse effects, which include increasing intraocular pressure and cataract progression (Jaffe et al., 2006).

5.6.4 Cyclodextrin

Cyclodextrins (CDs) are a family of cyclic oligosaccharides with a hydrophilic shell and a lipophilic central cavity (Figure 5.4). Drug–cyclodextrin complexation is a beneficial way to enhance the aqueous solubility of poorly water-soluble drugs without altering their molecular properties (T. Loftsson, Jarho, Masson, & Jarvinen, 2005). CDs improve topical drug delivery through the sclera into the posterior segment of the eye as they enhance permeation of lipophilic drugs through the aqueous tear film (Shelley, Grant, Smith, Abarca, & Jayachandra Babu, 2018; Valls, Vega, Garcia, Egea, & Valls, 2008).

Randomly methylated β-cyclodextrin (RMβCD) was utilized to enhance dexamethasone delivery into the posterior part of the eye (Thorsteinn Loftsson, Sigurdsson, Hreinsdóttir, Konrádsdóttir, & Stefánsson, 2007). Results from *in*

vivo ocular tissue distribution studies in rabbit eyes illustrated that aqueous eye drop solutions containing RMβCD yielded higher dexamethasone concentrations in vitreous, retina and optic nerve than commercial eye drops, Maxidex®. In addition, RMβCD worked as a penetrating enhancer into the lipophilic membranes owing to its lipophilic properties.

In another study, dexamethasone/γCD microparticles eye drop suspension enhanced topical dexamethasone delivery through the sclera into the posterior segment of the eye (T. Loftsson, Hreinsdottir, & Stefansson, 2007). High dexamethasone concentrations were obtained in the vitreous and retina while low concentrations were detected in the blood, indicating that dexamethasone/γCD is more site-specific. Microparticles were retained on the eye surface where they dissolved slowly, causing sustained drug saturation of the tear fluid. Furthermore, γCD increased the dexamethasone saturation concentration from about 0.16 mg mL^{-1} to almost 1mg mL^{-1}.

Cyclodextrins are also known to improve aqueous solubility of NSAIDs, highly lipophilic therapeutic agents. Valls *et al.* demonstrated that β-CD/diclofenac complex improved the solubility and bioavailability of diclofenac (Valls et al., 2008). Compared to free drug, CD/diclofenac enhanced drug transport across cornea up to six times.

5.7 Conclusion

The rising prevalence of posterior eye diseases makes the development of efficient drug delivery systems increasingly vital. Novel ophthalmic drug delivery systems are required to overcome the anatomical and physiological barriers of

the eye. From the pharmaceutical point of view, the ideal ocular delivery system should be easy to manufacture, minimize adverse effects and systemic exposure, improve patient compliance and maintain effective drug concentrations at the target site. The emergence of nanotechnology, new techniques, devices and their applications in ocular drug delivery enables the above –mentioned attributes. In the next few years, advanced ophthalmic drug delivery systems may replace invasive routes of drug administration to the posterior segment of the eye such as periocular and intravitreal injections.

5.8 References

Abdelkader, H., & Alany, R. G. (2012). Controlled and continuous release ocular drug delivery systems: pros and cons. *Curr Drug Deliv, 9*(4), 421-430.

Alavizadeh, S. H., Gheybi, F., Nikpoor, A. R., Badiee, A., Golmohammadzadeh, S., & Jaafari, M. R. (2017). Therapeutic Efficacy of Cisplatin Thermosensitive Liposomes upon Mild Hyperthermia in C26 Tumor Bearing BALB/c Mice. *Mol Pharm, 14*(3), 712-721. doi: 10.1021/acs.molpharmaceut.6b01006

Ashaye, A. O., Ubah, J. N., & Sotumbi, P. T. (2002). Respiratory arrest after retrobulbar anaesthesia. *West Afr J Med, 21*(4), 343-344.

Bachu, R. D., Chowdhury, P., Al-Saedi, Z. H. F., Karla, P. K., & Boddu, S. H. S. (2018). Ocular Drug Delivery Barriers-Role of Nanocarriers in the Treatment of Anterior Segment Ocular Diseases. *Pharmaceutics, 10*(1). doi: 10.3390/pharmaceutics10010028

Ban, J., Zhang, Y., Huang, X., Deng, G., Hou, D., Chen, Y., & Lu, Z. (2017). Corneal permeation properties of a charged lipid nanoparticle carrier containing dexamethasone. *Int J Nanomedicine, 12*, 1329-1339. doi: 10.2147/IJN.S126199

Banerjee, P. J., Bunce, C., & Charteris, D. G. (2013). Ozurdex (a slow-release dexamethasone implant) in proliferative vitreoretinopathy: study protocol for a randomised controlled trial. *Trials, 14*, 358. doi: 10.1186/1745-6215-14-358

Baranowski, P., Karolewicz, B., Gajda, M., & Pluta, J. (2014). Ophthalmic drug dosage forms: characterisation and research methods. *ScientificWorldJournal, 2014*, 861904. doi: 10.1155/2014/861904

Bourges, J. L., Gautier, S. E., Delie, F., Bejjani, R. A., Jeanny, J. C., Gurny, R., . . . Behar-Cohen, F. F. (2003). Ocular drug delivery targeting the retina and retinal pigment epithelium using polylactide nanoparticles. *Invest Ophthalmol Vis Sci, 44*(8), 3562-3569. doi: 10.1167/iovs.02-1068

Chang, D. F., & Wong, V. (1999). Two clinical trials of an intraocular steroid delivery system for cataract surgery. *Trans Am Ophthalmol Soc, 97*, 261-274; discussion 274-269.

Chin, E. K., Almeida, D. R. P., Velez, G., Xu, K., Peraire, M., Corbella, M., . . . Mahajan, V. B. (2017). Ocular Hypertension after Intravitreal Dexamethasone (Ozurdex) Sustained-Release Implant. *Retina, 37*(7), 1345-1351. doi: 10.1097/IAE.0000000000001364

Dalkara, D., Kolstad, K. D., Caporale, N., Visel, M., Klimczak, R. R., Schaffer, D. V., & Flannery, J. G. (2009). Inner limiting membrane barriers to AAV-mediated retinal transduction from the vitreous. *Mol Ther, 17*(12), 2096-2102. doi: 10.1038/mt.2009.181

Del Amo, E. M., & Urtti, A. (2008). Current and future ophthalmic drug delivery systems. A shift to the posterior segment. *Drug Discov Today, 13*(3-4), 135-143. doi: 10.1016/j.drudis.2007.11.002

Donnelly, R. F., Raj Singh, T. R., & Woolfson, A. D. (2010). Microneedle-based drug delivery systems: microfabrication, drug delivery, and safety. *Drug Deliv, 17*(4), 187-207. doi: 10.3109/10717541003667798

Freddo, T. F. (2013). A contemporary concept of the blood-aqueous barrier. *Prog Retin Eye Res, 32*, 181-195. doi: 10.1016/j.preteyeres.2012.10.004

Gaudana, R., Ananthula, H. K., Parenky, A., & Mitra, A. K. (2010). Ocular drug delivery. *AAPS J, 12*(3), 348-360. doi: 10.1208/s12248-010-9183-3

Gaudana, R., Jwala, J., Boddu, S. H., & Mitra, A. K. (2009). Recent perspectives in ocular drug delivery. *Pharm Res, 26*(5), 1197-1216. doi: 10.1007/s11095-008-9694-0

Haller, J. A., Bandello, F., Belfort, R., Jr., Blumenkranz, M. S., Gillies, M., Heier, J., . . . Li, J. (2011). Dexamethasone intravitreal implant in patients with macular edema related to branch or central retinal vein occlusion twelve-month study results. *Ophthalmology, 118*(12), 2453-2460. doi: 10.1016/j.ophtha.2011.05.014

Hironaka, K., Inokuchi, Y., Tozuka, Y., Shimazawa, M., Hara, H., & Takeuchi, H. (2009). Design and evaluation of a liposomal delivery system targeting the posterior segment of the eye. *J Control Release, 136*(3), 247-253. doi: 10.1016/j.jconrel.2009.02.020

Hornof, M., Toropainen, E., & Urtti, A. (2005). Cell culture models of the ocular barriers. *Eur J Pharm Biopharm, 60*(2), 207-225. doi: 10.1016/j.ejpb.2005.01.009

Jaffe, G. J., Martin, D., Callanan, D., Pearson, P. A., Levy, B., Comstock, T., & Fluocinolone Acetonide Uveitis Study, G. (2006). Fluocinolone acetonide implant (Retisert) for noninfectious posterior uveitis: thirty-four-week results of a multicenter randomized clinical study. *Ophthalmology, 113*(6), 1020-1027. doi: 10.1016/j.ophtha.2006.02.021

Jiang, J., Moore, J. S., Edelhauser, H. F., & Prausnitz, M. R. (2009). Intrascleral drug delivery to the eye using hollow microneedles. *Pharm Res, 26*(2), 395-403. doi: 10.1007/s11095-008-9756-3

Jung, J. H., Chiang, B., Grossniklaus, H. E., & Prausnitz, M. R. (2018). Ocular drug delivery targeted by iontophoresis in the suprachoroidal space using a microneedle. *J Control Release, 277*, 14-22. doi: 10.1016/j.jconrel.2018.03.001

Kaushik, S., Hord, A. H., Denson, D. D., McAllister, D. V., Smitra, S., Allen, M. G., & Prausnitz, M. R. (2001). Lack of pain associated with microfabricated microneedles. *Anesth Analg, 92*(2), 502-504. doi: 10.1097/00000539-200102000-00041

Kim, S. H., Csaky, K. G., Wang, N. S., & Lutz, R. J. (2008). Drug elimination kinetics following subconjunctival injection using dynamic contrast-enhanced magnetic resonance imaging. *Pharm Res, 25*(3), 512-520. doi: 10.1007/s11095-007-9408-z

Kim, S. H., Lutz, R. J., Wang, N. S., & Robinson, M. R. (2007). Transport barriers in transscleral drug delivery for retinal diseases. *Ophthalmic Res, 39*(5), 244-254. doi: 10.1159/000108117

Kimura, H., & Ogura, Y. (2001). Biodegradable polymers for ocular drug delivery. *Ophthalmologica, 215*(3), 143-155. doi: 10.1159/000050849

Kumar, C. M., Eid, H., & Dodds, C. (2011). Sub-Tenon's anaesthesia: complications and their prevention. *Eye (Lond), 25*(6), 694-703. doi: 10.1038/eye.2011.69

Loftsson, T., Hreinsdottir, D., & Stefansson, E. (2007). Cyclodextrin microparticles for drug delivery to the posterior segment of the eye: aqueous dexamethasone eye drops. *J Pharm Pharmacol, 59*(5), 629-635. doi: 10.1211/jpp.59.5.0002

Loftsson, T., Jarho, P., Masson, M., & Jarvinen, T. (2005). Cyclodextrins in drug delivery. *Expert Opin Drug Deliv, 2*(2), 335-351. doi: 10.1517/17425247.2.1.335

Loftsson, T., Sigurdsson, H. H., Hreinsdóttir, D., Konrádsdóttir, F., & Stefánsson, E. (2007). Dexamethasone delivery to posterior segment of the eye. *Journal of Inclusion Phenomena and Macrocyclic Chemistry, 57*(1-4), 585-589. doi: https://doi.org/10.1007/s10847-006-9253-4

Moiseev, R. V., Morrison, P. W. J., Steele, F., & Khutoryanskiy, V. V. (2019). Penetration Enhancers in Ocular Drug Delivery. *Pharmaceutics, 11*(7). doi: 10.3390/pharmaceutics11070321

Moshfeghi, A. A., & Peyman, G. A. (2005). Micro- and nanoparticulates. *Adv Drug Deliv Rev, 57*(14), 2047-2052. doi: 10.1016/j.addr.2005.09.006

Patel, S. R., Lin, A. S., Edelhauser, H. F., & Prausnitz, M. R. (2011). Suprachoroidal drug delivery to the back of the eye using hollow microneedles. *Pharm Res, 28*(1), 166-176. doi: 10.1007/s11095-010-0271-y

Peynshaert, K., Devoldere, J., Minnaert, A. K., De Smedt, S. C., & Remaut, K. (2019). Morphology and Composition of the Inner Limiting Membrane: Species-Specific Variations and Relevance toward Drug Delivery Research. *Curr Eye Res, 44*(5), 465-475. doi: 10.1080/02713683.2019.1565890

Raghava, S., Hammond, M., & Kompella, U. B. (2004). Periocular routes for retinal drug delivery. *Expert Opin Drug Deliv, 1*(1), 99-114. doi: 10.1517/17425247.1.1.99

Rizzo, L., Marini, M., Rosati, C., Calamai, I., Nesi, M., Salvini, R., . . . Brizzi, E. (2005). Peribulbar anesthesia: a percutaneous single injection technique with a small volume of anesthetic. *Anesth Analg, 100*(1), 94-96. doi: 10.1213/01.ANE.0000140951.65240.94

Saishin, Y., Silva, R. L., Saishin, Y., Callahan, K., Schoch, C., Ahlheim, M., . . . Campochiaro, P. A. (2003). Periocular injection of microspheres containing PKC412 inhibits choroidal neovascularization in a porcine model. *Invest Ophthalmol Vis Sci, 44*(11), 4989-4993. doi: 10.1167/iovs.03-0600

Schoenwald, R. D. (1990). Ocular drug delivery. Pharmacokinetic considerations. *Clin Pharmacokinet, 18*(4), 255-269. doi: 10.2165/00003088-199018040-00001

Schoenwald, R. D., & Stewart, P. (1980). Effect of particle size on ophthalmic bioavailability of dexamethasone suspensions in rabbits. *J Pharm Sci, 69*(4), 391-394. doi: 10.1002/jps.2600690407

Shelley, H., Grant, M., Smith, F. T., Abarca, E. M., & Jayachandra Babu, R. (2018). Improved Ocular Delivery of Nepafenac by Cyclodextrin Complexation. *AAPS PharmSciTech, 19*(6), 2554-2563. doi: 10.1208/s12249-018-1094-0

Tan, D. T., Chee, S. P., Lim, L., & Lim, A. S. (1999). Randomized clinical trial of a new dexamethasone delivery system (Surodex) for treatment of post-cataract surgery inflammation. *Ophthalmology, 106*(2), 223-231. doi: 10.1016/S0161-6420(99)90060-X

Thakur, R. R., Tekko, I. A., Al-Shammari, F., Ali, A. A., McCarthy, H., & Donnelly, R. F. (2016). Rapidly dissolving polymeric microneedles for minimally invasive intraocular drug delivery. *Drug Deliv Transl Res, 6*(6), 800-815. doi: 10.1007/s13346-016-0332-9

Vadlapudi, A. D., & Mitra, A. K. (2013). Nanomicelles: an emerging platform for drug delivery to the eye. *Ther Deliv, 4*(1), 1-3. doi: 10.4155/tde.12.122

Valls, R., Vega, E., Garcia, M. L., Egea, M. A., & Valls, J. O. (2008). Transcorneal permeation in a corneal device of non-steroidal anti-inflammatory drugs in drug delivery systems. *Open Med Chem J, 2*, 66-71. doi: 10.2174/1874104500802010066

Zafar, N., Fessi, H., & Elaissari, A. (2014). Cyclodextrin containing biodegradable particles: from preparation to drug delivery applications. *Int J Pharm, 461*(1-2), 351-366. doi: 10.1016/j.ijpharm.2013.12.004

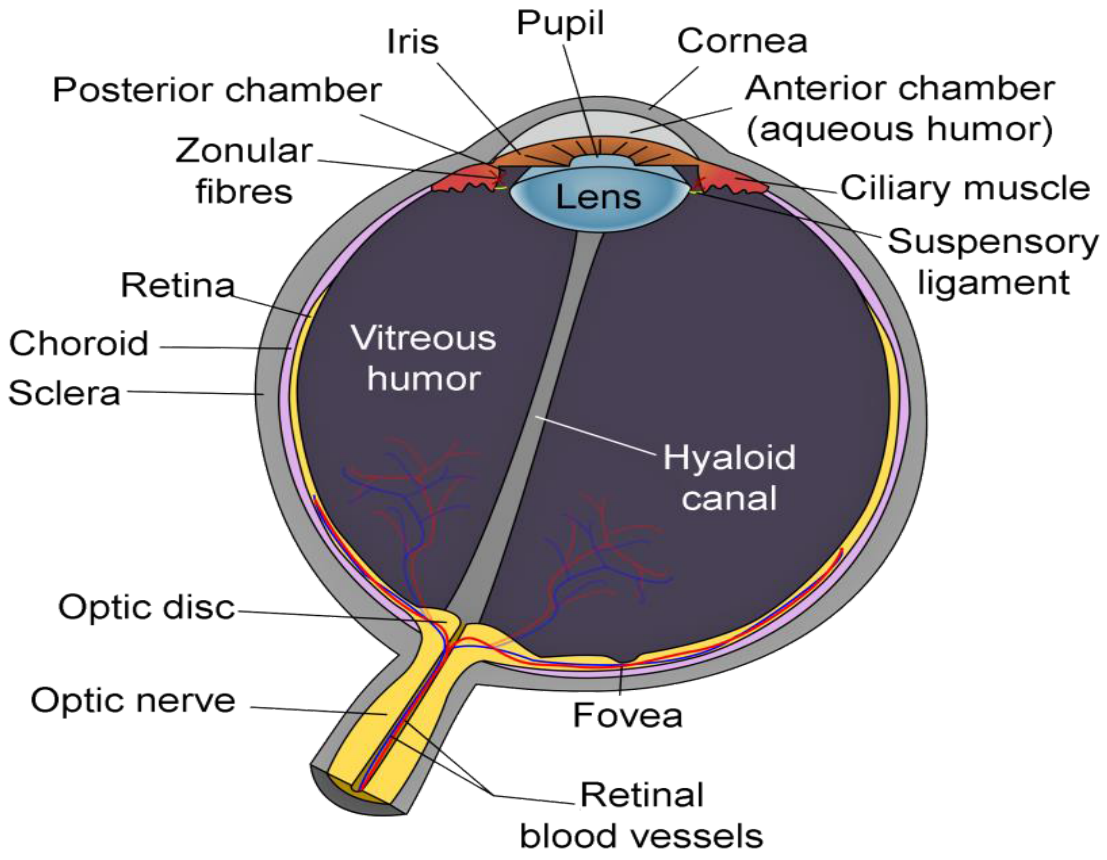

Figure 5.1: Anatomy of the eye

Table 5.1: Benefits and challenges of various routes of administration for ocular drug delivery

Route	Benefits	Challenges	Applications
Topical	High patient compliance and noninvasive	Higher tear dilution, cornea acts as barrier, efflux pumps	Keratitis, uveitis, conjunctivitis, scleritis, blepharitis
Oral/Systemic	Noninvasive route of administration	High dosing required, blood–aqueous barrier, blood–retinal barrier	Scleritis, episcleritis, retinitis, posterior uveitis
Subconjunctival	Delivery to anterior and posterior segment, enhances permeation of water-soluble drugs	Rapid elimination due to conjunctival and choroidal circulation	Glaucoma, age-related macular degeneration, retinitis, posterior uveitis
Subtenon	Fewer complications, high vitreal drug levels	Chemosis, subconjunctival hemorrhage	Uveitis, retinal vein occlusion, age-related macular degeneration
Retrobulbar/ Peribulbar	High local doses of anesthetics, minimal effect on IOP	Hemorrhage, respiratory arrest	Anesthesia
Intravitreal	Drug formulation directly inserted into the vitreous humor, sustains drug levels	Cataract, retinal detachment, endophthalmitis,	Retinitis, age-related macular degeneration, posterior uveitis, diabetic macular edema, cystoid macular edema,
Intracameral	Delivers drug to the anterior chamber	Toxic anterior segment syndrome, toxic endothelial cell destruction syndrome	Anesthesia, pupil dilation

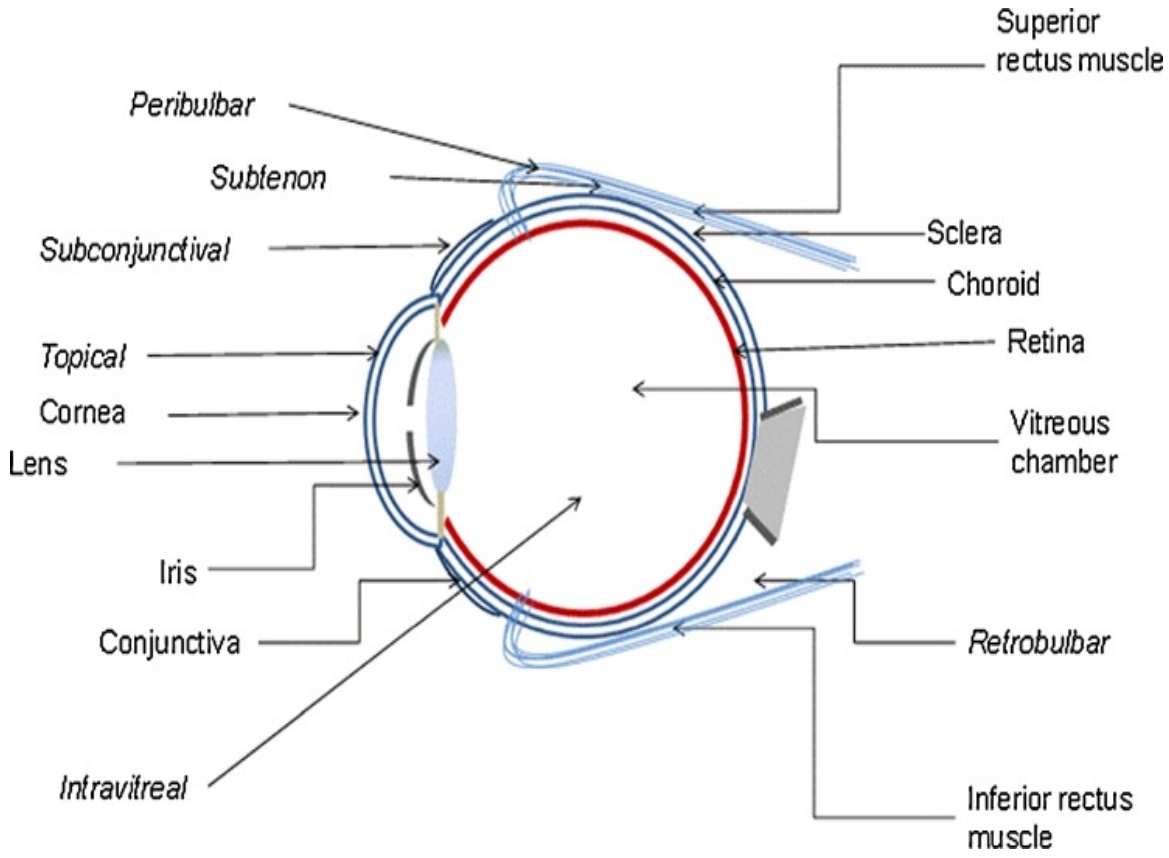

Figure 5.2: Routes of drug administration to eye (Gaudana et al., 2010)

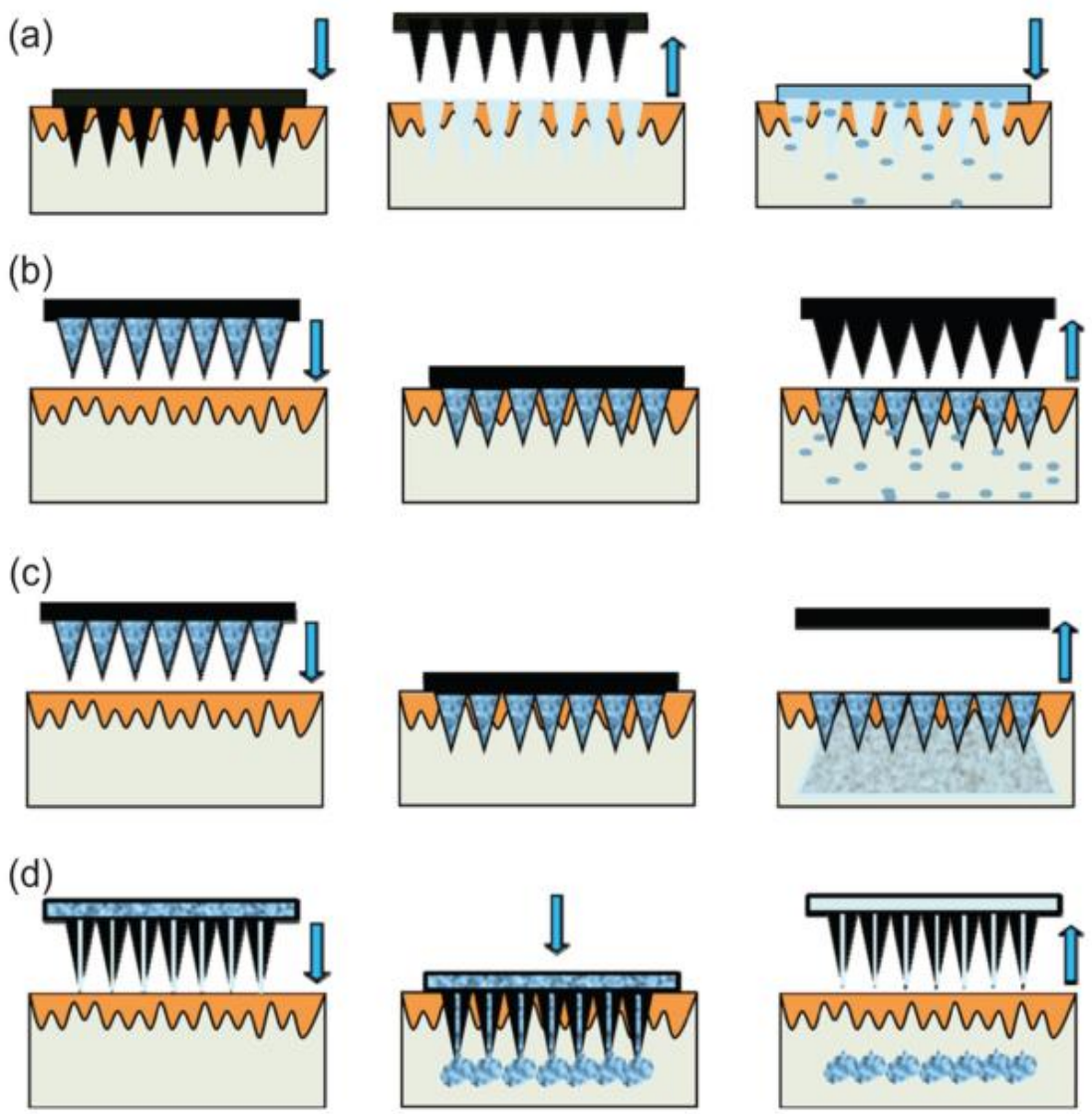

Figure 5.3: Schematic illustration of different methods of MNs application. (a) Solid MNs applied and removed to create micropores followed by the application of the drug (b) Solid MNs coated with drug applied for immediate delivery (c) Polymeric MNs remain in intended site and deliver drug over time as they slowly dissolve (d) Continuous drug delivery by hollow MNs (Donnelly, Raj Singh, & Woolfson, 2010)

.

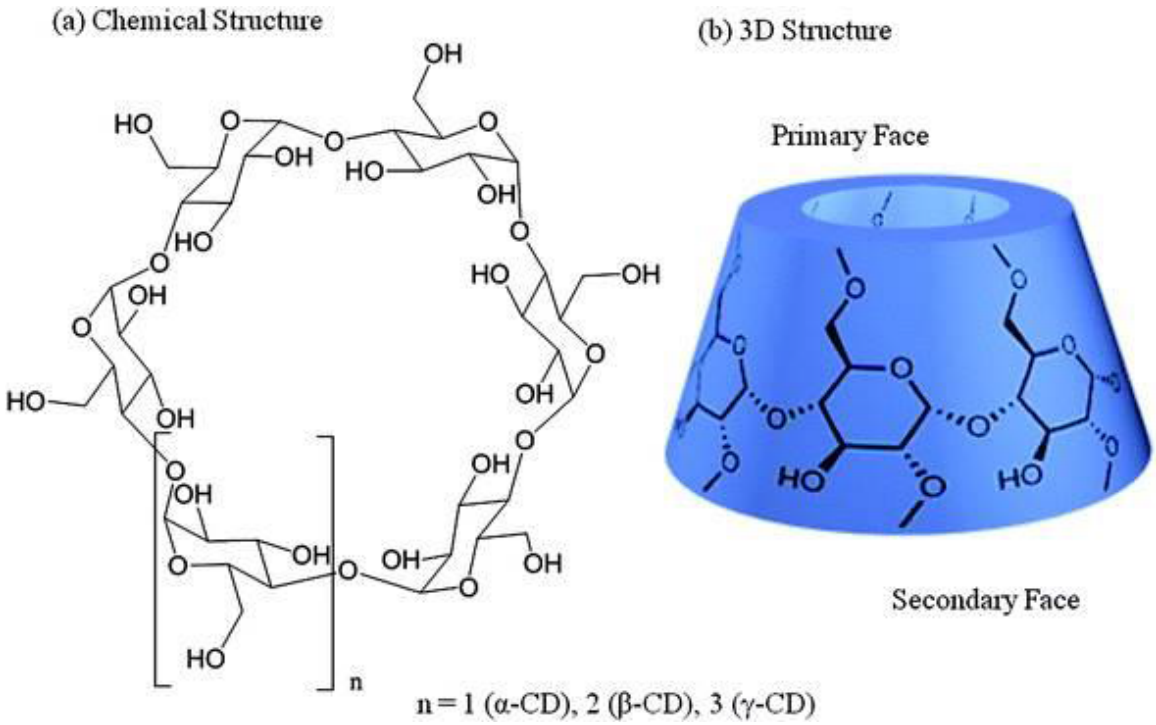

Figure 5.4: Cyclodextrins structures (Zafar, Fessi, & Elaissari, 2014)

Chapter 6. Rapidly Dissolving Polymeric Microneedles for Intraocular Delivery of Cyclosporine A

6.1 Abstract

Cyclosporine A (CsA) is a cyclic undecapeptide that belongs to the immunosuppressant class. CsA possesses anti-inflammatory activity in the treatment of ocular diseases such as uveitis, vernal keratoconjunctivitis and dry eye disease. However, due to its large molecular weight and hydrophobic nature (low aqueous solubility), the ocular bioavailability, especially of the posterior eye, is very low. Conventional topical formulations, such as a solution, emulsion or suspension, permeate poorly across the eye due to permeation barriers, lacrimation and lymphatic clearance. On the contrary, dissolvable microneedles (MNs) patches can be used to bypass the tear film and nasolacrimal drainage, thus maximizing the amount of CsA delivered to the posterior segment. The MN patches were fabricated using polyvinylpyrrolidone (PVP) and CsA and characterized for dissolution time and *ex vivo* permeation. PVP MNs dissolved within 5 minutes. *Ex-vivo* ocular drug distribution studies in a whole porcine eye perfusion model showed a significant increase of CsA levels in various ocular tissues of the posterior segment compared to a topically applied ophthalmic emulsion (Restasis®). Thus, dissolving MNs can deliver CsA to the posterior segment of the eye for the treatment of various inflammatory diseases.

6.2 Introduction

Treatment of posterior eye diseases, such as cytomegalovirus retinitis, diabetic retinopathy, age-related macular degeneration, posterior uveitis and retinitis pigmentosa, is currently accomplished by invasive methods such as surgical implants and ocular injections into vitreous humor. The invasive methods have many disadvantages such as fear of surgery, pain due to injection and the risk of infection. Conventional ophthalmic formulations, such as eye drops suspensions, and ointments, have a limited ability to deliver sufficient drug to the posterior segment due to the presence of various elimination mechanisms (tear turnover, nasolacrimal drainage, protein binding, and enzymatic degradation). In addition, complex penetration barriers (corneal, blood-aqueous and blood-retinal barrier) restrict drug transport from blood into the posterior segment. These barriers result in typically less than 5% ocular bioavailability of conventional ophthalmic formulations (Thrimawithana, Young, Bunt, Green, & Alany, 2011). Hence, microneedles (MNs) based ocular devices are being developed to overcome the many ocular barriers for effective delivery of drug in therapeutic concentrations (Gote, Sikder, Sicotte, & Pal, 2019; Patel, Lin, Edelhauser, & Prausnitz, 2011; Than et al., 2018).

Cyclosporine (CsA) (Figure 6.1) is a cyclic undecapeptide that possess a potent immunosuppressive activity. It inhibits T cell activation by blocking the transcription of genes responsible for production of interleukin-2 and interleukin-4 (Matsuda & Koyasu, 2000). Ocular administration of CsA became the preferred method of delivery for treatment of ocular inflammatory diseases because non-

ocular administration is associated with systemic adverse effects such as nephrotoxicity, hypertension and anemia (Palestine, Nussenblatt, & Chan, 1984) . However, due to its large molecular weight (1202.6 Da) and low aqueous solubility (40 µg/mL) (Czogalla, 2009), the ocular bioavailability of CsA following topical ophthalmic application is very limited (Agrahari et al., 2016). In addition, using topical formulations limit the amount of CsA capable of penetrating the posterior segment because of permeation barriers, lacrimation and lymphatic clearance (Lallemand et al., 2017).

Because of these limitations, strategies have focused on developing novel mechanisms to improve ocular bioavailability of CsA. Numerous innovative delivery systems such micelles (Di Tommaso et al., 2012), liposomes (Karn, Cho, Park, Park, & Hwang, 2013), *in situ* gelling systems (Wu, Yao, Zhou, & Dahmani, 2013), and hydrogels (Kapoor, Dixon, Sekar, & Chauhan, 2017) have been evaluated for the delivery of CsA to posterior eye. MNs have been recently employed as a minimally invasive method for localizing drug within the target ocular tissues with greater accuracy than conventional formulations. In addition, MNs offer less tissue trauma than injections or implants (Thakur Singh et al., 2017). A variety of MNs mechanisms have been attempted for ocular delivery such as hollow MNs (Jiang, Moore, Edelhauser, & Prausnitz, 2009; Y. C. Kim, Edelhauser, & Prausnitz, 2014), dissolvable MNs (Thakur et al., 2016) and solid coated MNs (Jiang et al., 2007). MNs can be fabricated long enough to penetrate the sclera and deliver the drug at a higher concentration to the posterior segment. MNs can be fabricated from a wide variety of materials and in different

shapes using slowly (e.g.PLA and PLGA) or rapidly dissolvable polymers (e.g. carboxymethyl cellulose, hyaluronic acid and chitosan) (Cheung & Das, 2016) so that drug release can be modulated. Rapidly dissolvable MNs advantages include (i) rapid drug release (ii) effective drug delivery by microchannels temporarily formed by the MNs (iii) ability to deliver a relatively large amount of drug (Park, Allen, & Prausnitz, 2005; Wang, Hu, & Xu, 2017). Dissolving MNs could avoid drawbacks associated with solid and hollow MNs, such as accidental retinal damage and detachment, since they dissolve within the ocular tissues (Bhatnagar et al., 2018).

Polyvinylpyrrolidone (PVP) is a water soluble, non-toxic and non-ionic amorphous polymer approved by the U.S. FDA for various purposes, such as tablet binder, disintegrant, and coating agent (Poonguzhali, Basha, & Kumari, 2017). Upon penetration, dissolving MNs will soften and dissolve rapidly within the eye, preventing ocular damage due to mechanical forces of needle application (Sriyanti et al., 2018).

The objective of this research was to develop dissolvable MNs for the rapid-release of CsA to the suprachoiroidal space (SCS), for treatment of posterior eye conditions. Targeting the SCS allows enhanced drug delivery to the posterior segment (retina) with higher bioavailability compared to topical formulations (Jung, Chiang, Grossniklaus, & Prausnitz, 2018).

6.3 Experimental Methods

6.3.1 Materials

CsA was procured from Letco Medical, Decatur, AL, USA. PVP (Plasdone™ K 29-32) was obtained as a gift from Ashland Inc, Covington, KY, USA. Fluorescein isothiocyanate (FITC) was obtained from Alfa Aesar, Ward Hill, MA, USA. Trypan Blue was purchased from Sigma Aldrich, St. Louis, MO. Room temperature vulcanizing (RTV) polydimethylsiloxane (PDMS) silicone microneedle molds were purchased from Micropoint Technologies Pte. Ltd, Singapore. All solvents used for high-performance liquid chromatography (HPLC) were of analytical or HPLC grade.

6.3.2 Preparation of CsA-loaded PVP hydrogels

PVP hydrogels were prepared in deionized water according to the composition presented in Table 6.1. A predefined amount of PVP was added to a known volume of deionized water and then vortexed for several minutes. The suspension was then sonicated at 37°C for an hour and kept for overnight hydration at room temperature. These gels were used to make CsA-containing hydrogel formulations. A stock solution (1 mg /ml) of CsA in acetonitrile (ACN) was prepared. CsA was added in a specified quantity to the PVP hydrogel to provide a final drug concentration of 0.5 mg/50µL hydrogel. The hydrogel was homogeneously dispersed for 5 h using magnetic stirring at 400 rpm at room temperature. All formulations were stored in the refrigerator (4–8°C) until further use.

6.3.3 Fabrication of Rapid Dissolving PVP Microneedles

50 µL of the formulation was pipetted into each RTV PDMS silicone MNs mold and centrifuged for 30 minutes at 3300 rpm using a Beckman Coulter Allegra™ 6R benchtop centrifuge (Indiananapolis, IN). Following centrifugation, PVP (without CsA) was placed into the MNs molds using a dropper, to serve as the backing. The MNs arrays were then left at ambient temperature under a chemical fume hood for two days for drying.

6.3.4 High Performance Liquid Chromatography (HPLC) Analysis

An Alliance Waters e2695 Separations Module and a Waters 2998 Photodiode Array Detector, Singapore, were used for CsA analysis. A Luna C18 (2) 5µm, 150mm x 4.60mm reversed-phase HPLC column was employed for CsA analysis. The mobile phase consisted of 80% acetonitrile in water containing 0.1% trifluoroacetic acid (TFA). Samples (20 µL) were eluted at a flow rate of 1mL/min at 60°C. The absorbance wavelength was set at 210 nm.

6.3.5 Characterization of Microneedle Patches Containing CsA

6.3.5.1 Scanning Electron Microscopy (SEM)

The MNs were analyzed to determine their structure and uniformity using a Jeol 7000f Scanning Electron Microscope, Peabody, MA, USA. Prior to analysis, each MN array was coated with a 20-22 nm gold coating.

6.3.5.2 Drug Content Determination in Microneedle

CsA content in MNs was determined by submerging the MN arrays in 8 mL of simulated lacrimal fluid (SLF, pH=7.4) in a water bath (34°C) for 5 min.

Due to the poor solubility of CsA, the SLF contained 30% ethanol was used. All samples were analyzed via HPLC.

6.3.5.3 Microneedle Array Dissolution Studies

To measure the release of CsA from the MNs, an individual array was attached to the bottom of the wells in a 6-well plate and submerged in 5 mL of the dissolution media (70:30 SLF:Ethanol) preheated to 34°C. The well plate was placed in a water bath at 34°C. The full volume of the well was removed at 1, 2, 3, 4, and 5 min, and replenished with fresh dissolution media. All samples were analyzed via HPLC.

6.3.5.4 Microneedle Failure Force

The strength of the MNs patches was determined by analyzing their failure force. Stress-strain curves were produced using a displacement-force test station, TA-HDi Texture Analyzer (Texture Technologies Corp, Hamilton, MA) An individual MN array was pressed against a stainless-steel surface at a rate of 1 mm/s until a preset distance was reached (1mm). Failure force was indicated by a sudden drop in applied force. Three runs were performed on each MN and the average value was calculated.

6.3.6 Visualizing MNs penetration and Insertion pathways

Trypan Blue staining was used to confirm the insertion and penetration of the MNs into the scleral tissue. Porcine eyes were obtained from Auburn University Lambert-Powell Meats Laboratory (Auburn University, Auburn AL) and all eyes were used within 4 hours of euthanasia to maintain the integrity of the entire globe. The animals were euthanized according to the Institutional Animal

Care and Use Committee (IACUC) approved protocol (SOP 2015-2727). The excess tissue was first cut from the globe and MNs were used to penetrate the scleral section for 5 minutes. After penetration, 50 uL of Trypan Blue was dispensed onto the injection site. After 60 seconds, excess Trypan Blue was rinsed from the sclera tissue and the sample was visualized by microscopy for defects and pictures taken. In addition, MNs were visualized to observe the dissolution of the PVP-based MN arrays after inserting MNs into the sclera for 1 minute.

6.3.7 Ocular Distribution of CsA and FITC in Isolated Perfused Eyes

Fresh porcine eyes were obtained as described earlier and used within 4 hours of euthanizing the animal. The excess adnexal tissue was trimmed from the ocular globe and placed in PBS pH 7.4 until ready for perfusion (Abarca, Salmon, & Gilger, 2013). The eyes were perfused with Dulbecco's Modified Eagle's Medium F12 (DMEM) under constant O_2 supply. The perfusion began 30 minutes prior to the drug application and maintained throughout the entirety of the study. A major artery of each eye was identified, split open with a 3.0 mm slit Eagle blade, cannulated and secured in place with Scotch® super glue gel. The eyes were then placed in a stainless-steel strainer on top of a beaker, which allowed collection of the DMEM medium from the veins. An Ismatec® peristaltic pump (Cole-Parmer GmbH, Wertheim, Germany) was employed to perfuse the oxygenated DMEM through the cannulated eyes. Perfusion was started at a flow rate 0.25–0.8 mL/min and increased to 1 ml /min (Mains, Tan, Wilson, & Urquhart, 2012). Adequate arterial perfusion was determined by observing flow

of media exiting the vortex veins. The MN patches were pressed into the sclera with the help of tweezers. For experiments, 50 µL of Restasis® was applied on the cornea surface. After two hours, the formulation was gently removed by rising and dabbing with a tissue. The eyes were frozen instantly using solid CO_2 and stored in a freezer at 80°C to prevent transfer of drug between tissues until dissection. For dissection, the frozen eye was placed on a cold ceramic tile and all ocular tissues were subsequently removed: cornea, lens, iris, vitreous humour, sclera, and retina. Each tissue was soaked in the HPLC mobile phase for 24 hours in individual vials, then filtered (0.45 µm Nylon membrane) and analyzed via HPLC.

To confirm CsA distribution within the ocular tissues, MNs made with FITC fluorescent probe were applied as described above. The eyes were quickly frozen and dissections were performed while frozen to avoid FITC transfer from one tissue to another. FITC fluorescence in the sclera and the retina was visualized immediately using a fluorescence microscope (EVOS fl, ZP-PKGA-0494 REV A, USA) at excitation and emission wavelengths of 495 and 519 nm.

6.3.8 Extraction Efficiency

The CsA extraction efficiency was determined in various ocular tissues. For these experiments, the tissues that were not in contact with CsA were exposed to 2 ml solution of CsA (0.5 mg/ml) in mobile phase. The recovery of CsA from the tissues was determined for various tissues such as cornea, sclera, retina, iris, and vitreous humor. The frozen tissue samples were minced in 5 mL polypropylene tubes with 2 mL of CsA solution and sonicated for 30 min and

stored overnight in a refrigerator. The following day, the samples were filtered (0.45-micron Nylon membrane) and assayed by HPLC. The CsA recovery (%) from the tissues was calculated as the ratio of the amount of CsA extracted from the spiked tissue to the amount of CsA extracted from the solution in the absence of the tissues, but processed by the same procedure.

6.3.9 Stability Study

MNs kept for one month protected from light in a desiccant container at room temperature. MNs were then analyzed to determine their structure and uniformity using SEM. In addition, they were analyzed for their CsA content.

6.3.10 Statistical Analysis

Data were analyzed using the Student t-test and one-way ANOVA. The amount of CsA in various ocular tissues was normalized to 1 gram of the tissue. In all cases, statistical significance was defined at the standard 5% level. GraphPad Prism Version 4.0 (GraphPad Prism Software Inc., San Diego, CA, USA) was used to analyze data.

6.4 Results & Discussion

6.4.1 Fabrication of Biodegradable Microneedles

The MN array size was 8x8 for a total of 64 individual MNs, 800 μm in length and a base height of 200 μm (Figure 6.2). The 800μm length was selected for easy insertion into the sclera to target drug release into the suprachoiroidal space (SCS) between choroid and sclera, without penetrating the chorioretina (Patel et al., 2011). Targeting delivery to the CSC yields enhanced bioavailability to the retina compared to intravitreal injections or topical formulations (Tyagi,

Kadam, & Kompella, 2012). The MN tips were 20 μm in diameter and the distance between needle tips was 680 μm. The final weight of the MNs was approximately 46, 32.5 and 28 mg for MN arrays made of 70, 50 and 30% PVP formulations, respectively. These polymer concentrations were sufficient enough to produce rigid MN arrays with encapsulated CsA without compromising the dissolution rate of MNs (discussed later).

6.4.2 Characterization of Microneedle Patches Containing CsA

6.4.2.1 Scanning Electron Microscopy (SEM)

SEM analysis of the MNs revealed that the arrays were uniform and sharp without the presence of any cracks, fractures or broken tips (Figure 6.3A&B). MNs must be strong and sharp enough to penetrate the ocular tissues without bending or breaking to deliver CsA to SCS.

6.4.2.2 Drug Content

The CsA content of MNs was determined to ensure dose accuracy and reproducibility. We were able to incorporate about 0.5 mg of CsA in the PVP MNs. The content of CsA in the MN arrays ranged from 93 to 98%. Dissolving MNs could be used to deliver a large dose of high molecular weight drugs because they allow entrapment of drugs within the polymeric matrix (Than et al., 2018).

6.4.2.3 Microneedle Dissolution Studies

The MNs began to dissolve within 30 seconds and they completely dissolved within 5 minutes for a 100% CsA release (Figure 6.4). Being fabricated from a hydrophilic polymer, PVP MNs rapidly dissolved within the ocular tissues

due to high water solubility. This rapid dissolution may increase the patient's compliance because wearing the patches for a long period of time is not necessary (Yang et al., 2012). In addition to rapid dissolution, polymer from dissolved MNs must not bind the drug and reduce its diffusion rate since sustained-release is not required. Complete CsA release from dissolved MNs indicates that the drug freely diffuses into the receptor solution.

6.4.2.4 Microneedle Failure Force

The failure force, which is the force required to break the MNs, is marked by the sharp decrease in applied force (Figure 6.5). The x-axis corresponds to the distance displaced by the upper stage after initial contact with the MN tips; the stage is then lowered until a preset distance of 1mm is reached. After the MNs are fractured, the applied force dips and then begins to increase again as it continues pressing against the MN backing until the pre-set distance is reached. The MN strength was in the order: F3>F2>F1. There is a proportional relationship between the applied compression force and the percentage of PVP polymer used to fabricate the MN arrays. MNs with low PVP%, F1, broke at a shorter distance. The mechanical properties of the dissolving MNs are affected by several factors including polymer type and concentration, and type and concentration of encapsulated drug (Thakur et al., 2016).

6.4.3 Visualizing MNs penetration and Insertion pathways

An essential factor in successful development and application of dissolving MNs is their ability to penetrate into the ocular tissue without fracture or delamination of MN arrays. Trypan blue was used to visualize MNs induced

defects in the sclera. As shown in Figure 6.6A, MNs were rigid enough to penetrate the sclera to deliver their drug payload into various ocular tissues. Once they penetrate the sclera, dissolving MNs will soften and rapidly dissolve (Figure 6.6B), preventing ocular tissues from damage, as extended mechanical force is not required.

6.4.4 Ocular Distribution of CsA in Isolated Perfused Eyes

The isolated perfused porcine eye model closely mimics *in vivo* conditions such as ocular temperature, circulation and tissue viability, which allows us to determine the distribution of CsA in the individual ocular tissues. Restasis® and MNs made with 70% PVP (F3) were studied. F3 has a similar release profile and drug content as F1 and F2. However, we have selected F3 since it has the best strength profile. The CsA quantification in various ocular tissues, as determined by the extraction efficiency experiments, suggests a recovery above 90%. F3 displayed drug detection in all ocular tissues while Restasis® had no detectable drug levels in the retina, sclera and vitreous humor (Figure 6.7). CsA topical formulations often display no detectable levels in the posterior segment because of the anterior permeation barriers, such as tear film layers and cornea (BenEzra, Maftzir, de Courten, & Timonen, 1990). Dissolving MNs successfully delivered CsA deeper into the posterior segment because they created microporated ocular tissue, rapidly dissolved and released CsA (H. K. Kim et al., 2018). MNs also increased drug retention time in the sclera by preventing removal by blinking and tear secretion (Than et al., 2018). To confirm drug distribution within the ocular tissues after application of MNs, FITC was traced within the ocular tissues.

As shown in Figure 6.8, MNs penetrated the porcine sclera and delivered FITC to both the retina and sclera.

6.4.5 Stability Study

The stability of MNs was studied over one month. The content of CsA in the MN arrays ranged from 95 to 96%. SEM analysis revealed that the arrays maintained their uniform shape and sharp appearance (Figure 6.9) with no cracks or fractures.

6.5 Conclusions

This study demonstrated the design and fabrication of rapidly dissolving MNs composed of PVP to overcome various ocular barriers to improve ocular drug delivery of CsA to the posterior segment. MNs dissolved rapidly (less than 5 minutes) within the sclera and encapsulated CsA effectively (around 98%). MNs were able to withstand the force needed for insertion in the eye and penetration of the sclera tissue without breaking. CsA level in posterior eye tissues was significantly higher than CsA ophthalmic emulsion (Restasis®). Taken all together, rapidly dissolving MNs fabricated with PVP is a promising platform to deliver CsA to the posterior segment of the eye.

6.6 References

Abarca, E. M., Salmon, J. H., & Gilger, B. C. (2013). Effect of choroidal perfusion on ocular tissue distribution after intravitreal or suprachoroidal injection in an arterially perfused ex vivo pig eye model. *J Ocul Pharmacol Ther, 29*(8), 715-722. doi: 10.1089/jop.2013.0063

Agrahari, V., Mandal, A., Agrahari, V., Trinh, H. M., Joseph, M., Ray, A., . . . Mitra, A. K. (2016). A comprehensive insight on ocular pharmacokinetics. *Drug Deliv Transl Res, 6*(6), 735-754. doi: 10.1007/s13346-016-0339-2

BenEzra, D., Maftzir, G., de Courten, C., & Timonen, P. (1990). Ocular penetration of cyclosporin A. III: The human eye. *Br J Ophthalmol, 74*(6), 350-352. doi: 10.1136/bjo.74.6.350

Bhatnagar, S., Saju, A., Cheerla, K. D., Gade, S. K., Garg, P., & Venuganti, V. V. K. (2018). Corneal delivery of besifloxacin using rapidly dissolving polymeric microneedles. *Drug Deliv Transl Res, 8*(3), 473-483. doi: 10.1007/s13346-017-0470-8

Cheung, K., & Das, D. B. (2016). Microneedles for drug delivery: trends and progress. *Drug Deliv, 23*(7), 2338-2354. doi: 10.3109/10717544.2014.986309

Czogalla, A. (2009). Oral cyclosporine A--the current picture of its liposomal and other delivery systems. *Cell Mol Biol Lett, 14*(1), 139-152. doi: 10.2478/s11658-008-0041-6

Di Tommaso, C., Bourges, J. L., Valamanesh, F., Trubitsyn, G., Torriglia, A., Jeanny, J. C., . . . Moller, M. (2012). Novel micelle carriers for cyclosporin A topical ocular delivery: in vivo cornea penetration, ocular distribution and efficacy

studies. *Eur J Pharm Biopharm, 81*(2), 257-264. doi: 10.1016/j.ejpb.2012.02.014

Gote, V., Sikder, S., Sicotte, J., & Pal, D. (2019). Ocular Drug Delivery: Present Innovations and Future Challenges. *J Pharmacol Exp Ther, 370*(3), 602-624. doi: 10.1124/jpet.119.256933

Jiang, J., Gill, H. S., Ghate, D., McCarey, B. E., Patel, S. R., Edelhauser, H. F., & Prausnitz, M. R. (2007). Coated microneedles for drug delivery to the eye. *Invest Ophthalmol Vis Sci, 48*(9), 4038-4043. doi: 10.1167/iovs.07-0066

Jiang, J., Moore, J. S., Edelhauser, H. F., & Prausnitz, M. R. (2009). Intrascleral drug delivery to the eye using hollow microneedles. *Pharm Res, 26*(2), 395-403. doi: 10.1007/s11095-008-9756-3

Jung, J. H., Chiang, B., Grossniklaus, H. E., & Prausnitz, M. R. (2018). Ocular drug delivery targeted by iontophoresis in the suprachoroidal space using a microneedle. *J Control Release, 277*, 14-22. doi: 10.1016/j.jconrel.2018.03.001

Kapoor, Y., Dixon, P., Sekar, P., & Chauhan, A. (2017). Incorporation of drug particles for extended release of Cyclosporine A from poly-hydroxyethyl methacrylate hydrogels. *Eur J Pharm Biopharm, 120*, 73-79. doi: 10.1016/j.ejpb.2017.08.007

Karn, P. R., Cho, W., Park, H. J., Park, J. S., & Hwang, S. J. (2013). Characterization and stability studies of a novel liposomal cyclosporin A prepared using the supercritical fluid method: comparison with the modified conventional Bangham method. *Int J Nanomedicine, 8*, 365-377. doi: 10.2147/IJN.S39025

Kim, H. K., Lee, S. H., Lee, B. Y., Kim, S. J., Sung, C. Y., Jang, N. K., . . . Lee, S. (2018). A comparative study of dissolving hyaluronic acid microneedles with trehalose and poly(vinyl pyrrolidone) for efficient peptide drug delivery. *Biomater Sci, 6*(10), 2566-2570. doi: 10.1039/c8bm00768c

Kim, Y. C., Edelhauser, H. F., & Prausnitz, M. R. (2014). Targeted delivery of antiglaucoma drugs to the supraciliary space using microneedles. *Invest Ophthalmol Vis Sci, 55*(11), 7387-7397. doi: 10.1167/iovs.14-14651

Lallemand, F., Schmitt, M., Bourges, J. L., Gurny, R., Benita, S., & Garrigue, J. S. (2017). Cyclosporine A delivery to the eye: A comprehensive review of academic and industrial efforts. *Eur J Pharm Biopharm, 117*, 14-28. doi: 10.1016/j.ejpb.2017.03.006

Mains, J., Tan, L. E., Wilson, C., & Urquhart, A. (2012). A pharmacokinetic study of a combination of beta adrenoreceptor antagonists - in the isolated perfused ovine eye. *Eur J Pharm Biopharm, 80*(2), 393-401. doi: 10.1016/j.ejpb.2011.11.006

Matsuda, S., & Koyasu, S. (2000). Mechanisms of action of cyclosporine. *Immunopharmacology, 47*(2-3), 119-125.

Palestine, A. G., Nussenblatt, R. B., & Chan, C. C. (1984). Side effects of systemic cyclosporine in patients not undergoing transplantation. *Am J Med, 77*(4), 652-656. doi: 10.1016/0002-9343(84)90356-5

Park, J. H., Allen, M. G., & Prausnitz, M. R. (2005). Biodegradable polymer microneedles: fabrication, mechanics and transdermal drug delivery. *J Control Release, 104*(1), 51-66. doi: 10.1016/j.jconrel.2005.02.002

Patel, S. R., Lin, A. S., Edelhauser, H. F., & Prausnitz, M. R. (2011). Suprachoroidal drug delivery to the back of the eye using hollow microneedles. *Pharm Res, 28*(1), 166-176. doi: 10.1007/s11095-010-0271-y

Poonguzhali, R., Basha, S. K., & Kumari, V. S. (2017). Synthesis and characterization of chitosan-PVP-nanocellulose composites for in-vitro wound dressing application. *Int J Biol Macromol, 105*(Pt 1), 111-120. doi: 10.1016/j.ijbiomac.2017.07.006

Sriyanti, I., Edikresnha, D., Rahma, A., Munir, M. M., Rachmawati, H., & Khairurrijal, K. (2018). Mangosteen pericarp extract embedded in electrospun PVP nanofiber mats: physicochemical properties and release mechanism of alpha-mangostin. *Int J Nanomedicine, 13*, 4927-4941. doi: 10.2147/IJN.S167670

Thakur, R. R., Tekko, I. A., Al-Shammari, F., Ali, A. A., McCarthy, H., & Donnelly, R. F. (2016). Rapidly dissolving polymeric microneedles for minimally invasive intraocular drug delivery. *Drug Deliv Transl Res, 6*(6), 800-815. doi: 10.1007/s13346-016-0332-9

Thakur Singh, R. R., Tekko, I., McAvoy, K., McMillan, H., Jones, D., & Donnelly, R. F. (2017). Minimally invasive microneedles for ocular drug delivery. *Expert Opin Drug Deliv, 14*(4), 525-537. doi: 10.1080/17425247.2016.1218460

Than, A., Liu, C., Chang, H., Duong, P. K., Cheung, C. M. G., Xu, C., . . . Chen, P. (2018). Self-implantable double-layered micro-drug-reservoirs for efficient and controlled ocular drug delivery. *Nat Commun, 9*(1), 4433. doi: 10.1038/s41467-018-06981-w

Thrimawithana, T. R., Young, S., Bunt, C. R., Green, C., & Alany, R. G. (2011). Drug delivery to the posterior segment of the eye. *Drug Discov Today, 16*(5-6), 270-277. doi: 10.1016/j.drudis.2010.12.004

Tyagi, P., Kadam, R. S., & Kompella, U. B. (2012). Comparison of suprachoroidal drug delivery with subconjunctival and intravitreal routes using noninvasive fluorophotometry. *PLoS One, 7*(10), e48188. doi: 10.1371/journal.pone.0048188

Wang, M., Hu, L., & Xu, C. (2017). Recent advances in the design of polymeric microneedles for transdermal drug delivery and biosensing. *Lab Chip, 17*(8), 1373-1387. doi: 10.1039/c7lc00016b

Wu, Y., Yao, J., Zhou, J., & Dahmani, F. Z. (2013). Enhanced and sustained topical ocular delivery of cyclosporine A in thermosensitive hyaluronic acid-based in situ forming microgels. *Int J Nanomedicine, 8*, 3587-3601. doi: 10.2147/IJN.S47665

Yang, S., Feng, Y., Zhang, L., Chen, N., Yuan, W., & Jin, T. (2012). A scalable fabrication process of polymer microneedles. *Int J Nanomedicine, 7*, 1415-1422. doi: 10.2147/IJN.S28511

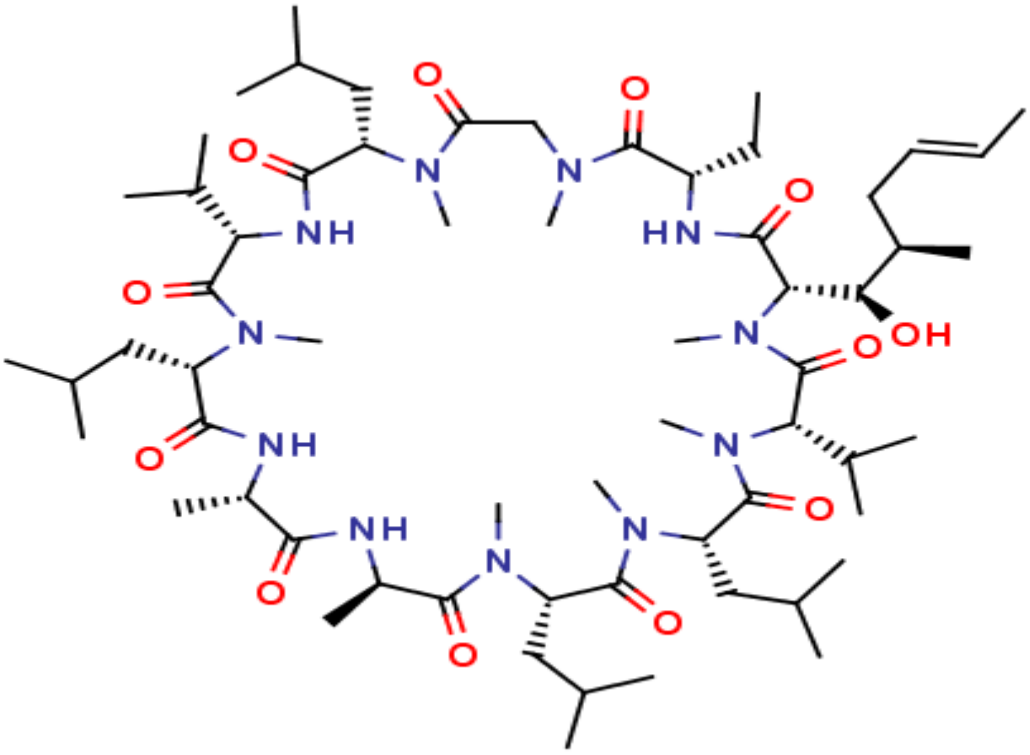

Figure 6.1: Structure of cyclosporine A (CsA), a cyclic undecapeptide

Table 6. 1: Composition of PVP-based MNs

Formulation	PVP concentration (%, w/w)*	CsA content (mg)
F1	30	0.5
F2	50	0.5
F3	70	0.5

* The backing layer not included

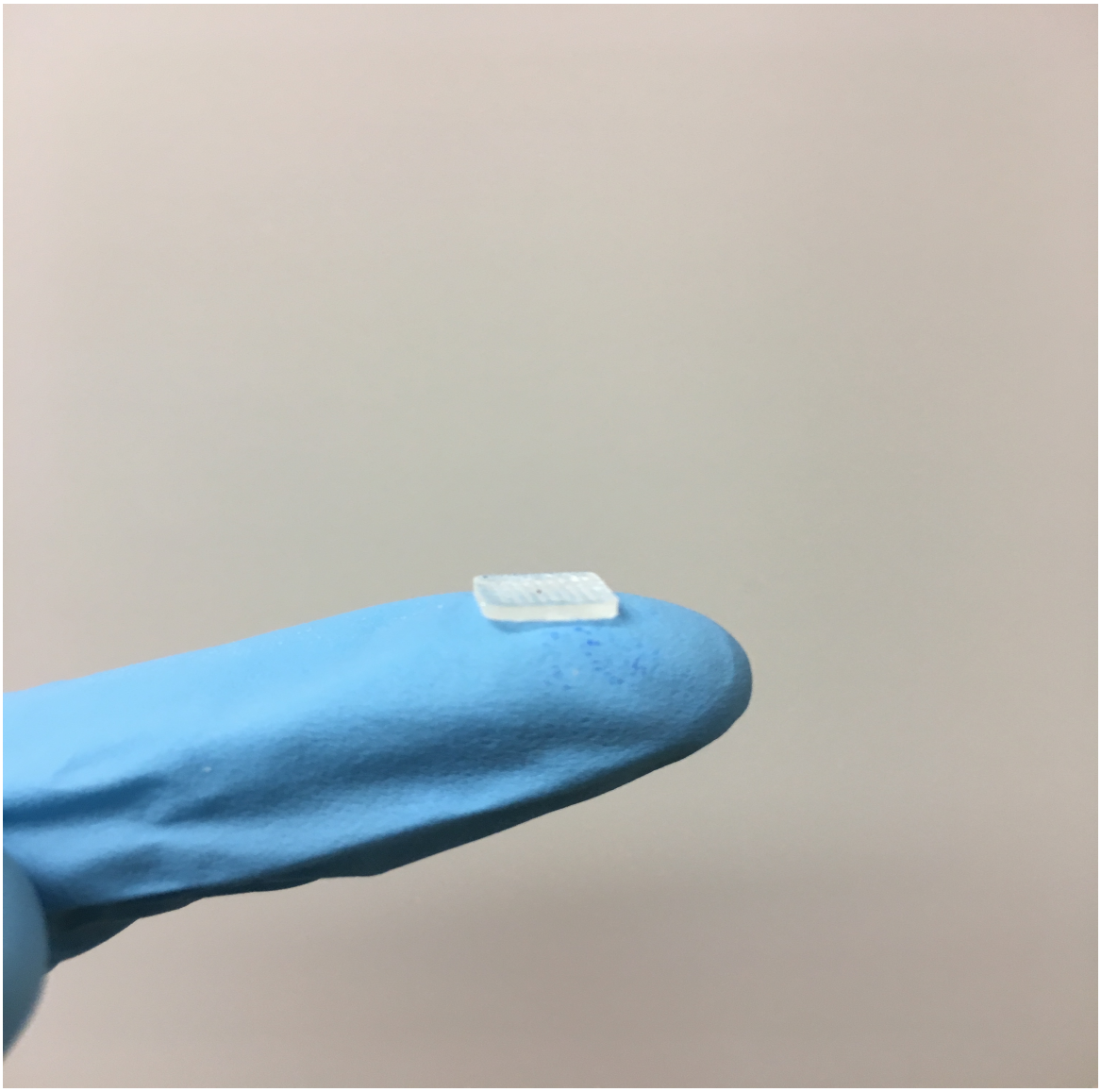

Figure 6.2: MN array relative to a fingertip. PVP-based biodegradable MN arrays (8mm x 8mm)

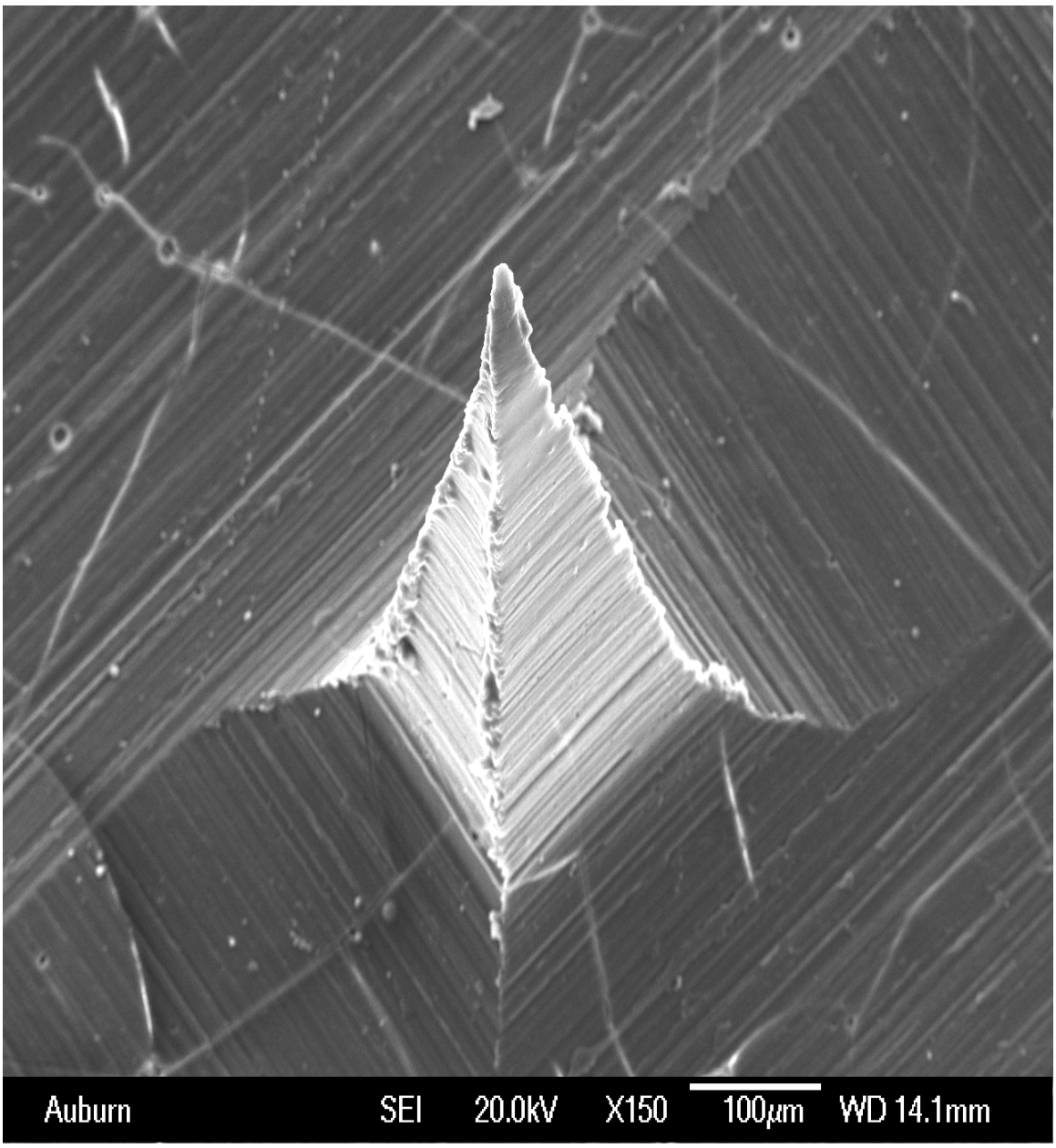

Figure 6.3A: SEM images revealing structure and uniformity of MNs, side-view of the MN

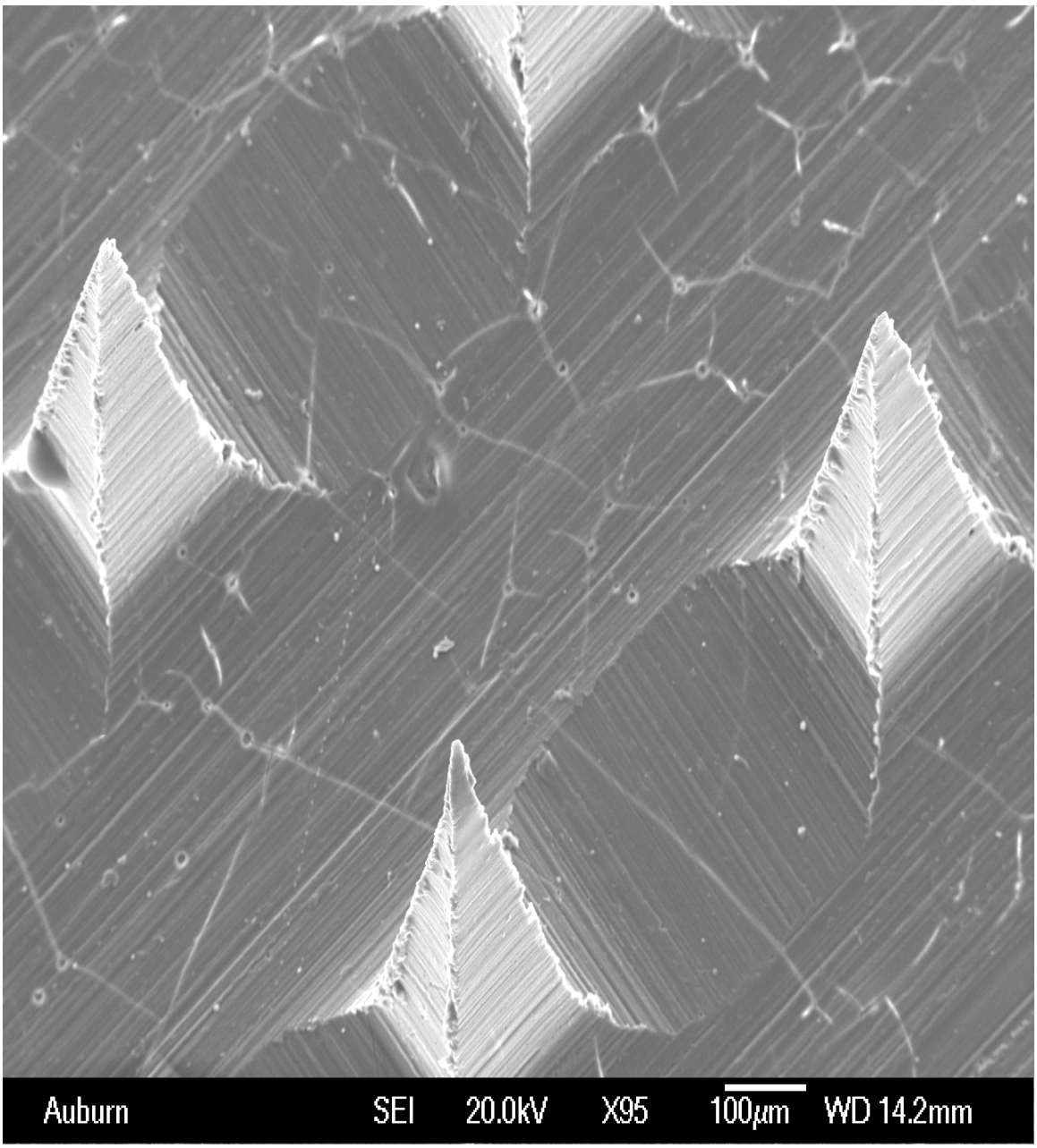

Figure 6.3B: SEM images revealing structure and uniformity of MNs, front-view of the MNs

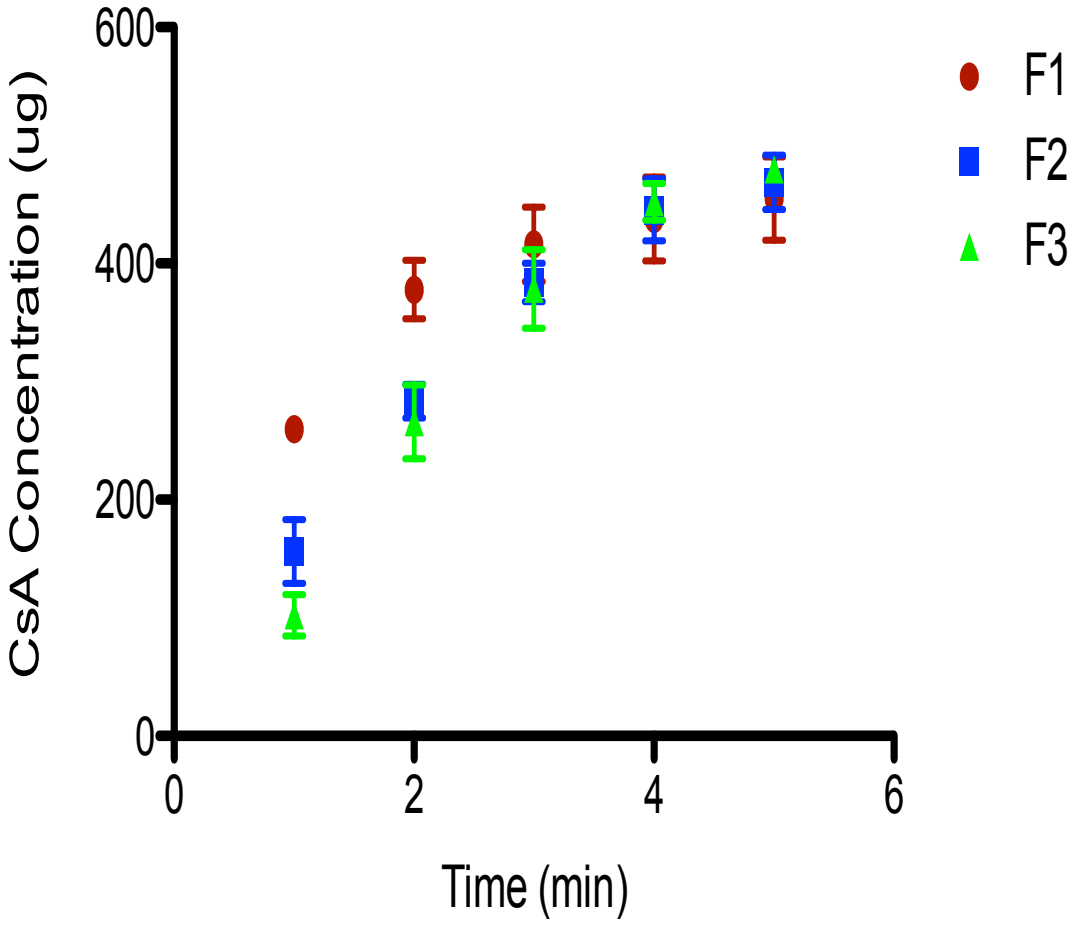

Figure 6.4: Dissolution of MNs. Values represented as mean ± SD, n = 3

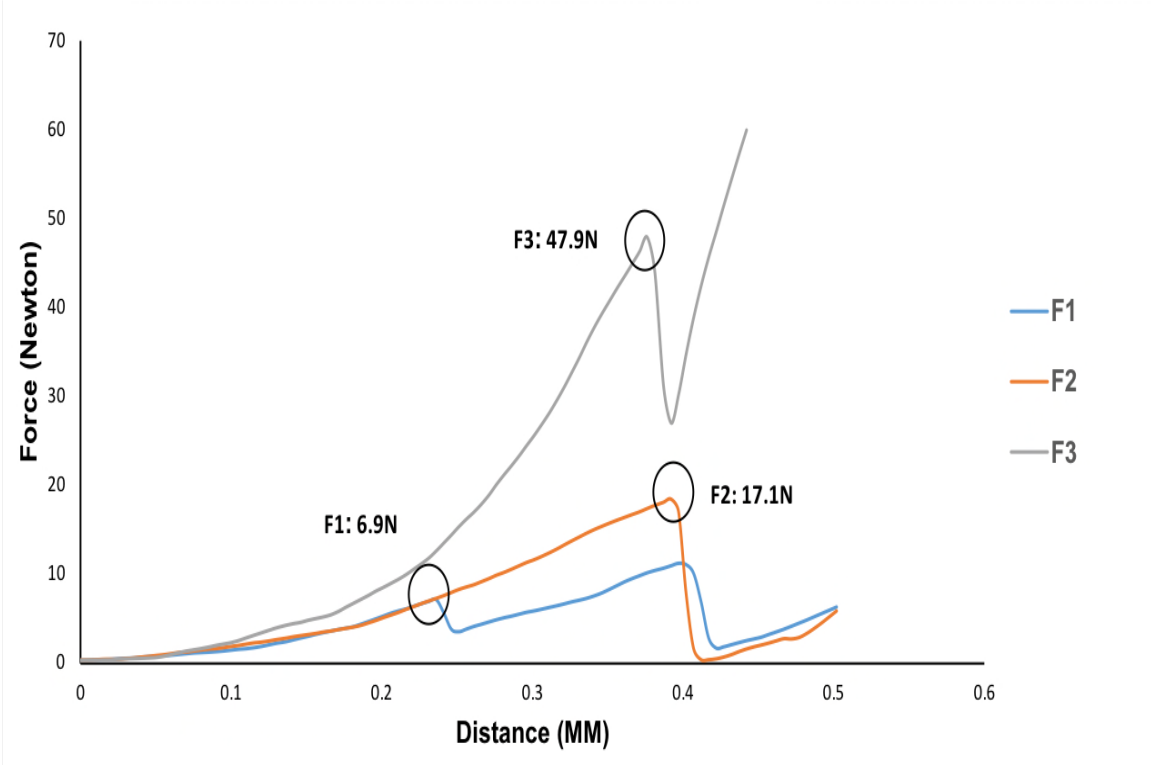

Figure 6.5: Stress-strain curves from Texture Analyzer. Plot shows data until MN failure point (dip in curve)

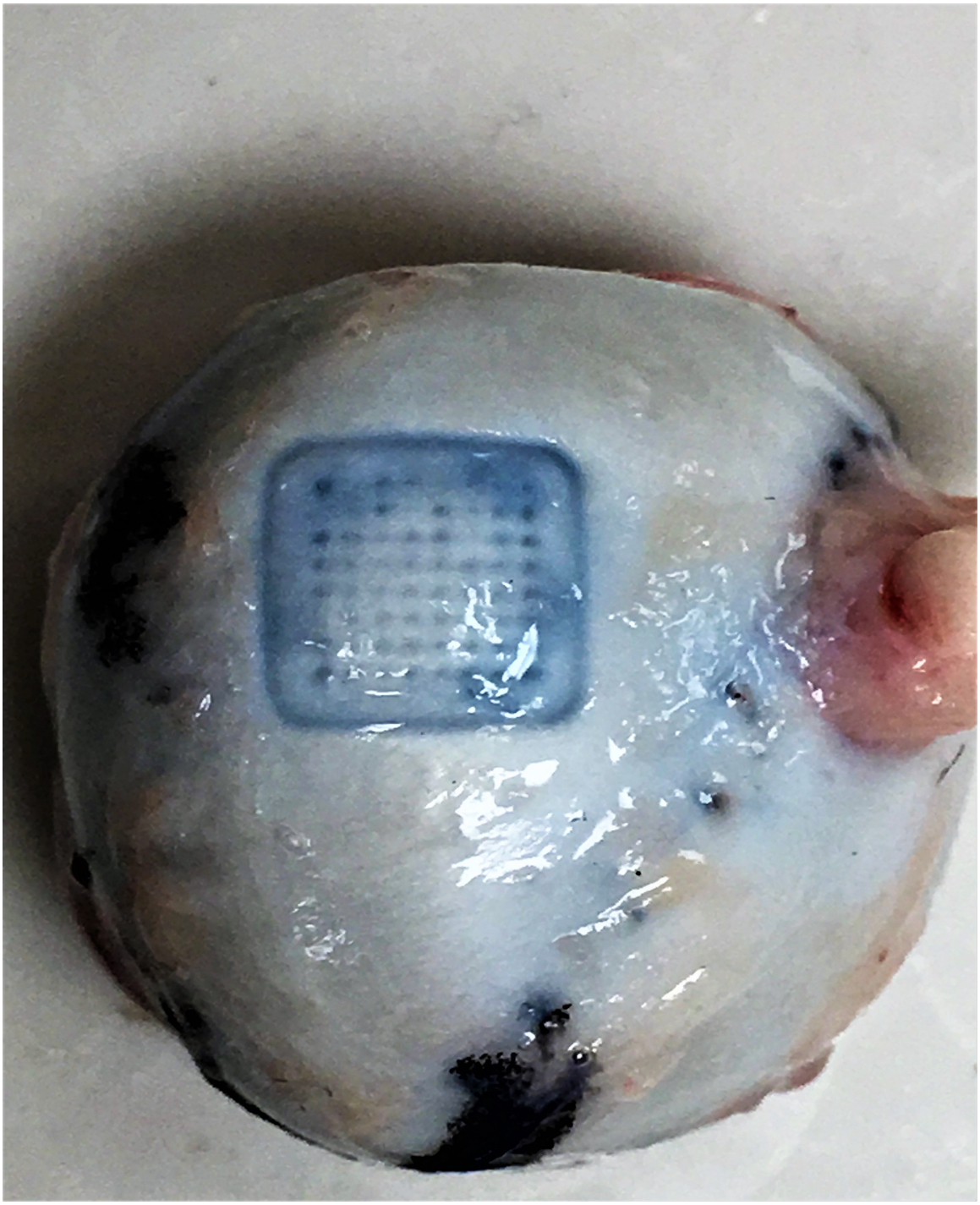

Figure 6.6A: MNs insertion points in the sclera after application

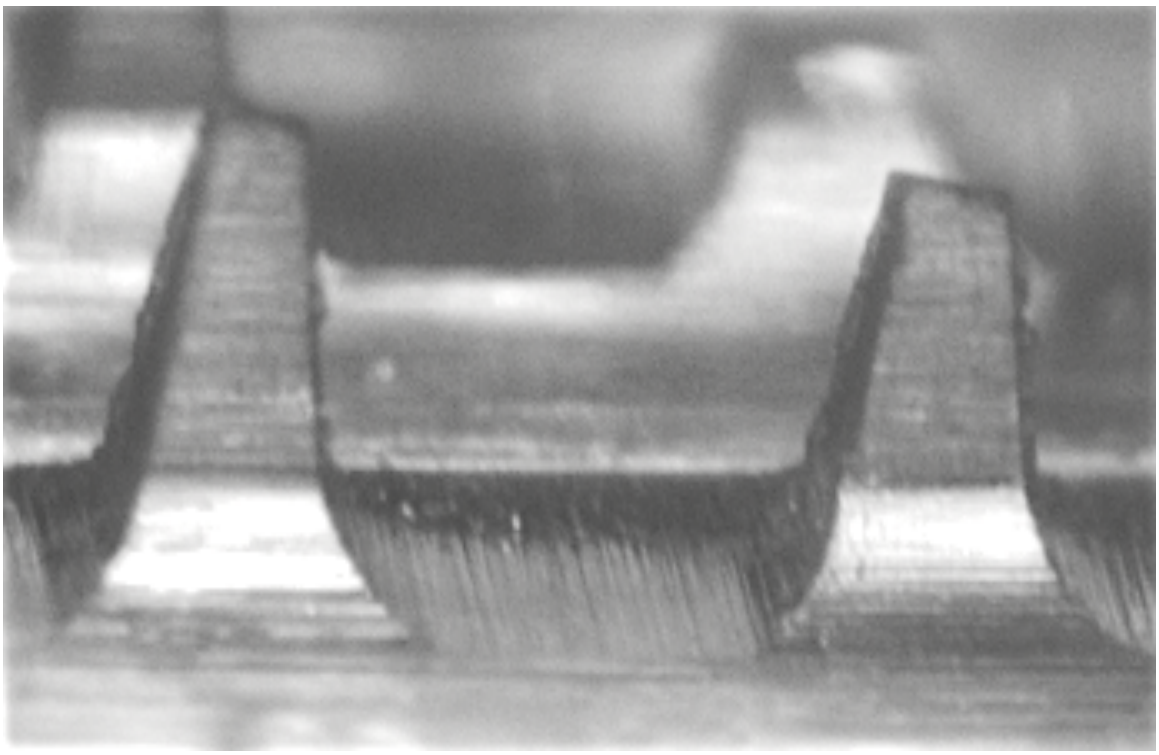

Figure 6.6B: Figure 6.6B: Images of PVP MN arrays (F3) encapsulating CsA after insertion into porcine scleral tissue for 60 seconds

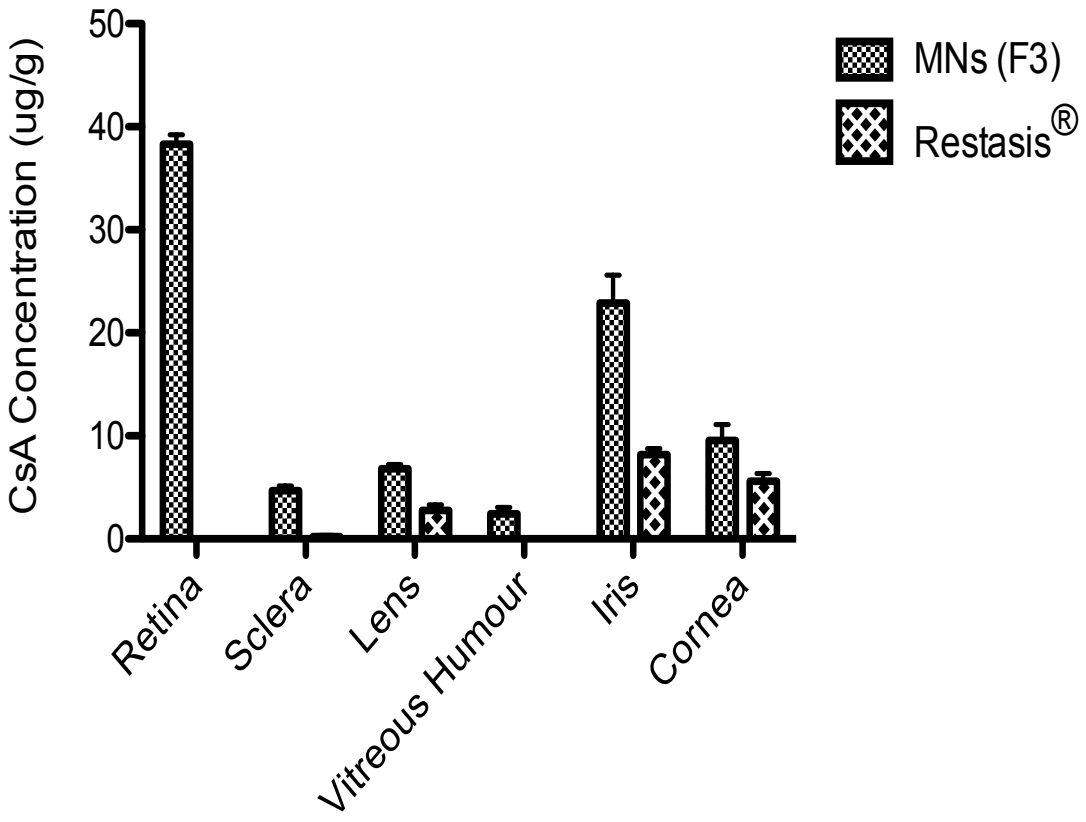

Figure 6.7: Ocular distribution of CsA in isolated porcine eyes in a continuous perfusion model after 2 hours. Values represented as mean ± SD, n = 3

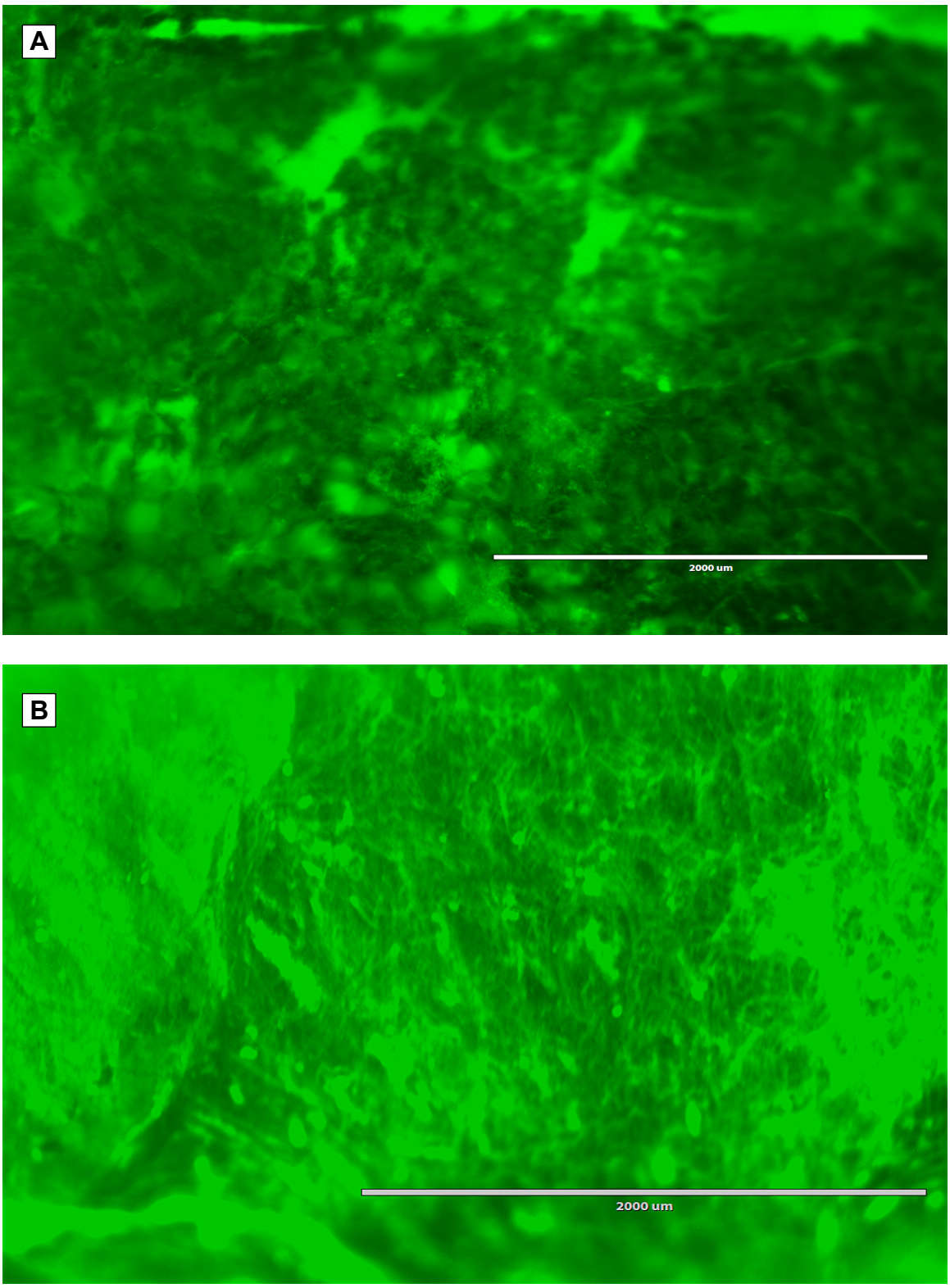

Figure 6.8: Image of the retina (A) and the sclera (B) after application of MNs (F3) loaded with FITC

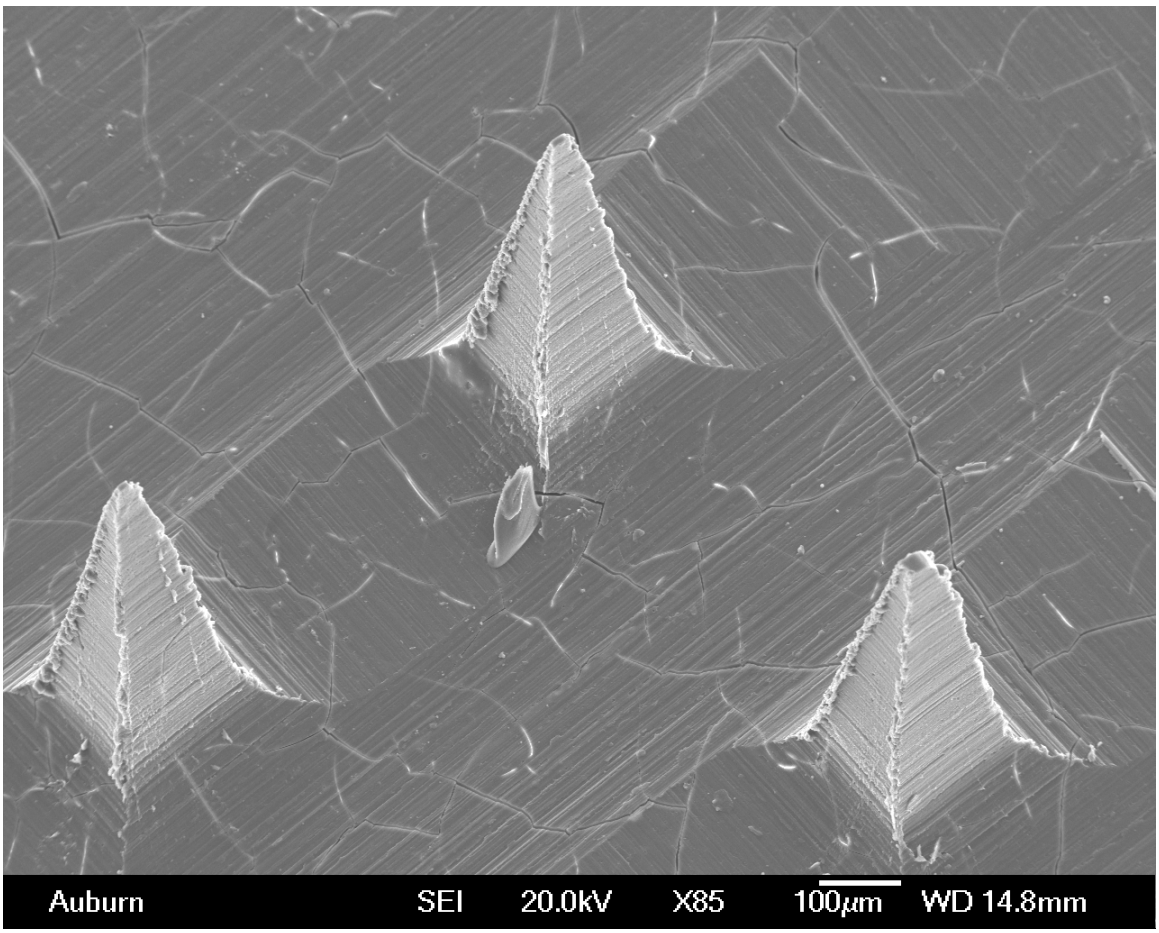

Figure 6.9: SEM images revealing structure and uniformity of MNs upon one-month storage

Chapter 7. Summary and Future Directions

The systemic administration of chemotherapeutic drugs is one of the main factors that lead to clinical failure in cancer treatment because limited drug reaches the tumor site. The non-targeted drug could exert cytotoxic effects on healthy tissues. The encapsulation of chemotherapeutic drugs in liposomes can limit the normal tissue uptake and target the desired site (tumor); however, an effective cellular uptake of drugs encapsulated in liposomes presents a significant challenge in cancer treatment. Stimuli-responsive liposomes are a promising approach to deliver and release chemotherapeutic drugs at the tumor site in a selective manner.

FDA has approved DaunoXome® (daunorubicin liposome composed of DSPC and cholesterol 2:1) as a first-line therapy for advanced HIV associated Kaposi's sarcoma. We designed and developed novel liposomal formulations to enhance circulation time, cellular uptake, and tumor-specific accumulation of daunorubicin against melanoma and breast cancer. To achieve this goal, PEGylated liposomal systems were developed using lipids that are known to induce cell membrane permeability (ceramide and cardiolipin) and/or lipids that are sensitive to specific internal (pH) or external (temperature) stimuli.

PEGylated liposomes, containing C6-ceramide, were prepared in the molar ratio 45:33:5:17 for DSPC/cholesterol/PEG2000-DSPE/C6-Cer to enhance the delivery and the cellular uptake of daunorubicin against melanoma cancer cells. These liposomes exhibited high drug encapsulation efficiency (>90%), small size (~100 nm), narrow size distribution (PI ~0.2) and good release and

stability profiles. Liposomes enriched with C6-ceramide exhibited the highest cytotoxicity against B16-BL6 melanoma cell lines, resulting in about a 10-fold and 6-fold higher cytotoxicity compared to daunorubicin solution and DaunoXome®, respectively.

Daunorubicin and cardiolipin were co-delivered using a pH- sensitive liposomal formulation to enhance the delivery, cellular uptake, and release of daunorubicin against melanoma cancer cells. PEGylated pH-sensitive liposomes, prepared in the molar ratio 40:30:5:17:8 for DOPE/cholesterol/DSPE-mPEG (2000)/ cardiolipin, exhibited high drug encapsulation efficiency (>90%), small size (~94 nm), narrow size distribution (PI ~0.16) and rapid release at acidic pH. In addition, the pH-sensitive liposomal formulation exhibited 12.5 and 5-fold higher cytotoxicity compared to daunorubicin solution and liposomes similar to DaunoXome®, respectively.

DPPC, MSPC, cholesterol, DSPE-mPEG (2000) and cardiolipin at a molar ratio of 57:40:30:3:20 were used to prepare a thermosensitive liposomal formulation to enhance the delivery, cellular uptake, and release of daunorubicin in MDA-MB-231 cell lines. The liposomes exhibited high drug encapsulation efficiency (>90%), small size (~115 nm), narrow size distribution (PI ~0.12) and rapid release profile under the influence of mild hyperthermia. In addition, the thermosensitive liposomal formulation exhibited ~4-fold higher cytotoxicity compared to daunorubicin solution or liposomes similar to DaunoXome®.

Owing to anatomical and physiological barriers of the eye, the delivery of therapeutic agents to the posterior segment of the eye remains a major challenge. Currently, periocular or intravitreal injection is the common route for delivery to the posterior segment; however, the injections are invasive and can result in pain, formation of cataract, retinal detachment, increased intraocular pressure and endophthalmitis. Biodegradable microneedles are less invasive and an efficient method to target and sustain drug levels in the posterior segment. They bypass the tear film and sclera and rapidly dissolve within the ocular tissues, due to high water solubility, to deliver the drug quickly and increase the patient's compliance.

Cyclosporine A ophthalmic emulsion (Restasis®) is approved for the treatment of keratoconjunctivitis sicca; however, its large molecular weight and hydrophobic nature limit its bioavailability in the posterior segment of the eye. We designed and fabricated rapidly dissolving microneedles composed of polyvinylpyrrolidone to improve ocular drug delivery of cyclosporine A to the posterior segment. Microneedles encapsulated cyclosporine A effectively and dissolved rapidly (less than 5 minutes) within the sclera. *Ex-vivo* ocular drug distribution studies in a whole porcine eye perfusion model showed a significant increase of cyclosporine A levels in various ocular tissues of the posterior segment compared to Restasis®.

Future work is directed to further explore the mechanism by which ceramide and cardiolipin enhanced the cytotoxic effects of liposomal formulations and the application of these novel liposomes in cancer treatment. In addition, the efficacy of the formulations should be determined in tumor-bearing mice.

In the case of the biodegradable microneedles, *in-vivo* studies using rabbits must be conducted to determine the irritation of the products as well as the *in vivo* drug distribution. Furthermore, *in vivo* studies comparing our biodegradable microneedles to the commercial formulations will provide valuable information.

Appendix: Publications and Conference Presentations

Publications

Alrbyawi, H., Poudel, I., Dash, R. P., Srinivas, N. R., Tiwari, A. K., Arnold, R. D., & Babu, R. J. (2019). Role of Ceramides in Drug Delivery. *AAPS PharmSciTech, 20*(7), 287. doi: 10.1208/s12249-019-1497-6

Chen, L., **Alrbyawi, H**., Poudel, I., Arnold, R. D., & Babu, R. J. (2019). Co-delivery of Doxorubicin and Ceramide in a Liposomal Formulation Enhances Cytotoxicity in Murine B16BL6 Melanoma Cell Lines. *AAPS PharmSciTech, 20*(3), 99. doi: 10.1208/s12249-019-1316-0

Alrbyawi,H, Arnold, R. D., Jayachandra Babu; Short-Chain Ceramide for Enhanced Cellular Uptake and Cytotoxicity of Liposome-Encapsulated Daunorubicin in Melanoma (B16-BL6) Cell lines (in preparation)

Alrbyawi,H, Arnold, R. D., Jayachandra Babu; Cardiolipin Based pH-Sensitive Liposomes for Enhanced Cellular Uptake and Cytotoxicity of Daunorubicin in Melanoma (B16-BL6) Cell Lines (in preparation)

Alrbyawi,H, Arnold, R. D., Jayachandra Babu; Cardiolipin for Enhanced Cellular Uptake and Cytotoxicity of Thermosensitive Liposome-Encapsulated Daunorubicin Toward Breast Cancer (MDA-MB-231) Cancer Cell Lines (in preparation)

Alrbyawi,H, Jayachandra Babu; Rapidly Dissolving Polymeric Microneedles for Intraocular Delivery of Cyclosporine A (in preparation)

Conference Presentation

1. H. Alrbyawi, J. B. Ramapuram. Rapidly Dissolving Polymeric Microneedles for Intraocular Delivery of Cyclosporine A, Auburn University Students Symposium, April 18, 2019
2. H. Alrbyawi, R. Arnold, J. B. Ramapuram, Short-Chain Ceramides for Enhanced Cytotoxicity of Liposome-Encapsulated Doxorubicin Toward Human Breast Cancer (MDA-MB231) and Prostate Cancer (PC-3) Cell Lines. American Association of Pharmaceutical Scientists Annual Meeting, San Diego CA, November 12-15, 2017. Poster* M7059
3. H. Alrbyawi, R. Arnold, J. B. Ramapuram, Short-Chain Ceramide for Enhanced Cellular Uptake and Cytotoxicity of Liposome-Encapsulated Daunorubicin Toward Melanoma (B16BL6) Cancer Cells. American Association of Pharmaceutical Scientists Annual Meeting, San Diego CA, November 12-15, 2017. Poster# M7060
4. RJ Babu, R Arnold, L Chen, H Alrbyawi, Co-delivery System of Doxorubicin and Ceramide in a Liposomal System for the Treatment of Melanoma, American Association of Pharmaceutical Scientist Annual Meeting, Denver, CO, November 13-17, 2016. Poster# 29TIOOO
5. Al Saqr, H. Alrbyawi, RJ. Babu. Evaluation of Diacetyl Boldine Loaded Microemulsion Formulations for Topical Drug Delivery: Preparation, Characterization, *In Vitro* Release and Cytotoxicity Studies. 4th Annual Nanobio Summit, Auburn, October 13-14, 2016. Poster# GP02

6. Al Saqr, H. Alrbyawi, RJ. Babu, Evaluation of Diacetyl Boldine Loaded Microemulsion Formulations for Topical Drug Delivery: Preparation, Characterization, *In Vitro* Release and Cytotoxicity Studies Shikimate Kinase (MtSK), Harrison School of Pharmacy Research Symposium, April 14, 2016
7. H Alrbyawi, RJ Babu, Short-Chain Ceramides for Enhanced Cytotoxicity of Liposome Encapsulated Doxorubicin Toward Human Breast Cancer Cells (MDA-MB231), Harrison School of Pharmacy Research Symposium, April 14, 2016
8. H Alrbyawi, RJ Babu, Short-Chain Ceramides for Enhanced Cytotoxicity of Liposome Encapsulated Doxorubicin Toward Human Breast Cancer Cells (MDA-MB231), Auburn University Students Symposium, April 13, 2016
9. Al Saqr, H. Alrbyawi, RJ. Babu. Evaluation of Diacetyl Boldine Loaded Microemulsion Formulations for Topical Drug Delivery: Preparation, Characterization, *In Vitro* Release and Cytotoxicity Studies. 4th Annual Nanobio Summit, Auburn, October 13-14, 2016. Poster# GP02